MOLECULAR PROBES FOR BIOLOGICAL FUNCTIONS

A thesis submitted

for the degree of

Doctor of Philosophy

by

J.R. Brocklehurst, B.A.,

St. John's College, Oxford.

December 1970

Department of Biochemistry

CONTENTS

Acknowledgements		(i)
Abbreviations		(ii)
Abstract		(iii)
CHAPTER 1.	Introduction	1
	Fluorescence	2
	Applications to proteins	13
	Applications to membranes	18
	Aim of this thesis	19
CHAPTER 2.	Experimental Methods	21
	Materials	21
	Biochemical preparations	22
	Probe preparations	27
	Instruments	35
	Procedures	39
CHAPTER 3.	Glutamate Dehydrogenase	43
	Introduction	43
	Results	46
	MNS	46
	Dansyl amino acids	49
	NADH	51
	Discussion	53

CHAPTER 4. Membranes 59

Introduction 59

Results 70

PS 70
Binding parameters 74
Uncoupling kinetics 76
Position of binding; covalent probes 82
Neutral probes 83
9-anilino acridine derivatives 90
Rapid reaction measurements 93

Discussion 93

Membrane changes 94
Probe structure 105

APPENDIX 1. R_F values 109

APPENDIX 2. Probe structures 110

References 111

ACKNOWLEDGEMENTS

I am grateful to Professor R.R. Porter for allowing me the facilities of his department, and to the British Petroleum Company Ltd., for a Research Studentship. I am also grateful to various members of this department for the loan of equipment.

I would like to thank Mr. R.L.J. Gardener for technical assistance, particularly with biochemical preparations, and Mrs. N. Williams for her accurate typing of this thesis.

I acknowledge many useful and informative discussions with my colleagues in the laboratory, especially R.B. Freedman and D.J. Hancock.

My main thanks are due to my supervisor, Dr. G.K. Radda, for his constant encouragement and inspiration, and for introducing me to biochemistry.

ABBREVIATIONS

The following non-standard abbreviations are used throughout this thesis:

GDH	L-glutamate-NAD(P) oxido-reductase (deaminating) EC 1.4.1.3.
αKg	2-keto-glutaric acid
ETPH	Electron transporting particles, prepared from heavy beef heart mitochondria by sonication.
TMPD	N,N,N',N' tetra methyl phenylene diamine
FCCP	Carbonyl cyanide p-trifluoromethoxy-phenylhydrazone
ANS	1-anilino-naphthalene-8-sulphonate
MNS	2-(N-methylanilino)-naphthalene-6-sulphonate
MNS-	2-(N-methyl anilino)-naphthalene-6-sulphonyl
DNS-) Dansyl)	1-dimethyl-amino-naphthalene-5-sulphonyl
PS	Pyrene-3-sulphonate
NPN	N-phenyl-1-naphthylamine
ABA) ABC) ABS)	2-methoxy,6-chloro, 9-acridinyl p-aminobenzene (arsonate (carboxylate (sulphonate

The structures of these and other probes are shown in Appendix 2.

ABSTRACT

The aim of this thesis was to develop the use of fluorescent probes for studying structural changes in biochemical systems. The investigation was carried out in two major ways:-

a) chromophoric molecules with different structures and fluorescence properties were used in an attempt to discover the structural characteristics needed to make a fluorescent molecule behave as a probe.

b) biochemical systems of differing complexity were studied using ANS (1-anilino-naphthalene-8-sulphonate) and other probes to see what sort of information this probe technique could give. The two main biochemical systems used were:- (i) the ligand induced conformational change of glutamate dehydrogenase (GDH) and, (ii) energy dependent structural changes in submitochondrial particles (SMP). (i.e. those changes induced in mitochondrial membrane fragments by oxidisable substrate which could be reversed by uncoupling agents).

a) MNS (2-(N-methyl anilino)-naphthalene-6-sulphonate) and MNS-Cl were synthesised in an attempt to label GDH covalently with an ANS type molecule. MNS was shown to behave in the same way as ANS, but with a larger blue shift of fluorescence on binding, and a larger enhancement accompanying the conformational change (3 fold instead of 2 fold). MNS-Cl denatured the enzyme

even under mild conditions of modification.

A variety of dansyl (1-dimethylamino-naphthalene-5-sulphonyl) amino acids were used to probe the conformational change of GDH. The dansyl derivatives of glutamate and inhibitors of the enzyme had their fluorescence quenched by NADH + GTP. In contrast the dansyl derivatives of the monocarboxylic amino acids (whose oxidation is activated by the conformational change) had their fluorescence enhanced by NADH + GTP. Despite this specificity there were large numbers of dansyl amino acid binding sites on GDH (ca 35 per oligomer).

Comparison of these responses with those of the MNS-amides showed that in order to detect the structural change in GDH, a probe needed to be negatively charged and to have the negative charge close to the aromatic part of the probe.

In order to detect energy dependent changes in SMP a probe again needed to be negatively charged. However, in this case the negative charge did not have to be as close to the aromatic part of the probe as with the GDH system. Neutral, non-polar probes bind in the lipid phase of the membrane where they cannot sense energy dependent changes in SMP or ionic strength changes in erythrocyte stroma. The negative charge is important in directing the probe to the area of the membrane where it can sense structural changes. In order to test what type of negative charge was required, three 9-anilino acridine derivatives with different acidic groups in the aniline ring were synthesised.

Only the sulphonate derivative responded to energy dependent changes in SMP, indicating a preference for this group rather than carboxylate or arsonate.

b) (i) A limited amount of information was obtained concerning GDH. L-Glu enhanced the fluorescence of bound NADH, while D-Glu had no effect and αKg was a potent quencher. These sharp differences are difficult to explain since all three molecules bind at the same site on GDH. αKg also shifted the conformational equilibrium, making GTP much more effective at inducing the conformational change. The reason for this is as yet unclear.

(ii) The responses of the polarity sensitive probes ANS and MNS, and of the excimer forming probe PS (pyrene-3-sulphonate) to the energy dependent changes in SMP were studied and compared. ANS and MNS bound rapidly to the membrane surface and slowly diffused to internal sites. The energy dependent response was a property of the internal sites only. On binding to SMP no excimer formation by PS was detectable. However, on energisation excimer fluorescence appeared, accompanied by a decrease in monomer fluorescence. This must be due to either an increase in PS concentration within the membrane or to decreased viscosity.

Comparison of the rates of fluorescence decrease following uncoupling revealed a common fast phase ($t_{\frac{1}{2}}$ = 2 sec) with a slow phase characteristic of each probe ($t_{\frac{1}{2}}$ = 12 (ANS), 30 (PS),

60 (MNS) secs). The rates of the slow phases of ANS and PS correlated well with those measured for probe efflux by independent methods. This suggested that the fast phase was a rapid membrane change, followed by a efflux of probe from the membrane (slow phase).

Binding parameters for ANS and MNS were measured by conventional fluorescence techniques. There was an increase in binding and in quantum yield of bound ANS and MNS on energisation of SMP. A novel filtration method was developed for measuring PS binding and showed a two fold increase in PS bound to SMP after energisation. However, this increase was not large enough to account for the observed excimer fluorescence. The technique was also used to verify the fluorescence results for ANS binding.

By measuring fluorescence polarisation and life-times of ANS and MNS in resting and energised SMP, it was possible to rule out viscosity changes as a cause of the PS fluorescence changes. It was therefore proposed that all the probe effects could be explained if energisation involved expulsion of water from the membrane.

This hypothesis was tested by examining the energy dependent responses of ANS and MNS in D_2O and H_2O. In free solution D_2O quenches ANS (and MNS) fluorescence less than H_2O giving an isotope effect of 2.8 (2.4). This effect was lowered for both probes on binding to SMP. On energisation, there was a further

lowering of the isotope effect on MNS. This suggested that the internal sites at which ANS and MNS bind are partially excluded from water and that on energisation this exclusion increases.

By comparing ANS with NPN (N-phenyl-1-naphthylamine) and other neutral probes, it was shown that the probe binding sites are close to the membrane protein, and are probably at interfaces between hydrophobic and aqueous regions within the membrane, i.e. in an area where the probe could easily sense water exclusion.

A theory of the energised state of SMP was proposed, based on the suggestion that energisation involves water expulsion. The theory accounted for the observed probe responses, as well as for proton uptake, and provided a driving force for phosphorylation.

One probe ABS (2-methoxy,6-chloro,9-acridinyl-p-amino benzene sulphonate) had an electron transport dependent response (as well as an energy dependent one), which appeared to follow the rate of oxidation of coenzyme Q.

INTRODUCTION

CHAPTER 1 INTRODUCTION

In recent years there has been a rapid increase in the application of physico-chemical techniques to biochemical problems. A major manifestation of this is the use of "probes" - small molecules or ions which provide a spectroscopic means of reporting local environment and changes in it. Substitution of a naturally occuring ion by one with interesting spectroscopic properties (e.g. of Mg^{++} by Mn^{++}) has led to the use of ESR, NMR, absorption spectra, and Mössbauer spectra[1] for studying a variety of enzyme and membrane systems. Use of Mn^{++} as a probe in NMR investigations on a number of enzymes has yielded much interesting structural information.[2,3] Spin labels are used in ESR studies on proteins and membranes.[4] Probably the best known types of probes are small organic molecules whose absorption and/or fluorescence spectra are sensitive to environmental changes. A very early example of this is the use of bromothymol blue to detect local pH changes.[5]

The use of fluorescent probes offers two main advantages over absorption probes: a) much greater sensitivity, b) several different parameters to measure, e.g. intensity, excitation and emission spectra, lifetime, polarisation. For this reason the work reported in this thesis is concerned with molecular probes which are fluorescent. One of the main difficulties with any experiment using a probe is the fact that the "foreign" probe is certain to perturb the biochemical system. The greater

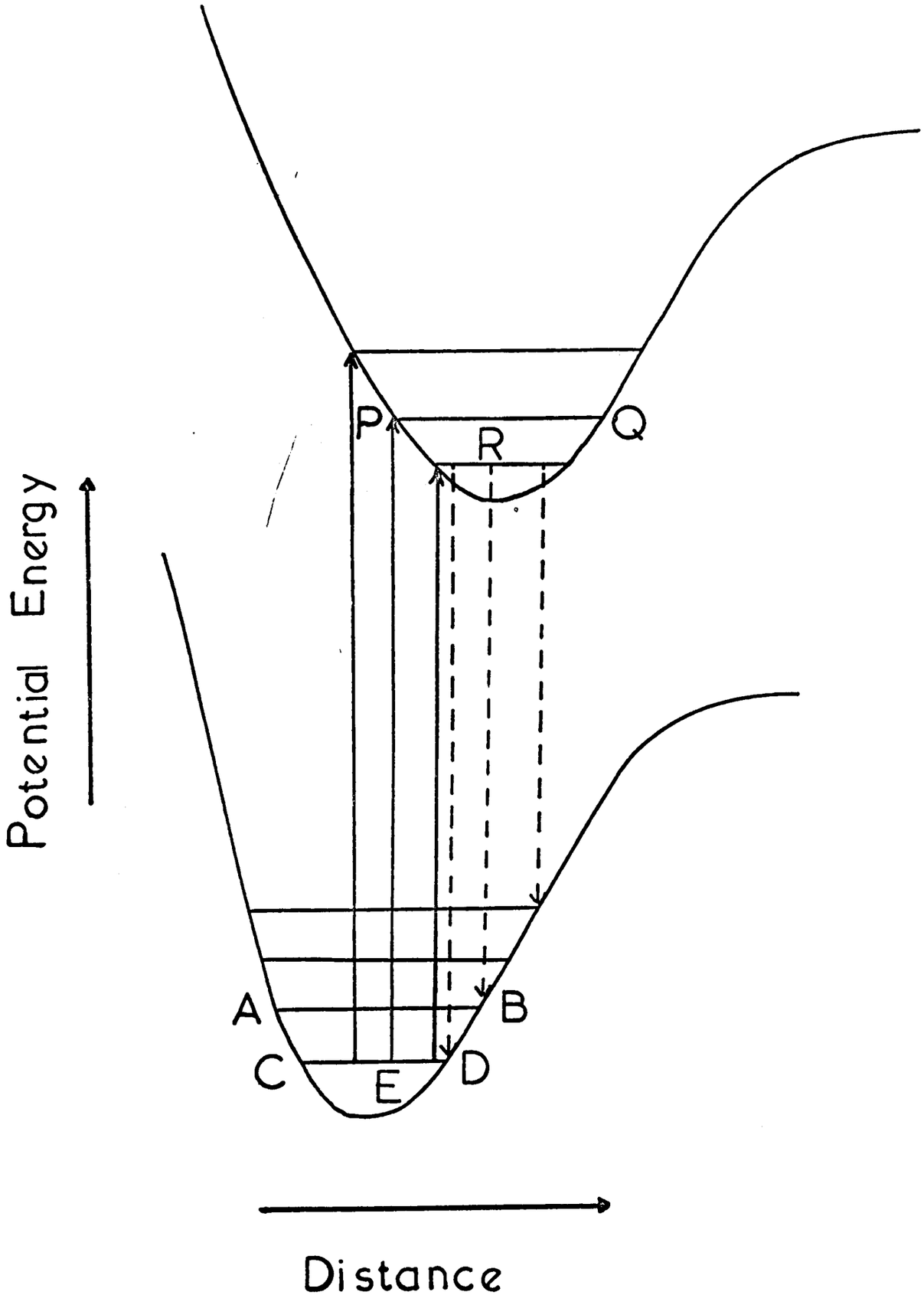

Fig.1. Morse curves for the ground and excited states.

sensitivity of fluorescence means that lower probe concentrations can be used. Wherever possible the continued proper functioning of the system must be checked by independent means.

Fluorescence

The way in which the environment affects the fluorescence of a molecule can only be understood by examining the nature of fluorescence. At room temperature most molecules will be in the lowest vibrational level of their ground state. On excitation they will be promoted to various vibrational levels of an excited state. In solution collisions will dissipate the vibrational energy rapidly ($\sim 10^{-12}$ sec) and the molecules will fall to the lowest vibrational level of the first excited state (Fig.1). In most organic molecules there is considerable overlap of the vibrational levels of the first and higher excited states, so by intersystem crossing and dissipation of vibrational energy all molecules arrive at the same energy level. Fluorescence occurs when a molecule drops back from the first excited state to the ground state vibrational levels. Most molecules will fall back to the upper levels and will lose excess vibrational energy by collision. Thus only the 0-0 transition occurs both in absorption and emission, and the main fluorescence band appears at longer wavelength than the absorption band (Stokes Law).

All the transitions in fig.1 have been indicated by vertical lines, representing the application of the Frank-Condon principle

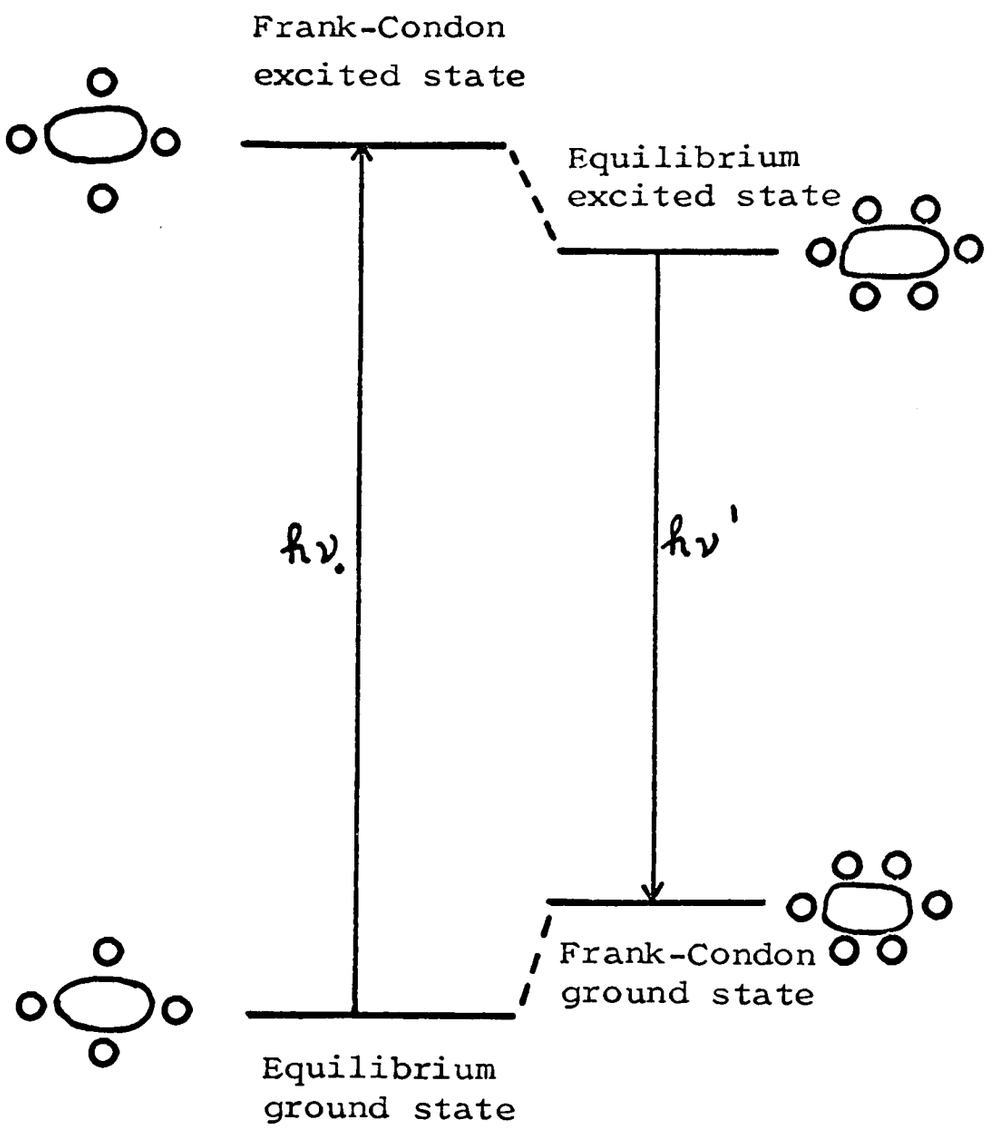

Fig.2. Solvent reorientation on excitation and emission.

that light absorption and emission processes take place too rapidly for molecular motion to occur during the transition. The most probable transitions are those from/to the mid-points of the lowest vibrational levels, and the extremes of the upper levels. Thus in fig.1 the most intense absorption will occur at the wavelength corresponding to EP. The most intense fluorescence will occur at the wavelength corresponding to RB. However, in solution interaction between the solute and solvent must be taken into account. Excitation involves movement of electrons within the molecule, and thus brings about a change in both dipole-moment and polarisability of the molecule. For many organic molecules the charge separation (and hence the dipole-moment) is larger in the excited state than in the ground state. This will cause greater dipole - induced — dipole interaction between solvent and excited state, than solvent and ground state i.e. solvation stabilises the excited state relative to the ground state and causes a red shift in absorption maximum. The extent of the interaction will of course depend on the polarisability of the solvent.

On excitation a molecule in ground state equilibrium with the solvent will be promoted to a Frank-Condon excited state (i.e. with the same solvation as the equilibrium ground state) - Fig.2. The solvent will then rearrange to give the equilibrium excited state, from which emission takes place. Emission produces a Frank-Condon ground state molecule (i.e. with the

solvent configuration of the excited state) which then rearranges to give the equilibrium ground state. Thus as a result of solute-solvent dipolar interactions, the 0-0 transitions in absorption and emission do not coincide - the fluorescence is red shifted. Increase of solvent polarity will obviously increase the interaction and cause larger red shifts of fluorescence. It should be noted that even with non-polar solutes in non-polar solvents there will be a small red shift due to dispersive (Van der Waals) interactions between solute and solvent[6].

Various attempts have been made to relate the observed solvent effects to measurable solvent properties such as dielectric constant and refractive index[6,7]. Using Lippert's[8] relation between band separation and "point-dipole"

$$\nu_{abs} - \nu_{fl} = \frac{2(D - 1)}{2D + 1} - \frac{2(n^2 - 1)}{2n^2 + 1}$$

and the Onsager[9] theory of solutions, it is possible to derive a very complex expression for the shift caused by change in solvent, in terms of dielectric constant, refractive index, and the energy of the solvent absorption band[6]:-

$$\Delta\nu_{fl} = \left[\frac{2}{a^3}\left(\frac{2n^2 + 1}{n^2 + 2}\right)\left\{\mu_e(\mu_g - \mu_e)\left(\frac{D-1}{D+2} - \frac{n^2 - 1}{n^2 + 2}\right) + \tfrac{1}{2}\left(\frac{n^2 - 1}{n^2 + 2}\right)\left(\mu^2_g - \mu^2_e\right)\right\}\right] + \left[\frac{2}{a^3}\left(\frac{n^2 - 1}{n^2 + 2}\right)\frac{E}{E + \varepsilon}\left\{|M_{12}|^2 + \varepsilon(\alpha_e - \alpha_g)\right\}\right]$$

where n,D are the dielectric constant and refractive index of the solvent, μ_g, μ_e are the ground and excited state dipole moments of the solute. α_g and α_e are the ground and excited state polarisabilities of the solute. $|M_{12}|$ is the transition moment for emission, and E and ε are the average absorption energies of the solvent and solute respectively. a is the Onsager radius. The first term represents dipole-induced dipole interaction between solute and solvent, while the second is the result of polarisation of the solvent by the transition moment dipole of the solute. For polar solvents an additional very complex term must be included to take account of dipole - dipole interactions. Clearly a complex expression like this is impractical for normal use. A simple empirical measure of solvent polarity has been suggested by Kosower[10]. He found that the transition energy (absorption) of 1-ethyl-4-carboxy-methylpyridinium iodide in different solvents correlated well with Y (the solvent ionising power) for alcohol/water and acetone/water mixtures, and suggested that these transition energies (Z) should be used to characterise the polarity of the solvent. Turner and Brand[11] extended this idea for use with fluorescent molecules, and used various probes to estimate the polarity of protein binding sites. However, they had no explanation for the fact that 1,8 ANS consistently predicted a lower polarity than related probes did. This could be due

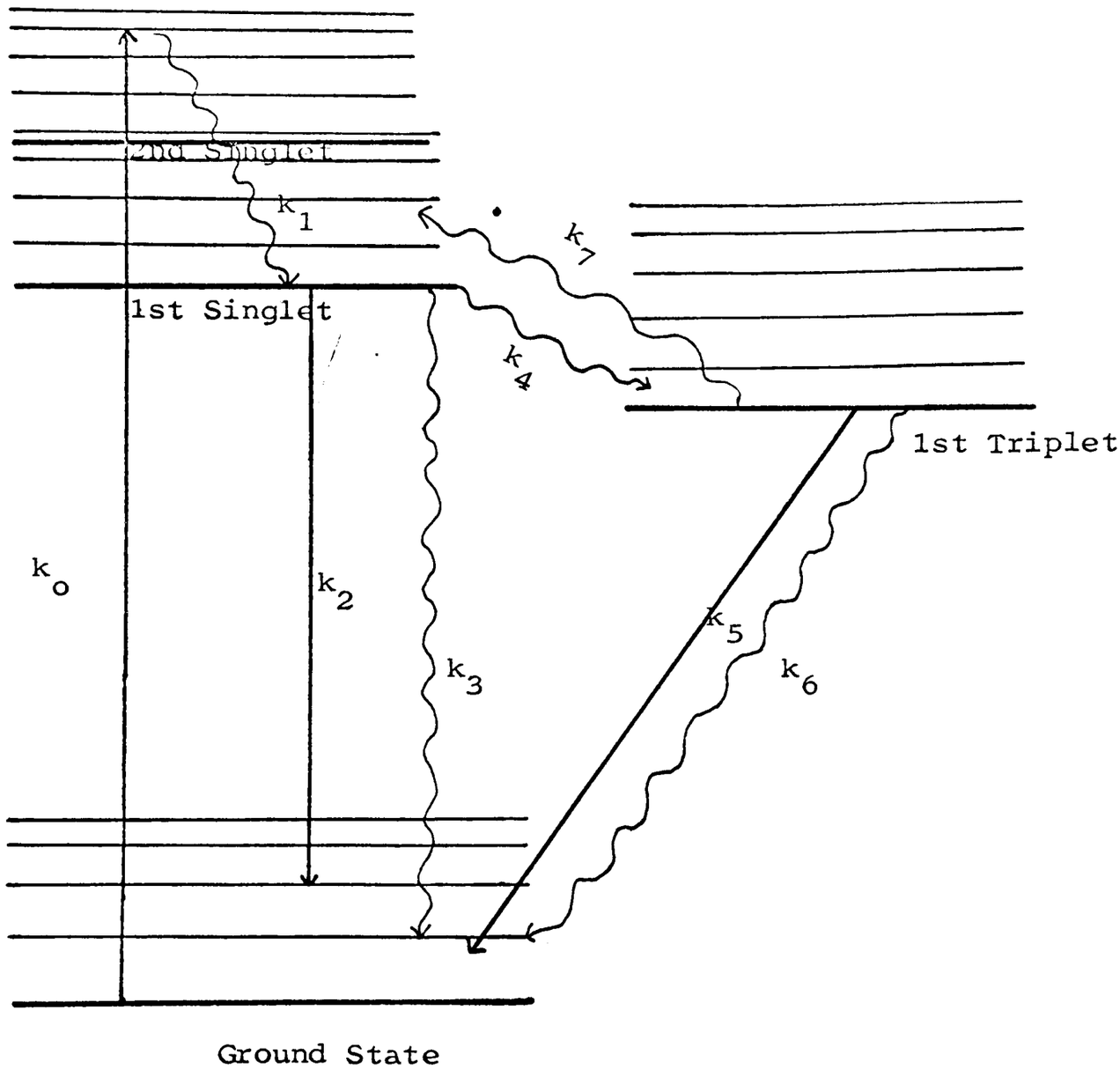

Fig.3. Jablonski diagram

to "peri" interactions between 1,8 substituents on the naphthalene ring[12].

Solute fluorescence is also affected by solvent viscosity. If movement of the solvent molecules is slowed down (e.g. by decrease in temperature or increase in viscosity) the Frank-Condon excited state will not have time to rearrange to the equilibrium excited state (Fig.2) before emission takes place. This leads to a blue shift in fluorescence (i.e. the 0-0 band separation decreases). This sort of effect is probably a very important factor in the binding of probes to macromolecules[13]. Some molecules change their shape on excitation (e.g. trans retinol)[14]. This will cause a distinct change in shape of the excited state potential energy curve (Fig.1) and separate the absorption and emission bands. Increasing solvent viscosity will restrain the change in shape, and hence will also bring down the 0-0 band separation.

The solvent effects discussed above have all involved changes in 0-0 band separation. Change of solvent frequently involves a change in fluorescence intensity (quantum yield) and this is much less well understood. Fluorescence is merely one of the many ways in which the energy of excitation may be lost by the molecule (Fig.3). As has already been seen k_1 is very rapid (10^{12} sec^{-1}). The rate at which energy is lost as fluorescence (k_2) is commonly 10^7 - 10^9 sec^{-1}. Obviously the fluorescence quantum yield (no of quanta emitted/no of

quanta absorbed) will depend on the relative rates of k_2 and the competing processes. If k_2 is much faster than k_3,k_4 etc the quantum yield will approach unity. k_3 is the composite constant for a number of processes, including quenching, and internal conversion. Normally internal conversion between the ground and first excited states is insignificant because of the large energy difference. k_4, the rate of intersystem crossing, will depend on the singlet-triplet separation energy. k_5 is the rate of phosphorescence, and k_6 is the quenching, intersystem crossing rate for the triplet ($\equiv k_3$ for the singlet). k_7 is the rate of repopulation of the singlet from the triplet. This is due to thermal excitation and results in delayed fluorescence[15]. k_4 is frequently as fast as k_2 and in rigid media (i.e. where k_3,k_6 are greatly reduced) the sum of quantum yields of fluorescence and phosphorescence is unity[16]. Obviously in the absence of other quenching mechanisms (low k_3) the fluorescence yield is larger the slower k_4 is. Any solvent, therefore, which increases the singlet-triplet separation, will increase the yield of fluorescence at the expense of phosphorescence. The dipole moment of the triplet excited state is usually between those of the ground and first singlet excited state. A decrease in the solvent polarity will, therefore raise the singlet energy more than that of the triplet, thus increasing the singlet-triplet separation, and increasing the

fluorescence yield. This is thought to be important in the enhancement of fluorescence of the anilino naphthalene sulphonates. Also important in the environmental sensitivity of these probes is the coplanarity of the anilino group with the naphthalene ring. X-ray diffraction studies on TNS crystals have shown[17] that in the anhydrous crystal TNS is planar, while in the hydrated crystal it is bent. The change in polarisation across the long wavelength absorption band used to excite ANS fluorescence suggests that two very close transitions are involved[11,18,18a]. The lower energy transition of the two probably has considerable intramolecular charge transfer character. Kasha[19] has proposed a new type of electronic transition intermediate in character between $\pi-\pi^*$ and $n-\pi^*$. This $1\text{-}a_\pi$ transition is from the lone pair of an aromatic substituent (e.g.$-NH_2$) to an antibonding molecular orbital of π origin (a_π). This transition is largely of intramolecular charge transfer character. A twisting parameter θ has been defined, which for sp^2 hybridised nitrogen is the angle between the plane of the aromatic ring, and the plane of the three nitrogen substituents. When $\theta=0$ the lone pair orbital in ANS (TNS) can readily become part of a molecular π orbital covering both aromatic rings, (hence giving a $\pi-\pi^*$ transition). However, as θ increases, the amount of $1\text{-}a_\pi$ character increases giving a decrease in the allowedness of the singlet-singlet

transitions, and an increased singlet-triplet mixing. In fact τ_o for phosphorescence can be correlated with θ for aromatic amines:-

$$\tau_o \propto \sin^2\theta\cos^2\theta$$

where $\sin^2\theta$ depends on the singlet-triplet mixing, and $\cos^2\theta$ on the projection of the N orbital onto the π orbitals of the aromatic ring. Thus as the molecule twists out of planarity (θ increases) the phosphorescence yield increases, and the fluorescence yield falls, as is indicated by the X-ray results.

Another possible reason for the low quantum yield of fluorescence of ANS in water is a specific quenching mechanism. Stryer suggested that the observed isotope effect in D_2O was due to a proton transfer mechanism (from solute to solvent)[20]. However, molecules with no transferable proton also exhibit an isotope effect.[21] Eisinger has proposed a tunnelling mechanism between ground and excited states via the solvation shell,[21] the efficiency of which is decreased in D_2O.

Quenching of fluorescence can occur by a variety of mechanisms. Various trivial mechanisms such as collisional quenching, ground state complex formation, concentration quenching can be a nuisance when studying fluorescence, especially of molecules with relatively long fluorescence lifetimes. However, two important quenching mechanisms can be useful in the use of probes in biological systems. These

are the possibility of excimer formation, and the possibility of energy transfer. Some fluorescent molecules, notably pyrene and its derivatives, exhibit concentration dependent fluorescence spectra. The low concentration fluorescence is quenched and is replaced by another band (usually longer wavelength) as the concentration is increased. This is due to the formation of excited state dimers[22] (excimers), between a molecule in the excited state, and one in the ground state:-

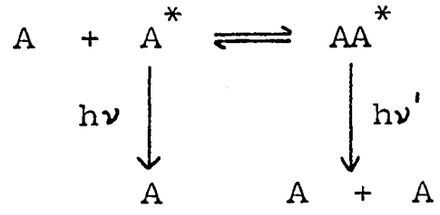

This process is obviously diffusion controlled and depends on concentration, solvent viscosity, etc.

The excitation energy of a molecule may be transferred to another molecule by a long range radiationless resonance mechanism[23]. The rate of transfer is proportional to $\frac{1}{R^6}$ (R = intermolecular distance) and a distance R_o (at which rate of transfer = rate of spontaneous fluorescence decay) can be calculated using the Förster theory. This transfer leads to quenching of the donor fluorescence, and sensitisation of the acceptor. Energy transfer may be used to probe the distance between different chromophores in biological systems, though assumptions about local refractive index etc. have to be made.

Three parameters of fluorescence (λ_{max} absorption and

emission, and quantum yield) have been extensively discussed. Polarisation of fluorescence and fluorescence lifetimes can also be used as probes in biological systems.

The fluorescence lifetime of a species is a measure of the average length of time an excited molecule spends in the excited state, before giving rise to emission. If emission is the only means of dissipating the excited state energy, the lifetime is $\tau_r = \frac{1}{k_f}$. k_f is defined by $\frac{dn}{dt} = -k_f n$ where n is the number of molecules in the excited state. τ_r is the mean <u>radiative</u> lifetime in the absence of all quenching and radiationless processes. In practice the measured lifetime is $\tau = q\tau_r$ where q is the quantum yield of fluorescence. Obviously changes in solvent which affect the quantum yield as discussed above (e.g. by altering the rate of intersystem crossing) will change the lifetime. Indeed one important way of deciding whether or not an interesting change is due to a quantum yield change is to determine the lifetime.

If polarised light is used to excite the fluorescence, only those molecules whose transition dipoles are parallel to the direction of polarisation will absorb light maximally. For others, the intensity of absorption will be $A\cos\theta$ where θ is the angle between their transition dipole and the direction of polarisation. If the molecules are rigidly held so that no rotation takes place during the excited state lifetime, the

emitted light has the same polarisation as the absorbed light provided that the absorption and emission dipoles are parallel. The polarisation (p) is defined as $p = \frac{I_{\parallel} - I_{\perp}}{I_{\parallel} + I_{\perp}}$ where $I_{\parallel}$ and $I_{\perp}$ are the intensities of the components of the beam resolved parallel and perpendicular to the initial direction of polarisation. Thus for rigidly held, randomly oriented molecules $p = p_o = 0.5$. If the molecules can rotate, the observed polarisation is less than 0.5, and will depend upon the lifetime of the excited state according to:-

$$\left(\frac{1}{p} - \frac{1}{3}\right) = \left(\frac{1}{p_o} - \frac{1}{3}\right)\left(1 + \frac{3\tau}{\rho}\right)^{24}$$ where τ is the lifetime and ρ is the rotational relaxation time of the molecule. (For a spherical molecule $\rho = 3V\eta/RT$ where V is the molar volume and η is the viscosity). However, in some molecules the excitation and emission dipoles are not parallel. If this is the case, the limiting polarisation is governed by $p_o = (3\cos^2\beta - 1)/(\cos^2\beta + 3)$ where β is the angle between the two dipoles. These equations apply only for polarised exciting light. The equations for natural light may be found in reference 24.

Applications

The applications of fluorescent probes to structural studies of proteins and/or membranes have been extensively reviewed[25-30], and are tabulated in Tables 1 and 2. Only the more significant or relevant papers will be discussed here.

Table 1 (Continued)

Probe	System	Information	Ref.
DNS	chymotrypsin	rotational relaxation times	82
	BSA	rotational relaxation times	83
	RNase	rotational relaxation times	84
	β-lactoglobulin A	rotational relaxation times	85
	ɣ-globulin G	molecular rigidity	86
	LDH	molecular rigidity	87
	thyroglobulin	freedom of rotation of label	88
Pβ	immunoglobulins	rotational relaxation times	88,89
Various		theoretical restrictions on rotation studies	90

(iii) protein fluorescence and energy transfer

Tyr, try	proteins and polypeptides	fluorescence characteristics	91
	hormones	structureless in solution	92
	G3-PDH	NAD binding	93,94
	papain, α chymotrypsin carbonic anhydrase	distribution of Try around the active site	95,96
Various	polypeptides	spectroscopic ruler, folding of chain	97,98

Table 1 (Continued)

Probe	System	Information	Ref.
TNS	poly-L-lys	specifically detects β structure	55
Amino naphthalene sulphonate	various proteins	binding site configuration	56
DNS amino acids	various proteins	specific interactions	57
DNS Cys	actin	detects polymerisation	58
DNS Lys	antibodies	antibody - hapten reactions	59
MNS	phosphorylase b	specifically detects AMP induced dimerisation	60
NADH	various dehydrogenases	binding studies	61
	GDH	binding studies	62,63
	GDH	effect of substrates, inhibitors	61,63-67
	alcohol DH	binding studies	68,69
	Glyerophosphate DH	binding studies	70
	malate DH	binding studies	71
	alcohol DH	effect of D_2O on binding	72
pyridoxamine 5' phosphate	phosphorylase b	structural changes	73
	aspartate amino transferase	binding studies	74
(ii) covalent			
DNS	BSA and anti-BSA	binding constant	75
DNS	various proteins	anomalous fluorescence properties	78-80
	various proteins	conformational changes	81

Table 1

Applications to Proteins

Probe	System	Information	Ref.
(i) non covalent			
ANS	myoglobin and haemoglobin	hydrophobic binding site in haemcrevice	18
	various proteins	binding site polarity	11
	BSA	binding parameters; theory and limitations	31-35
	BSA	heterogeneity of binding sites	37-40
	BSA and nitrite	dimerisation of ANS	41
	myosin	follows modification of ATPase activity	42
	"	change transfer follows structural changes	43
	GDH	detects ligand induced structural changes	44-46
	"	detects desensitisation by modification of tyr	47
	trans-aldolase	detects substrate induced conformational changes	48
TNS and ANS	immunoglobulins	hydrophobic binding sites	49,50
anilino acridines	"	hydrophobic binding sites	50,51
TNS	variety of protein	hydrophobic binding sites	26
TNS	pepsin	pepsinogen inter-conversion	52,53
	chymotrypsin	chymotrypsinogen inter-conversion	54

Applications to proteins

The three major ways in which fluorescence has been used to study proteins may be subtitled:- (i) non-covalent probes, (ii) covalent probes, (iii) coenzyme and protein fluorescence. These different approaches yield different types of information, much of which is complementary.

(i) non-covalent probes

The commonly used non-covalent probes are those of the anilinonaphthalene sulphonate type. As a result of factors which have been discussed above these molecules are nearly non-fluorescent in water, but are moderately fluorescent in non-aqueous environments e.g. when bound to a protein. Stryer used ANS as a probe of 'non-polar' binding sites in myoglobin and haemoglobin[18]. He found that ANS bound in the haem crevice, a very hydrophobic region, with a fluorescence quantum yield approaching unity. Subsequent work on various proteins[11,49,50] detected binding of ANS and TNS to hydrophobic regions, but this binding was not specific and yields little interesting information. Turner and Brand[11] measured the polarity of the hydrophobic sites of various proteins using Kosower's Z scale. However, some caution is needed in using this approach since, as was seen above, changes in local polarity are not the sole cause of changes in fluorescence intensity or wavelength maximum. While it may be true that 1,7 ANS is not affected by changes in viscosity[11], other

probes certainly are, and their properties will not correlate as well with the Z scale (this was found for 1,8 ANS[11]). It is important to realise that the quantum yields measured by Turner and Brand correlate well with the Z scale only for water/alcohol mixtures. For other solvents, especially ones where specific effects (e.g. ionisation in acetic acid, H-bonding in pyridine) may occur, the correlation is poor. These specific effects could be important in the binding to different proteins.

A number of methods are used for measuring the binding of probes to proteins. Weber and his collaborators have critically examined the limitations of the various extrapolation procedures[31-36] in terms of the information content. These methods are all based on the assumption that the various binding sites on a protein are equivalent and cause the same enhancements of the fluorescence of the probe. That this is not so has always been suspected since in many systems curved binding plots are obtained, indicating heterogeneous binding. Weber and Anderson have now shown that the five ANS binding sites on BSA are not equivalent, and do in fact cause different enhancements of ANS fluorescence[39,40]

A drawback of the above probes is the fact that nothing is known of where they bind. This problem has been tackled either by introducing a more specific group into the probe or by looking for "specific sites" which have a larger affinity for the probe than the rest of the protein. Chen was the first to attempt this

by using dansylated amino acids[57]. He found that different proteins caused different enhancements of DNS-amino acid fluorescence, BSA having the largest effect (see Table III of ref 57). "Specific sites" have been found for the ANS type of probe, e.g. Stryer's early work on haemoglobin. TNS was found to be enhanced by the β structure of poly-L-lysine[55], though the α helical and random coil forms caused only a slight enhancement. The effect is detected when the β form is produced by three different methods, and is accompanied by a marked increase in the polarisation of fluorescence. The β structure is held together by hydrophobic areas, and it is suggested that TNS binds preferentially to these areas (which are not present in the other structures).

Structural changes have been detected in several systems. The AMP induced dimerisation of phosphorylase b is detected by MNS[60], and not by ANS and similar probes. No explanation of this effect is offered - it may well be that ANS and MNS bind at different sites, and that the MNS one is involved in the dimerisation. The ligand induced structural changes in GDH as detected by ANS[44,45] will be discussed later. ANS has been used to study substrate induced changes in transaldolase[48]. The author postulated that addition of substrate caused a conformational change leading to the displacement of ANS. This was reversed by addition of the second substrate which led to regeneration

of substrate-free enzyme (and hence the ANS fluorescence was restored). An alternative explanation is that the conformational change causes a quenching of ANS fluorescence, or that the bound substrate quenches ANS. This cannot be ruled out in the absence of binding data for ANS to the enzyme-substrate complex. There is a growing tendency for changes in probe fluorescence to be interpreted as a conformational change without supporting evidence. TNS fluorescence is enhanced more by chymotrypsin than by chymotrypsinogen[53], and use is made of this to study the rate of activation of chymotrypsinogen.

(ii) covalent probes

Covalent attachment of a probe to a protein offers several advantages over the use of non-covalent probes. If necessary the actual position of binding can be determined by hydrolysis and identification of the labelled amino acid. More importantly information obtained is not confused by possible changes in binding. The main use of covalent probes has been to study rotational mobilities of proteins, and has yielded much useful information (Table 1). Careful selection of the probe is needed since if its fluorescence life-time is too short, the measurements will not be reliable. Anomalous results have been obtained, however, because of ignoring possible variation in life-time[90]. Multiple labelling often leads to anomalous fluorescence properties due to energy transfer[78]. The fluorescence properties

may also be modified by other effects such as change of acidity of the probe on conjugation. The acidity of the dansyl group is increased on conjugation with a protein, behaviour which Klotz has explained[79] in terms of structured water at the protein surface. This has been challenged[80] because ionic strength changes cause the pK_a to shift. However, it could well be that the ionic strength changes alter the water structure which is why the pK_a shifts.

(iii) coenzyme and protein fluorescence

One major disadvantage of all probe experiments is the possibility of perturbing the system under examination by addition of the probe (e.g. the BSA - anti-BSA binding constant is decreased two fold by dansylation of BSA[75]). In order to avoid this possibility a natural coenzyme may be used as a probe, or the natural protein fluorescence may be examined. NADH fluorescence has been widely used for studying coenzyme and substrate binding to dehydrogenases[61-72]. Of particular interest are the various effects of substrates and inhibitors on the fluorescence of the NADH/GDH complex (see below). Solvent perturbation (D_2O) of bound NADH was used to show that alcohol dehydrogenase partially restricts the access of bulk water to NADH bound at the active site[72]. The natural fluorescence of proteins is of particular use in probing distances on the protein surface. Thus energy transfer from

Table 2

Applications to Membranes

Probe	System	Information	Ref.
TNS	Pseudomonas aeruginosa	polymyxin effect on ion permeability	99
fluorescein		intracellular viscosity	100
ANS	erythrocytes and phospholipids	binding	101,102
Ethidium bromide	erythrocytes and phospholipids	binding	103
ANS, acridine orange	nerve fibres	response to electrical stimulation	104,105
ANS, DNS	electroplax	response to electrical stimulation	106,107
ANS	muscle microsomes	effect of ions	108
ANS	SMP	energy dependent structural changes	109,110

Try to an inhibitor has shown that a Try is within 10Å of the active site of carbonic anhydrase[95].

Applications to membranes

The use of fluorescent probes in the study of membranes has been restricted largely to non-covalent probes, particularly ANS. The earliest example was in 1954[99], when TNS was used to detect changes brought about in Pseudomonas aeruginosa cells by polymyxin. Fluorescence only appeared after polymyxin treatment, presumably due to diffusion of TNS into the cell membrane. Intracellular viscosity has been measured by polarisation of fluorescein fluorescence[100]. However, since no account was taken of possible life-time changes, this interpretation must be viewed with some caution. The interaction of ANS with simple membrane systems such as erythrocytes and phospholipid micelles has been widely studied. There is a typical shift and enhancement of fluorescence on binding, the extent of these being dependent on ionic strength and pH[101,102]. The low polarisation of fluorescence indicates that the probe is more mobile than when bound to proteins[102], and it is suggested that the probe binds at a hydrophobic/hydrophilic interface[101] where it responds to membrane changes brought about by osmotic shock. Similar studies have shown that the positively charged probe ethidium bromide will bind to whole mitochondria[103].

Structural changes have been detected by ANS and other probes in several membrane systems. Small increases in fluorescence of ANS and acridine orange bound to nerve fibres have been detected on electrical stimulation[104,105]. However, the size of the changes involved (ca 0.02%) leads one to suppose that significant structural alteration is absent. The observed changes could be the effect of changing electric field on the probe. Similar changes have been observed in the eel electroplax membrane using ANS and covalently attached DNS[106,107]. Metal ions induce structural changes in muscle microsomes which ANS detects[108], the ANS enhancement being associated with changes in the phospholipid part of the membrane.

By far the most interesting use of fluorescent probes, as far as this thesis is concerned is their use for following energy dependent structural changes in the mitochondrial membrane. Chance, Lee and Radda[109] first demonstrated that ANS detected a structural change, and subsequently showed that the ANS response was indicative of the "energy state" of the membrane[110]. Subsequent work in this field will be discussed later in the light of work presented in this thesis.

Aim

The aim of this thesis was to develop the use of fluorescent probes for studying structural changes in

biochemical systems - especially membranes. The fluorescence characteristics of a variety of organic molecules with differing structural features were examined for environmental sensitivity. Particular attention has been paid to series of related molecules whose structures differ only slightly (e.g. in charge). Potential probes were then tested in different biochemical systems of increasing complexity:-

a) Glutamate dehydrogenase, an enzyme with a known structural change. This was used to try to decide what particular structural characteristics were needed by the probe.

b) Simple membrane systems such as erythrocytes were used to see if the same factors found in a) were effective in a membrane.

c) Submitochondrial particles. The recently discovered energy dependent structural transition was to be fully investigated.

By using this type of logical approach it was hoped to determine (i) the molecular features needed for a fluorescent molecule to probe structural transitions.

(ii) the nature of the structural transitions, and their relation to biological events, particularly in membranes. The results will not necessarily be presented in the above order, since it has proved more convenient at times to rearrange them in order to bring together related ideas and themes.

EXPERIMENTAL

METHODS

CHAPTER 2 EXPERIMENTAL DETAILS

Materials

All materials used were supplied by BDH or Fisons, and were of the highest available quality, except the following:-

Biochemicals

Adenosine triphosphate (disodium salt, ATP), glutamate dehydrogenase (GDH) and nicotinamide adenine dinucleotide (reduced form, NADH) were supplied by Boehringer. Bovine serum albumin (BSA) was supplied by Armour Pharmaceuticals, and Sigma supplied guanosine triphosphate (GTP). p-Trifluoro-methoxy phenylhydrazone carbonyl cyanide (FCCP) was the kind gift of Dr. P.B. Garland.

Probes etc.

1-anilinonaphthalene-8-sulphonate (ANS) and pyrene-3-sulphonic acid (PS) were supplied by K & K Laboratories. Pyrene-1-butyric acid (PB) and dibutylaminopropanol (DBP) were supplied by Eastman. 6,9-dichloro 2-methoxy-acridine came from Aldrich. Koch-Light supplied 4-aminoisophthalic acid, dansyl-norvaline (DNS-Nor) and L-2,4-diamino n-butyric acid. Dansyl sulphonic acid (DNS-OH) came from Sigma, and p-arsonilic acid from Ralph Emanuel.

Solvents etc.

Absolute ethanol was supplied by J. Burroughs Ltd.

β-Scientific supplied D_2O and deuterated dimethylsulphoxide ($DMSOd_6$). Normal dimethylsulphoxide (DMSO) came from Koch-Light as did sodium dodecylsulphate (SDS). Sephadex resins were supplied by Pharmacia, and Dowex 50 resin came from BioRad. Oxygen-free nitrogen was supplied by British Oxygen.

All aqueous solutions were made up in water twice distilled from deionised water.

Biochemical Preparations

Mitochondria

Heavy beef heart mitochondria (HBHM) were prepared by a modification of the method of Crane, Glenn and Green[111]. Hearts from freshly slaughtered bullocks were obtained from the slaughter house and transported on ice. The preparation was carried out at 4°C. The muscle (1 - 1.5 kg. when free of connective fat and tissue) was cubed and minced. The mince was suspended in a buffer of 0.25M sucrose, and 0.01M Tris-Cl, pH 7.8 in the proportion 300g of mince to 400mls of buffer. To neutralise the acids released on mincing 1.8 mls. of 6M KOH were added with each 400 mls. of buffer since it proved impossible rapidly to neutralise the total 3-4 l of mixture. The pH of the total mixture was finally adjusted to 7.5 ± 0.1. The sucrose solution was then removed from the mince by squeezing in cheesecloth, or preferably by centrifugation

(2000 r.p.m. for 10 mins. in 1 l. pots on the MSE Mistral 6L*). The neutralised mince was then homogenised in a buffer of 0.25M sucrose, 0.01M Tris-Cl pH 7.8, 1mM Tris-succinate, and 0.2M EDTA (STSE). 200g of mince, 400mls of STSE, and 1ml of 6M KOH were placed in a Waring blender and homogenised at full speed for 15 secs. Another 1ml of KOH was added and the mixture homogenised for a further 5 secs. The pH of the viscous homogenate was adjusted to pH 7.8. This was most easily done by placing the homogenate (~41) in a plastic bucket, and stirring vigorously with a bent stainless steel rod attached to an electric drill while adding HCl or KOH. The homogenate was then centrifuged for 20 mins at 1200 r.p.m. on the Mistral. The supernatant was carefully decanted, strained through double cheesecloth to remove the lipid granules, and its pH was readjusted to 7.8. The preparation was usually left overnight at this stage.

The supernatant (~1500 mls) was then centrifuged for 20 mins in the 6 x 250 ml rotor of the Sorvall RC2-B ultra-centrifuge* at 13000 r.p.m. (or 16250 r.p.m. in the 21 head of the Spinco model L ultracentrifuge). The resulting pellet was swirled with a little STSE to remove the fluffy buff coloured layer (light beef heart mitochondria LBHM). The main brown layer (HBHM) was removed by stirring with ~10 mls

*Kindly loaned by Dr. K. Dalziel

of STAMS (0.25M sucrose, 0.01M Tris-Cl, pH 7.8, 1mM ATP, 1mM $MgCl_2$, 1mM potassium succinate) leaving a small very dark button in the bottom of the centrifuge pot. The suspension of HBHM was homogenised in a glass homogeniser with a Teflon pestle driven by an electric drill at ca.1400 r.p.m., with two short passes (5-10 secs). The homogenate (180 mls) was adjusted to pH 7.8 and spun in the Sorvall small head (8 x 50mls) at 18000 r.p.m. for 15 mins. The middle layer of this pellet was homogenised in STAMS and adjusted to ca. 60 mls pH 7.8. This was spun again as above, resuspended in STAMS and frozen in 15-20ml lots at -20°C for storage. (Yield: 60-80mls of HBHM suspension,~20mg/ml in protein).

Sub-mitochondrial particles (SMP).

ETPH (electron transporting particles)

This was essentially the method of Hansen and Smith[112]. 15mls of the mitochondrial suspension were thawed, diluted with an equal volume of STAMS, and adjusted to pH 7.8. This was spun in the 30 head of the Spinco model L ultracentrifuge for 15 mins at 17500 r.p.m. The HBHM were suspended in 50mls of a solution 0.25M in sucrose, 0.01M in Tris-HCl (pH 7.5), 1mM in ATP, 1mM in potassium succinate, 5mM in $MgCl_2$, and 10mM in $MnCl_2$, and adjusted to pH 7.5. 10ml lots of this solution were then cooled in an ice/salt bath and sonicated

at full power for two 30 sec bursts separated by 1 min (100 watt MSE ultrasonic disintegrator with a 9mm titanium probe*).

The pH was readjusted to 7.5, and the suspension was centrifuged for 7 mins at 20000 r.p.m. in the 40 rotor (Spinco Model L) to remove damaged mitochondria. The supernatant was carefully decanted from the pellet (taking care not to disturb the rather fluffy surface layer) and spun for 45 mins at 36000 r.p.m. in the 40 rotor. The small translucent brown pellet was suspended in a small volume of MST (225mM mannitol, 75mM sucrose, and 20mM Tris-HCl pH 7.4) and frozen in 2ml lots until required.

ESMP (EDTA treated submitochondrial particles)

This is a modification of the method of Linnane and Titchener[112a,113]. HBHM were prepared as above. A sample was thawed, spun down and suspended to a concentration of 10mg/ml (protein) in a solution 0.25M in sucrose, 0.01M in Tris-HCl pH 7.5, and 1mM in EDTA (STE_1). This suspension was centrifuged at 15000 r.p.m. for 7 mins in the 30 head of the Spinco model L ultracentrifuge and resuspended in 0.25M sucrose- 0.01M Tris-HCl pH 7.6 solution ($\sim$20ml). This was stored at -20^{o}C for a week during which time it was thawed and refrozen at least five times. It was then thawed, spun

*Kindly loaned by Dr. L.A. Stocken

down and suspended in the same volume of a solution 0.25M in sucrose, 0.01M in Tris-HCl pH 7.5, and 2mM in EDTA, (STE_2), sonicated as for ETPH, adjusted to pH 7.5, and centrifuged for 10 mins at 20000 r.p.m. in the 40 rotor (Spinco model L). The supernatant was carefully decanted and spun for 1 hour at 35000 r.p.m. in the 40 rotor. The resulting pellet was suspended in half the original volume of STE_1 and spun again as above. This procedure was repeated twice using the sucrose -Tris solution (i.e. excluding EDTA) and the final pellet was suspended in MST. This suspension was again frozen at -20°C in 2ml lots for storage.

Stroma

Aged human blood, preserved with citrate, was supplied by the transfusion service of the Oxford Regional Hospitals Board. Erythrocyte stroma were prepared by the method of Dodge, Mitchell and Hanahan[114] at 4°C. Red cells were spun down in the 6 x 250 head of the Sorvall RC2-B at 3000 r.p.m. for 20 mins. The cells were resuspended in isotonic phosphate buffer pH 7.4 (i.e. phosphate buffer with total ionic concentration 0.31M). After three such washes the cells were resuspended in this buffer and allowed to equilibrate for one hour at 4°C, before being spun down. The washed cells (pale pink by this stage) were rapidly poured into 20 vols of hypotonic phosphate buffer (total ionic conc. 0.02M) pH 7.4,

and stirred. This lysed cell suspension was spun down at 13000 r.p.m. for 45 mins. The resulting stroma were resuspended and spun again. After three such washes the pellet was colourless, and was resuspended to the original cell volume in hypotonic phosphate buffer and stored at $4^{o}C$. For use the membrane was spun down at 15000 r.p.m. and resuspended in the appropriate buffer.

Probe Preparations

MNS (N-methyl 2-anilino-6-naphalene sulphonate) and its derivatives

MNS was prepared by the method of Cory et al[115]. A mixture of 70g of 6-naphthol-2-sulphonic acid, 130g of sodium metabisulphite, 300ml of N-methyl aniline and 1l of water was refluxed for 48 hrs. This gradually turned yellow → orange → dark brown. The organic layer and solids (filtered from the aqueous layer while still hot) were cooled and washed with chloroform. Very little product appeared at this stage (see below), and had to be precipitated by excess 2N NaOH. This crude salt was recrystallised from dilute NaOH. The product had uv and nmr spectra which agreed with those published.

It was found (D.J. Birkett, personal communication) that a much better yield was obtained if it was assumed that the authors had used sodium methabisulphite (and not sodium sulphite as reported), and the full 250g was used. In this

case the product precipitated at the chloroform wash stage. It had the same uv and nmr spectra as above.

The sulphonyl chloride of MNS was also prepared by the method of Cory et al. 2 g of MNS were suspended in 10mls of pyridine. 1ml $POCl_3$ was added, and the mixture turned yellow. After refluxing for $1\frac{1}{2}$ hours the dark orange mixture was evaporated to dryness in vacuo, and the residue was extracted with acetone. It proved impossible to recrystallise the product from acetone-water mixtures, so it was extracted into chloroform, and obtained as an amorphous yellow solid by evaporation. For some labelling experiments the MNS-Cl was adsorbed onto celite[116]. MNS-Cl in $CHCl_3$ was mixed with ten times its weight of celite and the mixture was evaporated to dryness in vacuo.

Three sulphonamide derivatives were prepared by reacting equimolar quantities of MNS-Cl and the amine (ammonia, $C_2H_5NH_2$, $C_{10}H_{21}NH_2$) in chloroform/acetone solution. The resulting solutions were shaken with HCl to remove the excess amine, washed with water then dried on $MgSO_4$ and evaporated to dryness. The residue was dissolved in 80%aq. ETOH and stored. Concentrations were estimated from the published extinction coefficients of MNS and MNS-NH_2[115].

Labelling of GDH with MNS

Conventional methods of labelling GDH with MNS-Cl by adding

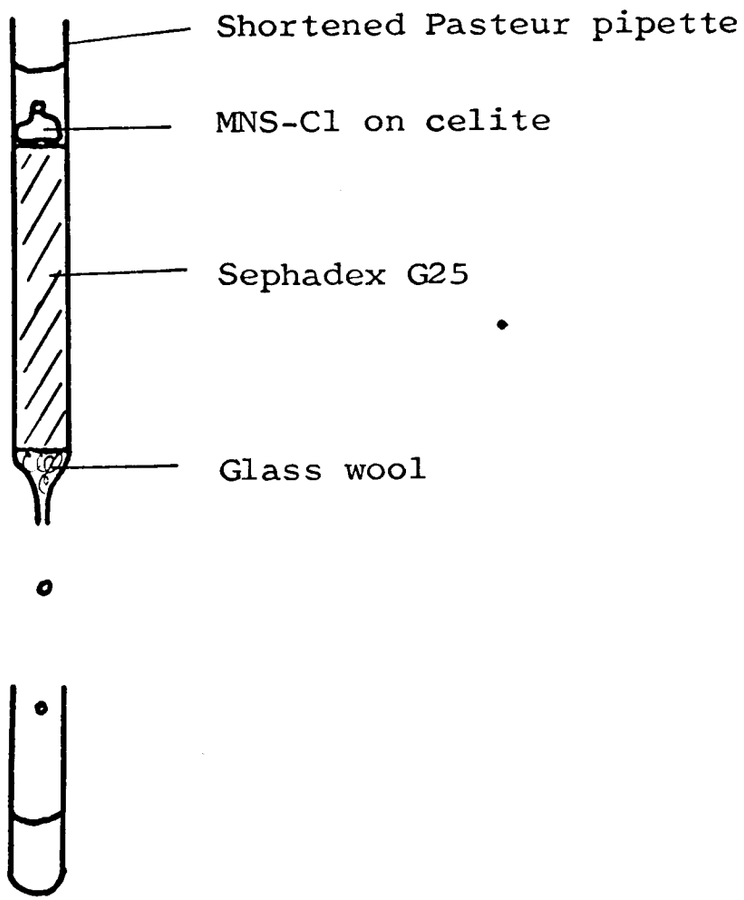

Fig.4a. Rapid pass apparatus.

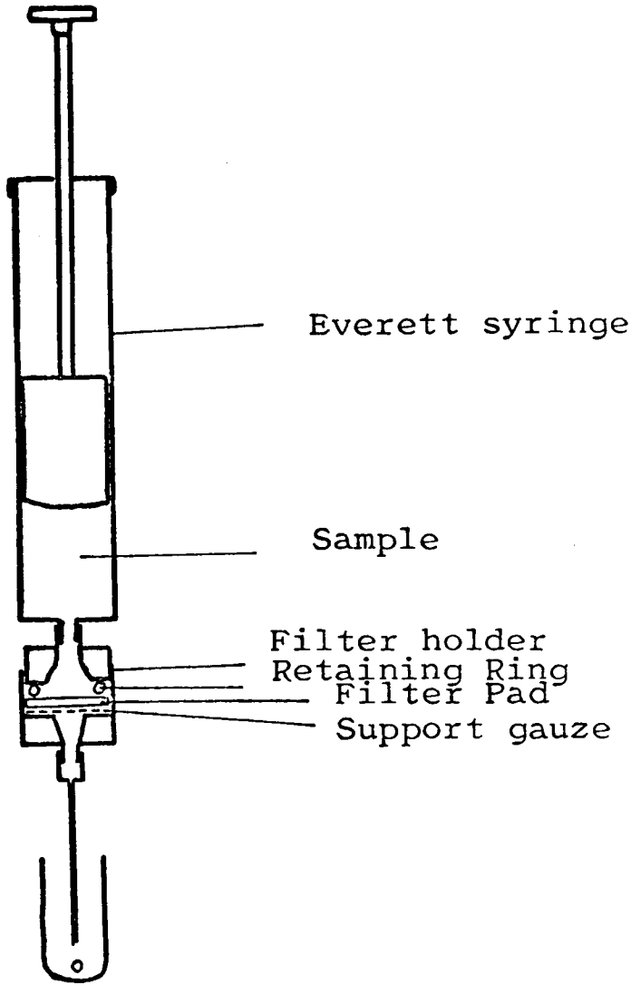

Fig.4b. Filtration apparatus

MNS-Cl dissolved in an organic solvent (e.g. ethanol, acetone) produced rapid denaturation of the protein, even at 0°C. Even Rinderknecht's method[116a] using MNS-Cl adsorbed on celite (normally a mild, rapid labelling technique) failed to give a viable labelled product. This problem was to some extent overcome by designing a system for bringing the protein into contact with the MNS-Cl for a very short time only. A small amount of MNS-Cl on celite (wrapped in cheesecloth for easy removal) was supported on a bed of coarse G-25 Sephadex (equilibrated with phosphate buffer) in a slightly shortened Pasteur pipette (Fig.4a). A concentrated solution of GDH (1-4 mg/ml) was passed rapidly through this column and washed through with buffer. Any MNS-Cl washed through the cheesecloth, and some of the free MNS produced by hydrolysis of MNS-Cl were retained on the Sephadex. The crude solution of labelled GDH was then passed down a longer column of G-25 Sephadex and the protein fraction was collected. Much later a fraction containing free MNS appeared. If necessary the protein solution was concentrated by stirring with dry Sephadex. The extent of labelling was determined by measuring optical densities at 280nm and 320nm, and using the known extinction coefficients.

$$O.D._{280} = GDH \times 0.3 + MNS \times 0.0105$$

$$O.D._{320} = GDH \times 0.02 + MNS \times 0.018$$

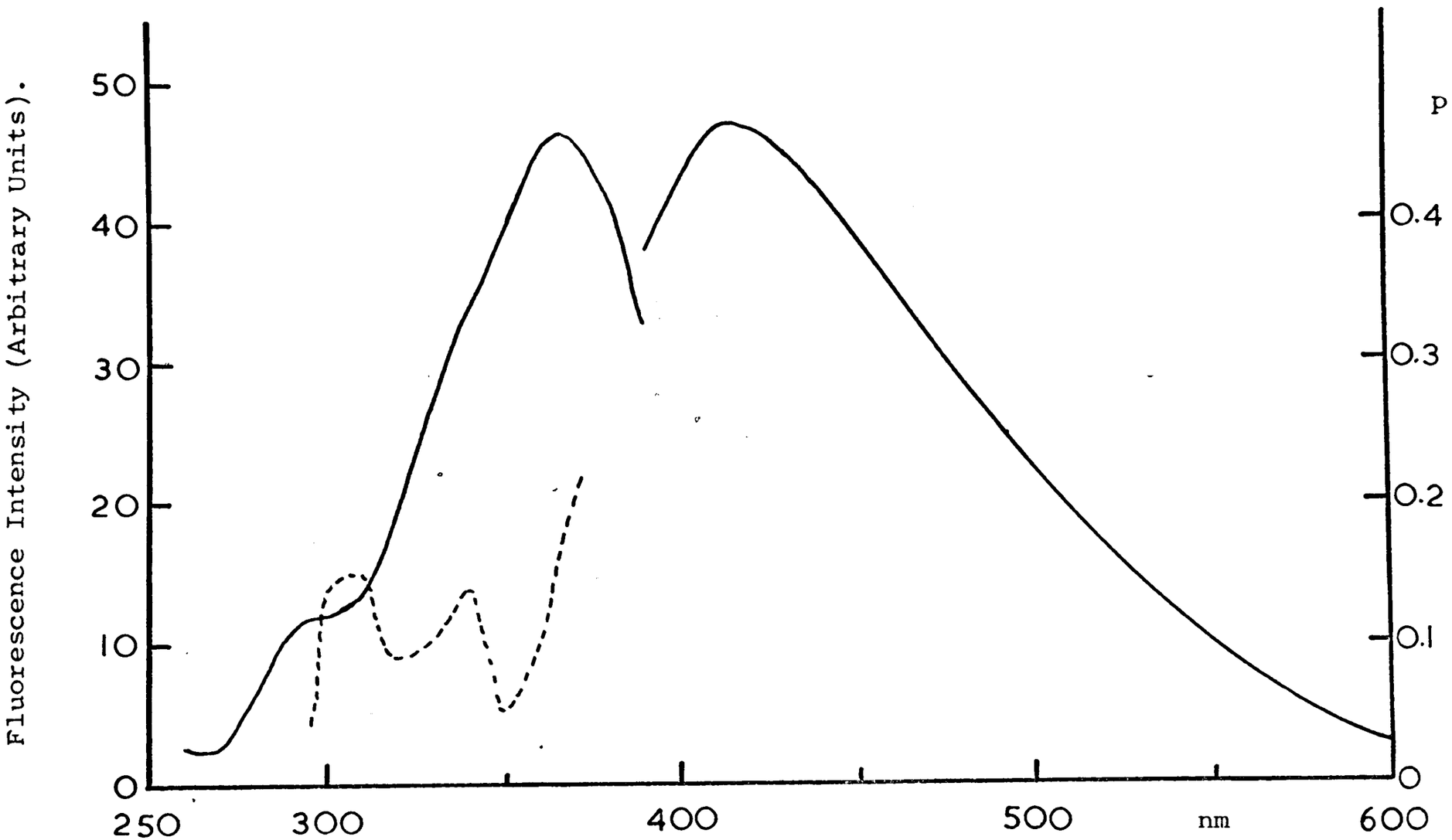

Fig.5. Fluorescence spectra of MNS-GDH. Excited at 350 nm. Emission at 450 nm.

Only one attempt at labelling GDH with MNS, using this rapid pass technique, was at all successful. It was necessary to include 0.1M NaCl in the buffer, and this produced GDH labelled with one MNS group per oligomer. The fluorescence and polarisation of fluorescence spectra of this sample are shown in fig.5. The bound MNS did not respond to the structural transition, nor was the MNS-GDH very active (ca 10%). It seems likely that MNS-Cl rapidly attacks groups which are important in maintaining the quaternary structure of GDH, leading to precipitation of most of the protein. The remaining protein then has MNS attached (by slow reaction) to some other groups.

Acridine derivatives.*

	X=
ABA	$-AsO_3^{2-}$
ABC	$-COO^-$
ABS	$-SO_3^-$

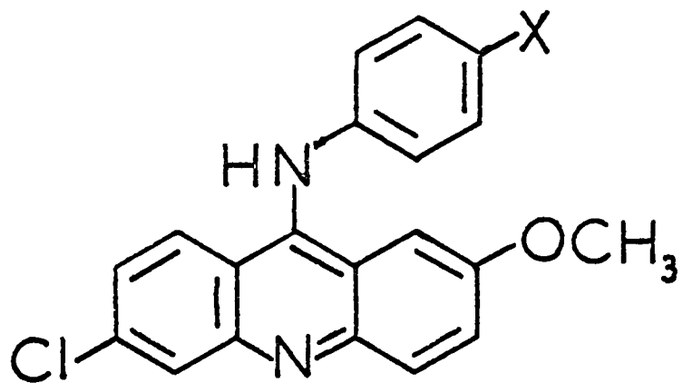

9-anilino acridine derivatives were prepared by the classical method (G. Weber, private communication)[117]. The sodium salts of the p-amino benzene acids were prepared by crystallisation from 5N NaOH. The acridine derivatives were prepared by heating 5g of the amino acid salt, 3g of 6,9-dichloro-2-methoxyacridine and 20g of phenol for two hours

*I am grateful to Mr. R.G. Bolton for much helpful advice on the preparations.

at 140°C. The resulting thick orange-red mixture was poured into 250mls of ether (cooled in ice) with vigorous stirring. The yellow precipitate was filtered off, washed with more ether and recrystallised from dil. NaOH. The arsonate proved very difficult to crystallise, and paper chromatography (pyridine 20 : butanol 40 : water 40) showed that it was very impure. The impurity appeared to be the 2-methoxy-6-chloro-acridone, - a likely byproduct caused by the hydrolysis of the intermediate 2-methoxy-6-chloro-9-phenoxyacridine. A sample of the acridone was prepared by hydrolysing 2-methoxy 6,9-dichloroacridine for 2 hours in N HCl. Chromatographically this behaved in the same way as the impurity. The preparation of ABA was repeated under various conditions, the best results being obtained by heating for $1\frac{1}{2}$ hours at 160°C. Even so a lot of the acridone was present. This was removed by precipitating the Mg salt of ABA by addition of $MgCl_2$. The Mg^{++} was removed from this by treatment with Na_2CO_3. The sodium salt of ABA was then crystallised from aqueous solution. The nmr spectra of these compounds were compatible with the expected structures.§

In order to determine the water content of these samples (water was present even after extensive drying) their nmr spectra were run in dry DMSO d_6. The solutions were prepared in a crude dry box consisting of a polythene bag containing

§ I am indebted to Mrs. E. Richards for running and interpreting the 100 Hz spectra. Dr. R.A. Dwek kindly instructed me in the use of the Perkin Elmer R12 nuclear magnetic resonance spectrometer.

silica gel inflated with a stream of nitrogen from a cylinder. Integration of the water peak (τ = 6.7) allowed a reasonable estimate of the number of moles of water present per mole of acridine.

NBD-Cl (7-chloro-4-nitrobenzo-2-oxa-1,3-diazole).

This was kindly donated by N.C. Price who synthesised it by the method of Boulton, Ghosh & Katritzky[118].

Dansyl amino acids

DNS-Glu, MNS-Met, DNS-isp, and DNS-NH_2 were synthesised by the method of Gray[119]. The amino acid (or ammonia for DNS-NH_2) was dissolved or suspended in 25 mls of 0.5M sodium bicarbonate to a concentration of 10mM. A 10mM solution of DNS-Cl in acetone was added to give a very slight excess ($\sim$ 2μM) of DNS-Cl. This mixture was shaken occasionally for 6-8 hours during which time the deep yellow colour of DNS-Cl turned to a very pale yellow. The mixture was carefully acidified (pH 3) with 50% glacial acetic acid and purified on Dowex 50[120]. Dowex 50, prewashed with 2N HCl followed by distilled water, was packed into a darkened column. The reaction mixture was added, and eluted first with 0.01M acetic acid. This removed the free sulphonic acid (DNS-OH). When the eluent was no longer fluorescent (λ_{max} $\sim$400-450nm) the column was washed free of acetate, and then eluted with 1M ammonia in 25% aqueous acetone. The dansyl amino acid

(intense yellow) fraction was readily identified, and was evaporated to dryness on a rotary evaporator. The residue was dissolved in 50% aqueous ethanol, and stored as this solution as it proved very difficult to recrystallise. Its concentration was estimated spectrophotometrically (ε_{330} = $4.3 \times 10^3 1.M^{-1} cm^{-1}$)[121].

DNS-2,4-diamino-n-butyric acid (DNS-γbut) was prepared by the method of Parker et al.[58] for ε-DNS-lysine. A mixture of 0.294 g of the amino acid and 1g cupric carbonate (precipitated by adding sodium carbonate to a cupric sulphate solution) was refluxed in 40mls of water for 1 hour. The resulting blue-black mixture was filtered to give a royal blue solution - the copper chelate complex of the α-amino acid. After cooling, 0.1g of sodium bicarbonate was added, followed by 0.75g of DNS-Cl in 27mls of acetone. The resulting muddy green solution gradually cleared to give a yellow precipitate in a pale green solution. The precipitate was filtered off, washed well with water, then ethanol, then ether (which removed XS DNS-Cl). It was then mixed with 3g of EDTA (disodium salt) and 15mls of water, and the pH adjusted to around 10 with 2N NaOH. When the precipitate had dissolved, 2N HCl was added to take the pH to 6. The resulting dark green solution slowly turned cloudy, and the slight precipitate was removed by centrifugation. This turned out to be the product. A much better yield was

obtained by crystallising out and filtering off the EDTA, and putting the filtrate onto a Dowex column. By careful washing and elution as above, it was possible to remove the DNS-γ-but while leaving the copper stuck to the resin.

The purity of all the dansyl amino acids (commercial and home-made) was checked by thin layer chromatography*. The plates were made from a slurry of 30g Silica Gel G with 65mls of 0.5% starch solution, which was degassed and then applied to the plates on a Shandon Unoplan Leveller (kindly loaned by Dr. J.M. Wilkinson). The plates were allowed to set for 30 mins, then dried at 110°C for 30 mins, and stored. Immediately prior to use, they were again dried in the oven, and a narrow strip ($\frac{1}{8}$") of gel was removed from each vertical edge to minimise edge effects. Solvent A[122] (benzene:pyridine: acetic acid, 80:20:2) produced little separation from impurities, so solvent E[123] (880 ammonia:isopropanol:methyl acetate, 20:35:4) was used. All the samples were pure except commercial DNS-Glu and DNS-Met. (Appendix 1, R_f values).

Methyl cellulose solutions were made up by suspending 2.25g of methyl cellulose in 100ml of hot water (60-70°). At this temperature, with constant stirring, a homogeneous bubble-free suspension was obtained. The fluorescent material was then dissolved by careful stirring.

*I am indebted to Miss Nancy Hogg for much helpful instruction and advice on the various chromatographic techniques used.

Instruments

An E.I.L. Model 23A direct reading pH meter (standardised with buffer tablets supplied by E.I.L.) was used for all pH measurements. Absorption spectra were recorded on a Cary 14 M-50 recording spectrophotometer, thermostatted at 25°C. Optical density measurements were made on a Unicam SP500 Mark II spectrophotometer, and kinetic experiments following absorption at a fixed wavelength were done on a Hilger and Watts spectrophotometer fitted with a Hilger-Gilford kinetic attachment.

Most fluorescence measurements were made on a commercial instrument or on a more sensitive instrument built in this laboratory[44]. The commercial instrument was a Zeiss PM QII spectrofluorimeter equipped with a 500 watt xenon lamp, and prism monochromators. Emission was detected at 90° to the exciting light through the bottom of a 1cm cuvette in a thermostatted (25°C) cell compartment. The xenon lamp intensity tended to fluctuate, and account was taken of this by routinely measuring the fluorescence of the sample relative to that of a fluorescent perspex block. The fluorescence was then standardised to a block reading of 600 on the most sensitive setting of the instrument. Polarisation of fluorescence measurements were made on the Zeiss by inclusion of 12mm Foucault prisms in the excitation and emission light paths. Each prism could be rotated through 90°. The polarisation

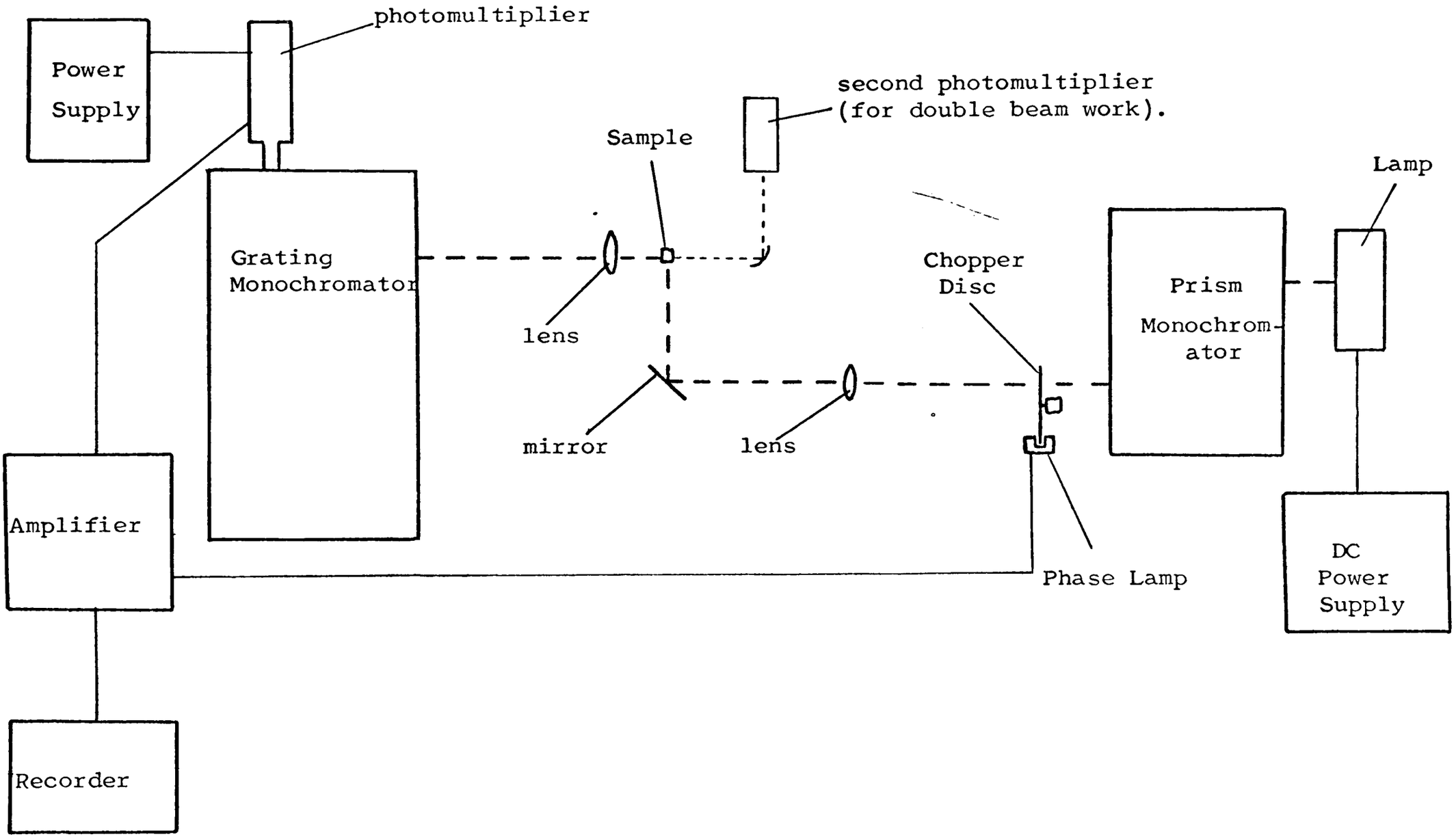

Fig.6. Block diagram of the home built fluorimeter.

was measured as:-

$$p = \frac{V_v - tH_v}{V_v + tH_v} \qquad \text{where } t = \frac{V_h}{H_h}$$ and the capitals denote the plane of polarisation of the exciting light while the subscripts denote the plane of polarisation of the emitted light. The polarisers were standardised using an FMN in glycerol solution (p = 0.45).

The more sensitive instrument was based on one built by C.A. Parker[124]. (Fig.6.) The light source was a 250 watt xenon lamp with a Bellingham and Stanley stabilised D.C. power supply, or a 24V 150W quartz halogen projector lamp with a Coutant Electronics power supply. The exciting light was passed through a Hilger and Watts prism monochromator, then a chopper disc, and focussed by a series of lenses and mirrors onto the sample. The emitted light was collected at 90^{o} by a Bausch and Lomb grating monochromator fitted with a thirteen stage (EMI 988B) photomultiplier. A phase sensitive amplifier (E.M. Wareham Type C366) was used, the phase being determined by a small reference lamp/photodetector on the chopper disc. The latter had 16 slots and was driven by an Evershed-Vignoles synchronised motor at 50cps (i.e. chopping the light beam at 800cps.) Readings were plotted out on a Servoscribe recorder (RE 511.20).

For measuring fluorescence intensities at two wavelengths simultaneously (e.g. with PS in SMP) the basic instrument was adapted slightly. It was possible to observe fluorescence on both sides of the cell, and so light from the second side was focussed by a concave mirror onto a photomultiplier guarded by a 400nm filter. This was connected to a second phase-sensitive amplifier and recorder, the second amplifier being driven by the main one. Fluorescence at other wavelengths was followed on the normal emission monochromator.

Fluorescence spectra of very concentrated solutions of PS were obtained using a thin film cell. This was made from two sides of a broken quartz cuvette, kept apart by two pieces of microscope cover-slip. This gave a film thickness of 0.3mm and cell capacity of 50λ. The cell was placed in the light beam at an angle of 25^{o} to the incident light beam to avoid reflecting the incident light into the emission monochromator. In this way spectra of concentrated solutions were obtained undistorted by self-absorption effects.

Some fluorescence spectra were recorded on a Hitachi-Perkin Elmer compensated recording spectrofluorimeter (MPF2A). All fluorescence spectra are uncorrected for wavelength variation of lamp intensity etc.

Fluorescence lifetimes were determined on a TRW 75A

decaytime fluorimeter. This used a TRW 31A nanosecond spectral source with a nitrogen lamp (operating at 5kcps - pulse duration ~20nsec.), and was linked to a Tektronix Type 556 dual beam oscilloscope with a Type 1S1 sampling attachment. The lamp shape was determined using a scattering sample (a ludol suspension). The signal was fed to the sampling beam of the oscilloscope. The main beams of the 'scope carried the computer simulated traces which were then fitted to the lampshape trace. The sample decay curve was then displayed (sampling beam), and the computer simulated decay trace was fitted to it, - the amount of adjustment from the lampshape being read out as the fluorescence lifetime. Oscilloscope traces were photographed using a Telford Model A oscilloscope polaroid camera. If necessary the decay trace could be fed out to a Servoscribe recorder. The excitation and emission wavelengths were selected by Corning filters e.g. for ANS

7-60 giving a 350nm peak for excitation

3-72 cut-off below 440nm for emission.

Oxygen Electrode

Oxygen uptake experiments were performed using an oxygen electrode[125]. This consisted of a platinum electrode protected by a polythene membrane, and incorporated a silver/silver chloride electrode for reference. This was coupled to a polarograph (Radiometer PO 4b) which applied a steady potential

of -0.6v across the electrode, and could record currents in the μamp range. The current under the experimental conditions was directly proportional to oxygen concentration. Measurements were performed in a darkened, thermostatted cell. This was filled with buffer, and the electrode was inserted carefully so as to expel excess buffer and exclude all air. Submitochondrial particles, substrates etc., were then added from a disposable syringe via a small slot in the electrode assembly.

Procedures

GDH was dialysed against buffer for 18 hours at 0-4°C, spun in a bench centrifuge to remove denatured protein, and the supernatant used. Its concentration was determined using the published extinction coefficient $\mathcal{E}_{280}^{0.1\%} = 0.97$[126]. All experiments were performed in 0.1M phosphate buffer pH 7.6. NADH and GTP solutions were made up by weight (NADH in Tris since it decomposes in phosphate buffer) and their concentrations were checked spectrophotometrically[44].

Membrane concentration was determined, in triplicate, as protein by the method of Lowry et al[127] using crystalline BSA as standard. Buffer blanks were always run since Tris in the buffer interferes with the determination. All membrane experiments were performed in MST (see above) pH 7.4.

Fluorescence experiments were carried out in the normal

way, due care being taken to allow for scattering by the macromolecule. The necessary amounts of effectors, probes etc. were added in small volumes (e.g. 10λ). When it was necessary to obtain rapid addition and mixing (as in some of the SMP experiments) the small volume to be added was placed on the tip of a glassrod, and added and stirred simultaneously (usual mixing time $\leq$ 1 sec). The binding parameters of probes to macromolecules were determined in two ways:-

a) Conventional fluorescence technique.

A small concentration of probe (e.g. 10 μM) was titrated with macromolecule by starting with a high concentration of macromolecule (plus 10 μM probe) and progressively diluting it with a 10 μM probe solution. The variation of fluorescence with macromolecule concentration was then plotted as a double reciprocal plot to find the limiting enhancement of fluorescence at infinite macromolecule concentration. A constant concentration of macromolecule was then titrated with probe by successive small additions of probe solution (e.g. 10λ). The fractions of probe free and bound could then be calculated for each point on the titration curve.

b) Filtration technique

For probes whose fluorescence is not enhanced on binding it was necessary to find a method for separating the free probe from bound probe and the macromolecule. Centrifugation

is the obvious method, and is useful for proteins and membranes at static equilibrium. However, for systems in dynamic equilibrium (e.g. energised membrane) the method is too slow. A novel filtration method was devised for measuring probe binding to such systems. 2mls of the sample was taken up into an Everett 2ml glass syringe via a disposable needle. The latter was then replaced by a Millipore "Swinny" filter holder (No.XX30 012 00) containing a Whatman GF/B glass fibre filter paper (This was cut to size from a 2.5cm circle using a cork-borer kindly loaned by Dr. R. Cecil). The assembly (Fig.4B) was then inverted and the syringe plunger gently pressed to expel all the air from the filter assembly. It was found that the most reproducible way of doing this was to expel the air plus one drop of liquid. Three drops of the filtrate ($\sim$0.075ml) were then collected in a small test-tube (5 x 1cm). By this stage 0.2ml of liquid had passed through the filter pad - a small enough volume not to affect the equilibrium appreciably.

In order to measure the free probe concentration 0.05ml of the filtrate was diluted with buffer or a 5mg/ml BSA solution (for PS and ANS measurements respectively) and its fluorescence measured relative to a blank. The blank was treated identically except that it had no membrane in it. This was necessary in

order to take into account adsorption of the probe by the filter pad. The concentration of free probe was then:

$$\frac{F_{sample}}{F_{blank}} \times \text{total probe concentration}$$

A protein determination on various samples of filtrate showed that no membrane came through the glass filter if only a small volume (< 0.5ml) of sample was passed through it.

GLUTAMATE

DEHYDROGENASE

CHAPTER 3 GLUTAMATE DEHYDROGENASE

Introduction

L-Glutamate dehydrogenase is a multi-subunit enzyme which undergoes a reversible, concentration dependent aggregation[126]. On denaturation (urea, pH, guanidine) a subunit of M.W. ca 53,000 is obtained[128]. This is a single polypeptide[129] possessing no catalytic activity (regardless of the denaturing conditions[130]). The molecular weight of, and hence the number of subunits in, the active species of the enzyme has been a matter of some controversy. It was once thought[131] that a high M.W. aggregate was the active form, but it was later shown that the specific activity did not vary with enzyme concentration[132]. The low concentration M.W. now accepted is 312,000, corresponding to six subunits of M.W. 52,000[133]. As the enzyme concentration is increased this "oligomer" aggregates to give a linear polymer (at 8mg/ml, M.W.$\sim 2\times10^6$) [133-135]. The hexameric oligomer model is supported by electron microscope studies[136,137].

The enzyme catalyses the oxidative deamination of glutamate using either NAD^+ of $NADP^+$, both of which activate the deamination[138] (neither NADH nor NADPH activates the amination of αKg[139]). This is explained in terms of negative cooperativity between the subunits[138,139]. The enzyme will also catalyse the deamination of several mono-carboxylic amino acids[140]. It is

competitively inhibited by dicarboxylic acids like isophthalic acid, and will not oxidise asparate, which suggests that the substrate binding site contains two positive centres ca 7.5A apart[141].

The activity of the enzyme is affected by a large number of small molecules including steroids and nucleotides[131,142] GTP inhibits and ADP (at pH 7.6-8.0) activates glutamate deamination[131], while the alanine dehydrogenase activity is affected in the opposite sense[143]. GTP tends to disaggregate the enzyme, while ADP prevents the disaggregation[131]. It was these observations that led Frieden to the erroneous conclusion that the polymeric species was the most active. This GTP inhibition was interpreted in terms of two distinct conformations of the oligomer[144], one of which possessed GDH activity and could aggregate, the other having AlaDH activity but which could not aggregate[145].

Binding studies have shown that there is one active site per subunit[63,146] and one GTP site per subunit in the absence of coenzyme[147]. In the presence of coenzyme there is a cooperative interaction between the six GTP sites in the oligomer[147]. This cooperativity in binding has yet to be displayed kinetically (unlike the NAD^+ effect above). GTP enhances the fluorescence of NADH bound to GDH[63,67] by tightening the binding. Glutamate

also enhances the NADH fluorescence[64,65] while αKg quenches it[61]. The glutamate effect is also due to tighter binding - the αKg effect is as yet unexplained.

Further evidence for the allosteric nature of the GTP effect has been obtained from physical measurements. A conformational change has been detected by ORD[63], an immunological technique[148] and particularly by the use of fluorescent probes[149,44]. The fluorescence of ANS is enhanced ca 100 fold on binding to GDH. A further enhancement (ca 2 fold) occurs when the conformational change is brought about by NADH and GTP. Stopped flow measurements[44] show that this second enhancement is biphasic, consisting of a rapid phase ($t_{\frac{1}{2}}$ = 34msec) and a slow phase ($t_{\frac{1}{2}}$ = 240msec). This was interpreted as a rapid change in the structure of the subunits followed by a slower rearrangement of the subunits. This interpretation has been challenged[46] on the basis of unpublished observations that the GTP inhibition of GDH appeared faster than the fastest phase of the structural transition. Desensitisation of GDH by modification of tyrosine lowers the response of ANS to the ligand induced change[47].

This thesis

The NADH/GTP induced conformational change (hereafter referred to as the structural transition) was used to study the characteristics of several probes of different types:-

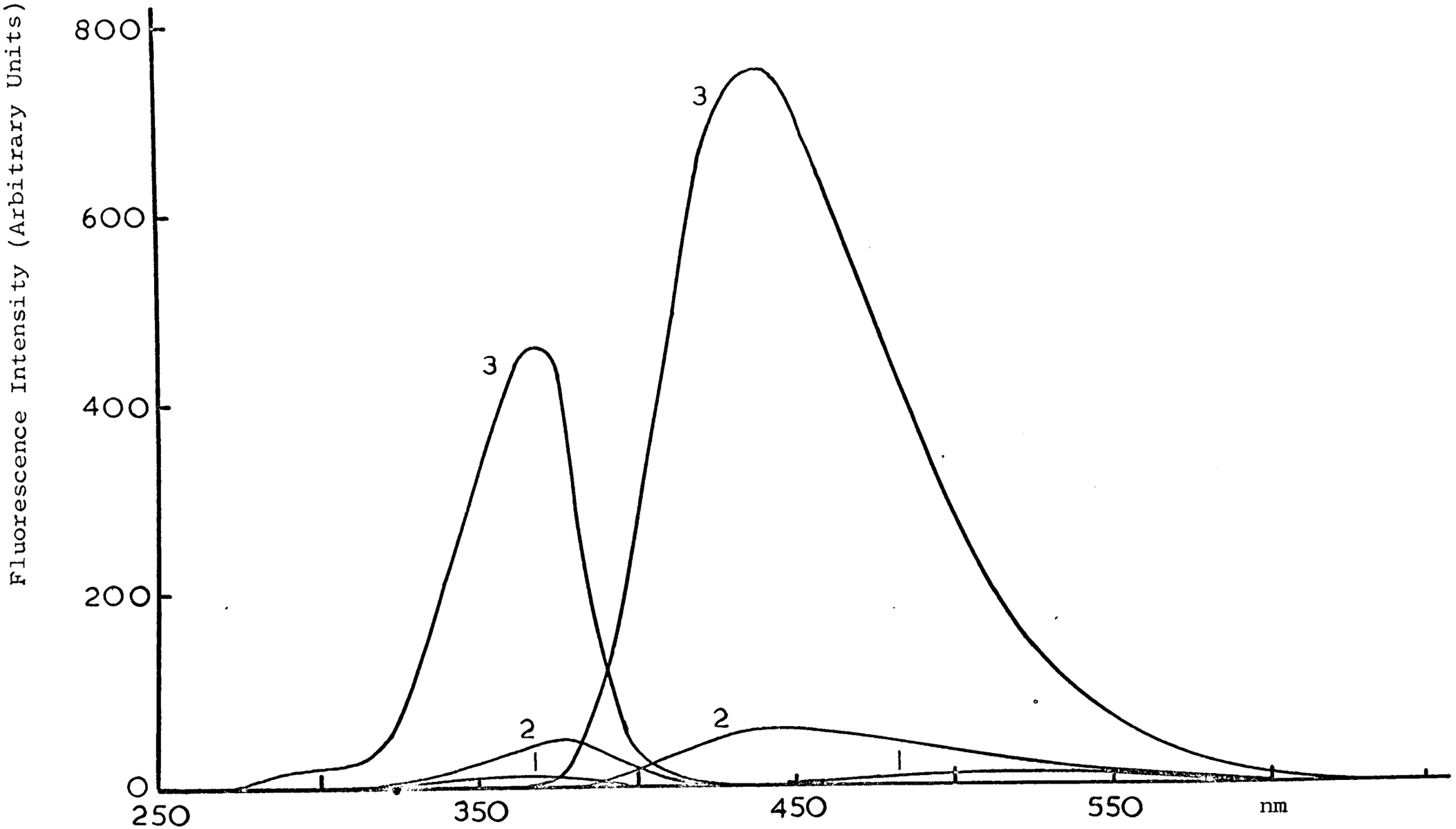

Fig.9. Fluorescence spectra of MNS (20 μM), Excited at 370 nm, Emission at 480 nm.

1. Buffer pH 7.5 2. GDH, 0.5 mg/ml. 3. Ethanol.

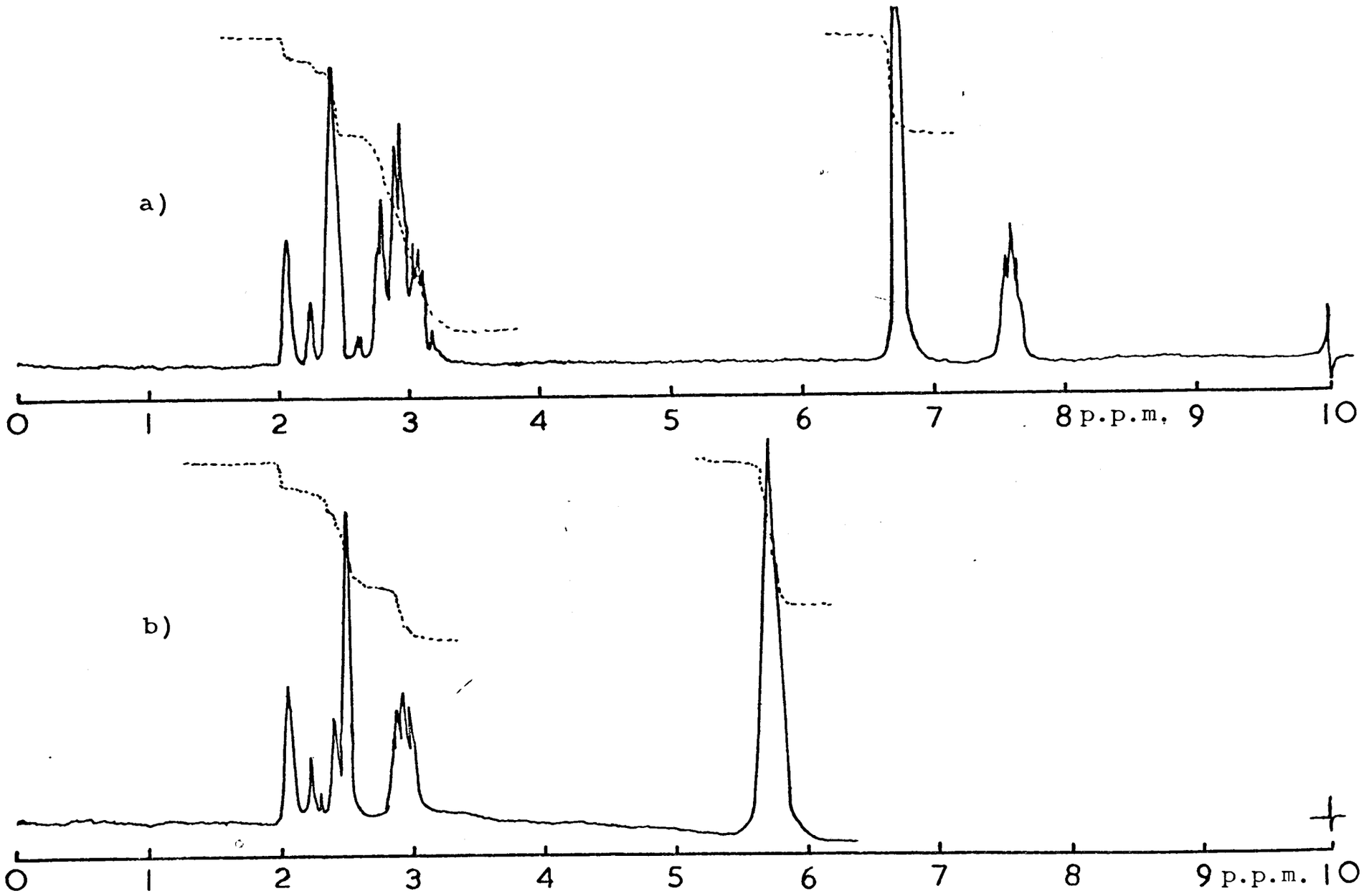

Fig.8. Nmr spectra of a) MNS in DMSO d_6 b) 2-naphthol-6-sulphonic acid in DMSO.

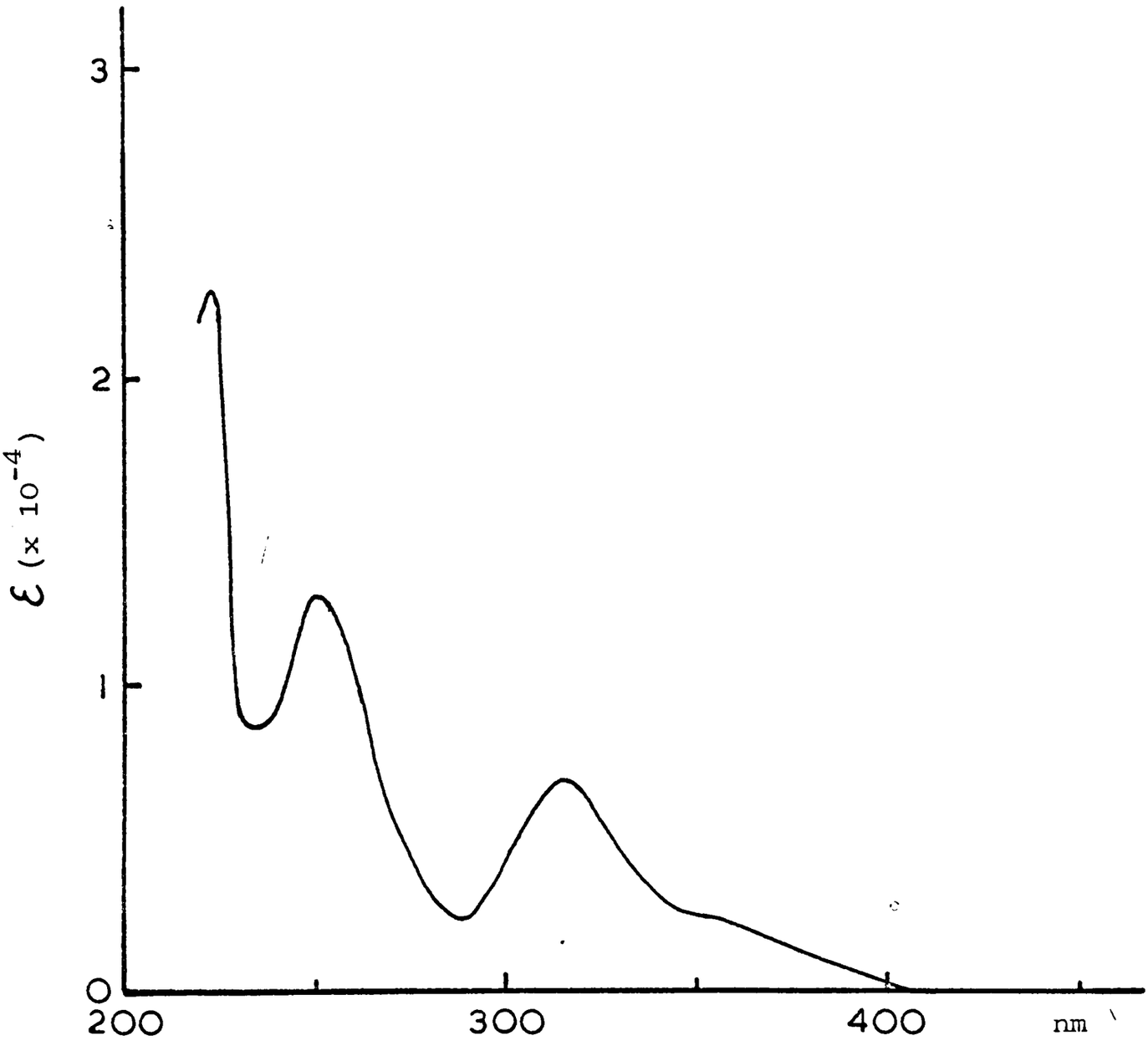

Fig.7. Absorption spectrum of MNS in buffer (pH 7.5).

(i) MNS and derivatives. MNS-Cl was synthesised to provide a covalent version of ANS in order to study the response of a covalently bound probe to the structural transition. Three sulphonamides of MNS were prepared to see how replacement of the negative charge of MNS by a polar or non-polar neutral group altered its ability to act as a probe.

(ii) Dansyl amino acids. An environmentally sensitive fluorescent label of the ANS type was attached to various amino acids in an attempt to see what specificity if any the amino acid conferred on the fluorophore.

(iii) NADH fluorescence. This was studied as an intrinsic property of the system. The effect of various amino acids could be tested without perturbing the system with bulky extrinsic molecules (such as ANS,MNS).

Results

(i) MNS

MNS was synthesised as described in the experimental section (p.27). Its absorption and nmr spectra (figs.7,8) agreed with the data published by Cori et al[115]. The fluorescence spectra (fig.9) were quite similar to those of ANS, except that MNS underwent a much larger blue shift on being transferred from water to ethanol (540nm to 440nm, instead of 550nm to 480nm). In water/ethanol mixtures there

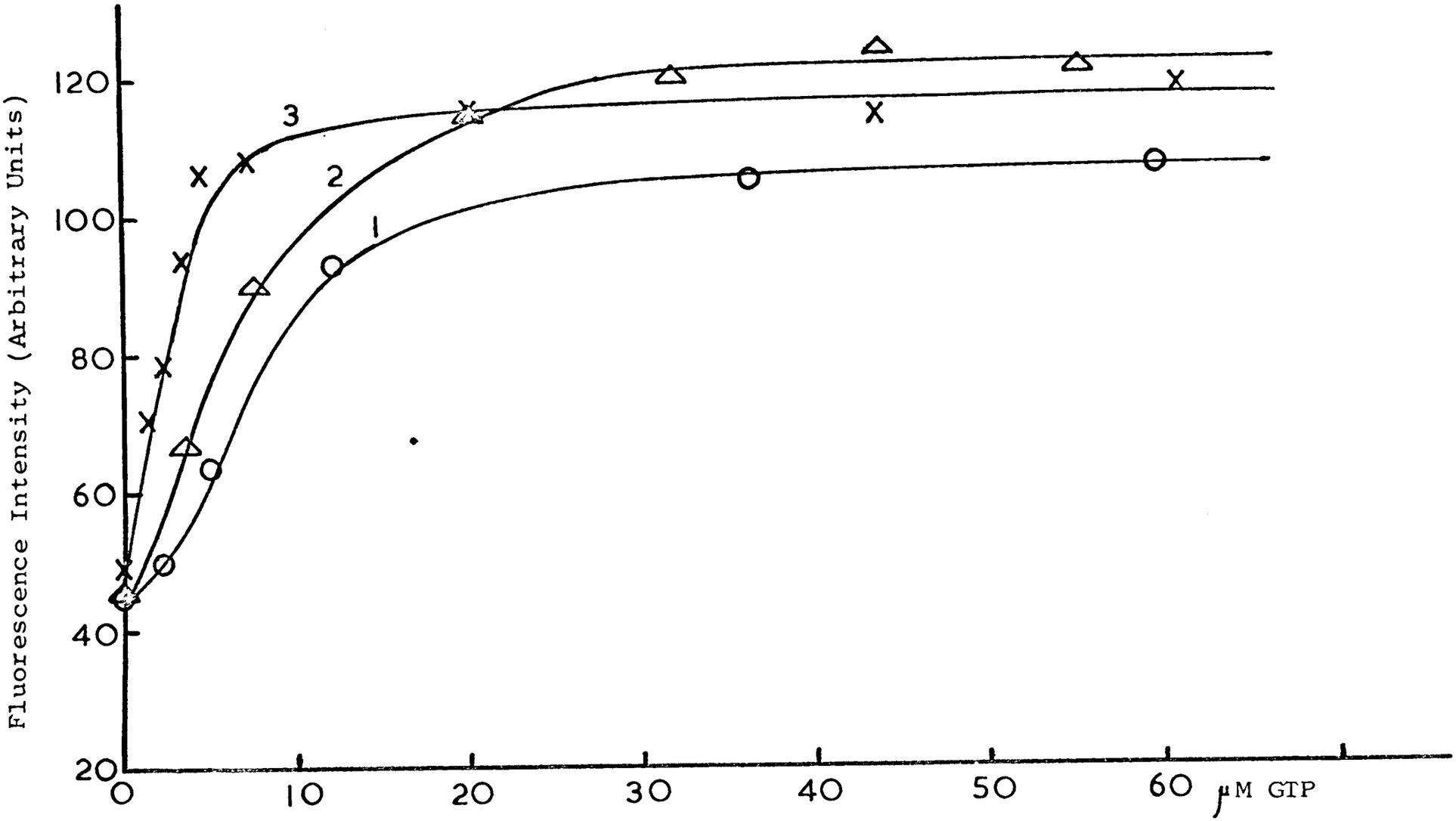

Fig.14. Effect of αKg on the conformational change of GDH.

MNS 60 μM (excited at 365nm, emission at 450nm)

GDH 1 mg/ml, NADH 100 μM. αKg concentrations:-

1. 6 μM; 2. 60 μM; 3. 600 μM.

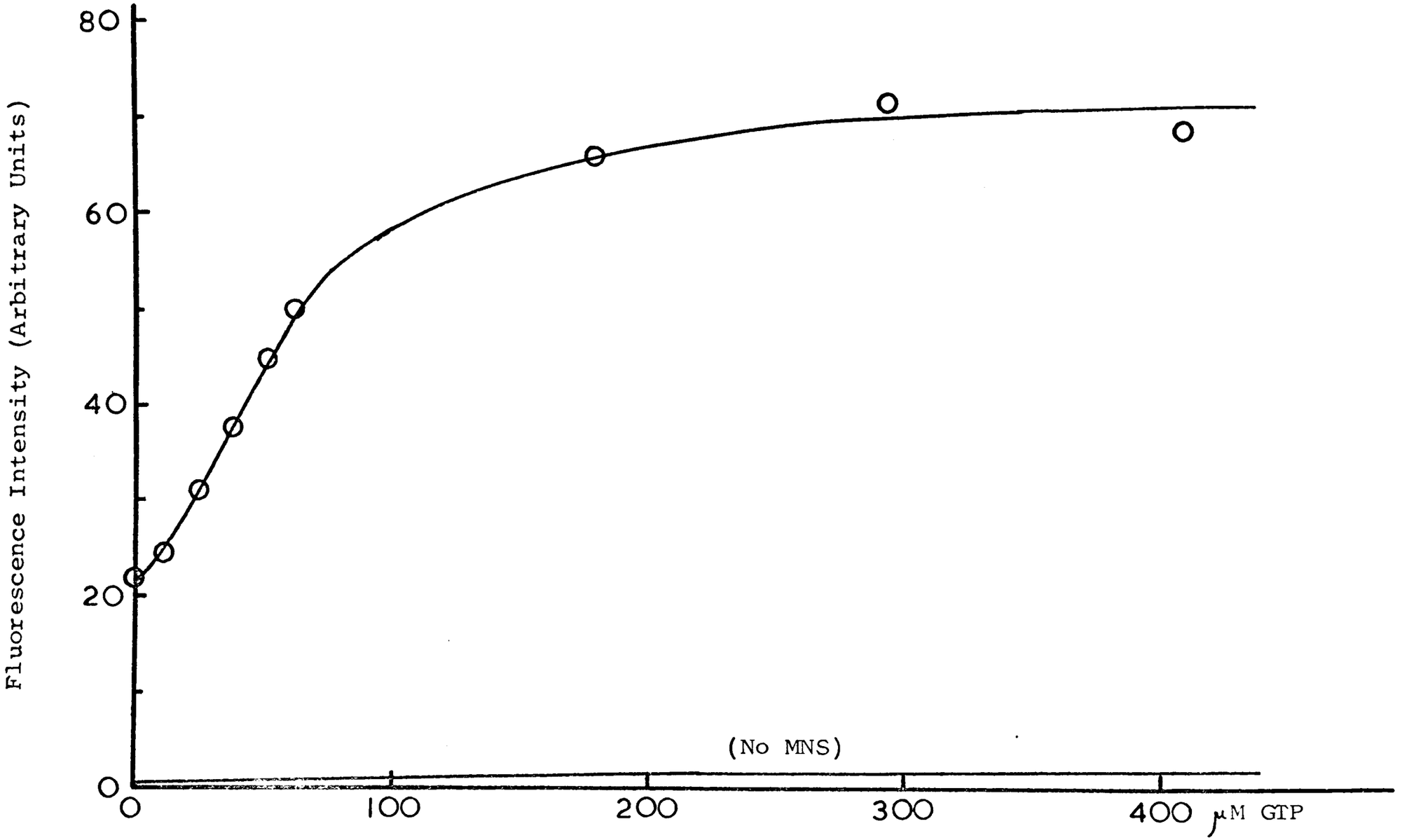

Fig.13. The conformational change of GDH detected by MNS.
MNS 60 μM (excited at 380 nm, emission at 450 nm)
NADH 60 μM, GDH 1 mg/ml.

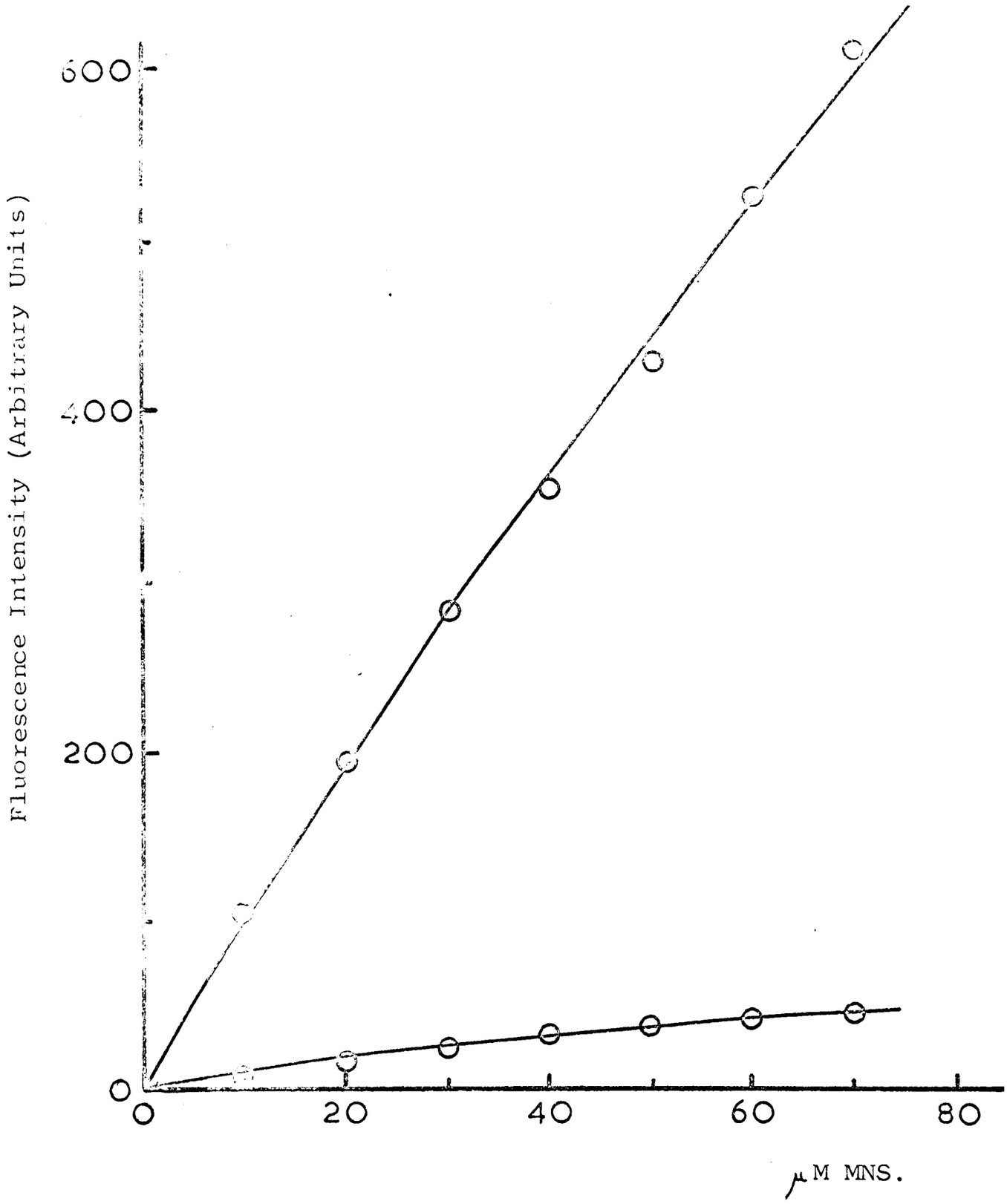

Fig.12. GDH (1 mg/ml) titrated with MNS.

Excitation at 380 nm. Emission at 450 nm.

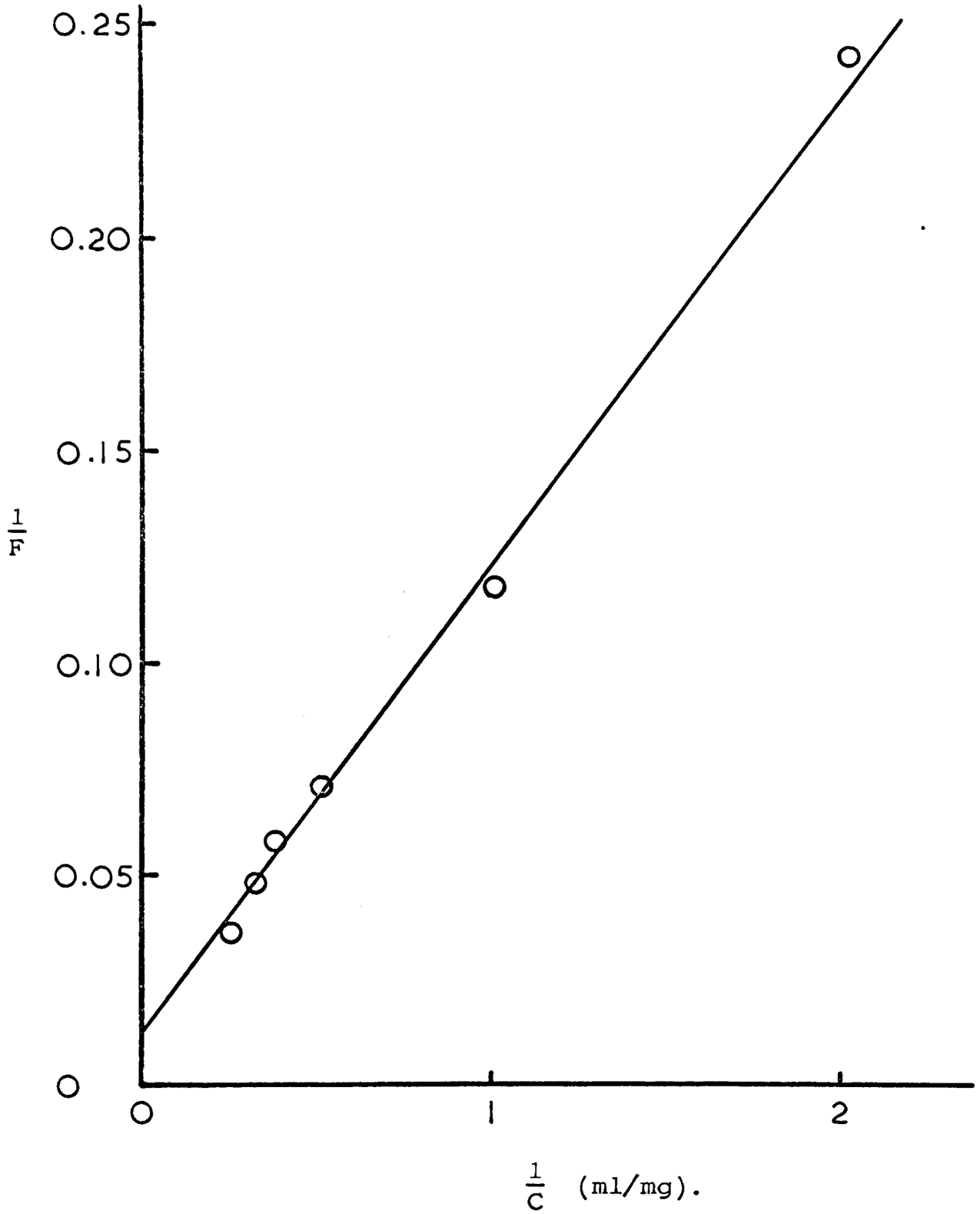

Fig.11. Double reciprocal plot of MNS (10 μM) binding to GDH.

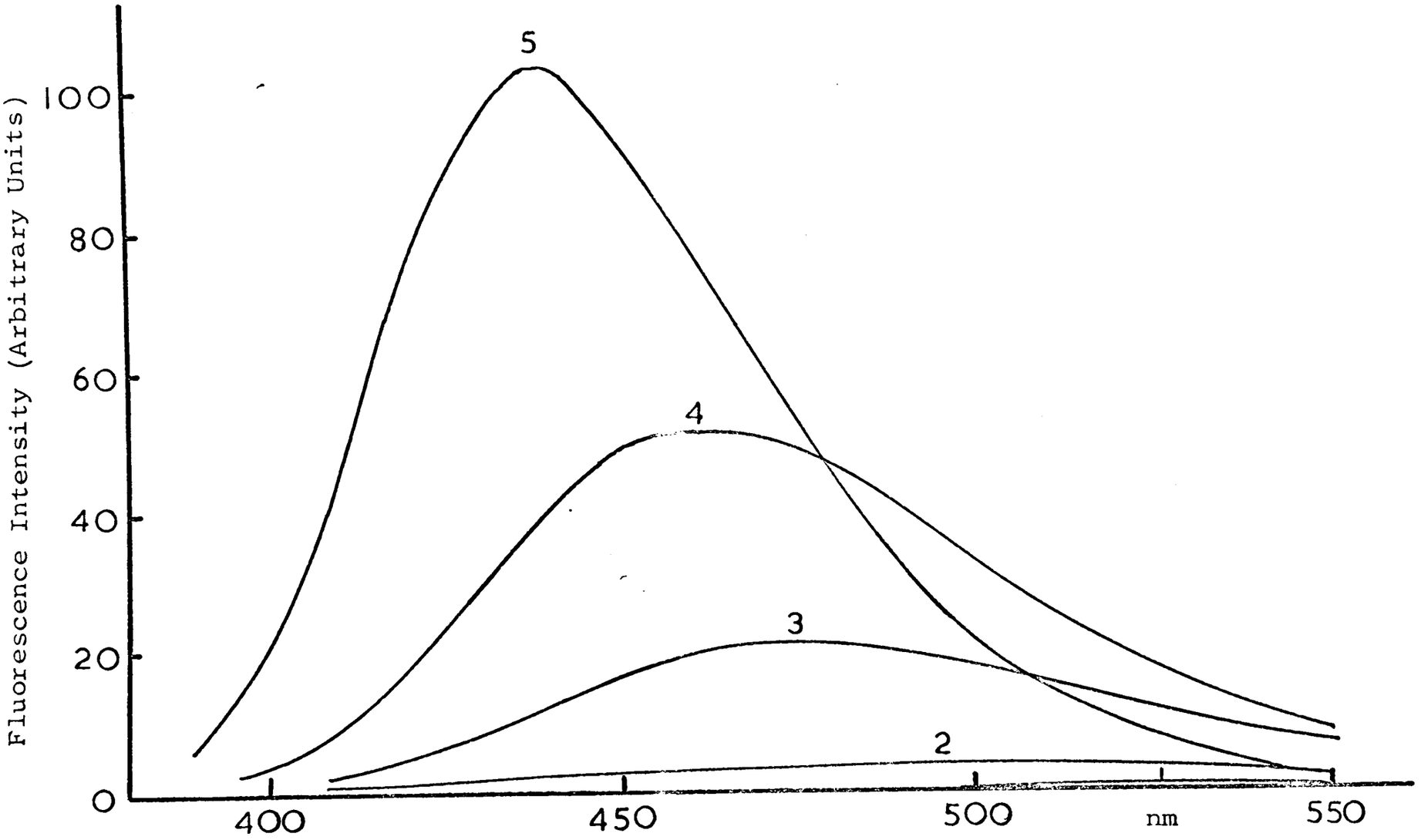

Fig.10. Fluorescence emission spectra of MNS (10 μM) in water/ethanol mixtures. Excited at 370 nm. Bandwidths 7 nm for emission and excitation.

1. H_2O; 2. 25% EtOH; 3. 50% EtOH; 4. 75% EtOH; 5. EtOH.

was the characteristic increase in intensity and shift in emission maximum with increasing ethanol concentration (fig.10). In the presence of GDH (1mg/ml), MNS (20 μM) fluorescence was enhanced ca 6 fold and shifted 100nm to the blue i.e. the same shift as in ethanol but a much smaller enhancement. The small enhancement as compared with ethanol is due to the fact that only a small amount of the MNS is bound at this relatively low probe:protein ratio. The enhancement of fully bound MNS was found from a double reciprocal plot (fig.11), obtained by titrating a low concentration of MNS with GDH. This value (96) was very nearly the same as that caused by ethanol. Unlike ANS, it was impossible even to approach the saturation of the enzyme by MNS (fig.12), and so no binding data could be obtained.

Attempts to use MNS as a probe for the structural transition of GDH failed at first because the blue shifted MNS fluorescence coincided with the NADH emission band. However, by making use of the fact that αKg quenches the fluorescence of bound NADH (see below) it was possible to reduce the NADH fluorescence to a low, constant background signal. MNS gave a three fold enhancement of fluorescence on titration with GTP (fig.13). By varying the αKg concentration it was possible to alter the shape of the titration curve (fig.14). Analysis of these changes showed that increasing the αKg

Table 4

	Lifetimes (nsec)			
	ANS		MNS	
GDH	5.6		6	10
GDH + NADH + αKG	5.4		6	10
do. + GTP	5.4	7.5	8	14
do. + GTP	5.4	8.1	6	18
do. + GTP	5.4	8.8	6	16.5
do. + GTP	5.4	9.6	7	19
do. + GTP		10.5	7	19

Each addition of GTP was a concentration increment of 10 μM.

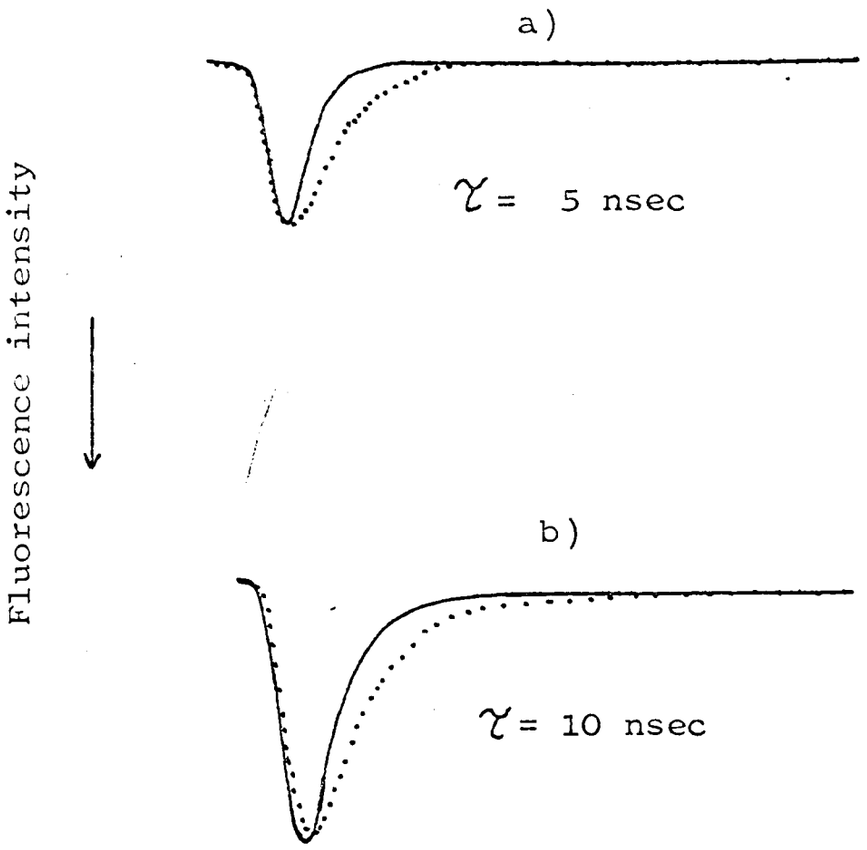

Fig.15. Fluorescence decay curves of ANS in the presence of a) GDH (1 mg/ml), b) GDH, (1 mg/ml). NADH (100 μM), αKg (100 μM) and GTP (100 μM).

Table 3

α Kg concentration(μM)	MNS $S_{0.5}$(μM)	ANS $S_{0.5}$(μM)
0	(50)	8
6	7.5	9.6
60	5.75	5.6
600	3.0	3.4
6000		3.6

concentration lowered the concentration at which GTP effected the structural transition (as shown by $S_{0.5}$, Table 3). In contrast, increasing concentrations of L-glu had no effect on the structural transition detected by ANS.

The enhancement of ANS and MNS fluorescence caused by the structural transition could be due to an increase in binding and/or to an increase in quantum yield. Because of the difficulty in obtaining reliable binding data, a possible change in quantum yield was investigated by measuring fluorescence lifetimes of the probes at various points in an NADH/GTP titration of GDH. The life-time of ANS (and MNS) in buffer was too short to be measured (i.e. < 1 nsec) but increased to 5.6 nsec on addition of 1mg/ml GDH. Addition of NADH and αKg lowered this slightly to 5.4 nsec (αKg had to be used to quench bound NADH with both MNS and ANS since the filters used would not entirely exclude NADH fluorescence). Successive additions of GTP produced decay curves which could not be fitted to a single exponential, but corresponded approximately to two:- one giving a constant life-time of 5.4 nsec, the other giving an increasing life-time (Table 4). In the presence of excess GTP, a single long life-time (10.5 nsec) was obtained (fig.15). This indicates that the ANS life-time doubles during the GTP titration. With MNS there was a three fold increase in life-time though in this case there was a multiple

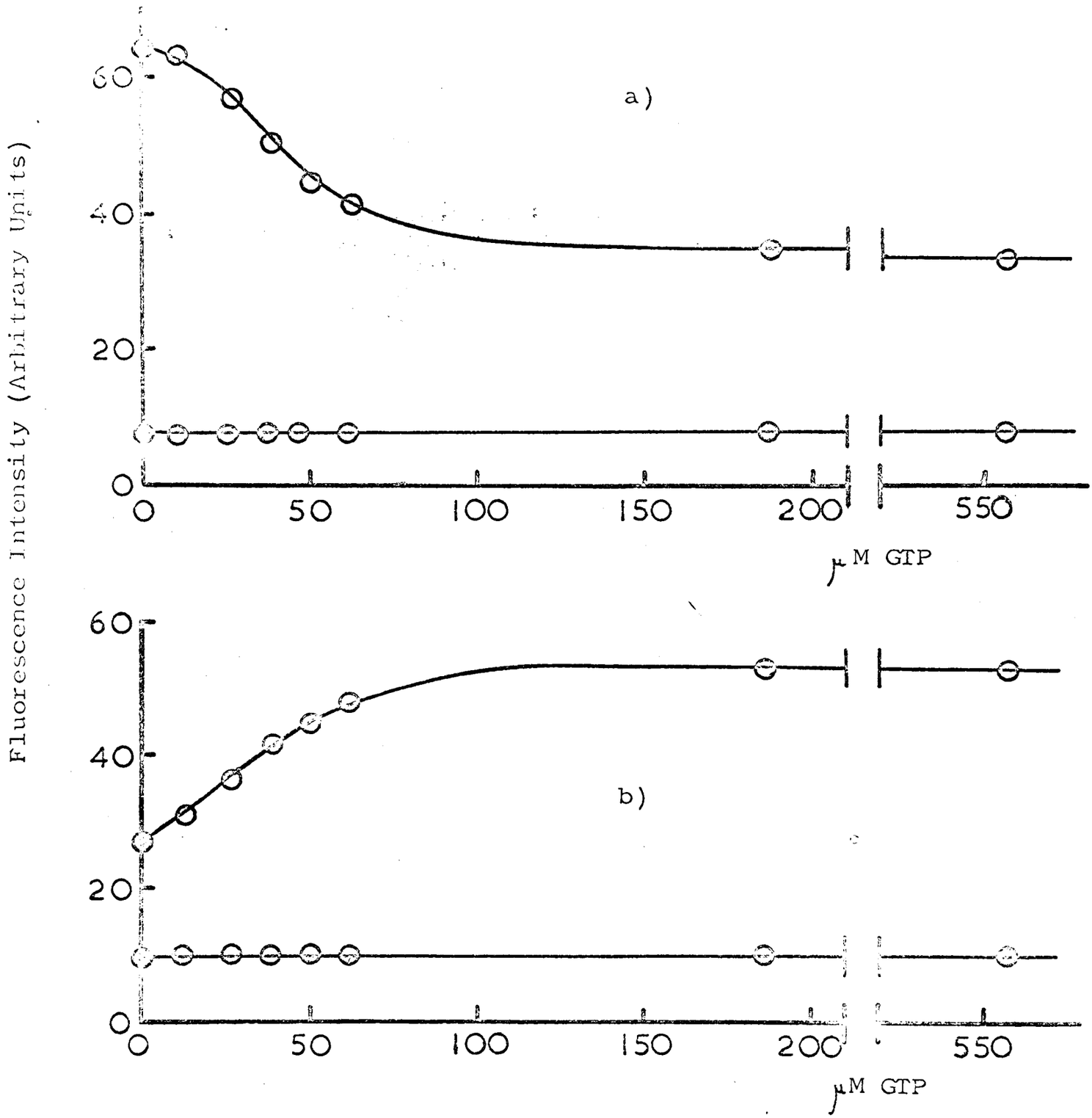

Fig.17. Response to DNS amino acids to the structural change. GDH, 1 mg/ml; NADH, 100 μM; DNS amino acids 18 μM. a) DNS-Cys, b) DNS-Ala

Table 6

DNS Amino Acid	(550 nm) Enhancement (520 nm)			
	0	300 μM (GTP)	0	300 μM (GTP)
DNS-Cys	8.66	4.37	14.9	8.0
DNS-Glu	5.8	3.17	9.1	4.7
DNS-isp	1.79	1.15	2.38	1.39
DNS-Pro	1.57	1.4	2.19	2.9
DNS-γ-but	1.0	1.0	1.16	1.36
DNS-Leu	1.39	1.54	1.22	2.11
DNS-Hist	1.46	2.27	1.83	2.94
DNS-Nor	1.89	2.17	2.44	3.25
DNS-But	1.86	3.45	2.37	5.46
DNS-Ser	2.82	8.08	4.05	16.0
DNS-Ala	2.57	5.26	3.62	8.87
DNS-Asp	3.85	6.00	5.95	15.42
DNS-Met	2.0	4.2	2.78	7.15
DNS-Try	2.55	13.13	6.36	22.4

Table 5

DNS Amino Acid	(550 nm) Enhancement (520 nm)			
	10 μM	20 μM	10 μM	20 μM
DNS-Cys	3.26	2.92	4.2	3.58
DNS-Glu	2.87	2.77	3.6	3.56
DNS-Asp	2.21	2.12	3.4	3.16
DNS-Ala	1.72	1.70	2.4	2.2
DNS-Try	1.47	1.79	1.9	1.92
DNS-Ser	1.43	1.43	-	-
DNS-isp	1.43	1.40	1.6	1.53
DNS-Met	1.32	1.32	1.43	1.51
DNS-Nor	1.24	1.20	1.42	1.52
DNS-But	1.20	1.16	1.45	1.32
DNS-Gly	1.20	1.23	-	-
DNS-Glm	1.19	1.14	1.33	1.28
DNS-Phe	1.17	1.15	-	-
DNS-Leu	1.13	1.13	-	-
DNS-Pro	1.12	1.15	1.2	1.17
DNS-His	1.086	1.02	1.07	1.02

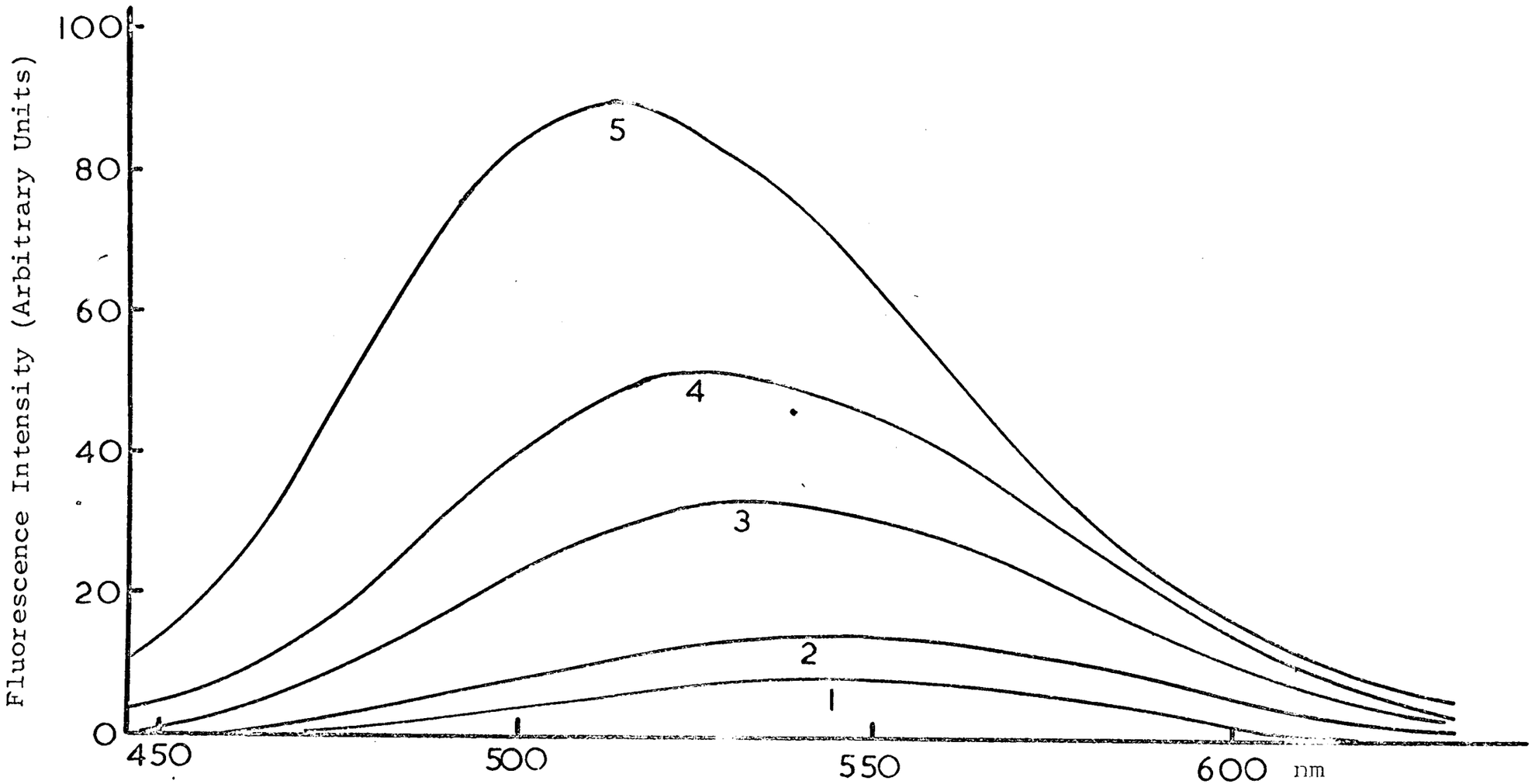

Fig.16. Fluorescence emission spectra of DNS-Try (49 μM) in ethanol/water mixtures.
1. H_2O; 2. 25% EtOH; 3. 50% EtOH; 4. 75% EtOH; 5. EtOH.

exponential throughout the titration (Table 4). These results correlate well with the observed enhancement in intensity for the two probes, and suggest that these enhancements are due primarily to increased quantum yield, and that τ_o does not change during the titration.

(ii) Dansyl amino acids*

Unlike ANS, the DNS group is fluorescent in water, and is only enhanced ca 10 fold on changing from water to ethanol. There is a typical blue shift in the emission (550nm to 520nm; fig.16). In water/ethanol mixtures there is a more or less linear variation of relative quantum yield (Intensity/OD at exciting wavelength) and emission wavelength with ethanol concentration. The interaction of GDH with the DNS derivatives of a number of amino acids (including substrates e.g. Glu, Nor, Met, Ala, Pro[140], substrate analogues e.g. Cys, Asp, Glm and inhibitors e.g. p-amino isophthalic acid (isp)[141]) was studied. GDH enhanced the fluorescence of all the derivatives studied (Table 5), the effect being greater for the dicarboxylic acids. Most of these probes responded to the structural transition in GDH (Table 6). However, while the fluorescence of the dicarboxylic substrate and inhibitor derivatives was quenched, that of the others was enhanced (fig.17). Thus while the enhancement caused by GDH alone appears to be governed by the amount

*Much of the work on DNS amino acids has already been submitted in a Part II Thesis (ref[150]).

of negative charge on the amino acid, irrespective of its substrate/inhibitor properties, the response to the structural transition seems to depend on the substrate/inhibitor properties of the amino acid. These results predicted that Cys ought to be a competitive inhibitor, and this was later demonstrated.

Despite this apparent specificity there are a large number of sites for DNS amino acids on GDH. By careful titration of GDH with DNS-Glu and DNS-Ala, in the presence and absence of excess NADH/GTP, it was possible to derive average numbers of binding sites per oligomer:-

	DNS-Glu	DNS-Ala
GDH	35	40
GDH + NADH/GTP	43	30

The value for DNS-Glu was in good agreement with the limiting value obtained more rigorously by a Weber titration[35,31]:- -n=37. Obviously the structural transition induced by NADH/GTP has a very marked effect on the fluorescence properties of these probes. A 20% increase in binding of DNS-Glu is accompanied by a 50% drop in fluorescence, while a 25% decrease in binding of DNS-Ala is accompanied by a 100% increase in fluorescence.

All the probes used above have been negatively charged. The next step was to determine whether or not neutral probes (e.g. MNS amides) would respond to binding and the structural transition. Three amides of MNS were prepared as described in

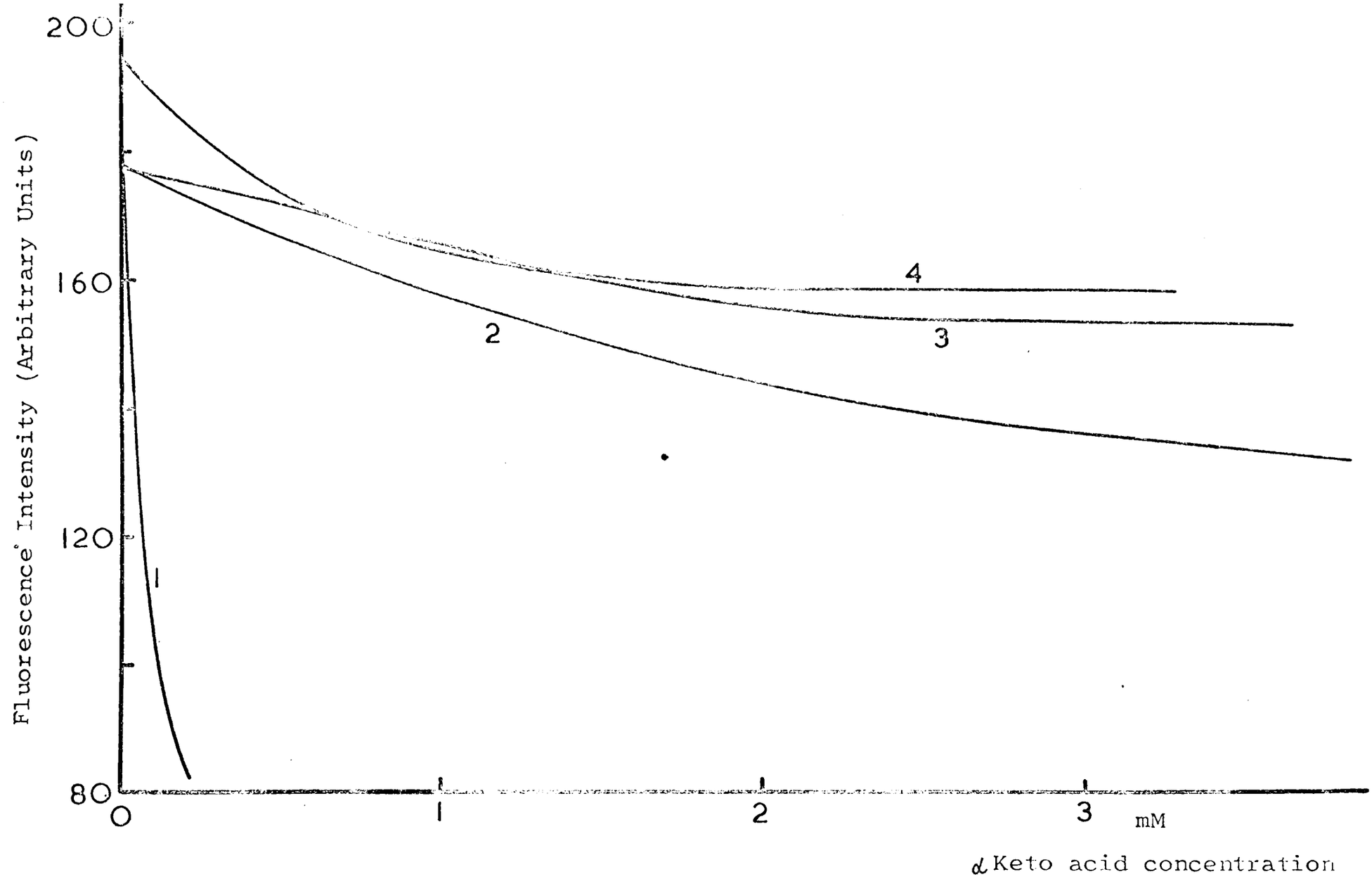

Fig.26. Effect of α Keto acids on bound NADH fluorescence. NADH, 30 μM; GDH, 1 mg/ml; excited at 380 nm, emission at 470 nm.

1. αKg; 2. pyruvate; 3. αK caproate and αK isocaproate; 4. αK butyrate.

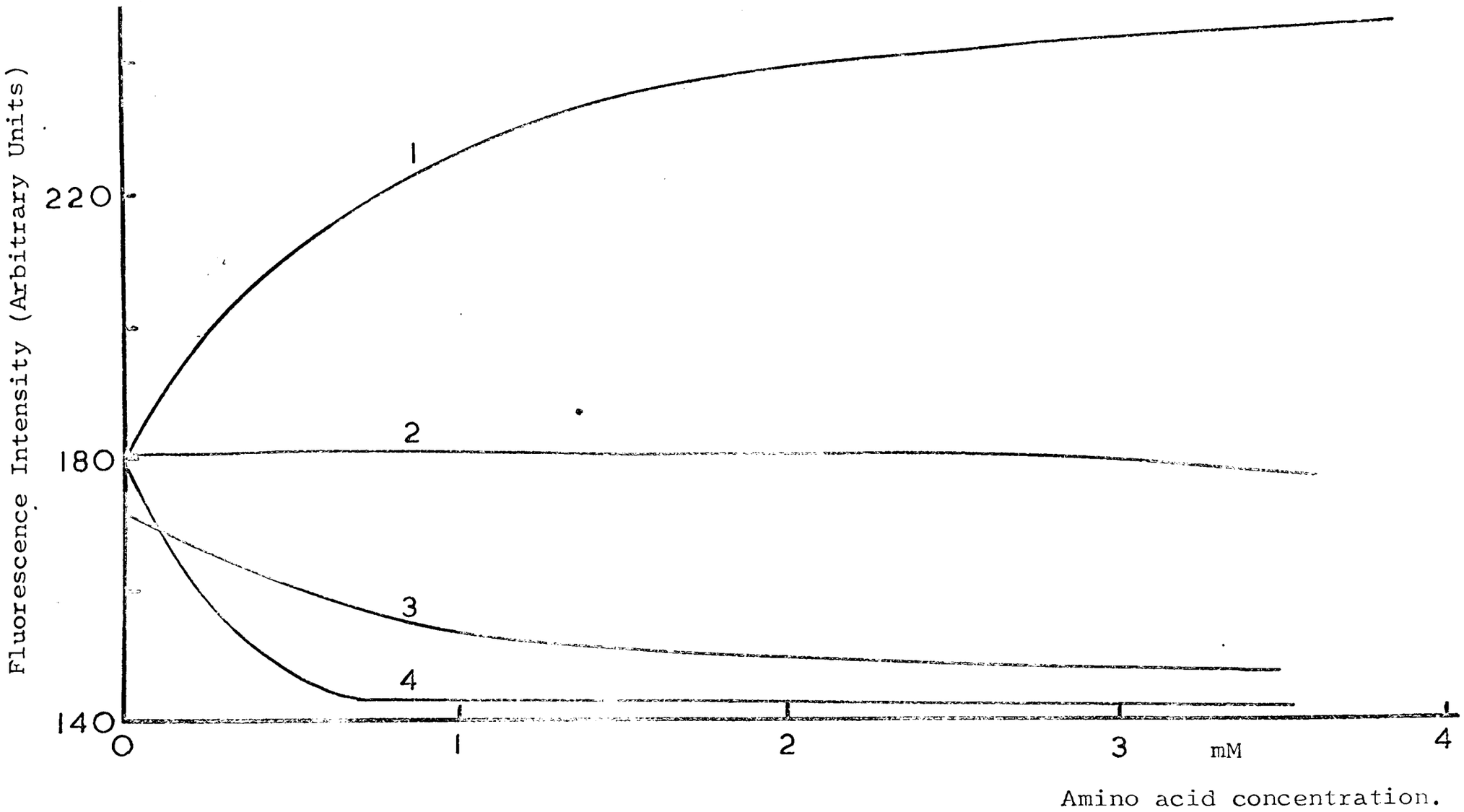

Fig.25. Effect of amino acids on bound NADH fluorescence. NADH, 30 μM; GDH, 1 mg/ml; excitation at 380 nm, emission at 470 nm.
1. L-glu; 2. D-glu; 3. Nor; 4. Leu

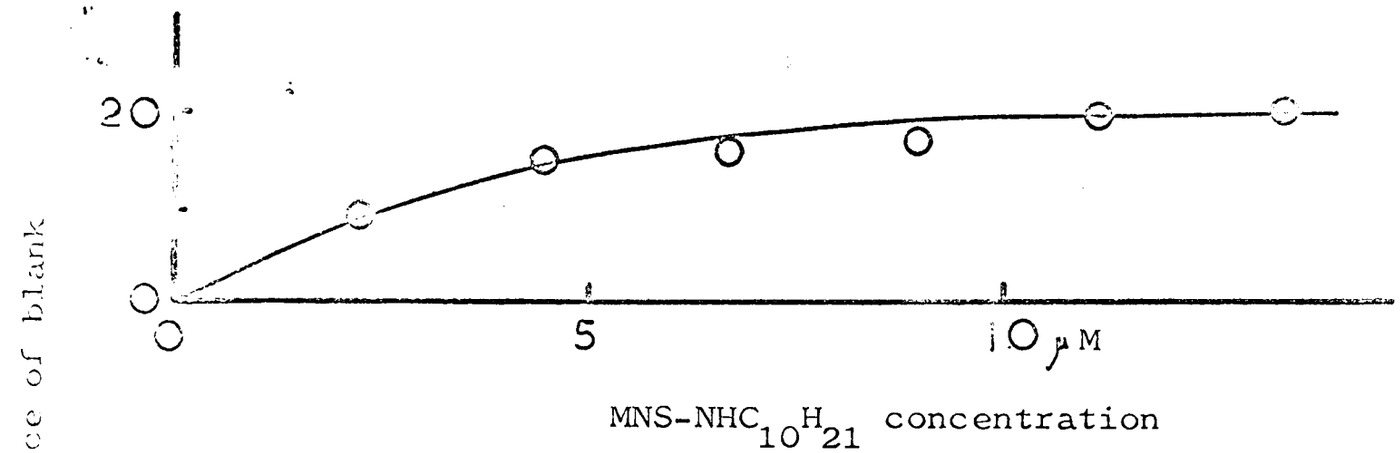

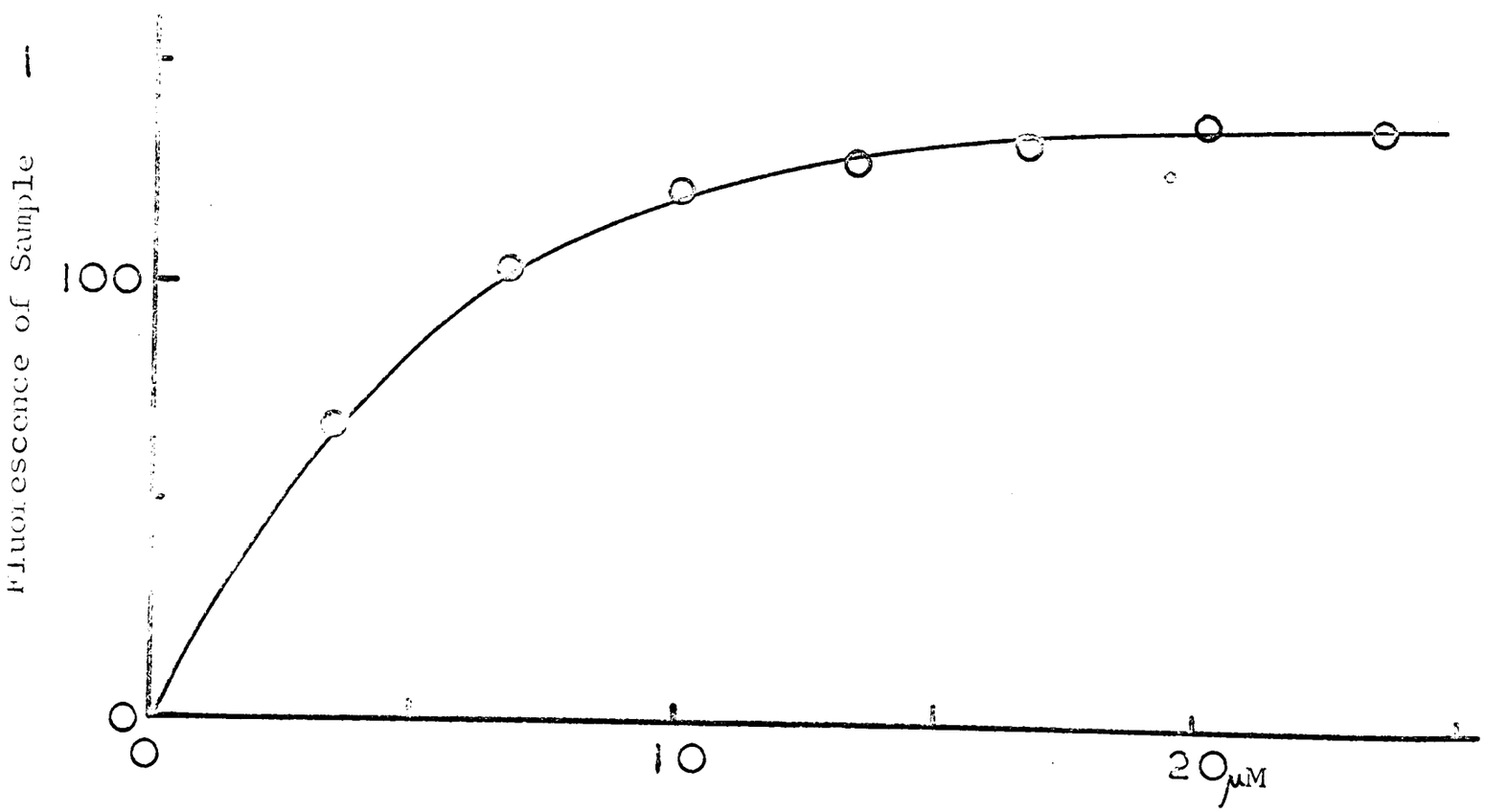

Figs.23 and 24. Titration of GDH(1mg/ml) with MNS NHC_2H_5 and MNS $NHC_{10}H_{21}$. Excited at 375nm. Emission at 470nm.

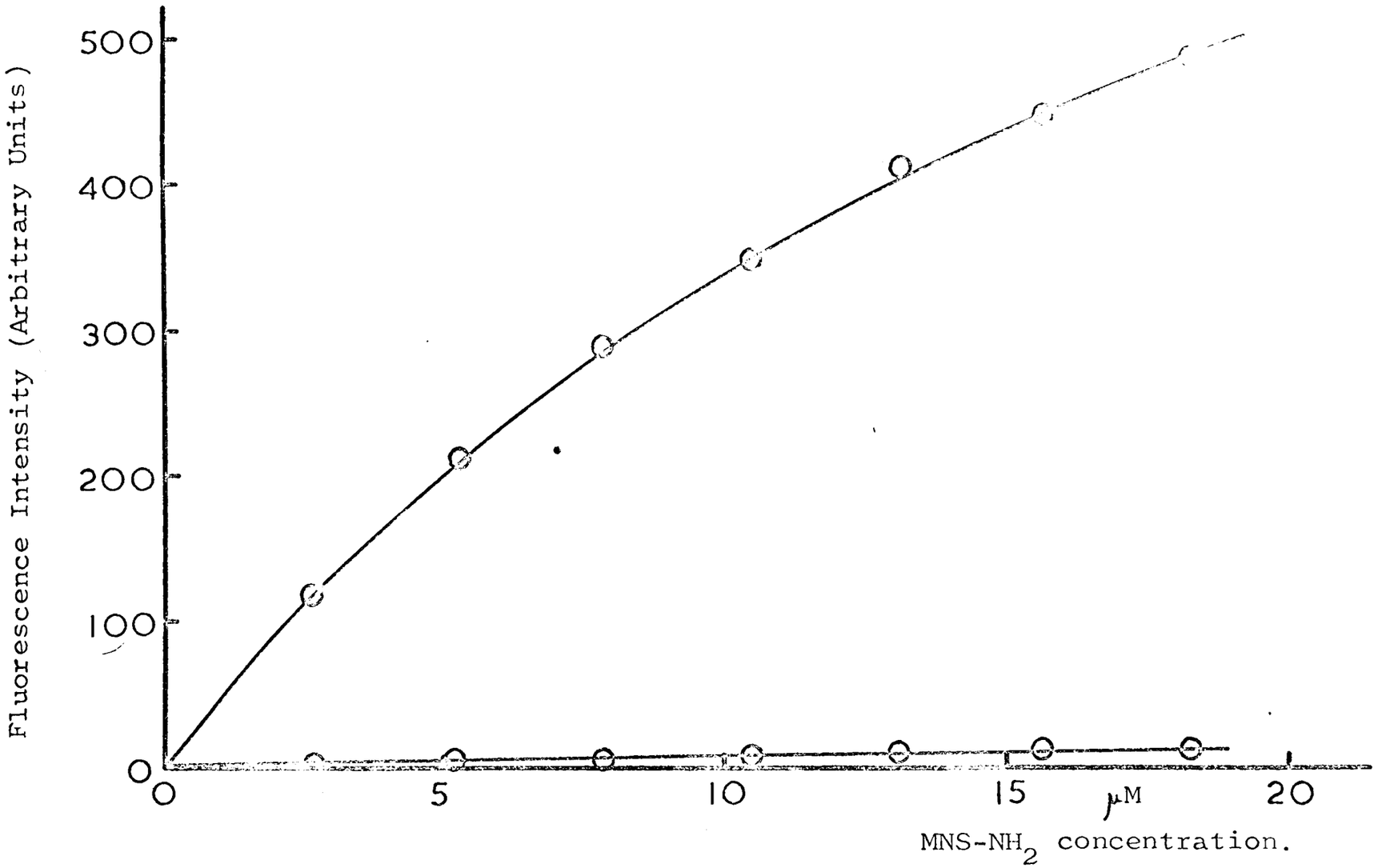

Fig.22. Titration of GDH (1mg/ml) with MNS-NH_2.

Excitation at 375 nm, emission at 470 nm.

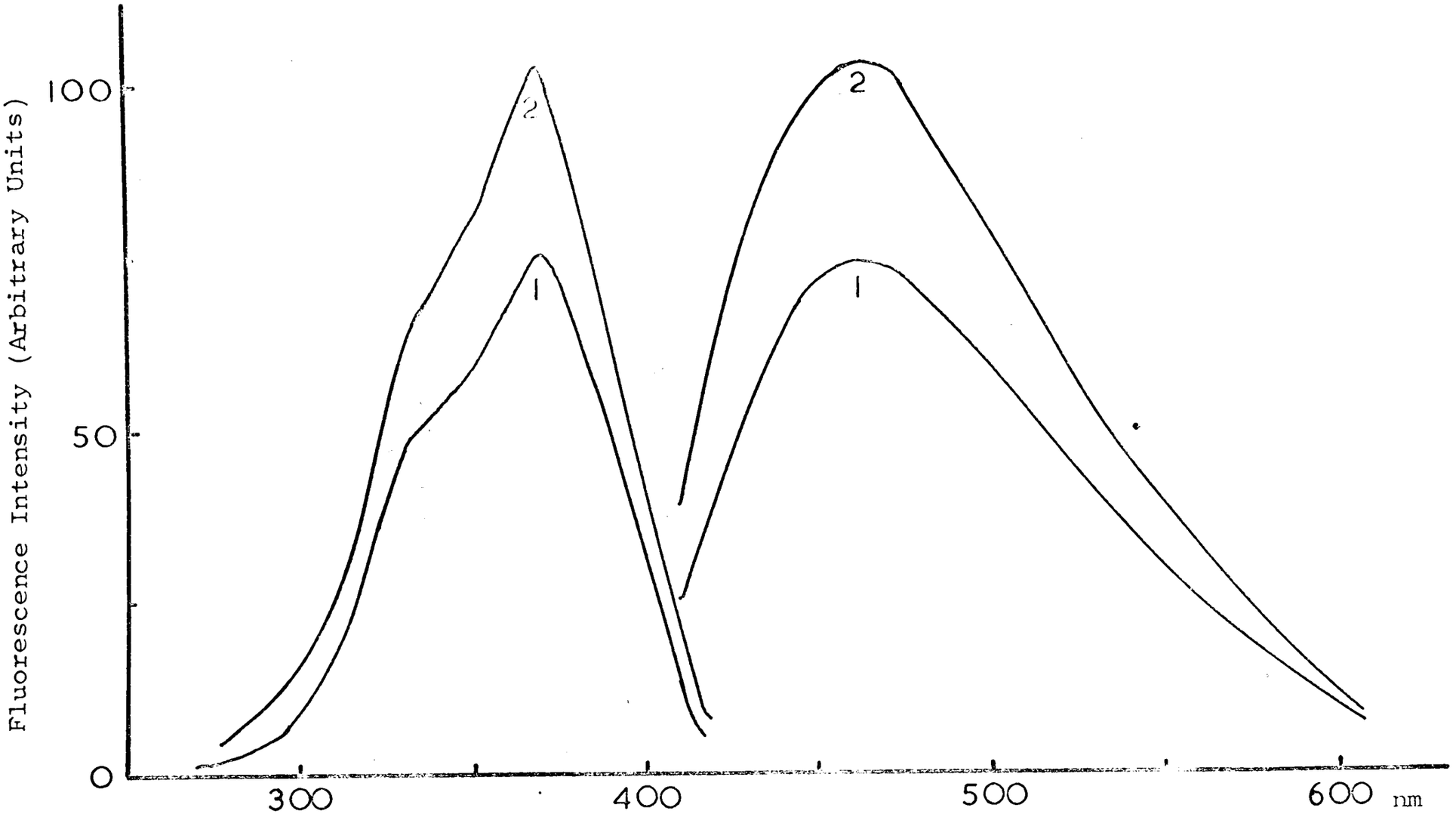

Fig.21. Fluorescence spectra of MNS-$NHC_{10}H_{21}$ in the presence and absence of GDH. 1. 13 μM MNS-$NHC_{10}H_{21}$; 2. 13 μM MNS-$NHC_{10}H_{21}$ + GDH (1 mg/ml). Excited at 375 nm, Emission at 470 nm.

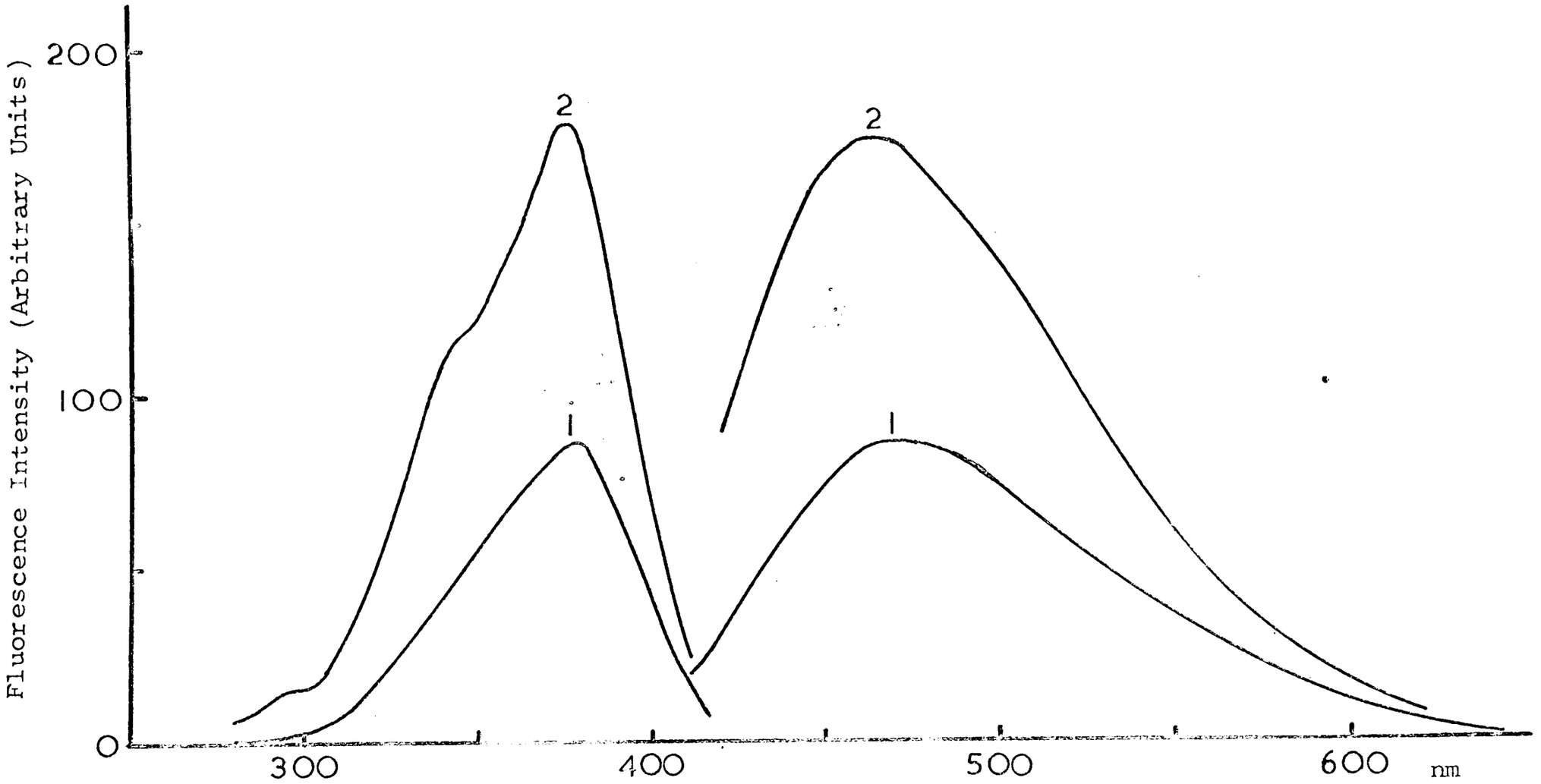

Fig.20. Fluorescence spectra of MNS-NHC_2H_5 in the presence and absence of GDH.

1. 20 μM MNS-NHC_2H_5. 2. 20 μM MNS-NHC_2H_5 + GDH (1 mg/ml).

Excited at 375 nm, Emission at 470 nm.

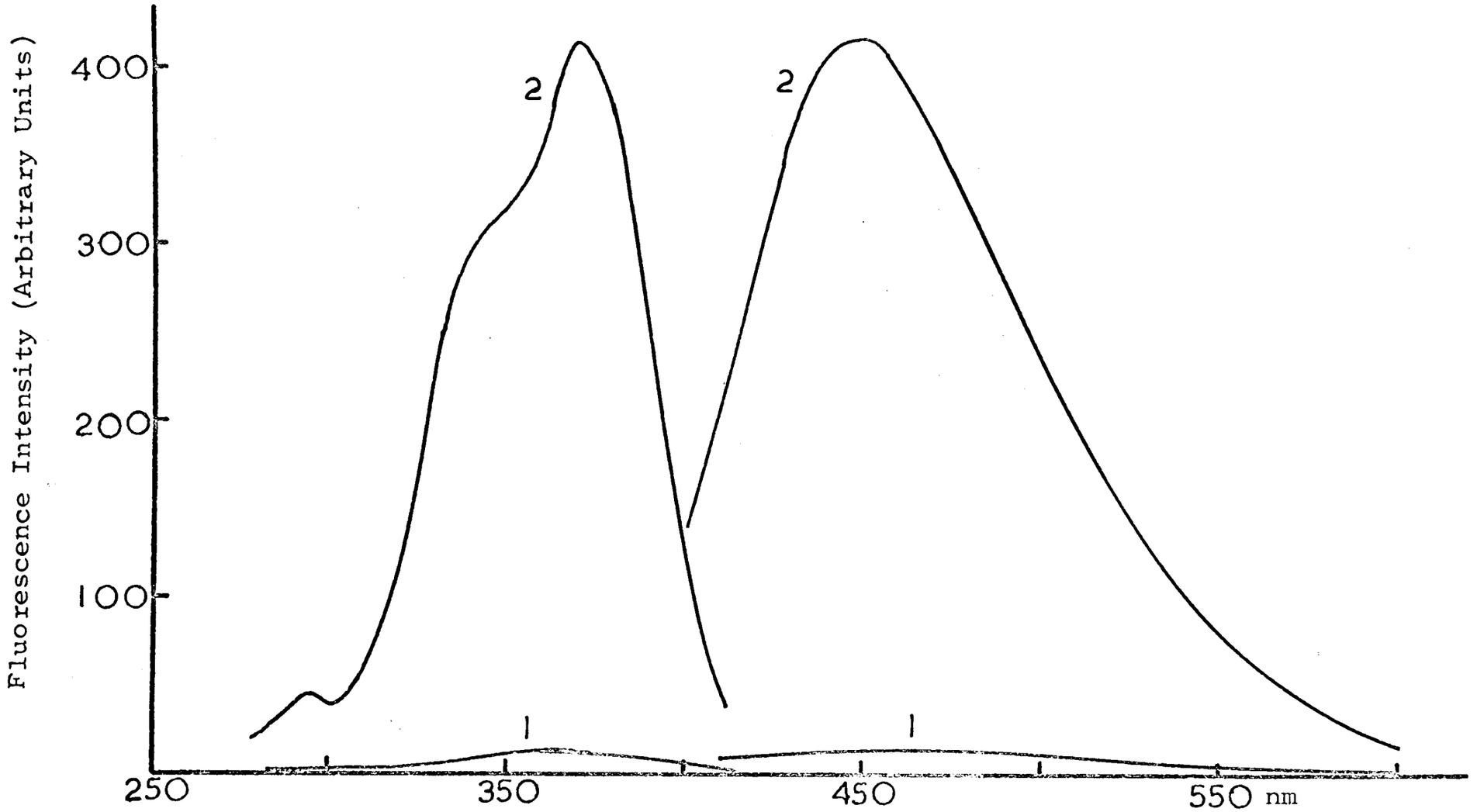

Fig.19. Fluorescence spectra of MNS-NH_2 in the presence and absence of GDH. 1. 15.5μM MNS-NH_2. 2. 15.5μM MNS-NH_2 + GDH (1mg/ml). Excited at 375nm, emission at 450nm.

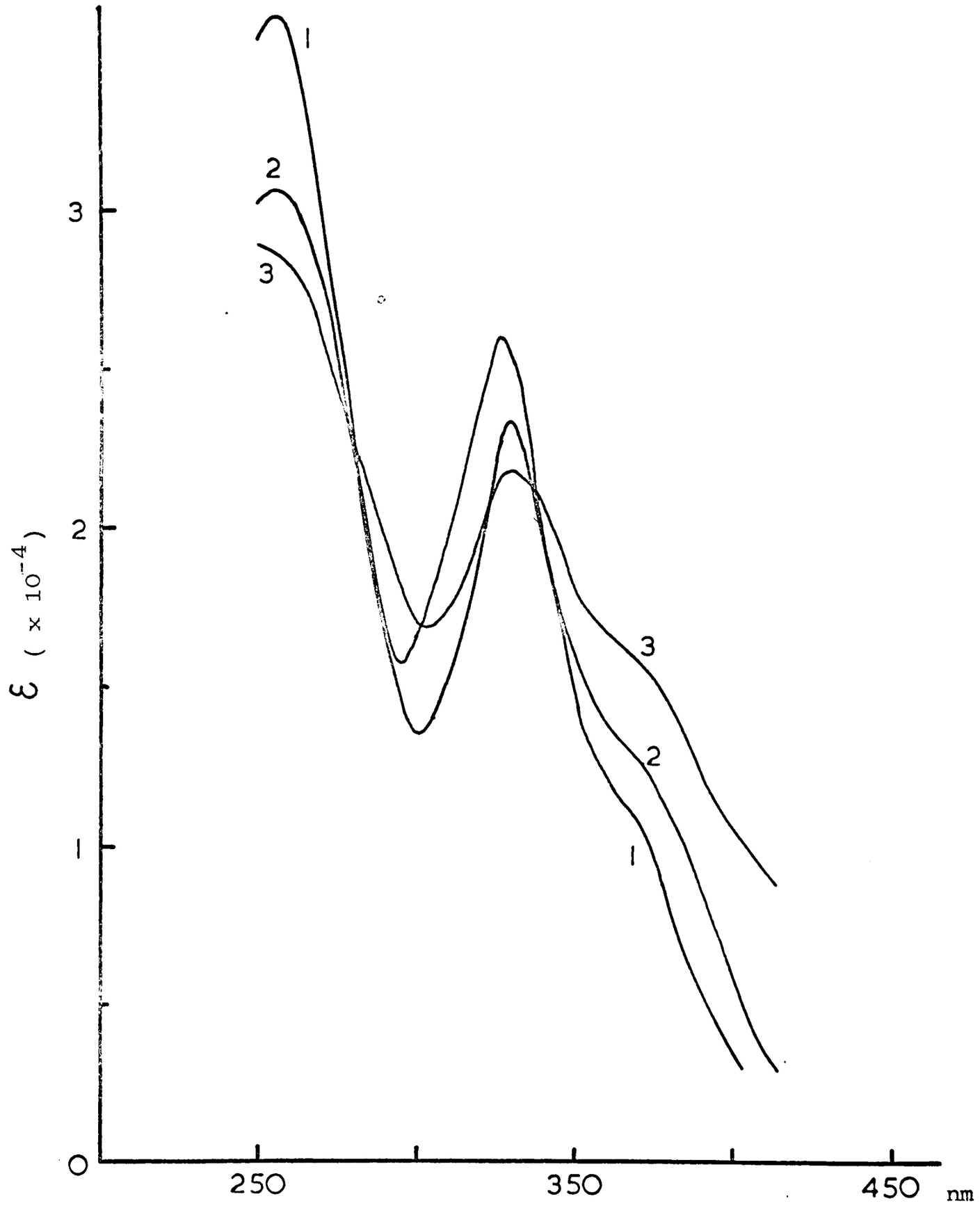

Fig.18. Absorption spectra of MNS amides in buffer (pH 7.6)

1. MNS-NH_2; 2. MNS-NHC_2H_5; 3. MNS-$NHC_{10}H_{21}$.

the experimental section. While their absorption spectra were very similar (fig.18) their fluorescence properties were quite different. Their fluorescence in water was in the order $MNS\text{-}NH_2 < MNS\text{-}NHC_2H_5 < MNS\text{-}NHC_{10}H_{21}$ while the enhancements and shifts caused by GDH were in the reverse order (figs.19-21). Obviously increasing the length of the alkyl chain, decreased the similarity in behaviour between the probe and MNS. Titration of GDH (1mg/ml) with these probes showed that like MNS, $MNS\text{-}NH_2$ saturated the enzyme only at very high probe concentrations. However, $MNS\text{-}NHC_2H_5$ and $MNS\text{-}NHC_{10}H_{21}$ both saturated at quite low concentrations - 6.3μM, approx 2 binding sites per oligomer (fig.22-24). The lack of a negative charge did not prevent these probes from interacting with GDH. However, none of them responded to the structural transition.

(iii) NADH

Carefully dialysed, ammonia free GDH was used (to prevent any reaction when α-keto acids were used) and GDH (1mg/ml) with 30μM NADH was titrated with the amino (α-keto) acids. The results are shown in figs. 25, 26. The most striking observation was that while most of the acids which affected bound NADH fluorescence (either by quenching or enhancement) did so at around 1mM, αKg was effective at concentrations as low as 10μM. While L Glu enhanced NADH fluorescence, D Glu had no effect. Obviously the influence of these three molecules must

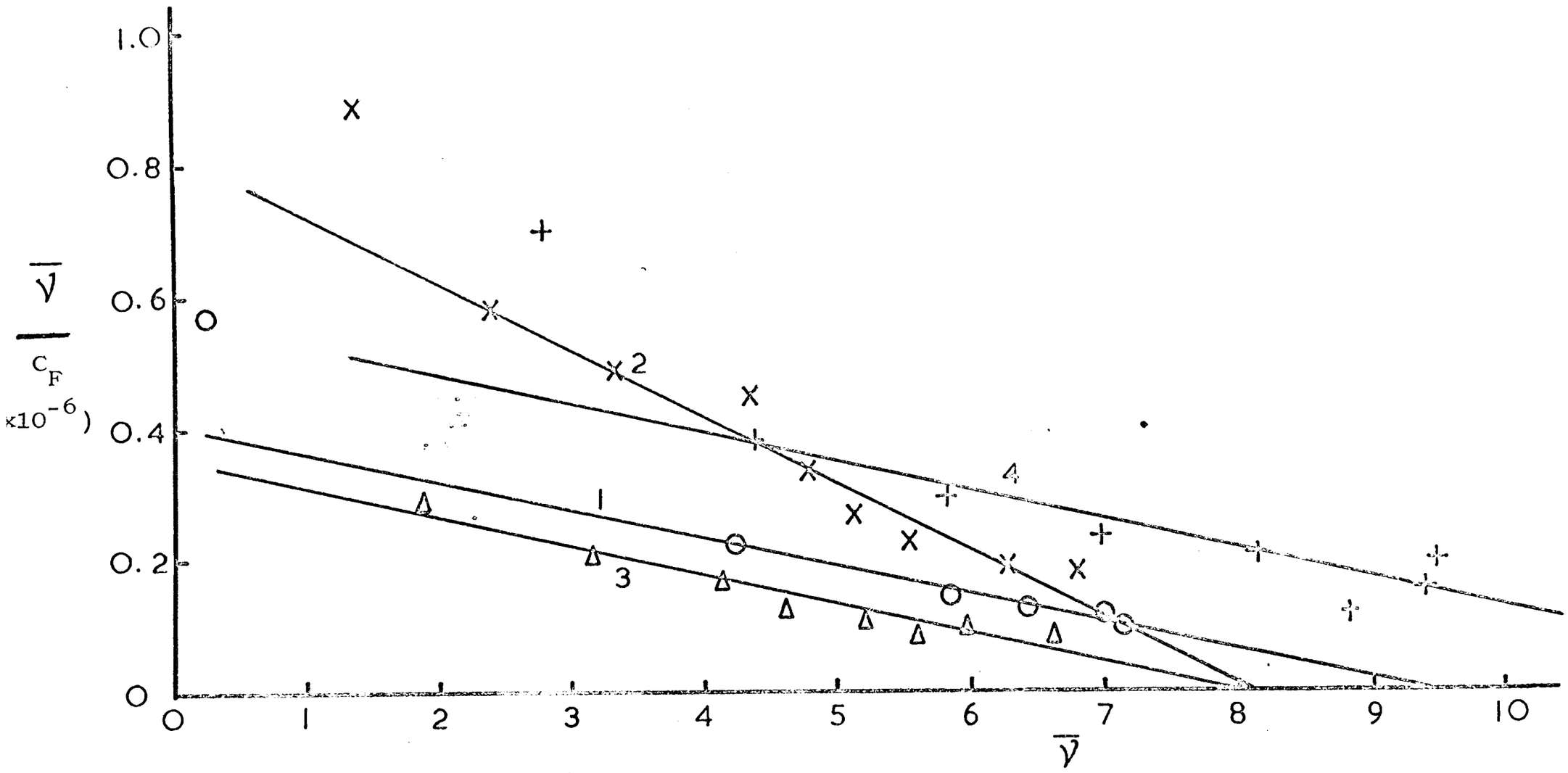

Fig.27. Scatchard plots of NADH binding to GDH. Each line represents a different experiment.

1. n = 9.5; K_D = 23 μM; 2. n = 8.1, K_D = 9.8 μM; 3. n = 8, K_D = 22.4 μM;

4. n = 12.8, K_D = 22.5 μM.

be very powerful and localised since they are thought to bind at the same site[141].

One possibility is that while binding at the same site, they have different effects on the binding of NADH to GDH, altering the fluorescence by changing the binding rather than by altering the quantum yield. Attempts were therefore made to measure the binding parameters for NADH in the presence of the different amino (α-keto) acids. This was done by titrating GDH (1mg/ml) and amino (α-keto) acid (5mM) with NADH to obtain the saturating concentration of NADH and the limiting fluorescence. In order to get reasonable titration curves (i.e. a straight free NADH base-line) it was necessary to move the excitation wavelength away from the absorption peak to avoid the "inner filter" effect. Normally excitation at 380nm (emission 470nm) was used. In this way it was shown that Glu and αKg had little effect on the number of NADH binding sites on GDH:-

Acid	$[NADH]_{sat}$ μM	No. of binding sites	F_∞ / F_f
none	21.4	6.6	2.3
L Glu	21.4	6.6	4.0
α Kg	20	6.2	0.11

Binding data obtained for NADH in the absence of substrates gave a spread of dissociation constants and numbers of binding sites (fig.27).

Discussion

MNS has very similar properties to ANS in that it binds to GDH with a marked shift and enhancement of fluorescence, and responds to the structural transition of GDH. The observed rather small enhancement serves to underline the fact that when enhancements are quoted, the experimental conditions relating to the amount of dye bound must also be quoted, as well as the wavelengths of emission and absorption. The enhancement of MNS caused by the structural transition is larger than that of ANS (three fold and two fold respectively). The increases in life-time of the two probes were also three fold and two fold. This suggests that the intrinsic life-times of the two probes are unaltered by the structural transition, and that the increases in intensity (quantum yield) result from decreased quenching, this being larger for MNS. Similarly, the fluorescence changes of the two probes on going from water to ethanol where for ANS an intensity increase of ca 125 fold is accompanied by a ca 100 fold change in life-time. Thus Kasha's theory on the dependence of τ_o on the rotation of the substituted amino group (p. 8) cannot be used to explain the enhancements of ANS and MNS fluorescence in water/ethanol mixtures, or on the structural transition of GDH. However, the fluorescence properties of N-phenyl-1-naphthylamine (NPN) do illustrate the Kasha theory. This molecule behaves

Table 7

Amino acid	Rel.rate[a]	GTP rate[b]	Fluorescence enhancements 550nm	520nm
L Glu	100	.11	.55	.52
L Nor	17	1.38	1.15	1.33
L But	2.3	3.74	1.85	2.30
L Leu	1.7	3.82	1.11	1.73
Val	1.6	3.30		
Norleu	1.6	3.36		
iso Leu	0.95	5.37		
Met	0.82	5.90	2.1	2.57
Ala	0.27	8.44	2.05	2.45
Orn				
Lys				
Pro			.89	1.32
Asp	< 0.1		1.56	2.59
Thre				
D Leu				
Methyl Glu				
isp			.64	.58
Cys			.50	.37

a Data from ref.140.

b GTP rate = rate in presence of GTP/rate in absence of GTP. Data from ref.145.

similarly to ANS in that its fluorescence is very solvent dependent being blue shifted by less polar solvents. However, unlike ANS its τ_o (not the quantum yield) changes on changing the solvent e.g. τ_o doubles on changing from hexane to benzene[151].

The DNS amino acid results proved to be especially interesting. Chen had found that GDH enhanced DNS-Glu more than DNS-Gly and DNS-Try[78], but made no attempt to explain the differences. Investigation of this effect with a large number of DNS amino acids showed that GDH enhanced most of them, but that the extent of the enhancement was governed largely by the amount of negative charge on the amino acid. However, the response to the structural transition seemed to be governed by the substrate properties of the amino acid. Table 7 lists the efficiencies of the various amino acids as substrates of GDH, and the effect of GTP on each of them. Where GTP is an inhibitor, the DNS amino acid fluorescence is quenched, where GTP is an activator, the fluorescence is enhanced i.e. the fluorescence response mirrors the substrate properties of the amino acid. However, the extents of fluorescence change, do not correlate with the efficiencies (Table 7). Particularly noticeable is the change-over of DNS-Asp, which is like Glu (dicarboxylic acid) in the interaction with GDH, but like Ala in its response to the structural transition.

In order to respond to the structural transition it seems

that the DNS group must be near to the carboxyl group since DNS-γ-but does not respond, unlike DNS-But. This does not apply to DNS-isp which responds despite the separation between DNS and the carboxyl groups. It is possible to imagine that unlike DNS-γ-but where the DNS group is free to move relative to the carboxyl group, DNS-isp is bound in such a way that the DNS group cannot escape perturbation by the neighbouring protein side-chains. However, Baker[152] found that 4-methyl isophthalate was 40 times less effective as an inhibitor of GDH than isophthalate (isp). He envisaged a binding site cleft into which Glu fits γ-carboxyl first, and in which there is just room for isp. However, the 4-methyl derivative is too big and binds like salicylic acid, in an external orientation across the mouth of the cleft. It seems likely that DNS-isp will be even less able to fit into the cleft. However, if it does bind externally it is difficult to explain why it does not behave in the same way as DNS-γ-but.

The apparent contradiction between specificity on the one hand, and the large numbers of binding sites found on the other, is probably due to the different probe to protein ratios at which the two measurements are made. At low probe:protein ratios, where the response to the structural change is observed, the binding is probably dominated by a few strong sites. On the other hand, the binding data are obtained at high probe:protein

ratios, where the response to the structural change is observed, the binding is probably dominated by a few strong sites. On the other hand, the binding data are obtained at high probe: protein ratios where a large number of weak sites are saturated, as well as the strong sites. Thus the number of sites obtained from a series of Weber titrations increases to a limit as the probe:protein ratio is increased[150].

Removal of the negative charge of MNS abolished its response to the structural transition. The gradation in properties of the MNS amides as the side chain becomes more hydrophobic is quite marked, especially in their binding to GDH. $MNSNHC_2H_5$ and $MNSNHC_{10}H_{21}$ appear to bind quite tightly at two sites per oligomer. These must be non-polar sites away from the normal DNS amino acid and MNS sites since the MNS amides do not respond to the structural transition.

The binding of NADH to GDH has been a matter of some controversy. A whole range of binding constants have been derived by various methods. Bayley and Radda[63], and Churchich[153] obtained values of 2μM and 3-4μM by fluorescence enhancement and polarisation of fluorescence. Yielding et al found 7.8μM by fluorescence[67] and 200μM by equilibrium dialysis[154], but did not comment on the discrepancy. Various workers in Oxford have found values in the range 14-28μM[155]. It is interesting that most of the values obtained in the present work fall within

this latter range. This variation might be explained by work which shows (by very careful fluorescence titration) that the NADH binding is sigmoidal[156]. The variation in the numbers of sites is also puzzling. Even taking into account a recent increase in the M.W. (from the sequence of Smith[157]), the numbers of sites vary from six upwards, i.e. there are more NADH molecules bound than there are active sites. It is possible that these additional sites are the second NADH sites originally discussed by Frieden[158].

The effect of αKg on the structural transition as detected by MNS and ANS (i.e. a lowering of the concentration at which GTP becomes effective) must be as a result of one of two things:

a) αKg tightens GTP binding, or

b) αKg tightens NADH binding.

For a) to be the cause there would have to be cooperativity between αKg and GTP. If αKg tightens the binding of NADH (b) an enhancement of NADH fluorescence would be expected by analogy with Glu (which enhances the NADH fluorescence by tightening the binding, not by changing the quantum yield[159]). However, it is possible that αKg tightens NADH binding and complexes with it, when the carbonyl group might be expected to quench the NADH fluorescence.

The above investigations lead to the conclusion that in order to respond to the structural transition in GDH, a probe

needs to be negatively charged, and that in general the fluorophore needs to be close to the negative charge. The logical progression from here is to see if tne same is true in membrane systems. The investigations have also yielded a certain amount of information (albeit limited) about the GDH system itself.

MEMBRANES

CHAPTER 4 MEMBRANES

Introduction

Biological membranes exhibit a number of functions attributable either to the 'membrane' itself, membrane bound proteins, or both. The membrane frequently acts as a barrier to protect sensitive metabolic processes, to mediate in the flow of substrates, products etc, or to contain the different sections of a complex process which would otherwise diffuse away from each other. It also serves as an anchorage for functional protein complexes such as the mitochondrial electron transfer chain. For the purpose of this thesis, erythrocytes will be treated like phospholipid or lipo-protein micelles, i.e. simple membranes with no ATPase, or ion translocating activity. On the other hand, with sub-mitochondrial particles the membrane bound electron transfer chain will be the main focus of attention.

Membrane structure

Membrane structure has been the subject of a number of recent reviews[160-162]. In addition specific reviews on the erythrocyte membrane[163], and mitochondrial membrane structure and function[164,165] have appeared.

Natural membranes consist of a complex mixture of lipid, protein, polysaccharide and water. The amount of bound

(structurally essential) water is usually 20-30% wrt. the dry weight[162] (as found by low angle X-ray scattering). The protein:lipid ratio varies widely from 0.25 for myelin to 3.6 for the inner mitochondrial membrane[160]. The type of lipid present is just as variable. Thus half the mitochondrial lipid is phosphatidyl choline (twice as much as in myelin or erythrocytes) while myelin contains 21% cerebroside, erythrocytes and mitochondria have none[166].

Structure determination

X-ray diffraction and electron microscope studies have contributed a great deal to our knowledge of membrane structure. The classical trilaminar structure of membranes originally emerged from the work of Fernandez-Moran and Finean on myelin[167]. A combination of positive staining electron microscopy and low angle X-ray diffraction enabled them to obtain dimensions of 20-30Å for the electron opaque outer layers, and 40-50Å for the less opaque central layer. Similar structures were observed for outer membranes[168]. Recent work seems to indicate that the trilaminar structure is an artifact caused by high concentrations of staining agent. If low concentrations are used a structure more like a membrane composed of subunits is observed[169]. By using negative staining (e.g. phosphotungstic acid) the membrane is shown as a light structure on a dark background. This technique enables much finer structure to be detected. Elegant

work by Fernandez-Moran and others has thus enabled detection of the fine structure of the inner mitochondrial membrane[170-172], and of sub-mitochondrial particles[173], as well as "configurational" changes between mitochondria in different metabolic states[174]. Attempts have been made to correlate these configurational changes with the primary step of energy conservation[175,176].

The mitochondrion appears as an ellipsoid contained by a double membrane, the inner one having thin invaginations known as "cristae"[172] into the mitochondrial interior. The surface of the cristae is covered with knobs which have a dumb-bell like structure:- a spherical head 80-100Å in diameter, a stalk 30Å wide by 50Å long and a base piece (which with its neighbours forms the continuous inner membrane) 40x112Å [171]. This elementary particle has a protein molecular weight of 1.4×10^6 as compared with one of 0.9×10^6 for the complete electron transfer chain. It was originally assumed that the electron transfer chain was spread throughout this particle[171]. However, the reconstitution studies of Racker showed that in sub-mitochondrial particles the heads and stalks could be stripped off (by a trypsin/urea or sephadex/urea treatment) leaving the electron transfer chain intact, but removing the ability to phosphorylate. Thus it seems likely that the electron transfer chain is situated in the base piece, while the final ATPase

needed for phosphorylation is the head piece[177,178] (The head piece is the F_1 coupling factor). Various studies have shown that the sub-mitochondrial particles prepared by sonication (e.g. ETPH as used in this thesis) are "inside-out" i.e. they are formed by nipping off the cristae near the main wall of the mitochondrion leaving the elementary particles on the outside (in contact with the bulk medium instead of with the matrix in whole mitochondria)[173,179].

Freeze etching studies have shown that both mitochondria and erythrocyte membranes have a knobbly surface[180,181]. When erythrocyte ghosts are stretched on a plastic film they appear to be fibrous, even after lipid extraction[182] indicating again the importance of protein in the structure.

Spectroscopic studies

In addition to the fluorescence techniques mentioned earlier, other spectroscopic techniques have been used to study membrane structure. The membrane proteins and protein-lipid interactions have been studied largely by ORD and CD. Lenard and Singer found that the proteins of erythrocytes seemed like α helical proteins, and were probably a mixture of proteins with both α helical and random coil conformations. They were certainly not in the β-form required by the classical membrane models (see below)[183]. These techniques have also been used to detect pH induced conformational changes in SMP[184]. By using a

combination of CD and nmr, Singer et al have shown that ~60% of the lipid of red blood cell membranes can be removed by phospholipase C without disturbing the protein conformation (CD) but that the nmr spectrum of the remaining lipids was markedly changed. Conversely increase in temperature altered the protein conformation, but did not affect the lipid[185].

Infra-red studies of frozen/dried erythrocytes also show that the protein is predominantly random coil with some αhelical structure[186]. Similar studies on mitochondrial membranes have detected energy dependent protein conformational changes[187]. High resolution nmr of erythrocyte membranes by Chapman et al has given characteristic spectra in which certain amino acid and phospholipid protons may be picked out[188]. However, Chapman's assignments have been doubted by other workers[189]. Metcalfe has used small organic molecules such as benzyl alcohol to probe membranes. Changes in the nmr spectra of the probes and/or the membrane indicate a certain mobility within the membrane[190].

The use of free radicals as probes for the lipid phase of membranes has recently advanced rapidly[191,192]. The small nitroxide radicals used by McConnell appear to rotate freely in the lipid phases of a number of membranes, though anaesthetics cause strong immobilisation[191]. McConnell attributes this ability to rotate to the occurrence of 'holes'

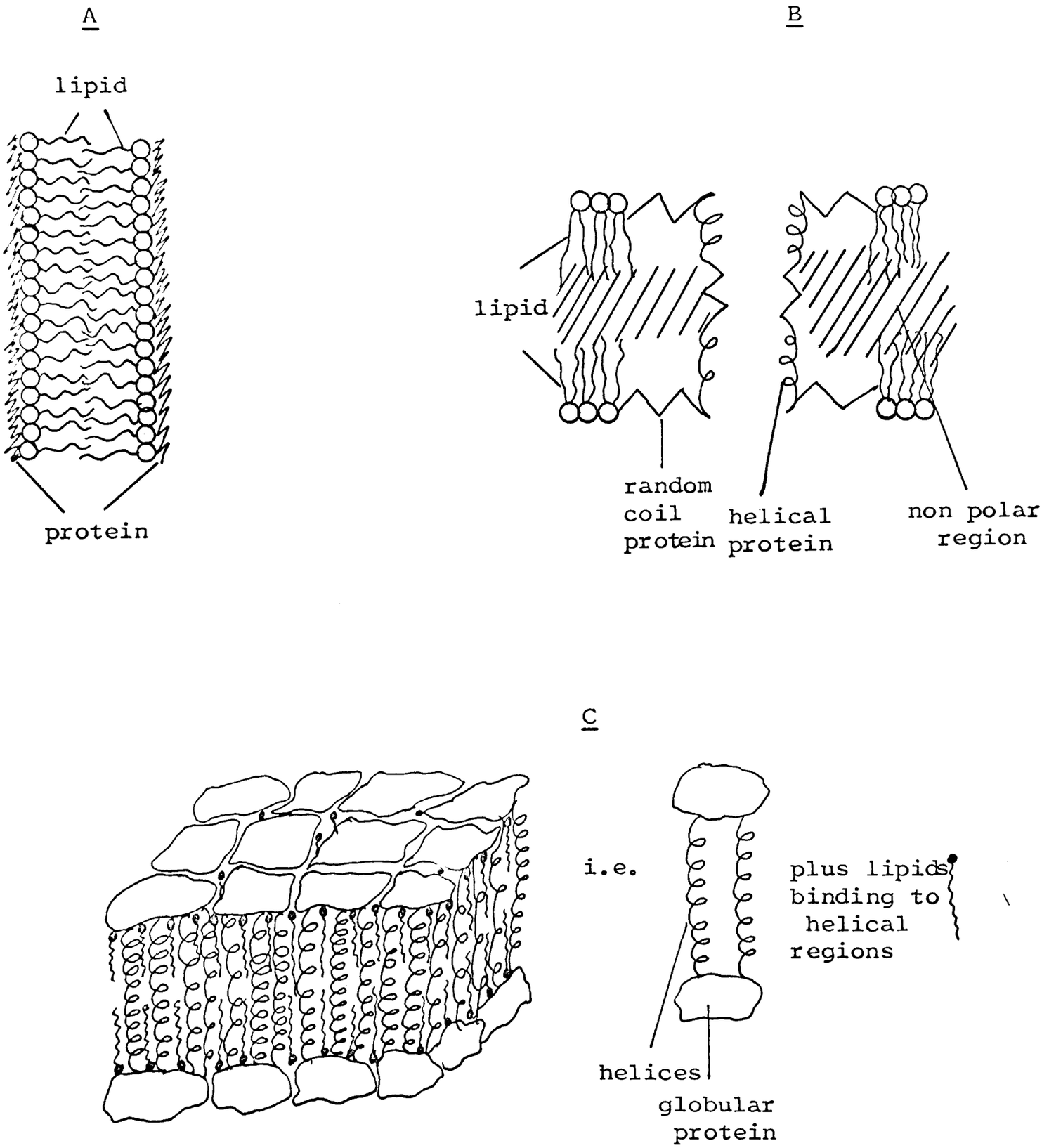

(After Zahler ref.197)

Fig.28. Membrane models

within the lipid phase, caused by unsaturation in neighbouring lipid side-chains[193]. Steroid spin labels cannot rotate so well and appear to bind at the lipid-water interface[191]. Similarly spin labels attached to long chain fatty acids give spectra characteristic of molecules in an oriented environment[193]. Calvin et al have used biradicals to study the differences in interaction between the two radicals in different environments. Although there is strong interaction in water, there is none in nerve membranes (resting or excited) though the probe appears to be highly mobile. The conclusion is that the probe must be binding in the lipid phase, at a point removed from any structural changes connected with nerve excitation[194]. In contrast, water insoluble spin labels have been claimed to detect energy dependent changes in ETPH[195]. However, interference by reduction of the spin label cannot be ruled out in such a complex system.

Membrane models

As a result of the spectroscopic studies the various models proposed for membrane structure have been considerably modified. The first electron microscope pictures appeared to reinforce the Davson and Danielli[196] model (fig 28A) of a lipid bilayer with a coating of protein on each surface. While this may in fact be close to the structure of myelin which contains very little protein, there are several objections for other

membranes. As mentioned above, removal of a large proportion of the lipid does not alter the structure as seen on electron micrographs and by ORD[161,185]. The Davson-Danielli model requires the protein to be stretched out over the surface in a β-pleated sheet or at least in a random coil configuration. Thus the large amounts of α-helical protein found in various membranes[183] are not accounted for. These observations led Singer and Lenard to propose a new model[183] where the protein was the main structural determinant (fig 28B). This has random coil protein on the surface, and α-helical protein in the interior of the membrane. A similar model for red cell membranes has been proposed by Zahler[197] (fig 28C) which consists of globular protein at the surface, joined through the membrane by α-helical protein chains. The lipid is then arranged in the hydrophobic region around the α-helical chains. The fact that the inner mitochondrial membrane had a sub-structure of elementary particles prompted several unit models of membrane structure, including various micellar models[198]. However, it is unlikely that all membranes are made up of the same sub-units, indeed probably no one model will be able to account for all membranes[161].

Mitochondrial membrane functions

In the presence of oxidisable substrate and oxygen,

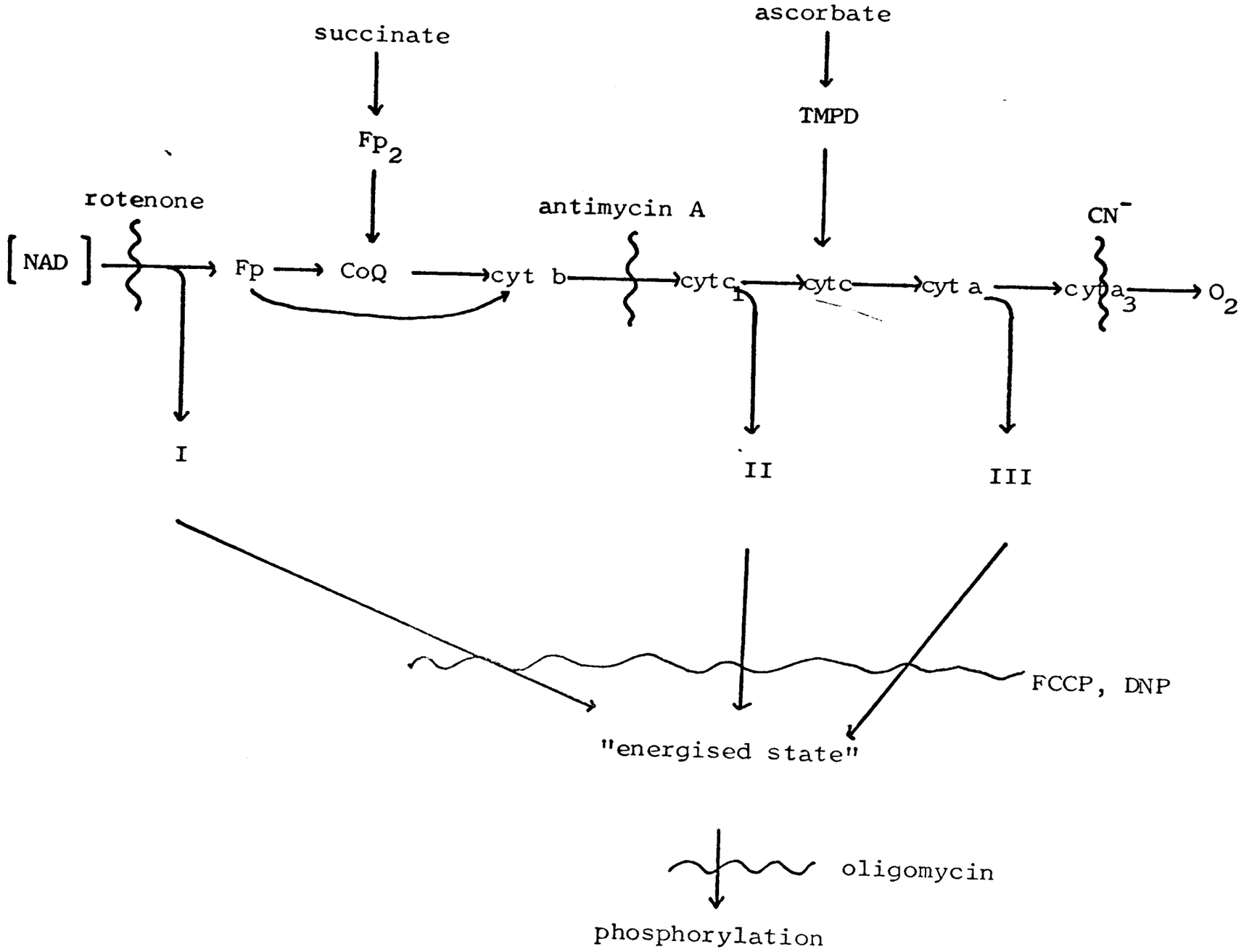

Fig.29. The mitochondrial electron transfer chain (adapted from Mahler, H.R. & Cordes, E.H. "Biological Chemistry", Harper (1966) p.607.

mitochondria (and sub-mitochondrial particles) are capable of a number of functions including active translocation of cations and protons, and phosphorylation of ADP. Ion translocation has been the subject of a number of recent papers[199-201] and theories[200,202,203] (of varying mathematical complexity), and will not be further discussed here.

The degradation products of a number of metabolic pathways are finally oxidised in the mitochondrion by the electron transfer chain. The nature of the components of the chain, and their order are now fairly well understood though there is still considerable discussion about the position of ubiquinone. Chance et al[204] prefer to place it off the direct pathway between the NAD complex and cytochrome b, while Mitchell et al place it on the pathway at various points, usually between cyt b and cyt c_1[205]. The elegant spectrophotometric work of Chance and Williams[206] did much to elucidate the order of the components, and the positions of the three phosphorylating sites (fig.6). There has been some disagreement about the position of the first phosphorylation site, and the site of action of inhibitors like rotenone (which isolate site I and the NADH dehydrogenase from the rest of the chain). Recent work suggests that the rotenone site must be on the oxygen side of the non-haem iron of the NADH dehydrogenase complex[207]. It is also suggested that -SH

groups are important in the contribution of this complex to the whole chain[208].

The most animated discussion in mitochondriology is between the protagonists of the various theories of oxidative phosphorylation. These theories and the experimental data relevant to them have been reviewed[209,210-213], though some of these (refs 210-212) tend to be biased in favour of the author's personal view-point. The original chemical theory of Slater[214] has been considerably modified, but essentially maintains that a high energy chemical intermediate is formed during electron transfer, the breakdown of which drives ATP synthesis and ion transport. The major disadvantages of the theory are that it does not easily explain the action of uncouplers, it does not give a clear reason why the system needs to be membrane bound, and a high energy intermediate has never been detected. The recent discovery of a high energy form of cyt b may go some way towards solving the latter difficulty[204], as may the work of Wang on arsonate inhibition[215] and model systems involving phosphorylated intermediates[216].

The other major theory is the chemi-osmotic hypothesis of Mitchell[217] which proposes that the primary energy conservation step is the production of a proton gradient across the membrane, as a direct result of the oxidation/reduction steps of the electron transfer chain. This theory emphasises the barrier

nature of the membrane, and readily accounts for the action of uncouplers. It has been critisised on the grounds that the ion gradients required to drive ATP synthesis are far too high to be maintained by the membrane[216] ($1:10^{19}$), that it requires a completely sealed membrane vesicle in SMP[213], that it requires specific ion translocating proteins[219] and that it requires specific hydride carriers where (e.g. at the cytochrome oxidase end of the chain) manifestly none exist,[218]. This latter objection is somewhat trivial since a two electron carrier (e.g. metallo protein) will suffice. Liberman, Skulachev et al have obtained data on energy dependent cation and anion transport which seem to support many (but not all) of Mitchell's ideas[220,218].

At about the same time as the Mitchell hypothesis appeared, Williams suggested that the protons generated by the electron transfer chain were in fact involved in energy coupling, but that they diffused out of the membrane slowly. Inside they had a high thermodynamic activity enabling them to remove water and thus drive ATP synthesis by dehydration[221]. The phosphorylating sites correspond to points on the electron transfer chain where electron transfer is slowed down by changing from a single electron to a two electron (i.e. $H^- \rightleftharpoons H^+$) mechanism[213]. Conformational changes have also been cited as the primary energy conservation step[175,210,222]. In

view of recent work with fluorescent probes[110], and the work reported in this thesis, it seems that this hypothesis merits further investigation.

This thesis

The use of ANS to detect energy dependent structural changes in SMP[109,223], and studies of ANS binding to other membranes such as erythrocyte stroma[223,102] have raised several questions regarding both the nature of the structural changes which ANS and similar probes detect, and the characteristics necessary for a fluorescent molecule to act as a probe. These questions may be posed as follows:-

a) What happens in the membrane to cause the probe to respond?

b) The related problem:- where in the membrane are the probe binding sites?

c) What structural characteristics are needed for a fluorescent molecule to be a good probe?

In order to find the answers to the first two questions, the ANS work was extended using pyrene-3-sulphonate (PS), a probe whose fluorescence is concentration dependent[22]. The third question was tackled by using a whole variety of probes of differing structural characteristics.

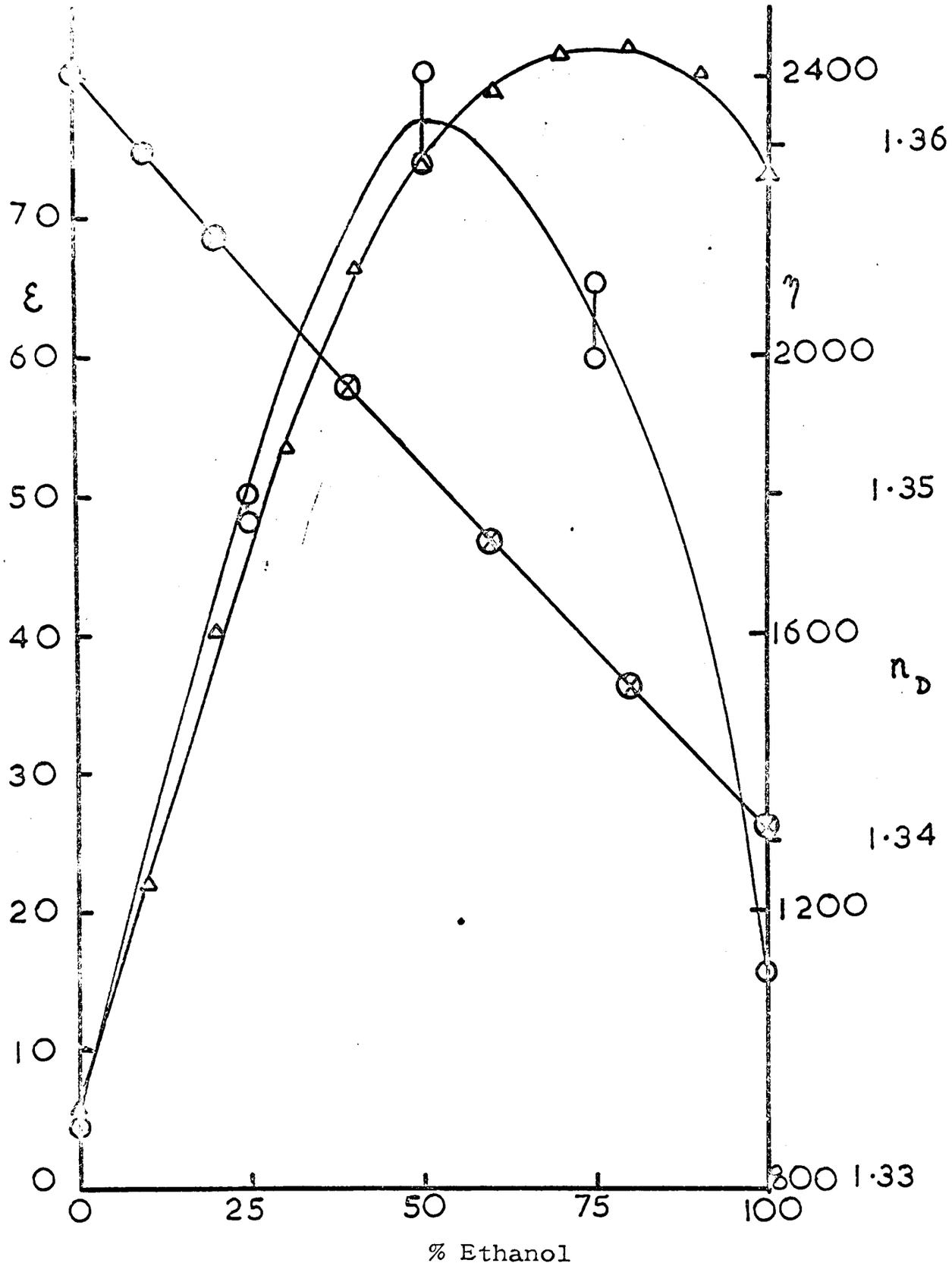

Fig.34. Physical properties of water/ethanol mixtures.

⊗ Polarity (ε); o Viscosity (η); Δ Refractive Index (n_D).

Data from ref.235.

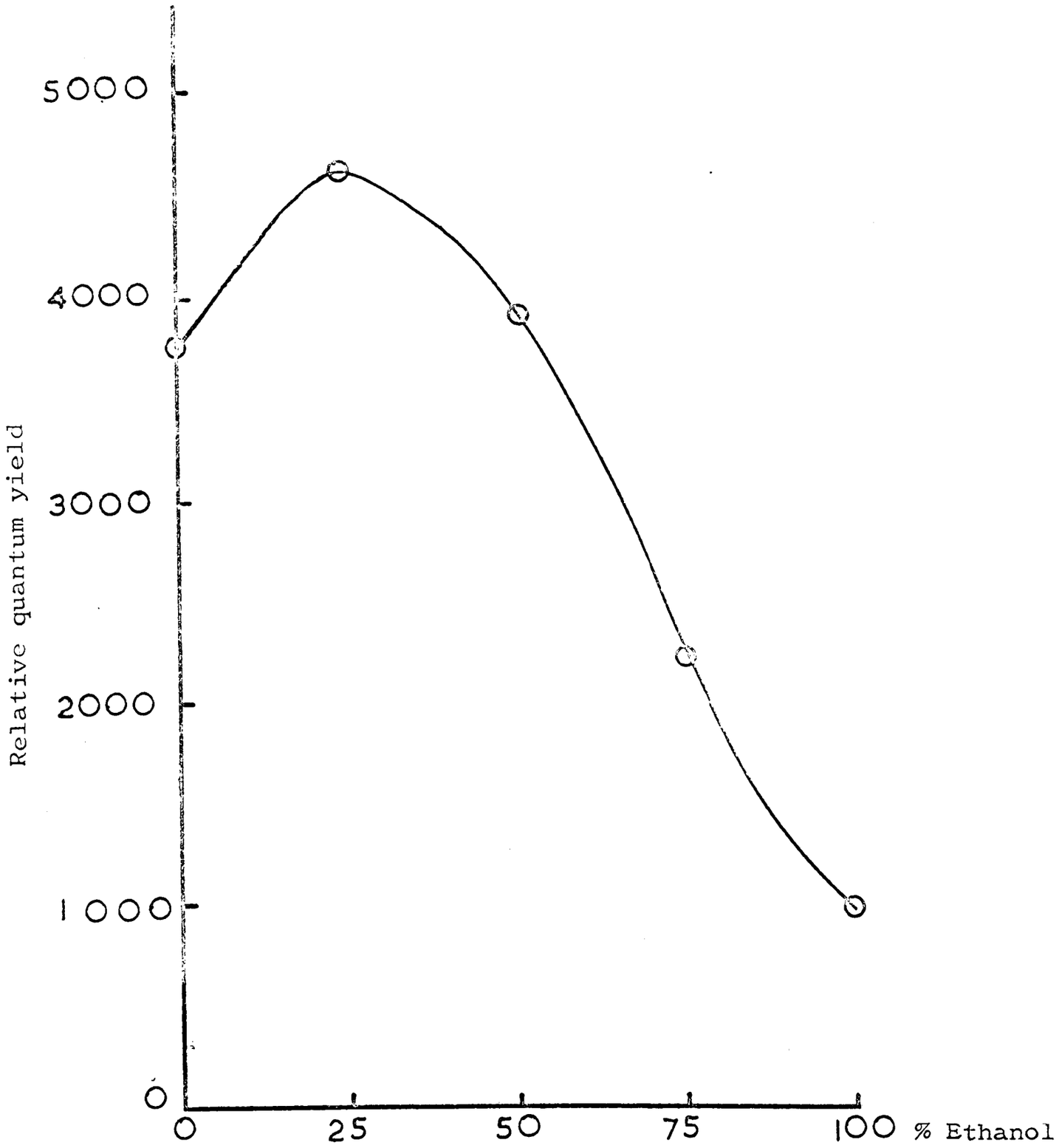

Fig.33. Relative quantum yield of PS (5μM) in ethanol/water mixtures.

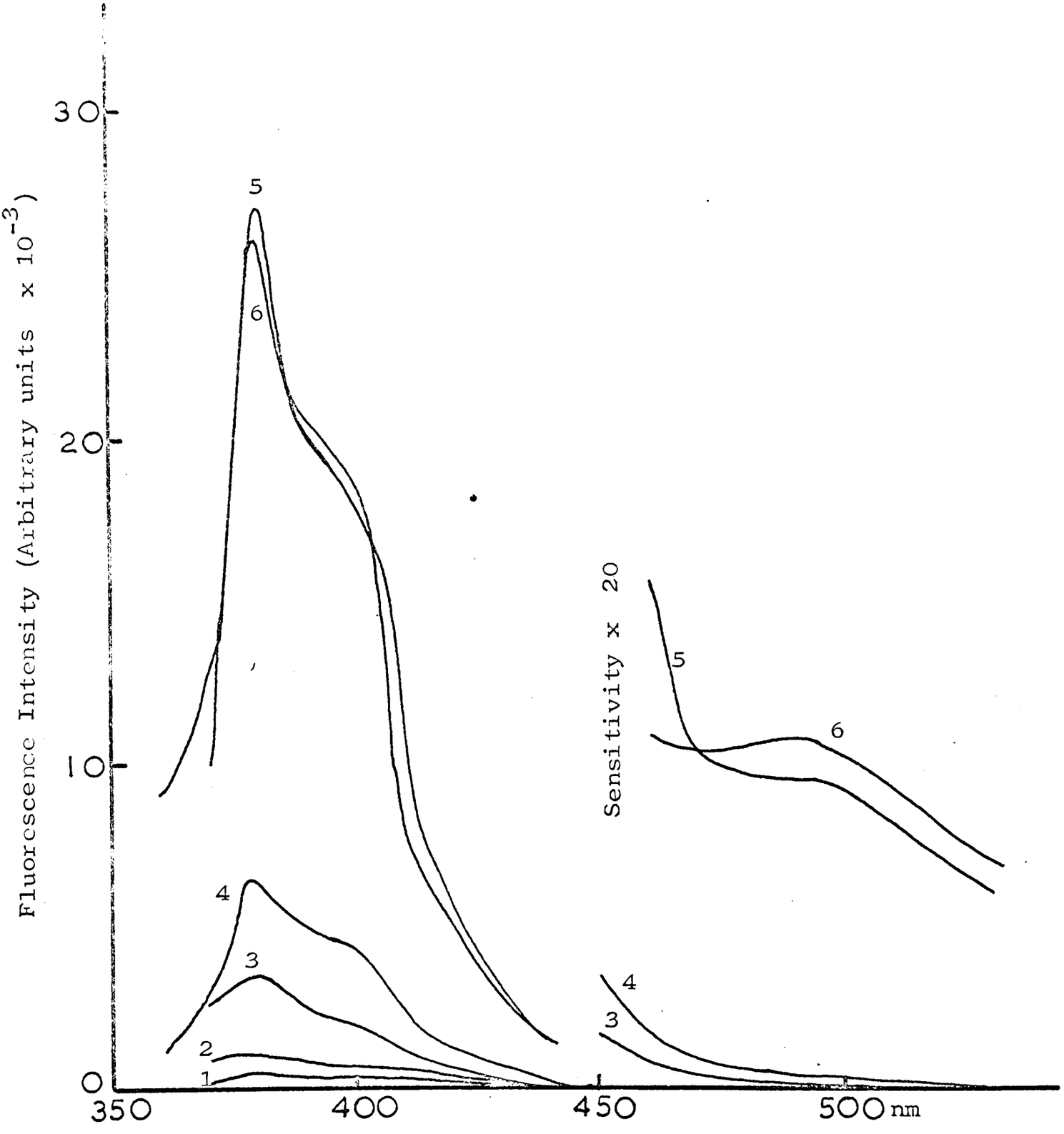

Fig.32. Concentration dependence of PS fluorescence emission spectrum. Excited at 340nm.

1. 5μM; 2. 25μM; 3. 50μM; 4. 100μM; 5. 500μM; 6. 1mM.

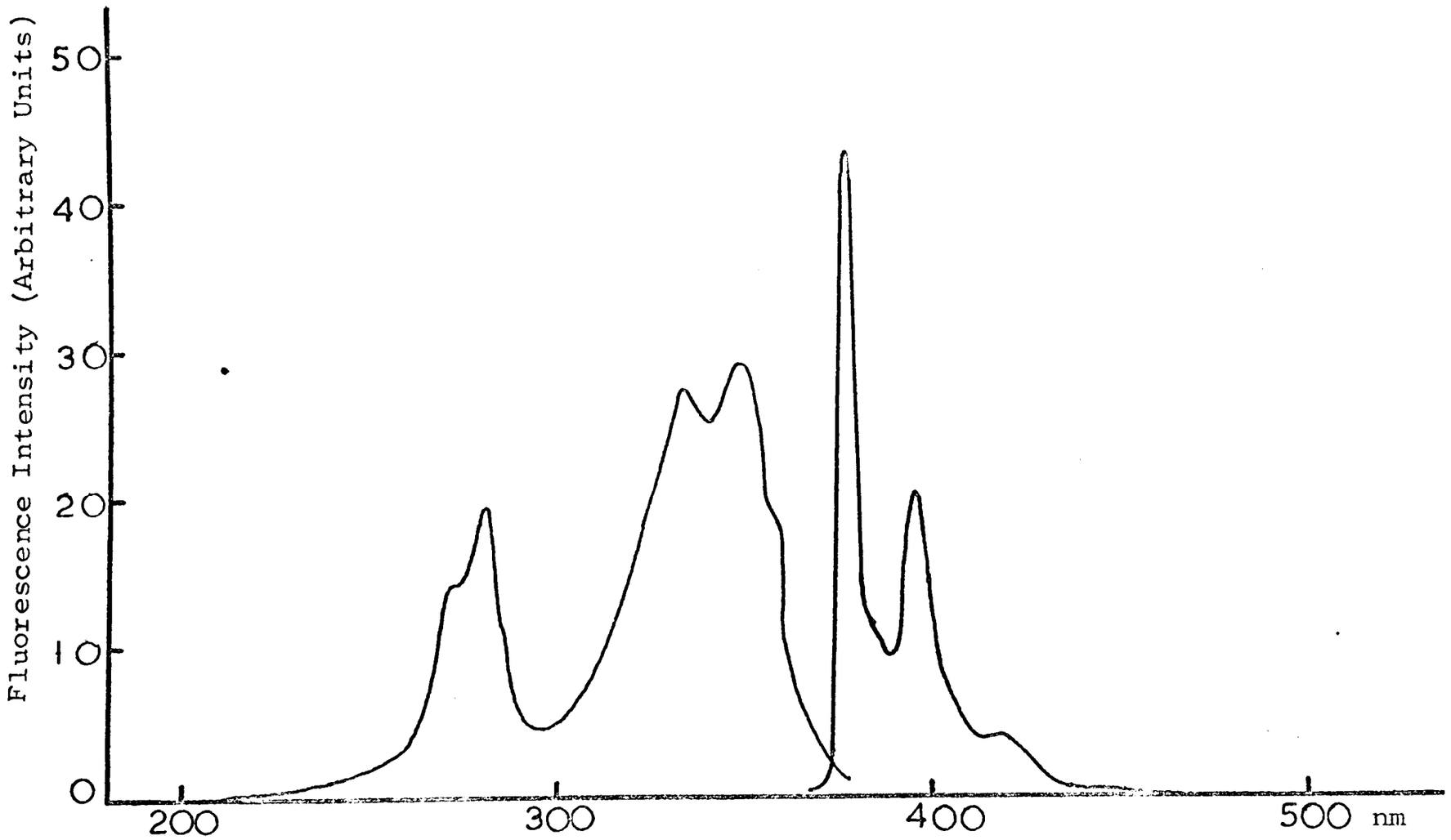

Fig.31. Fluorescence spectra of PS (25μM) in buffer. Excited at 340nm, emission at 380nm. Bandwidths for excitation and emission are 7nm.

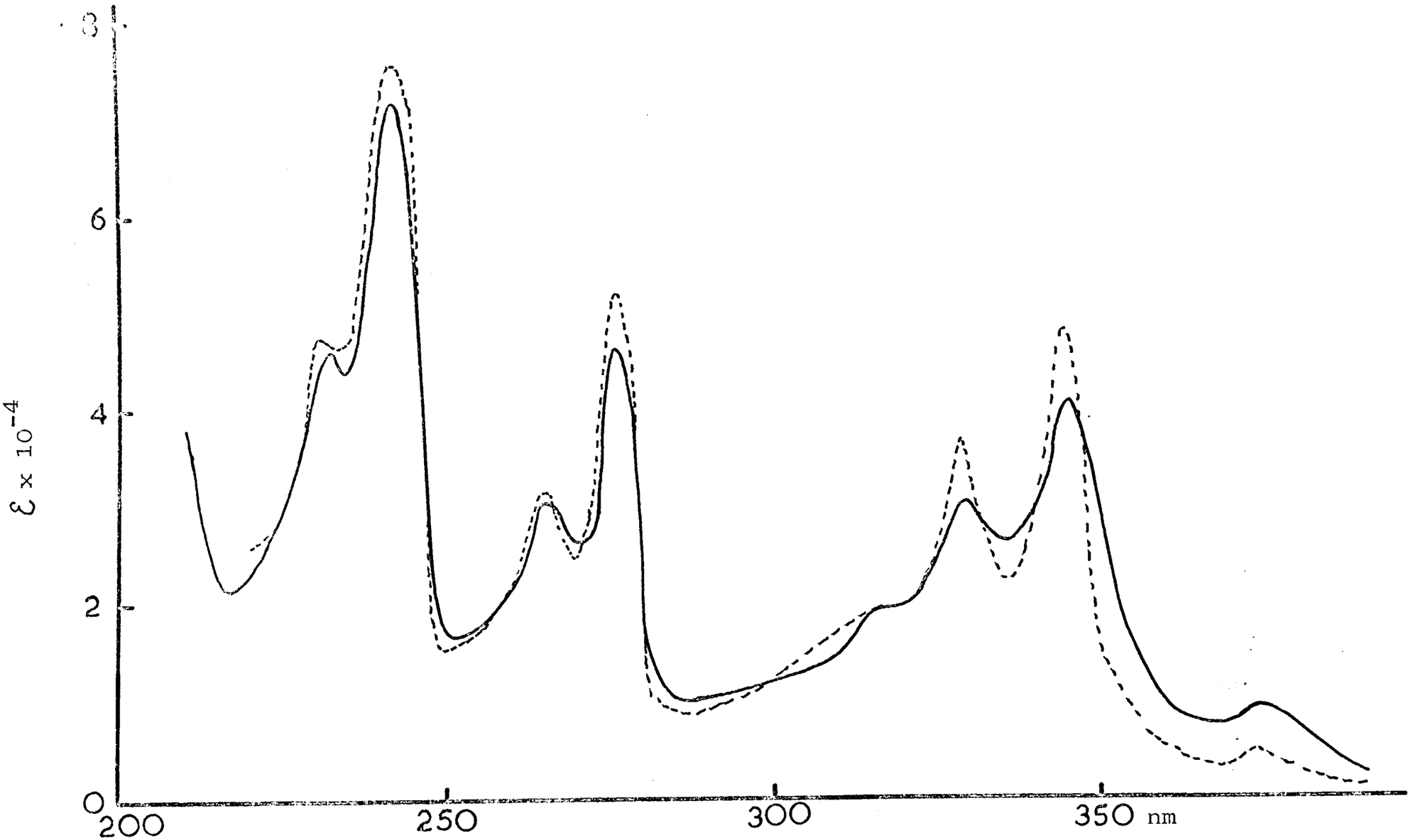

Fig.30 Absorption spectra of PS. (—) in buffer pH 7.4 (-----)in ethanol.

Results

Pyrene-3-sulphonate

The results with GDH and those with ANS in submitochondrial particles suggested that an amphiphilic probe was needed to detect structural changes in SMP. What was also needed was a probe to distinguish between the possible mechanisms causing enhancement of ANS fluorescence (i.e. polarity, viscosity, rigidity). Pyrene-3-sulphonate with its ability to form excimers[22] (i.e. to probe environmental viscosity and rigidity) was chosen to attempt this distinction. The absorption and fluorescence spectra of pyrene-3-sulphonate (PS) in water are shown in figs.30, 31. The concentration dependence of PS fluorescence was studied using a thin film cell (p.37). At low concentrations (ca 10 μM) fluorescence at around 400nm only is seen, whereas at high concentrations (ca 1mM) a longer wavelength peak (500nm) appears (fig.32). This is due to excimer formation by interaction of a molecule in its excited state with one in its ground state (see p.10.) At low PS concentrations in water/ethanol mixtures there was a complicated variation in intensity with ethanol concentration (fig.33). The plot of relative quantum yield v. ethanol concentration (fig.33) has the same general shape as the variation of viscosity with solvent composition (fig.34). Obviously, with this probe the effect of viscosity on fluorescence intensity is much more marked than that of solvent

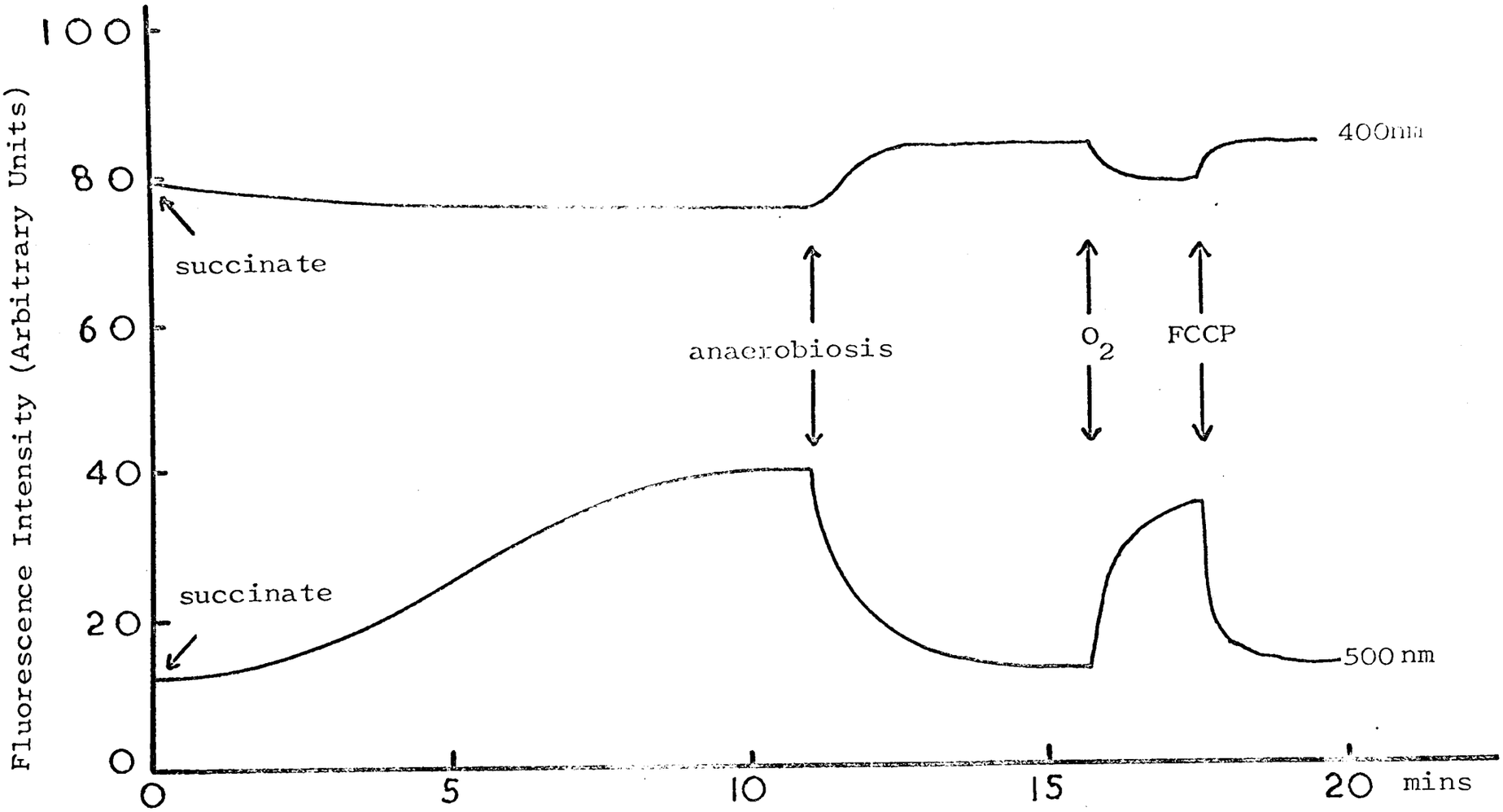

Fig.36. Excimer fluorescence of PS in ETPH.

PS (25μM); ETPH (0.5 mg/ml); FCCP (2μM); Succinate (25mM).

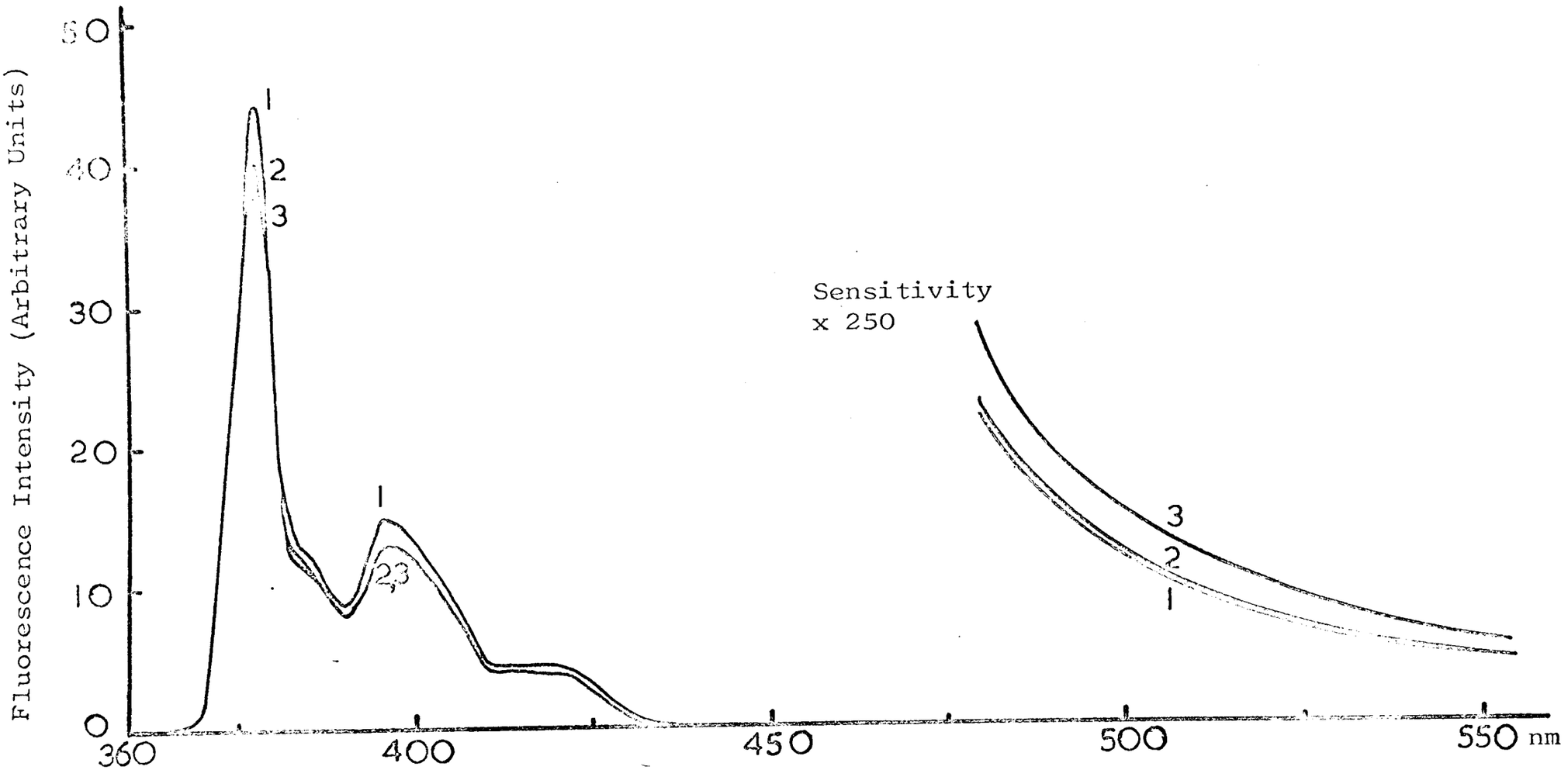

Fig.35. Fluorescence emission spectra of 25μM PS excited at 340nm.
Bandwidths Excitation, 7nm, Emission, 1nm.

1. Buffer pH 7.4. 2. With resting ETPH (0.33mg/ml) 3. With energised ETPH (0.33mg/ml)

polarity. Comparison of the concentration dependence in water with that in glycerol showed that even at 1mM there was no detectable excimer formation in glycerol. This was as expected since the increase in viscosity would be expected to hinder collision and hence decrease the probability of dimer formation.

Addition of 0.5 mg/ml ETPH to a 25μM solution of PS caused very little change in the fluorescence spectrum. The drop in 400nm fluorescence could be accounted for as attenuation by scattering. The slight difference at 500nm is negligible. However, energisation of the ETPH produced an increase in the 500nm emission and a simultaneous small decrease in the 400nm emission (fig.35). Similar opposite changes at the two wavelengths were observed when various energy dependent changes were brought about (fig.36). On energisation there is a lag phase in the 500nm fluorescence. The increase in 500nm fluorescence must result from an increase in excimer formation (apparently an increase in local concentration within the membrane), and as such should be simultaneous with the quenching of the 400nm fluorescence. One reason for the lag phase in the 500nm fluorescence could be that the excimer quantum yield is much lower than that of the monomer. This would mean that the observed monomer fluorescence is much more sensitive to changes in concentration than is that of the excimer. Hence the monomer fluorescence will start to decrease before the excimer fluorescence

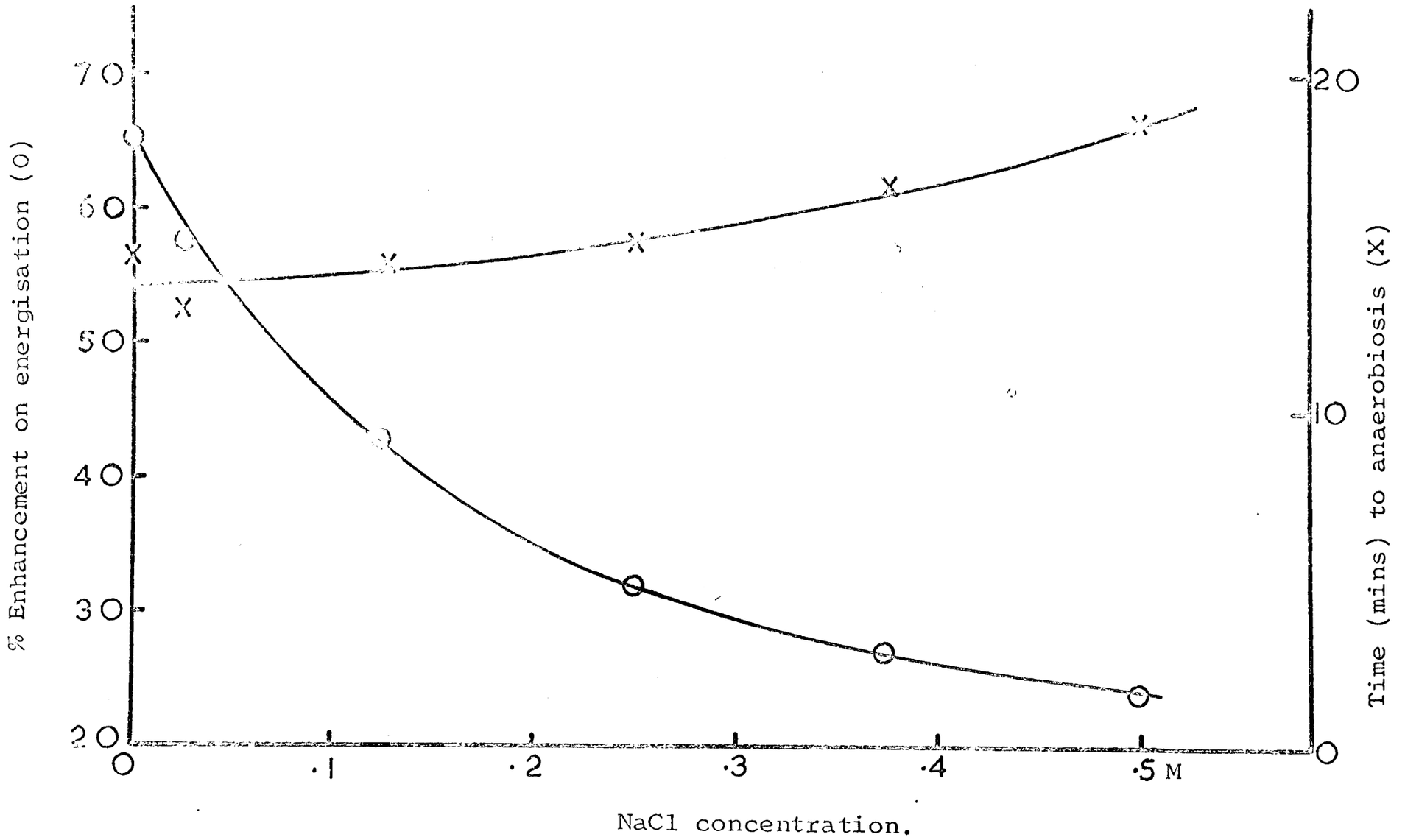

Fig.37. Effect of salt concentration on PS response at 500nm.

Conditions as in fig.36.

is detectable. That this was indeed an excimer formation was demonstrated by the absence of a detectable change in the absorption spectrum. Using divided cells, difference spectra over the range 270nm - 370nm showed very little difference in PS absorption between resting and energised ETPH. Such differences as there were could be accounted for by instrument drift.

This apparent increase in excimer concentration could be caused by increased binding, decreased viscosity, or decreased volume of the pocket in which PS binds. To investigate this further several approaches were adopted.

The extent of these energy dependent changes was found to depend on the ionic strength of the buffer (c.f. ANS where increasing ionic strength increases the fluorescence of ANS bound to resting SMP, but has no effect on the energy dependent response[124,224]). The length of time for which the particles remained aerobic increased, and the extent of the response decreased (both at 500nm and at 400nm) as the ionic strength was increased with sodium chloride (fig.37). This indicates a slowing down of the rate of oxidation of succinate with a corresponding increase in energy leakage (hence a decrease in probe response). Measurement of the pH dependence of the response was rather limited by the fact that the particles only respired within a fairly narrow pH range (6 - 8). Maximal

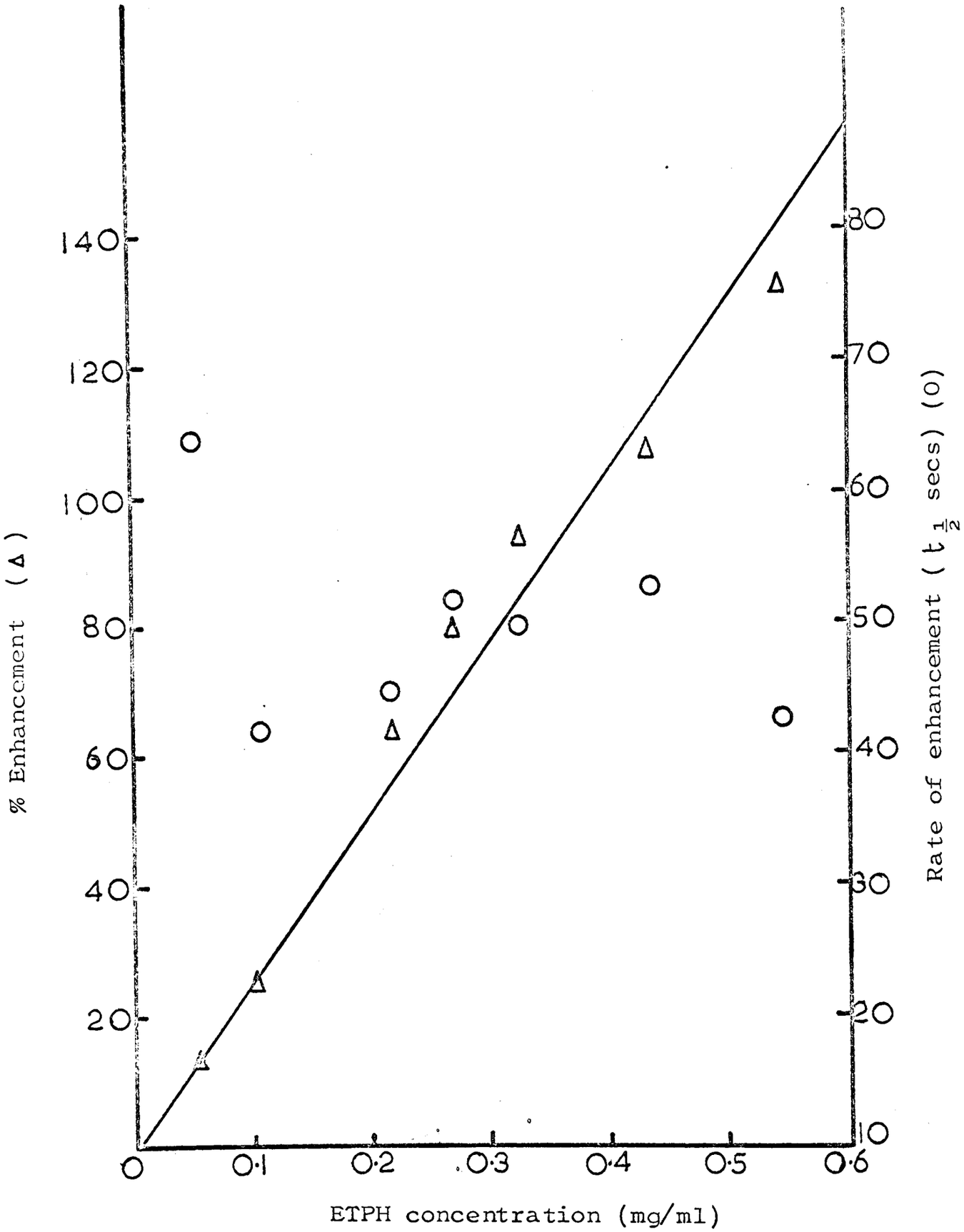

Fig.40. Effect of varying ETPH concentration on PS response.

PS 25 μM other conditions as in fig.36.

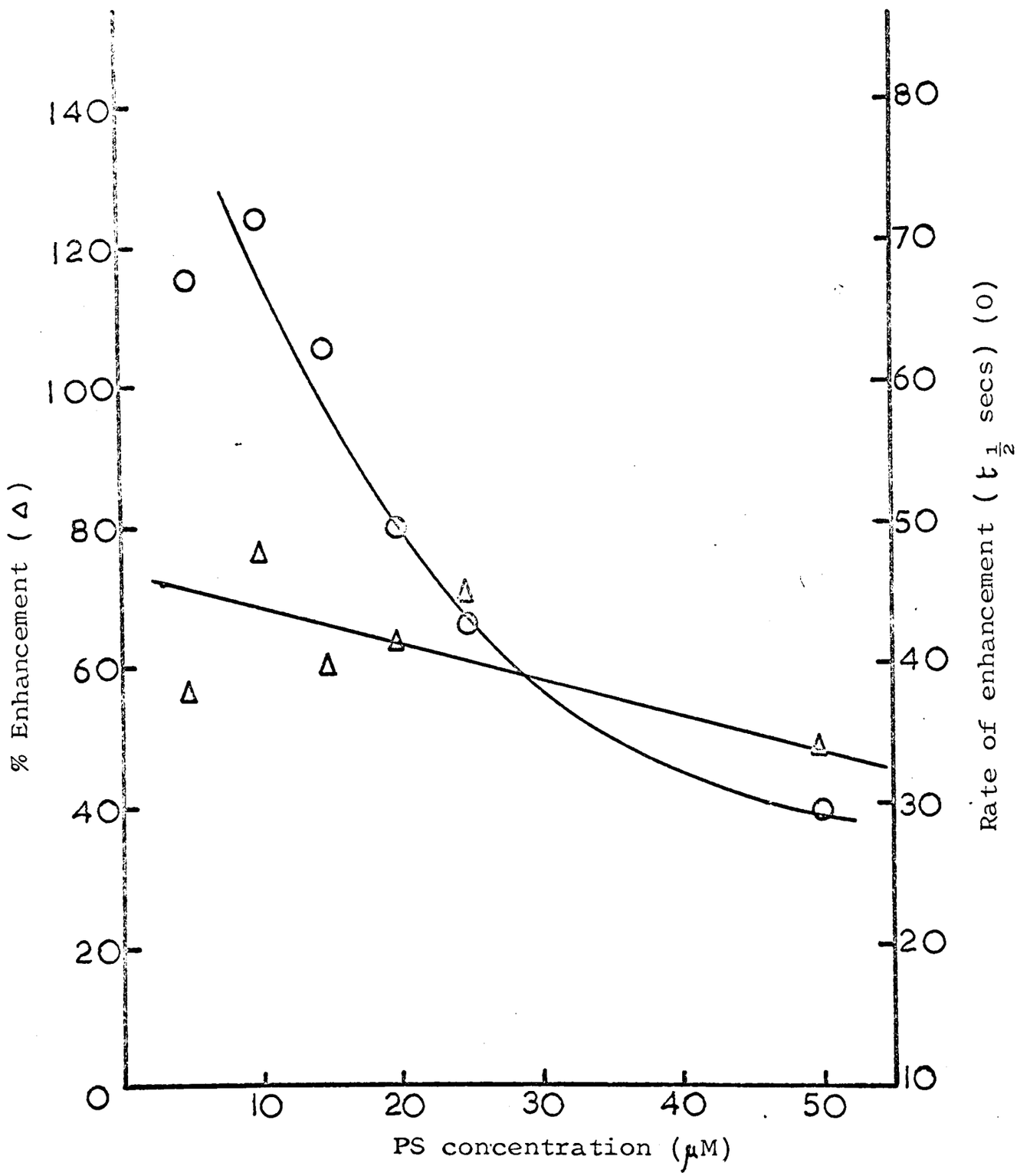

Fig.39. Effect of varying PS concentration on PS response.

ETPH 0.28 mg/ml, other conditions as in fig.36.

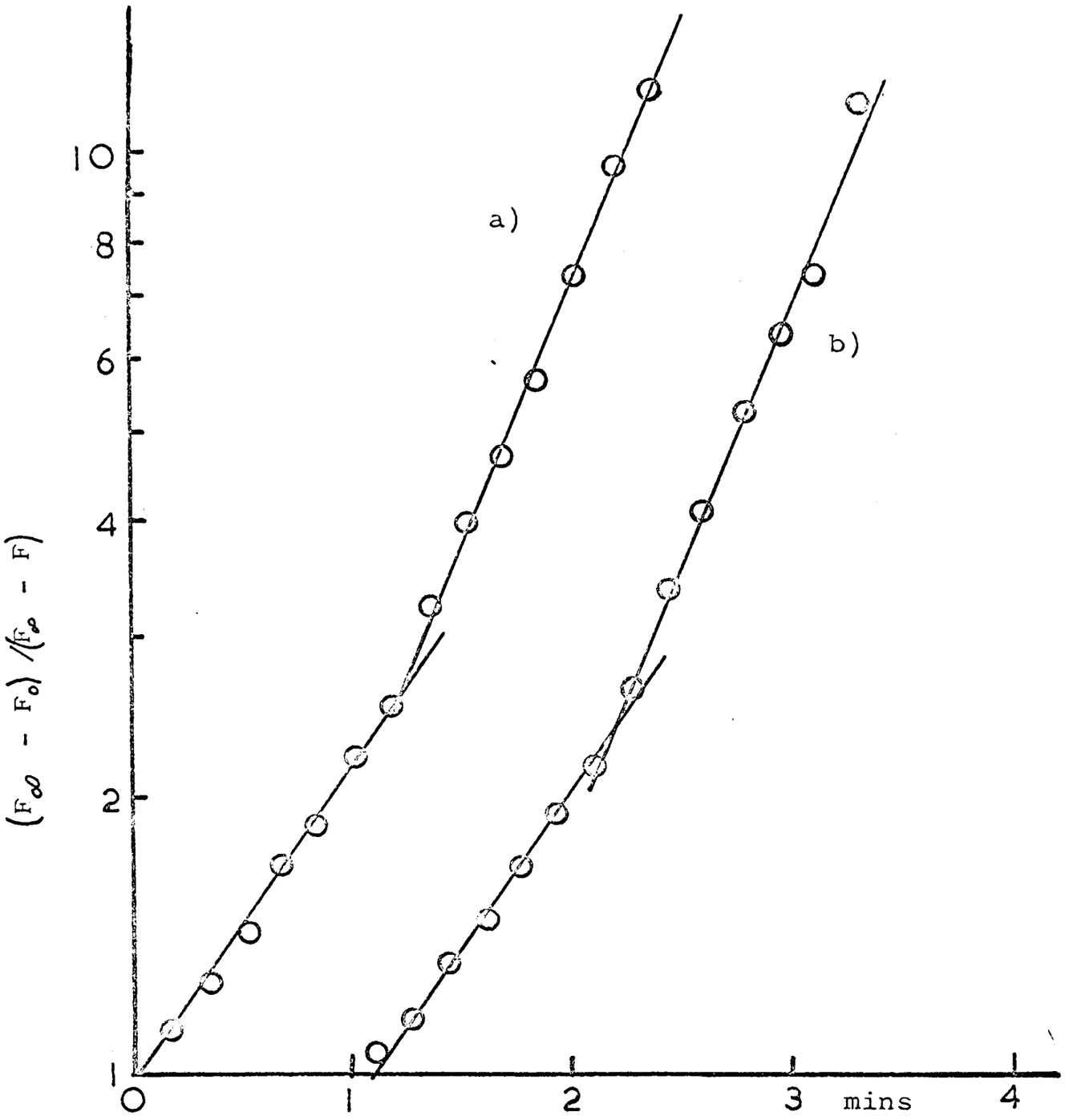

Fig.38. Kinetics of PS response to energisation.

Conditions as in fig.36.

a) PS added before energisation

b) PS added after energisation

Table 8

	Life-time (nsec)	
	400nm	500nm
1mM	46	48
0.5mM PS	52	44
250μM PS	54	38
125μM PS	50	23 + 42
25μM PS	53	10 + a longer
25μM PS (deoxygenated)	56	14 + 30
25μM PS + ETPH	34	11
25μM PS + ETPH(energised)	34	24

response was at pH 6.8.

There was very little change in polarisation of PS fluorescence on energisation or on increasing PS concentration ($p \approx 0$). Measurement of PS life-times was complicated by the difficulty in separating the excimer and monomer fluorescence with the filter system of the instrument. This difficulty is particularly well illustrated by the variation in life-time measured at 500nm with concentration (Table 8).

A more fruitful approach was to examine the kinetics of the PS response. Energisation of the ETPH/PS complex produced a biphasic increase in fluorescence at 500nm, an almost identical plot being obtained by adding PS to ETPH which had been respiring for 5 mins (fig.38). With ANS the enhancement caused by energisation is monophasic. The biphasic PS response is probably a result of the fact that the excimer fluorescence (used to follow the kinetics) is proportional to $[PS]^2$. Variation of the concentrations of PS and ETPH caused changes both in the extent of the enhancement, and in the rate of enhancement (figs.39, 40). Increasing ETPH concentration increased the % enhancement almost proportionately but had little effect on the rate. However, increasing PS concentration decreased the rate and slightly decreased the % enhancement. Variation in ETPH concentration will alter the amount of PS bound (and hence the enhancement) but should have no effect on the rate at which the energised

state is produced. On the other hand, increasing PS concentration will increase the proportion of free PS causing a decrease in the observed enhancement. High concentrations of PS apparently inhibit ETPH.

Probe binding parameters

Binding parameters were determined for ANS and MNS in the conventional way by measuring the limiting enhancements of fluorescence, and treating the data by Scatchard's methods[225]. These results showed that on energisation there was an increase in binding of the two probes, and also an increase in quantum yield (as also shown by increased life-time - see below). This approach, however, makes assumptions about the homogeneity of binding sites etc., and is not applicable to PS where there is no enhancement on binding. An independent method was needed. The first approach to the problem was to use BSA to "mop up" free ANS, and to measure the ANS concentration by the enhancement caused by BSA. Addition of BSA to a mixture of ETPH and ANS should give a rapid rise in fluorescence as free ANS binds to BSA, followed by a further slow change as ANS diffuses out of the membrane. However, it was found that BSA not only mopped up the free ANS, it also pulled ANS off the ETPH too rapidly for the two processes to be distinguished. With rapid mixing a titration curve could be obtained, but this yielded a meaningless Scatchard plot. The binding constant of PS could

not be derived from the variation of PS response with PS and ETPH concentration since a limiting response could not be obtained at high ETPH concentration where the bound PS concentration was too low for excimer formation to be detected.

A filtration method was then developed (p.41). A small sample of membrane-free solution was filtered off from the equilibrium mixture of probe and SMP (energised and resting). It was found that the best results were obtained using a glass fibre filter, rather than a Millipore one, since the latter tended rapidly to clog with membrane particles. The total amount of solution passed through the filter in order to obtain a small sample was always less than 10% of the total volume used. Protein determinations on the filtrate showed that under these conditions, no membrane passed through the filter. The concentration of free probe could then be determined by finding the concentration of probe in the small sample. For ANS this was done by adding a 5mg/ml BSA solution and measuring the resulting enhancement relative to a standard ANS solution. With PS the 400nm fluorescence was intense enough for the concentration to be measured by diluting the sample into buffer and measuring the fluorescence. With both probes it was necessary to measure the fluorescence relative to a blank to allow for probe adsorbed by the filter (ca 15%). The method was first checked using ANS, and a direct correlation between the results from fluorescence and those from

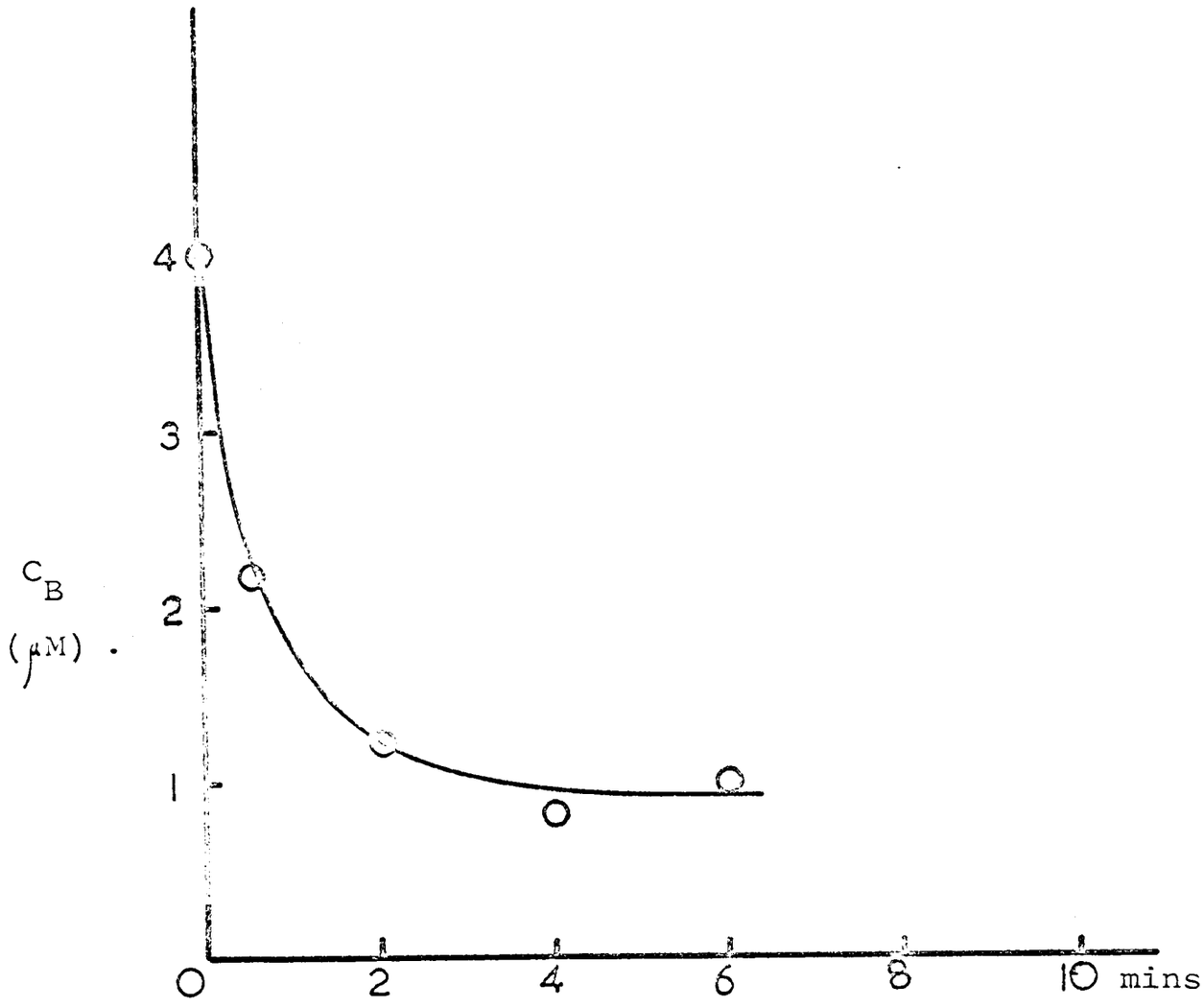

Fig.42. Uncoupling kinetics followed by direct binding (filtration technique). PS 12.5 μM, ETPH 0.45mg/ml. Succinate 25 mM, FCCP 1.25μM.

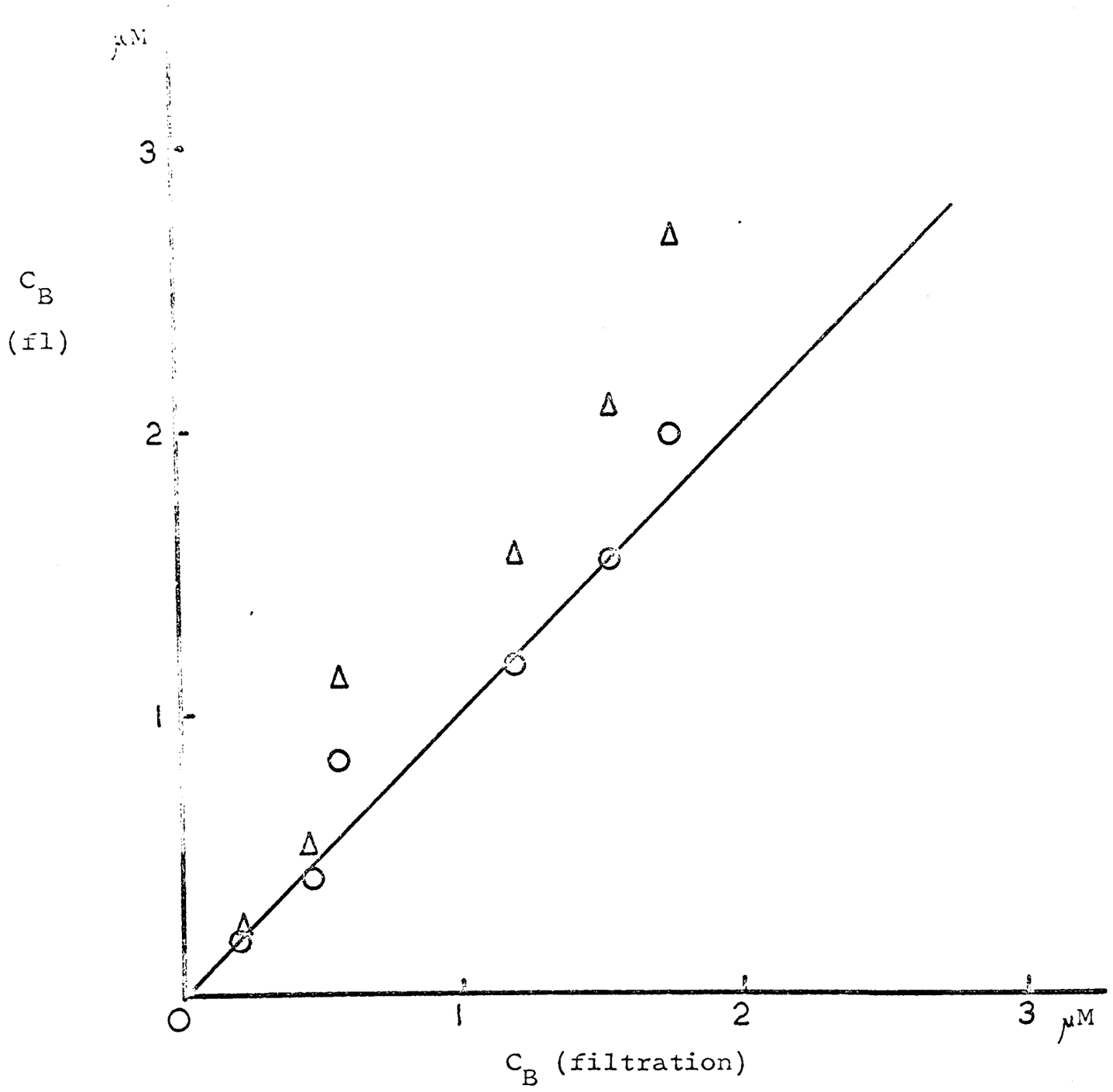

Fig.41. Correlation of binding results by fluorescence and the filtration technique. ANS 7.5 μM, ETPH 0.09-1.0 mg/ml. The line represents 1:1 correlation.

the filtration method was obtained (fig.41). The binding of PS to ETPH was then measured and an increase in binding was found on energisation, e.g. at a total PS concentration of 25 μM, the fraction bound to 0.5 mg/ml ETPH increased from 0.175 to 0.35. However, it proved impossible to obtain reproducible Scatchard plots. The method is only really reliable for comparing directly the amount of PS bound to resting and energised ETPH at given concentrations of PS and ETPH. This technique was also used to follow the rate of efflux of PS from energised particles after uncoupling (fig.42). The results confirmed those derived from fluorescence measurements (see below).

Uncoupling kinetics*

It was not possible to interpret the different rates of response of PS, ANS and MNS to energisation for three reasons:-

(i) the energisation process is limited by the sluggish turnover of succinate dehydrogenase.

(ii) the probes move into the membrane at a similar rate to that of energisation.

(iii) the response of PS (at 500nm) to energisation involves a lag phase. The first difficulty could have been overcome by using oxygen pulses on anaerobic particles, but this would still have involved a lag phase in the PS response and probe movement. If the PS lag phase was in fact due to a sensitivity limitation,

*These experiments on uncoupling kinetics were performed in collaboration with R.B. Freedman[223] and D.J. Hancock[226].

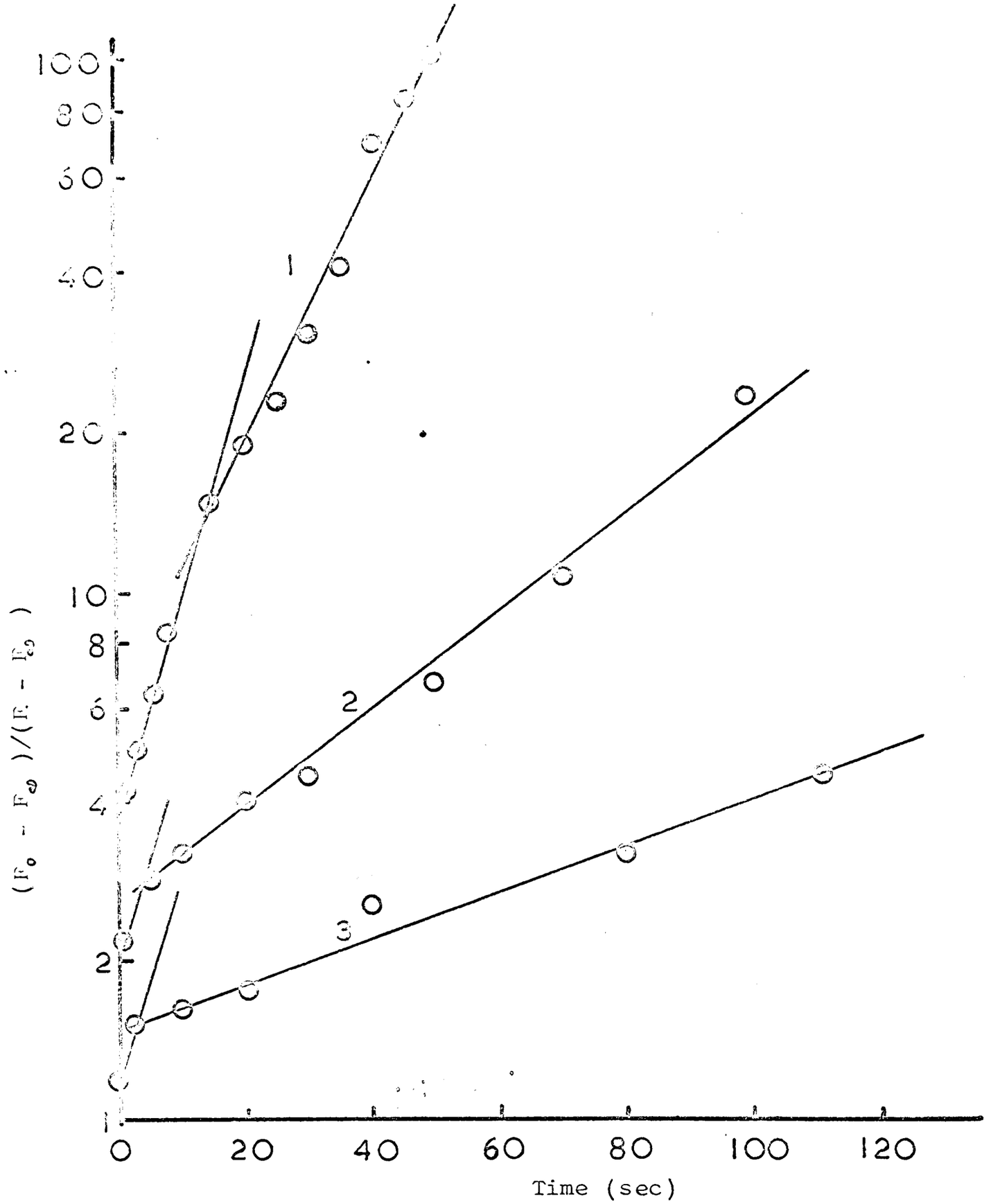

Fig.43. Uncoupling kinetics of ANS(1), MNS(3) and PS(2). Conditions as in fig. 36. Probe concentrations: 10μM.

de-energisation should have had an advance phase at the end of the change (i.e. the PS excimer fluorescence detected would disappear before the change was complete). In order to investigate this possibility, the kinetics of the responses of the probes to uncoupling by FCCP were examined. It was hoped that the uncoupling process would not be rate limiting (as succinate dehydrogenase is rate limiting), and that this would be separate from probe movement. This was in fact found to be the case. FCCP was added rapidly to energised particles in the presence of the three probes, and the decrease in fluorescence was followed on a recorder set at high chart speed. The results were plotted as a semi-log plot ($\log (F_o - F_\infty)/(F - F_\infty)$ vs t) and are shown in fig.43. All three probes showed a biphasic decrease in fluorescence. The fast phases had the same half time of 2 sec, while the slow phases had different half times:- ANS, 12sec; MNS, 60sec; PS, 30sec. (N.B. the two ANS half times are very similar, and allowance had to be made for the contribution of the slow phase to the fast phase). These results indicated a common rapid phase - interpreted as a structural transition of the membrane, followed by a slower phase characteristic of the different probes - interpreted as the different rates at which they are expelled from the membrane after uncoupling. Increase in ETPH concentration caused no slowing down of the explusion

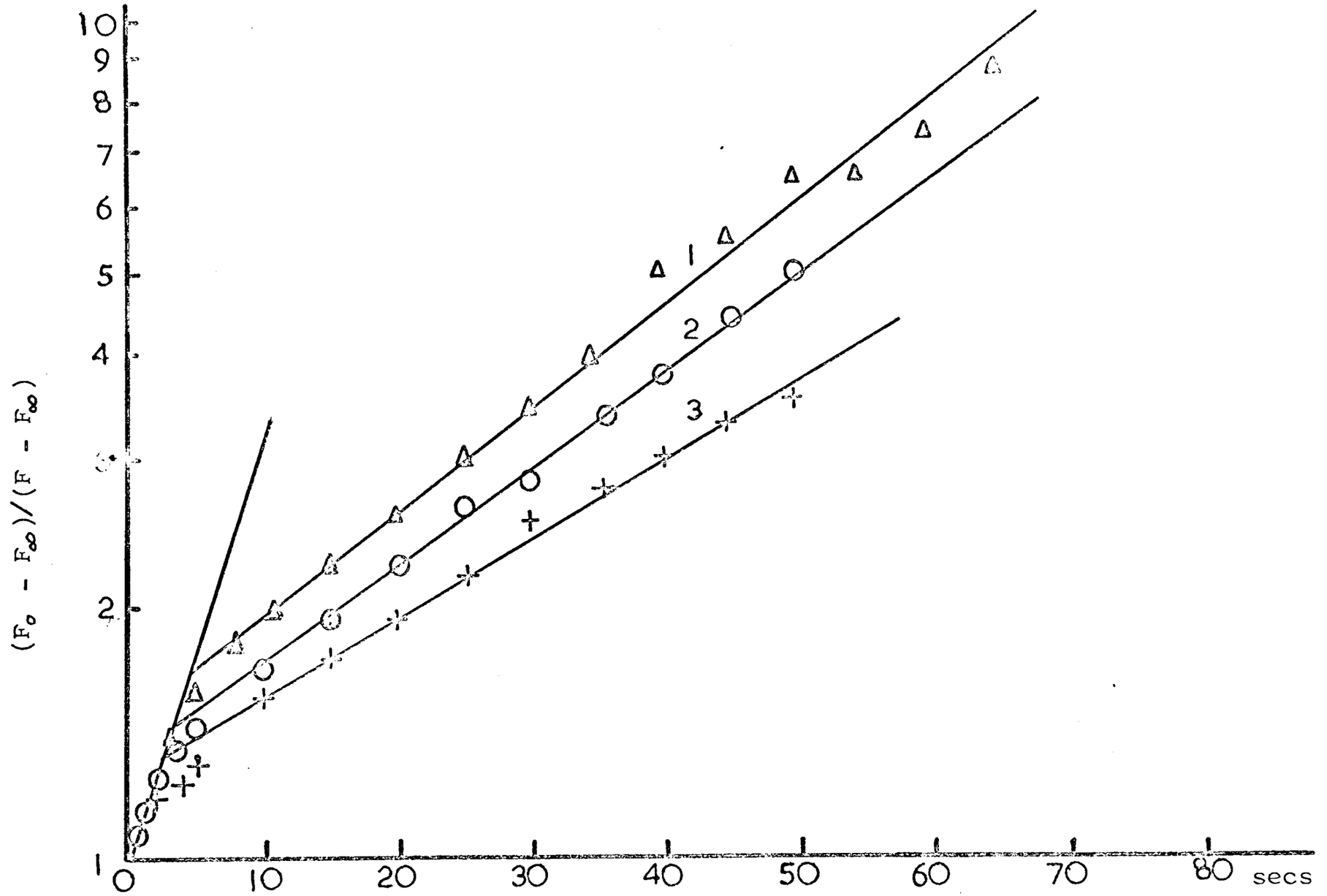

Fig.44. Effect of varying ETPH concentration on PS response to uncoupling. 1. 0.12 mg/ml; 2. 0.24 mg/ml; 3. 0.36 mg/ml. Other conditions as in fig.36.

of PS (fig.44). For comparison the rate of expulsion of ANS on dilution of ETPH was determined. Small volumes of ETPH (20λ of a 15mg/ml soln.) and a probe (10λ of a 10mM soln.) were equilibrated and then rapidly diluted into a cuvette of buffer. The rate of decrease of fluorescence was mono-phasic with a half time of 12 ± 2 sec.[225]. The expulsion of PS as determined by the filtration method had a half-life of 30 ± 5 secs.

Since the three probes appear to detect the same rapid membrane change it is reasonable to assume that they bind to the same or similar areas of the membrane. Comparison of the fluorescence polarisation and fluorescence life-times of MNS and ANS in the presence of resting and energised ETPH suggested that the viscosity of their microenvironment increased slightly on energisation

	γ_R	γ_E	P_R	P_E
ANS	5	9	0.22	0.18
MNS	4	8	0.17	0.14

applying the formula $\frac{p_2}{p_1}\left(\frac{p_o - p_1}{p_o - p_2}\right) = \frac{\eta_2\,\gamma_1}{\eta_1\,\gamma_2}$ (obtained from the formula on p.12) it can be seen that $\frac{\eta_2}{\eta_1} = 1.25$.

This small change is hardly likely to affect the fluorescence of PS very much, and in any case would cause a <u>decrease</u> in excimer formation on energisation. Trivial depolarisation of the emitted

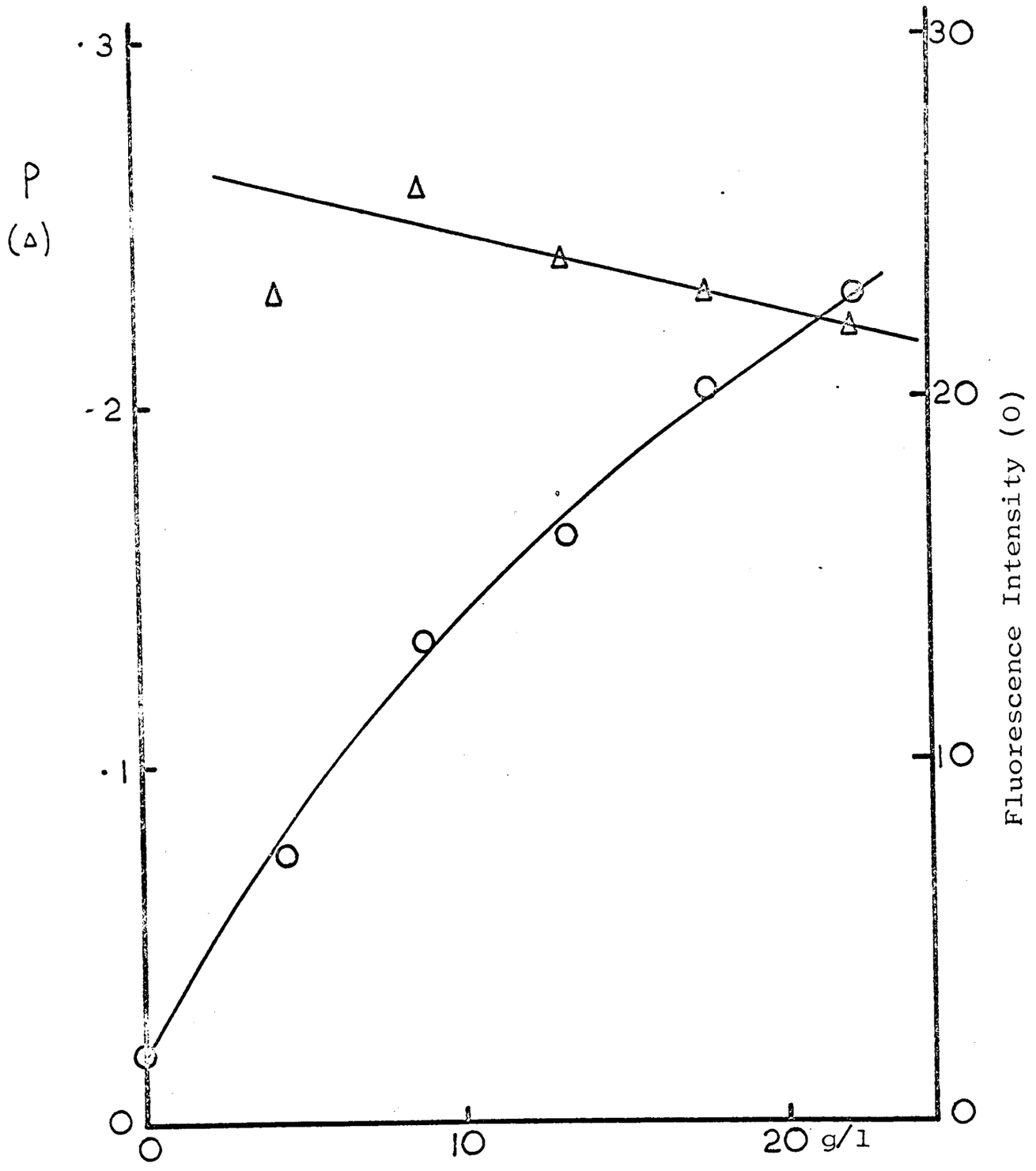

Fig.45. Fluorescence properties of ANS (5μM) in methyl cellulose solutions.

light was ruled out by determining the polarisation of DNS-BSA in the presence and absence of ETPH. A small change (0.2 to 0.17) was observed on addition of ETPH with no further change on energisation with succinate.

The above values of fluorescence polarisation indicate that MNS and ANS are not as restricted in the membrane as ANS bound to protein ($p = 0.4$)[44,225]. This would suggest that they bind in the lipid phase rather than to protein in the membrane. However, the variation of polarisation of ANS in methyl cellulose solutions (fig.45) showed a similar value of $p = 0.22$.

The above results could be explained in terms of an extrusion of water from the membrane on energisation. This would:- a) decrease the volume of the pocket in which the probes bind,

b) decrease the polarity of the probe environment, and hence increase the ANS and MNS quantum yields.

c) increase ANS and MNS quantum yields by decreased quenching. (See discussion).

What was now needed was an independent method of looking at membrane bound water to see if it did in fact move. One possibility was the use of nmr. The nmr signal due to water protons is relaxed by paramagnetic ions such as Mn^{2+}, and the rate of relaxation changes with the environment of the manganese and water. This technique has been successfully used to detect

conformational changes in enzymes[3]. *Initial experiments showed that normal ETPH contained high concentrations of Mn^{2+} (ca 1mM estimated by esr) which complexed with the succinate used for energisation. This caused marked changes in the observed relaxation rates. By using SMP prepared in the absence of Mn^{2+} [112], it was possible to overcome this problem. 30% increases in relaxation rate were observed on energisation, but it became obvious that these changes were very complex, depending to a large extent on the oxygen concentration.

A second possibility was to look for an isotope effect on the ANS fluorescence changes when the experiments were performed in a D_2O buffer (prepared simply by replacing water by D_2O - hence it contained ca 5% water). Water is thought to quench ANS fluorescence[20], and an isotope effect of 2.8 was found in free solution. If ANS in the membrane is in contact with water (either bulk phase or pockets of structured water) an isotope effect should be detected. If energisation produced a movement of water there may be a difference in isotope effect between energised and resting ETPH. Experiments were carried out to compare the ANS fluorescence enhancements and rates of uncoupling in H_2O and D_2O at a variety of ETPH concentrations.

At all ETPH concentrations, D_2O caused a dramatic slowing

*I am indebted to Dr. R.A. Dwek for performing the proton relaxation measurements.

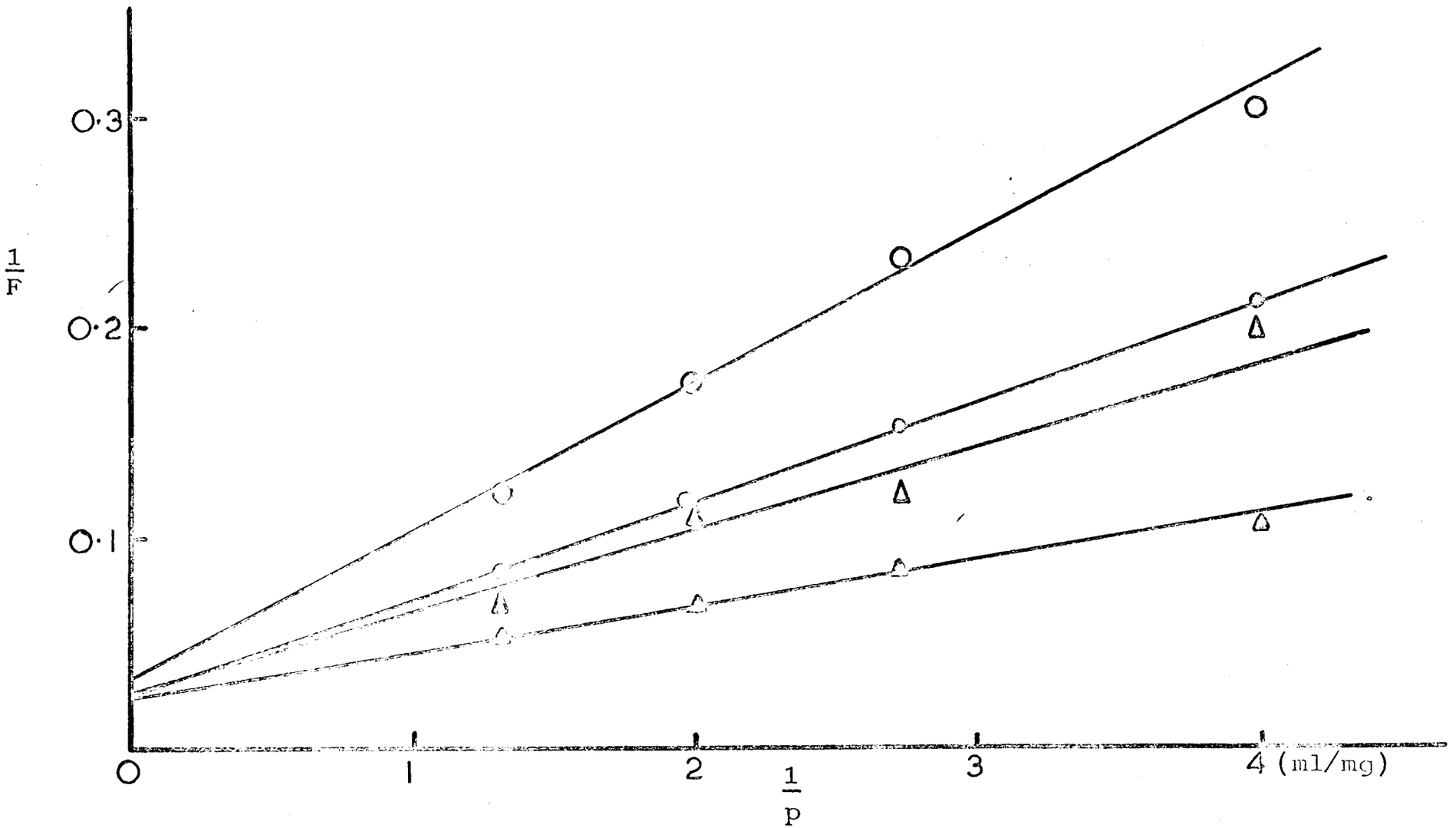

Fig.49. Double reciprocal plots for ANS binding to energised and resting ETPH in D_2O and H_2O. O resting in H_2O, Δ energised in H_2O; ○ resting in D_2O; ▲ energised in D_2O.

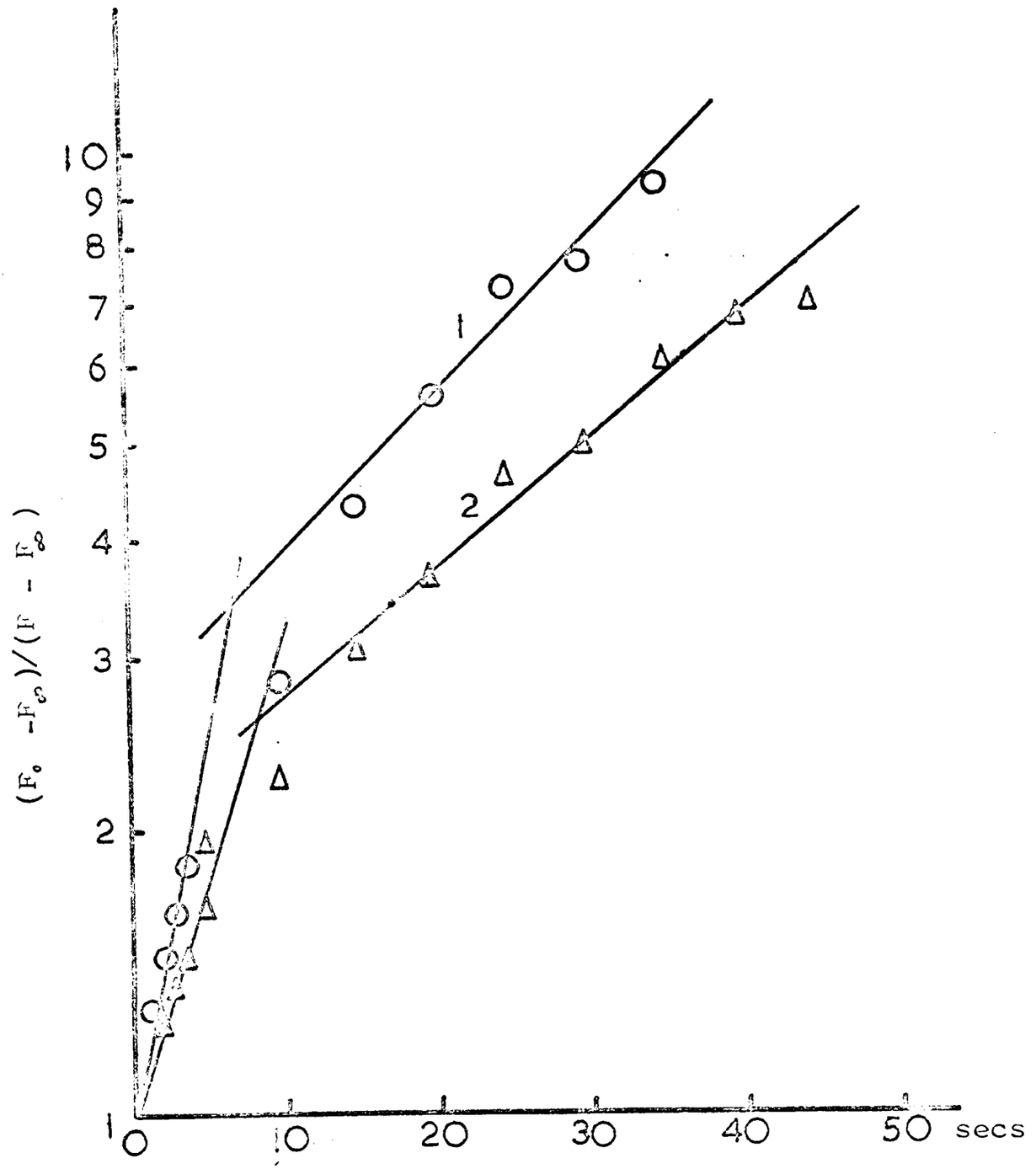

Fig.48. Effect of D_2O on the uncoupling kinetics of ANS. ANS 10 μM, ETPH 0.25mg/ml, Succinate 25 mM, FCCP 2μM.

1. H_2O; 2. D_2O

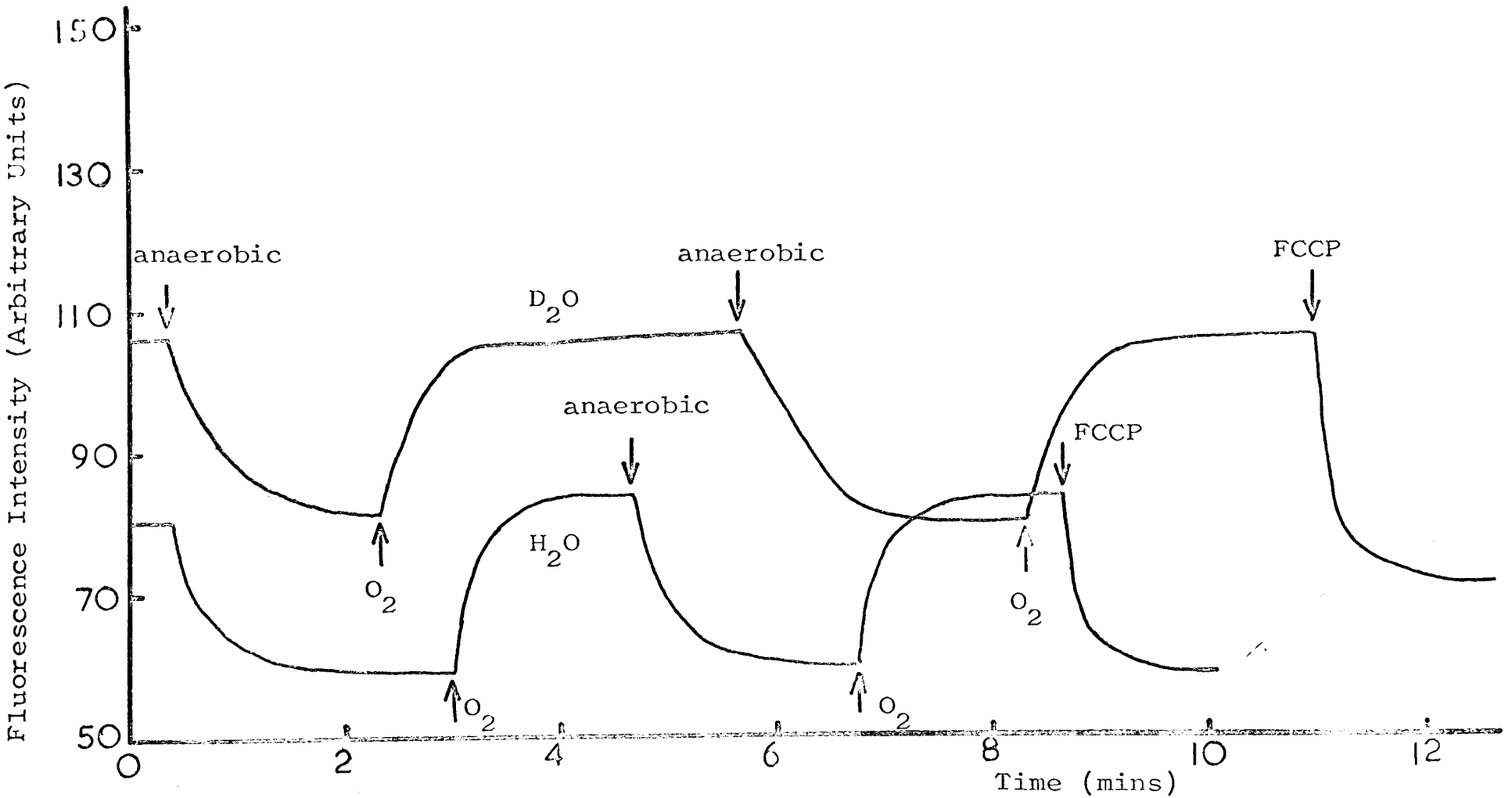

Fig.47. Effect of D_2O and H_2O on the ANS response to oxygen pulses. ETPH 0.75 mg/ml. Other conditions as fig.36. O_2 was added by rapidly bubbling 20mls of air through the solution.

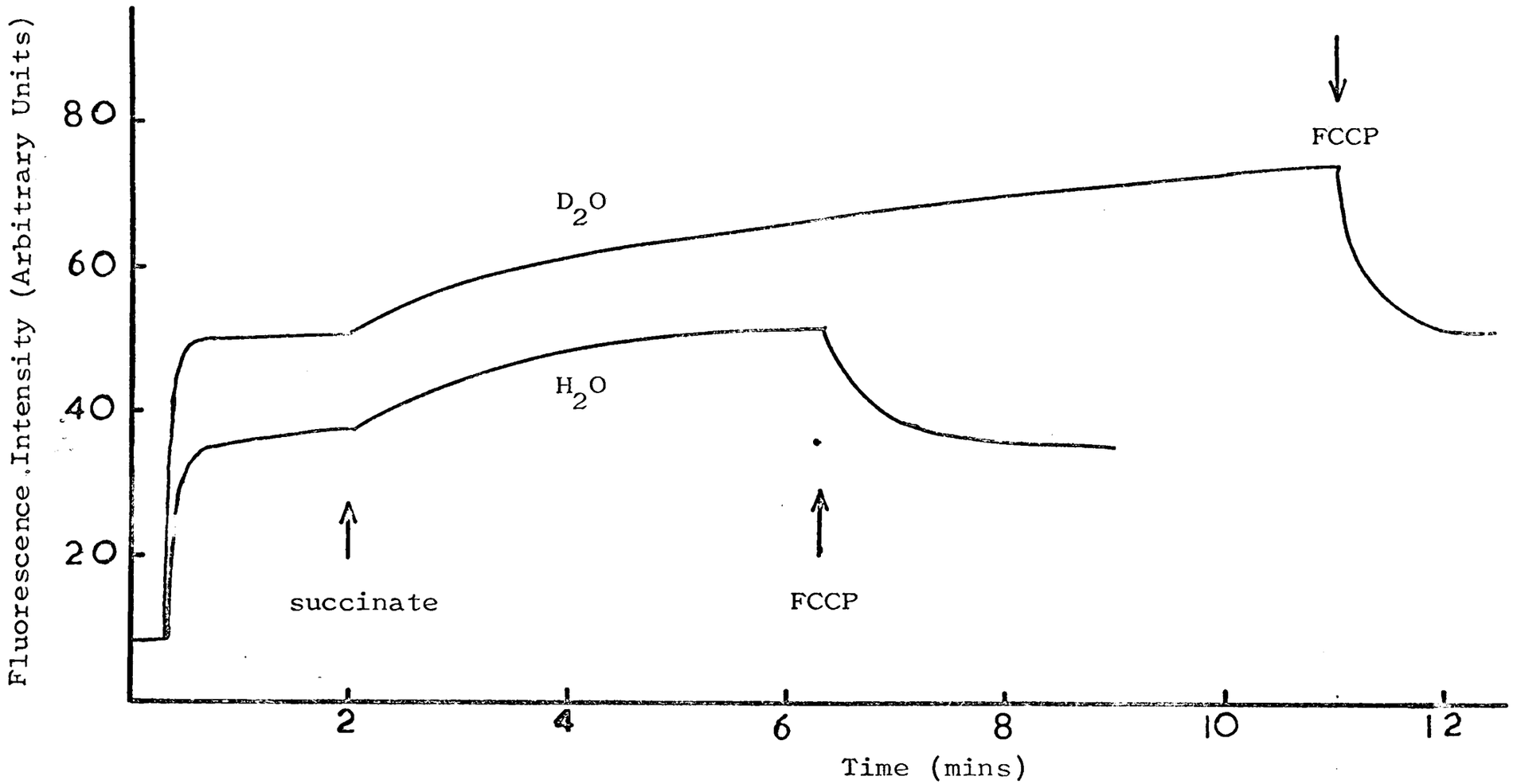

Fig.46. Effect of D_2O and H_2O on the ANS response to energy dependent changes in ETPH (0.5 mg/ml). ANS (10 μM) fluorescence emission at 480nm, excited at 380nm.

down of the energisation process (fig.46). ANS also appeared to bind to ETPH more slowly in D_2O. The isotope effects were measured as:-

Buffer	ETPH (resting)	ETPH (energised)
2.8	1.5 ± 0.2	1.6 ± 0.2

The effect for energised ETPH must be regarded as a lower limit because the membrane took longer to become energised in D_2O, and hence must have leaked more energy away giving an observed enhancement below the true value. Energisation could make H_2O/D_2O exchange easier within the membrane giving a progressive increase in enhancement on repeated oxygen pulses. This was not observed (fig.47), leading to the conclusion that there is rapid exchange in both resting and energised particles.

The isotope effects on the kinetics of the changes were less marked. That for the slow phase of the uncoupling kinetics was 1.2 (fig.48). Contrary to what was observed above, this suggests that D_2O has little effect on the rate at which ANS moves in and out of the membrane. Double reciprocal plots (fig.49) for resting and energised ETPH showed that the change in ANS quantum yield on energisation was lower in D_2O (1.2) than in H_2O (2.0).

The isotope effect on MNS bound to ETPH is slightly larger relative to the isotope effect in water, than is that of ANS.

Buffer	ETPH (resting)	ETPH (energised)
2.4	1.5	1.2

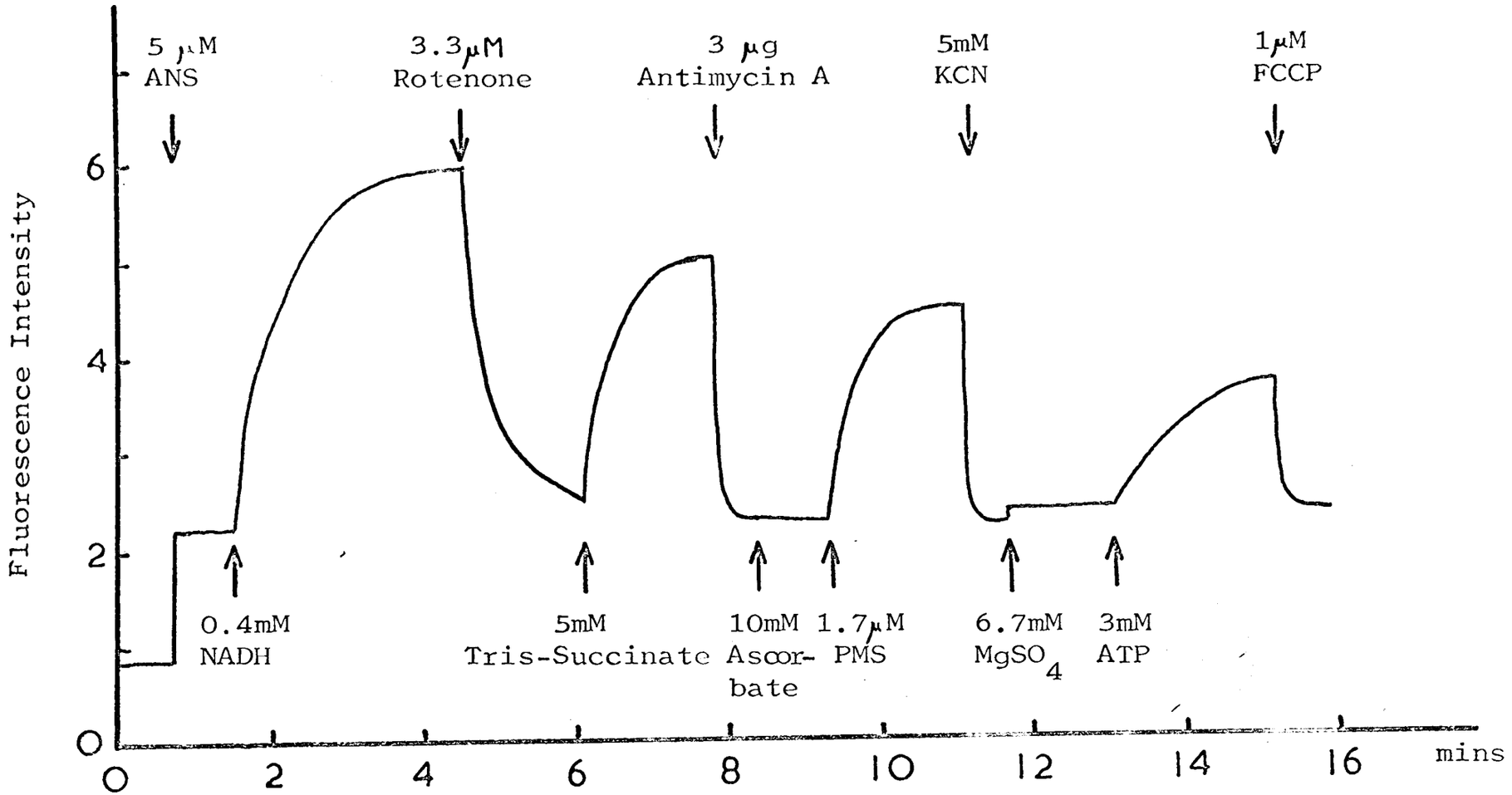

Fig.50. ANS responses in ETPH energised by different substrates.

170 mM sucrose, 30 mM Tris Acetic pH 7.5 + 0.9 mg ETPH.

Final Vol.3ml.

Data from ref.227

Position of binding

In an attempt to discover more about the nature of the membrane change detected by the three probes, the particles were energised at different points along the electron transfer chain. An ANS response was obtained using NADH, succinate or ascorbate/TMPD as substrates, though the extent of the response fell along this series (fig.50 - this data, kindly supplied by Dr. C.P. Lee of the Johnson Research Foundation, Philadelphia, illustrates the point better than that obtained by the author).

Covalent probes

A way of overcoming the difficulty of probe movement on energisation, is to attach the probe covalently to the membrane. Preliminary experiments showed that erythrocyte stroma could be labelled with FITC (fluorescein isothiocyanate) or MNS-Cl on celite, but that the attached label did not respond to ionic strength or pH changes, unlike the corresponding non-covalent probes[226]. The renewed interest in the possible importance of -SH groups in various components of the electron transfer chain[208] prompted an attempt to label ETPH with the -SH reagent, NBD-Cl. This reagent is not fluorescent, but produces a fluorescent adduct[228].

The reagent reacted very slowly with resting ETPH, and apparently very rapidly with ETPH oxidising NADH. However, it

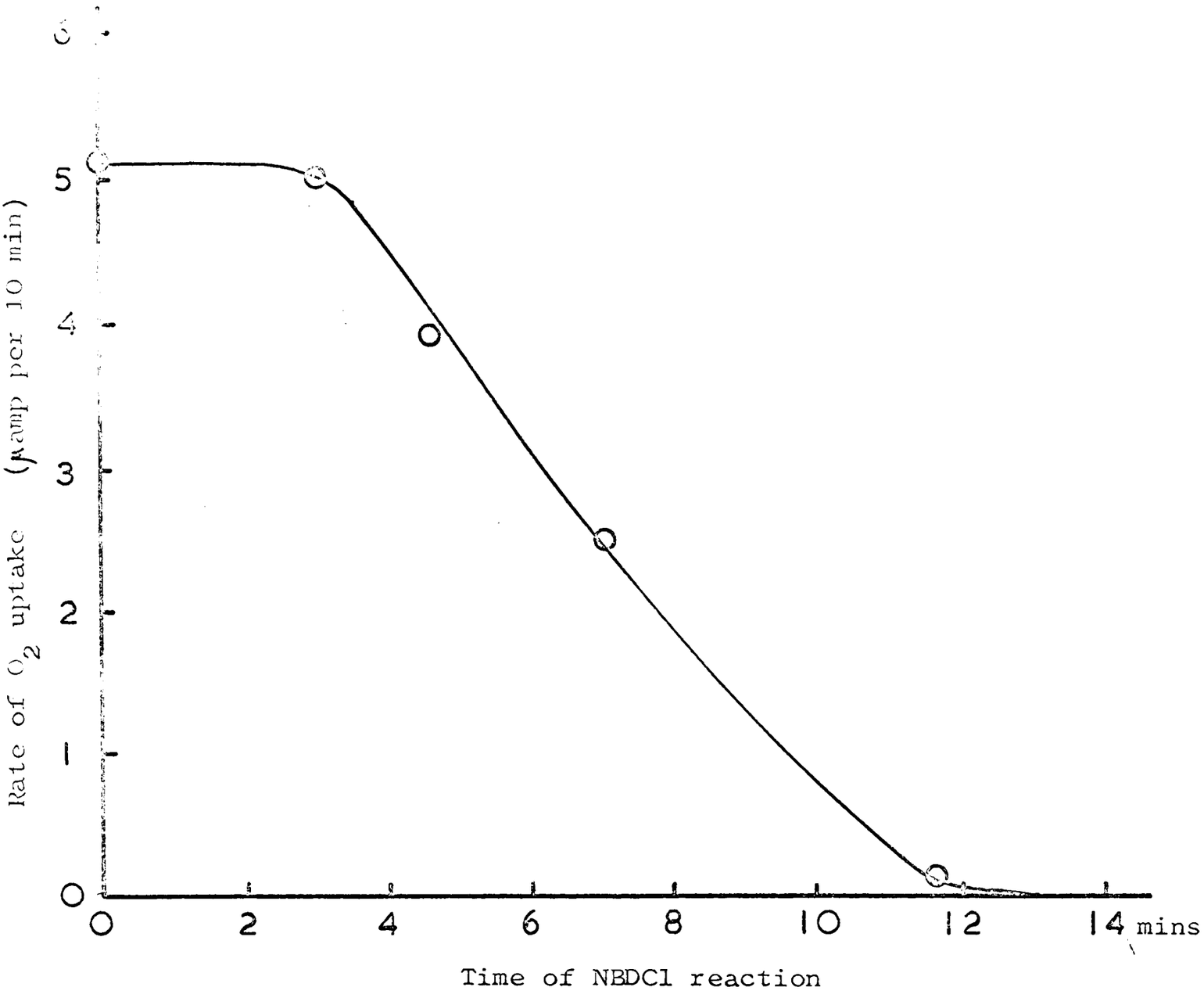

Fig.52. Inhibition of ETPH (0.5mg/ml) by reaction with NBD-Cl (375μM).

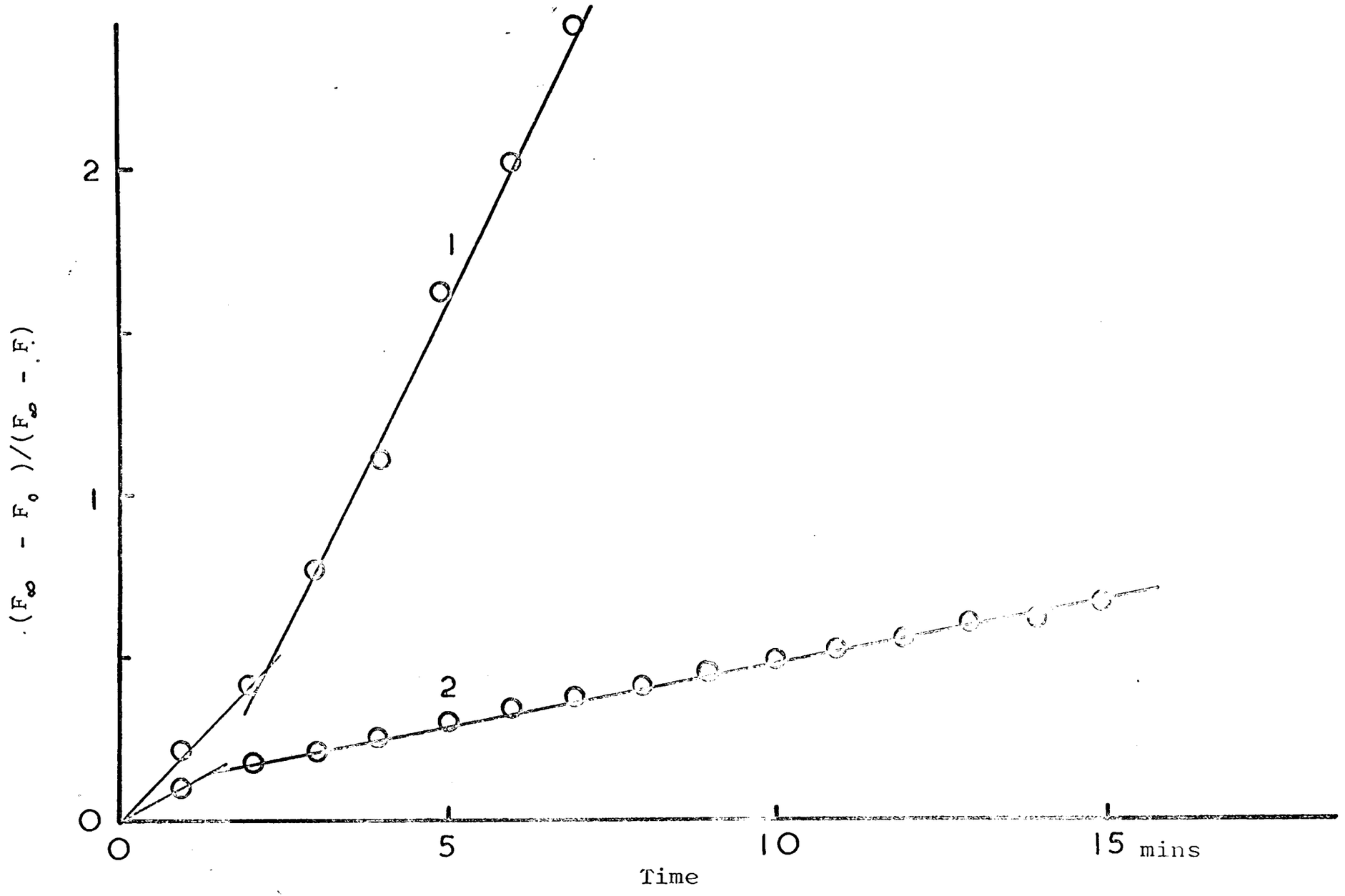

Fig.51. Rates of reaction of NBD-Cl with ESMP(1) and ETPH (2) (0.34 mg/ml).

turned out that the latter was in fact the rapid formation of a charge transfer complex between NADH and NBD-Cl which disappeared just as rapidly, as the two reacted. ETPH energised with succinate reacted faster than resting ETPH which suggested that the -SH groups were more exposed after energisation. Further investigation of the reaction of NBD-Cl with both ETPH and ESMP showed that the apparent rate of reaction increased with the elapsed time of energisation. Analysis of the data on a semi-log plot showed that in fact the rates of reaction were very similar, it was merely the extents of reaction that were different i.e. more -SH groups were exposed on energisation. It appeared that ESMP reacted much faster (but less extensively) than ETPH (fig.51).

However, the labelled membrane was totally inhibited with respect to succinate oxidation (fig.52) before sufficient label had been introduced for examining energy dependent changes in the fluorescence of the bound probe.

Neutral probes and others

The experiments reported in the previous sections have gone some way towards answering the first two questions posed on page 69, i.e. "What happens to the membrane to cause the probe to respond?" and "Where is the probe binding?" The current section investigates the third question i.e. "What structural characteristics are needed for a fluorescent molecule to probe

energy dependent changes?" Neutralisation of the negative charge of MNS had abolished its probe response in the GDH system (p.51). This was the logical structural modification to make here since it was quite possible that the negative charge on ANS, MNS and PS was important in directing the probe to the area in which it could sense the energy dependent changes. The three amides of MNS provided an opportunity of studying the effect both of neutralising the charge, and of increasing the lipophilicity of the molecule. The fluorescence of all three was enhanced by ETPH, but none of them responded to energisation. However, the least lipophilic (MNS-NH_2 and MNS-NHC_2H_5) had fast and slow phases like those observed with ANS and MNS, while the most lipophilic had a slow phase only[225]. Thus it was apparent that a negative charge is necessary for a probe to respond to the energy dependent change, and that altering the hydrophobic nature of the probe altered the way in which it bound to SMP. The questions now to be answered were:-

a) How do even more lipophilic fluorescent molecules behave (even the MNS amides have a marked dipole moment due to the -SO_2NH- group)?

b) Will a positively charged probe show the same behaviour?

c) Does the negative charge have to be close to the fluorophore as was found with GDH?

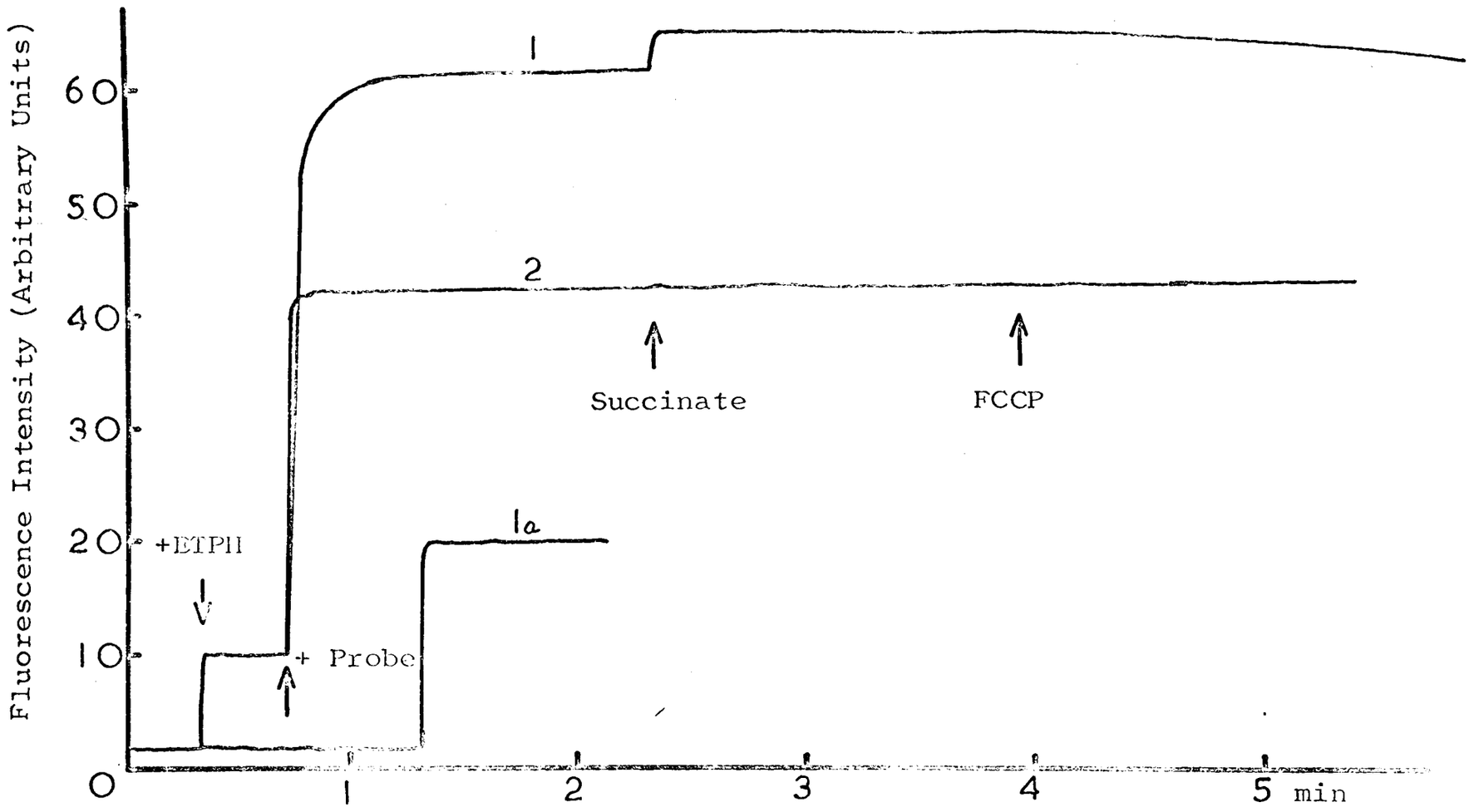

Fig.55. Responses of NPN and retinol to energisation of ETPH.

1. Retinol excited at 355 nm, emission at 465 nm. 1a Retinol in buffer.

2. NPN excited at 350nm, emission at 420nm. Other conditions as in fig.3

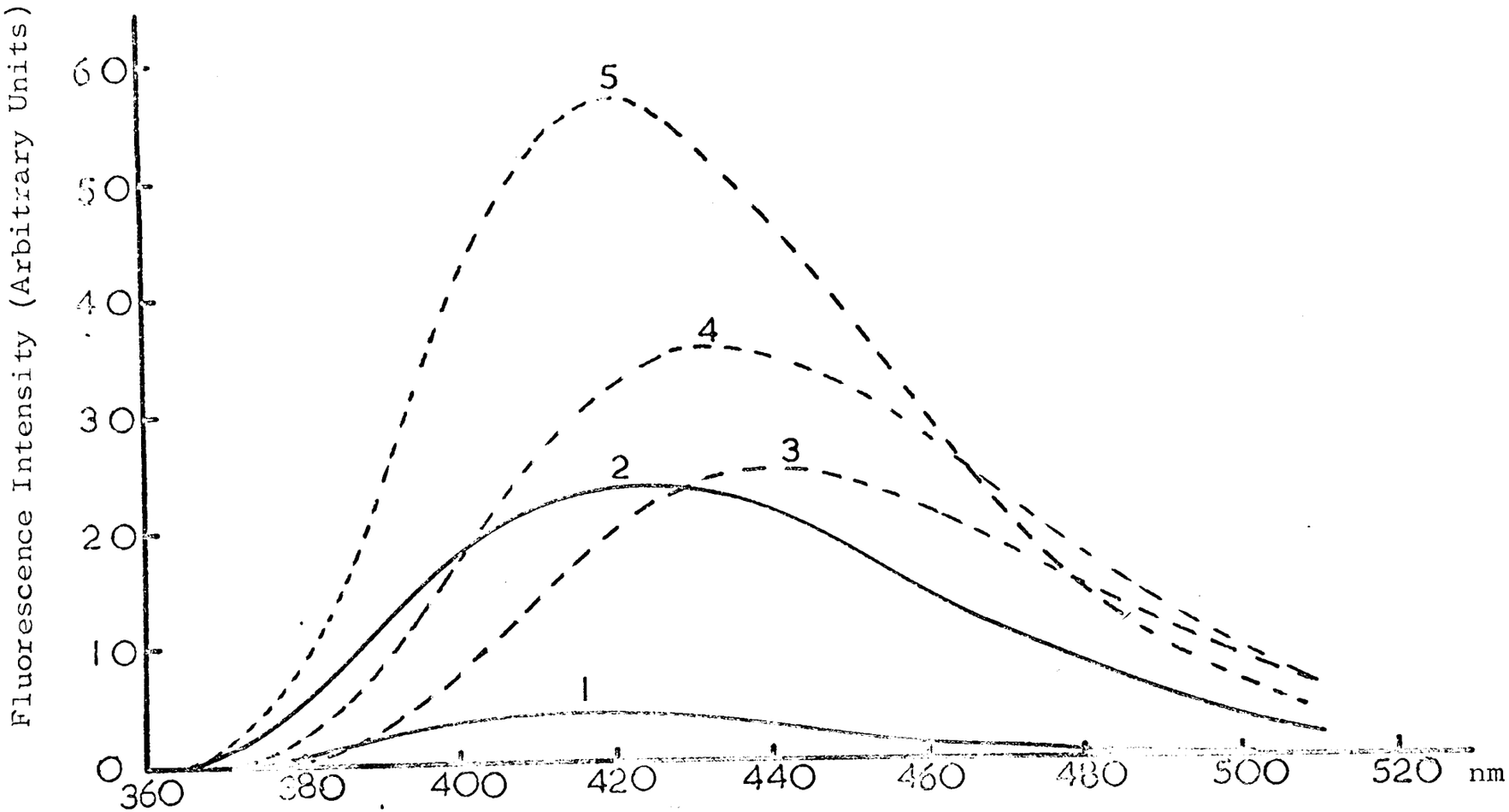

Fig.54. Fluorescence emission spectra of 10 μM NPN in ETPH, excited at 340nm.

Bandwidths: 10nm for excitation, 2mm for emission.

1. Buffer 2. ETPH (0.33 mg/ml) resting and energised.

3. 50% EtOH 4. 75% EtOH 5. 100% EtOH

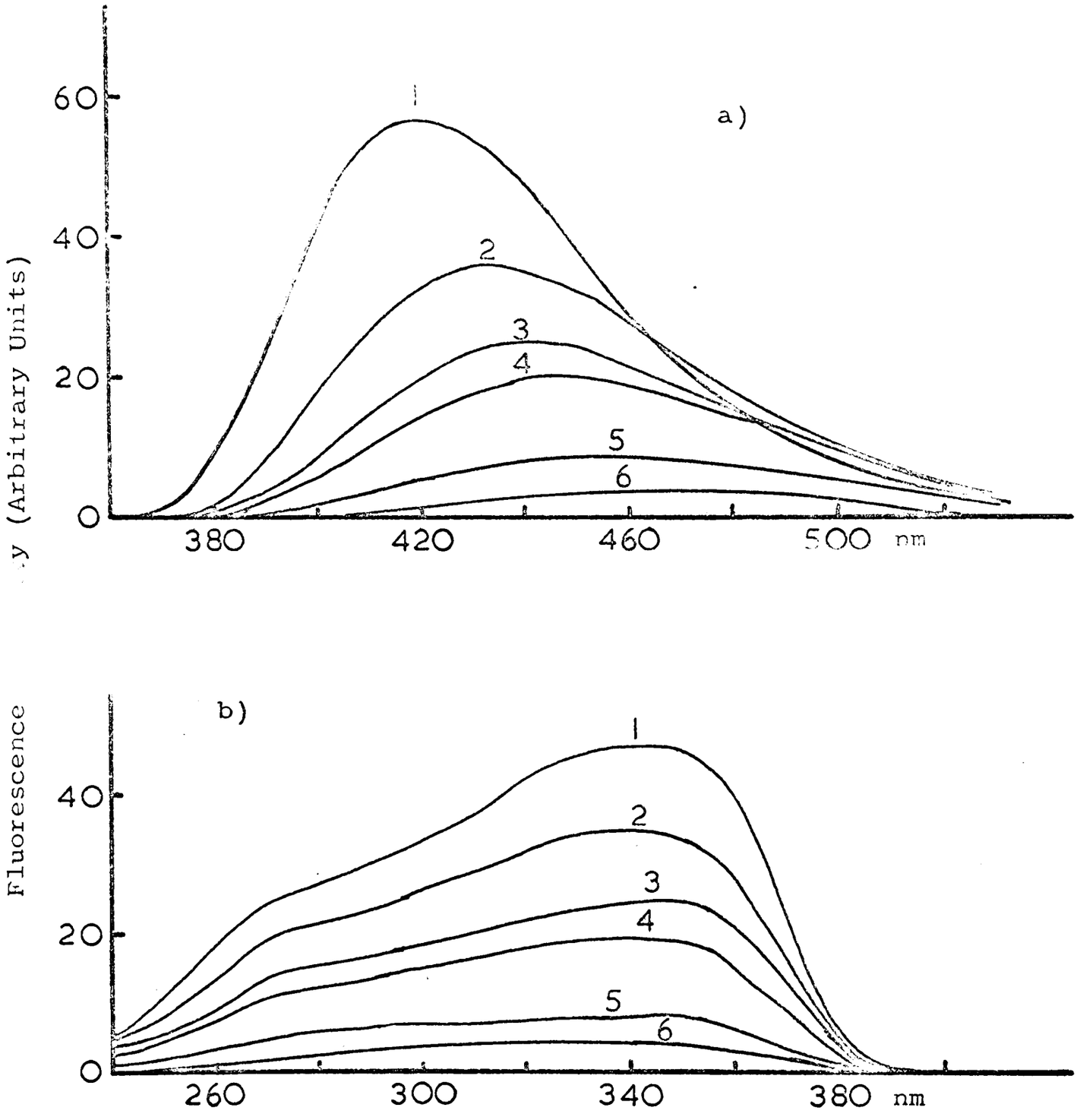

Fig.53. Fluorescence spectra of 10 μM NPN in ethanol/water mixtures a) excited at 340nm (10nm band width) with 2nm band width b) observed at 440 nm (2nm band width) with 10nm band width.

1. EtOH 2. 75% EtOH 3. 50% EtOH 4. 40% EtOH 5. 25% EtOH 6. H_2O

d) Will any negative charge do, or does it have to be a sulphonate group?

Two less polar probes were chosen to investigate question a):- N-phenyl-1-naphthylamine (NPN) is ANS without the sulphonate group, and ought to have similar fluorescence properties; retinol, the fluorescence of which depends upon the constraint placed upon the conjugated side chain. NPN showed the expected blue shift and enhancement of fluorescence in water/ethanol mixtures (fig.53) with a shift of ca 50nm between water and ethanol. Addition of ETPH produced a rapid enhancement of fluorescence with a small slow phase, indicating rapid binding to the membrane (cf MNS-$NHC_{10}H_{21}$ above). However, there was no further change on energisation of the ETPH (figs. 54 and 55). It is interesting that although the intensity corresponds to ca 50% ethanol the wavelength maximum corresponds to ca 90% ethanol (fig.54), another example of the danger of equating intensity with binding site polarity. Similar results were obtained with retinol (and retinol palmitate) though retinol appeared to bind to ETPH more slowly than NPN. There was a rapid enhancement of fluorescence on addition of ETPH, followed by a slow phase (fig.55). There was also a small response to energisation which was not reversed by FCCP (i.e. not, therefore, energy dependent).

The obvious conclusion is that these two molecules are

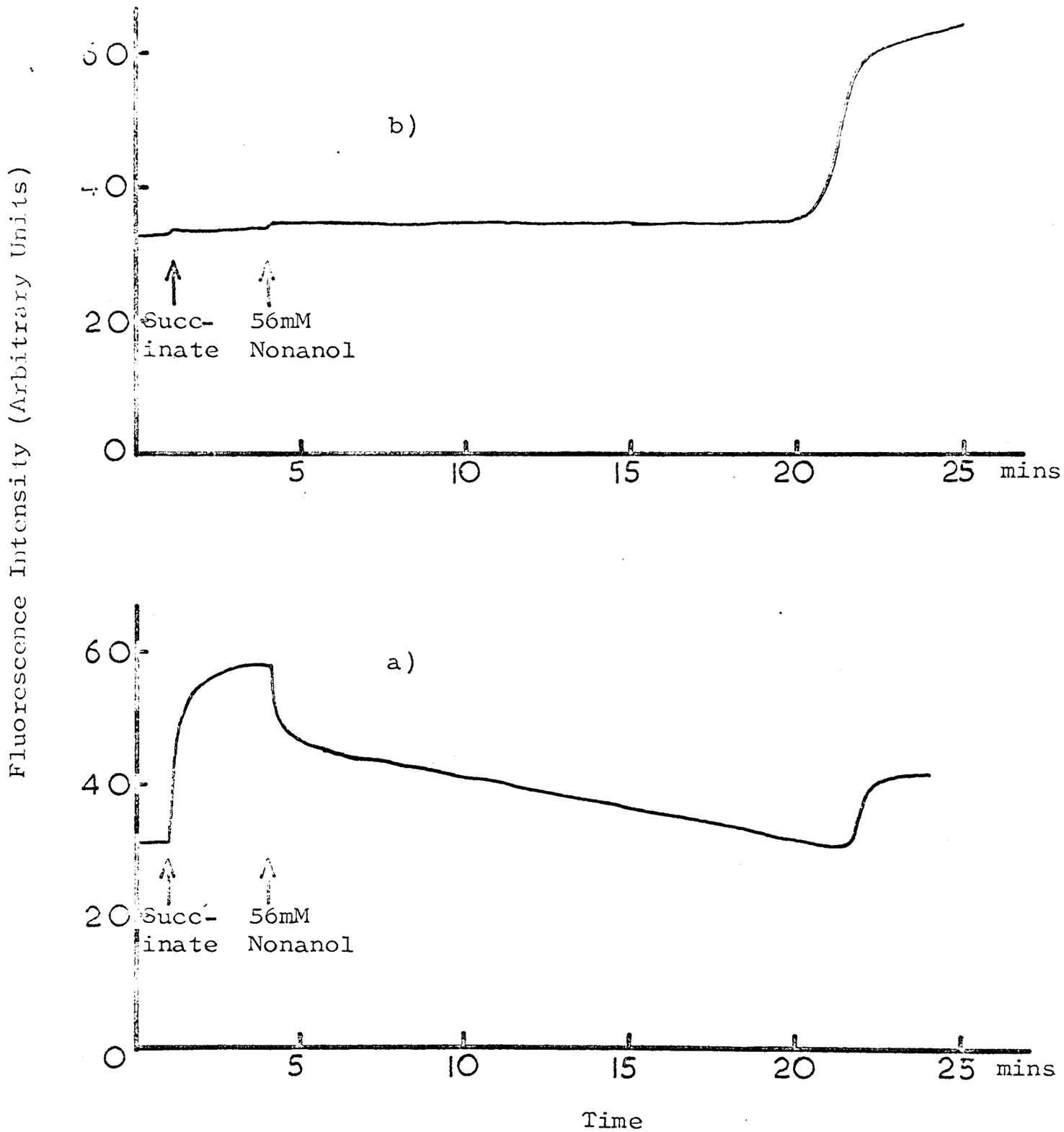

Fig.56. Effect of nonanol on ANS and NPN responses. Conditions and wavelengths as in figs.36 and 55. a) ANS b) NPN

able to penetrate right into the lipid phase of the membrane where there are no structural changes. It has since been shown that both NPN and retinol will respond to structural changes induced in lipid micelles by cholesterol[229]. The probes' insularity from structural changes in SMP was investigated further by inducing gross membrane changes e.g. by protein denaturing agents such as SDS, or by high concentrations of anaesthetics (e.g. benzyl alcohol, nonanol, ether). The effects were compared with those on ANS and other probes which bind where they can sense energy dependent changes. With energised particles saturating concentrations of chloroform and ether caused slight quenching of ANS fluorescence, and benzyl alcohol quenched ANS, MNS, PS, NPN and Retinol slightly. Nonanol was the only molecule to cause drastic effects. 56mM nonanol caused a sharp decrease in ANS fluorescence not unlike that caused by uncouplers, followed later by a small increase. Nonanol had no initial effect on NPN fluorescence but after a time corresponding to that taken for untreated particles to reach anaerobiosis, there was a sharp rise in fluorescence (fig.56). It is interesting to note that both ANS and NPN appear to see the same effect. However, in view of the complexity of the system it is impossible to say what nonanol is doing.

This sort of approach was also adopted with a simple

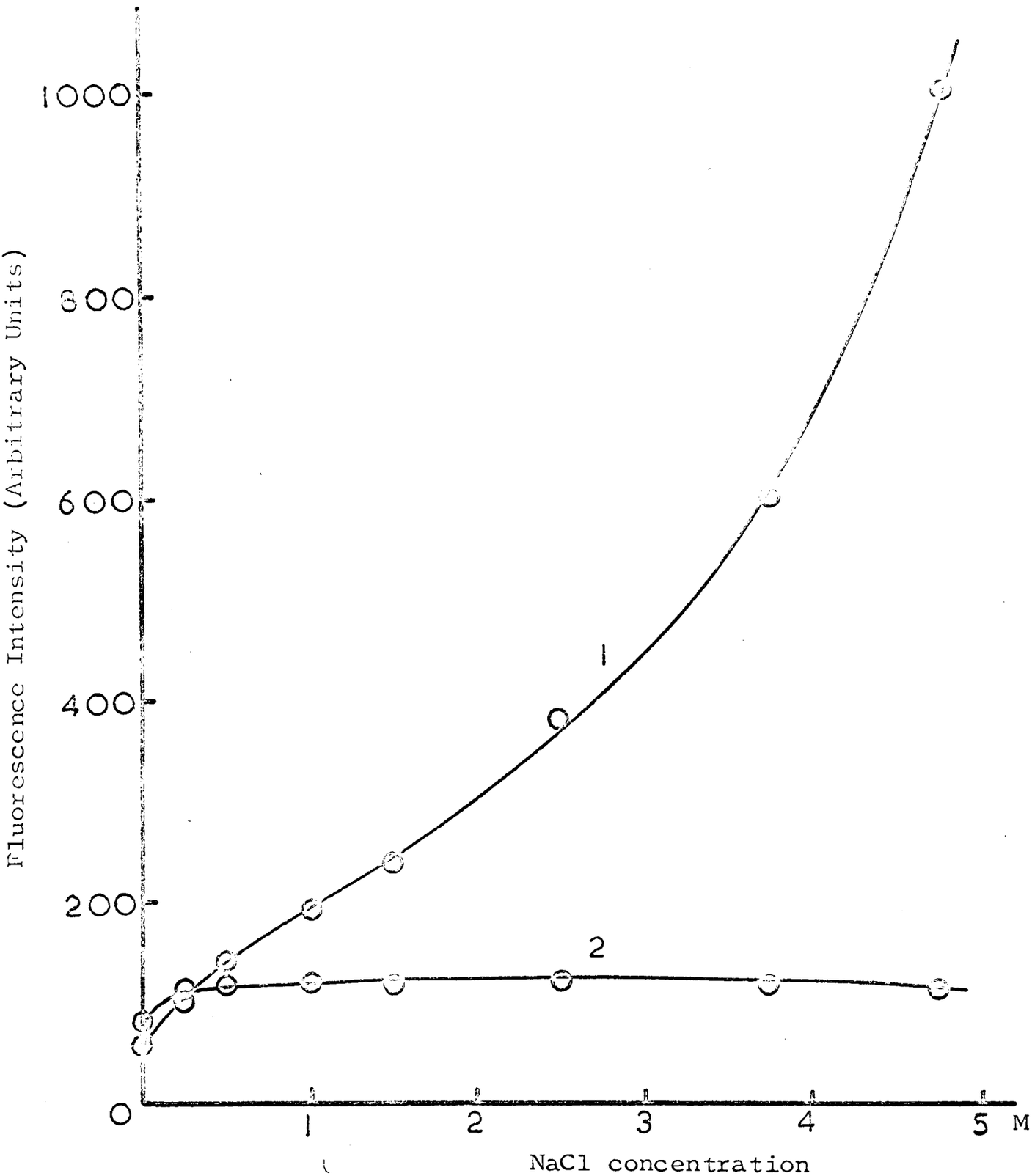

Fig.57. Effect of NaCl concentration on the fluorescence of ANS (10μM, 1) and NPN (10μM, 2) bound to 0.07 mg/ml erythrocyte stroma.

membrane system (i.e. erythrocyte stroma). Nonanol only had a very slight quenching effect on the fluorescence of ANS, NPN and PS bound to erythrocytes, so it seems that the above effects were a special property of the mitochondrial membrane. An alternative approach was to denature the stroma protein with SDS and to see how this affected ANS and NPN fluorescence. 0.05% SDS decreased the fluorescence of stroma bound ANS by ca 65% while it increased the fluorescence of NPN by ca 20%. This enhancement of NPN fluorescence could be accounted for by binding of NPN to SDS micelles (determined in the absence of stroma) but it was found that ANS did not bind to SDS micelles[230]. Obviously ANS binding is associated to a large extent with the membrane protein, while NPN is in the lipid phase where it cannot detect changes in the protein. A further test of this conclusion was to investigate the effect of ionic strength on ANS and NPN fluorescence, since ions will presumably only interact with probes in an environment accessible to the bulk aqueous phase. Thus it was expected that ANS would be affected by changes in ionic strength while NPN would not be. Increasing concentrations of sodium chloride had a marked effect on the ANS fluorescence, but only a very small effect on the NPN fluorescence (fig.57). Magnesium chloride has similar effects except that at high $MgCl_2$ concentrations a time dependent enhancement of NPN

fluorescence appeared.

Obviously a negative charge was necessary to prevent the probe from becoming completely buried in the lipid phase of SMP where it was unable to sense energy dependent changes. Since there are positively and negatively charged groups on the surface of a membrane, it was quite possible that a positive charge on the probe would also prevent its entry into the lipid phase. In an attempt to obtain a probe capable of carrying a positive charge, the O-dansyl derivative of N-di t-butyl 3-aminopropanol (an analogue of butacaine) was synthesised. Its fluorescence was not enhanced by ETPH nor was it sensitive to energisation. There have been several reports in the literature of the use of the positively charged probe ethidium bromide (extensively used for studying DNA and RNA[231]) for studying erythrocytes[103], SMP[103,232], and whole mitochondria[233]. However, it was found impossible to repeat Gitler's work (refs. 103, 232) except that ethidium bromide fluorescence was enhanced by SDS micelles[230]. To check that the experiments were performed under the correct conditions (ethidium bromide concentration, λ_{max} etc) DNA was added to a solution of ethidium bromide. A 20 fold enhancement was observed. The discrepancy with Gitler's work could be due to the fact that at the long wave-lengths involved his filters did not entirely exclude light scattering effects. The work of Chance[233] seems to indicate that this

Table 9

Probe	Enhancement(ETPH)	Shift (nm)	Enhancement(energisation)
DNS-NH_2	+	-20	0
-Try	+	-10	+
-His	-	0	0
-Cys	+	-10	+
-Nor	(-)	0	0
-isp	-	?	+
-Glu	-	0	0
-Gly	-	0	0
- But	-	0	-
-Asp	(-)	0	0

probe binds to whole mitochondria and has its fluorescence enhanced by energisation. This indicates that the inside out relation of SMP to mitochondria causes a different charge specificity, and presumably means that positively charged probes will not act as probes in SMP.

It was now apparent that a negative charge was absolutely essential, though the type of negative charge, and its distance from the fluorophore remained to be defined. The DNS amino acids and PB (γ-1-pyrenyl-butyrate) offer a way of investigating both unknowns, since in them the negative charge is at varying distances from the fluorophore, and it is a carboxyl group, not a sulphonate. A selection of DNS amino acids was tested for a response to energisation of ETPH, and the results are shown in Table 9. DNS-NH_2, DNS-Try and DNS-Cys fluorescence was enhanced on binding to ETPH, but the rest were quenched. DNS-Try and DNS-Cys were further enhanced on energisation, while the quenching of DNS-isp was reversed and that of DNS-γ-But was increased. Interestingly DNS-NH_2 does not respond to energisation (cf MNS-NH_2). However, it is difficult to draw any conclusions about the specificity of these probes. In marked contrast to ANS (and NPN) DNS-OH binds to ETPH with a small enhancement of fluorescence, but does not respond to energisation. Dimethyl naphthylamine neither binds to ETPH (as judged by fluorescence enhancement) nor responds to energisation.

Even from these few results it is possible to conclude that at least with DNS as the fluorophore, a carboxyl group is as effective (if not more so) as the $-SO_3^-$ group, and that unlike in the GDH system, increased distance between the negative charge and the fluorophore does not prevent response (cf DNS-γ-but and DNS-But p.55).

PB (γ-(1-pyrenyl)-butyrate) was found to have very similar fluorescence properties to PS, but had a much longer life-time (presumably due to the removal of the acidic group from direct substitution in the ring system) and so was sensitive to quenching by oxygen. Addition of ETPH to a solution of PB caused no enhancement of excimer fluorescence, but addition of succinate caused a slow increase which could be reversed by FCCP. i.e. PB detects the same energy dependent change as PS does. However, unlike PS, anaerobiosis caused only a small drop in the fluorescence of PB. This is presumably due to the fact that the drop associated with anaerobiosis is counterbalanced by an increase in fluorescence due to the removal of oxygen (and hence a lowering of quenching).

9-anilino-acridine derivatives

The above investigations have suggested that a probe needs a negative charge in order to respond. What was now needed was a series of closely related molecules in which the acidic group can readily be changed. Such a series is based on acridine and

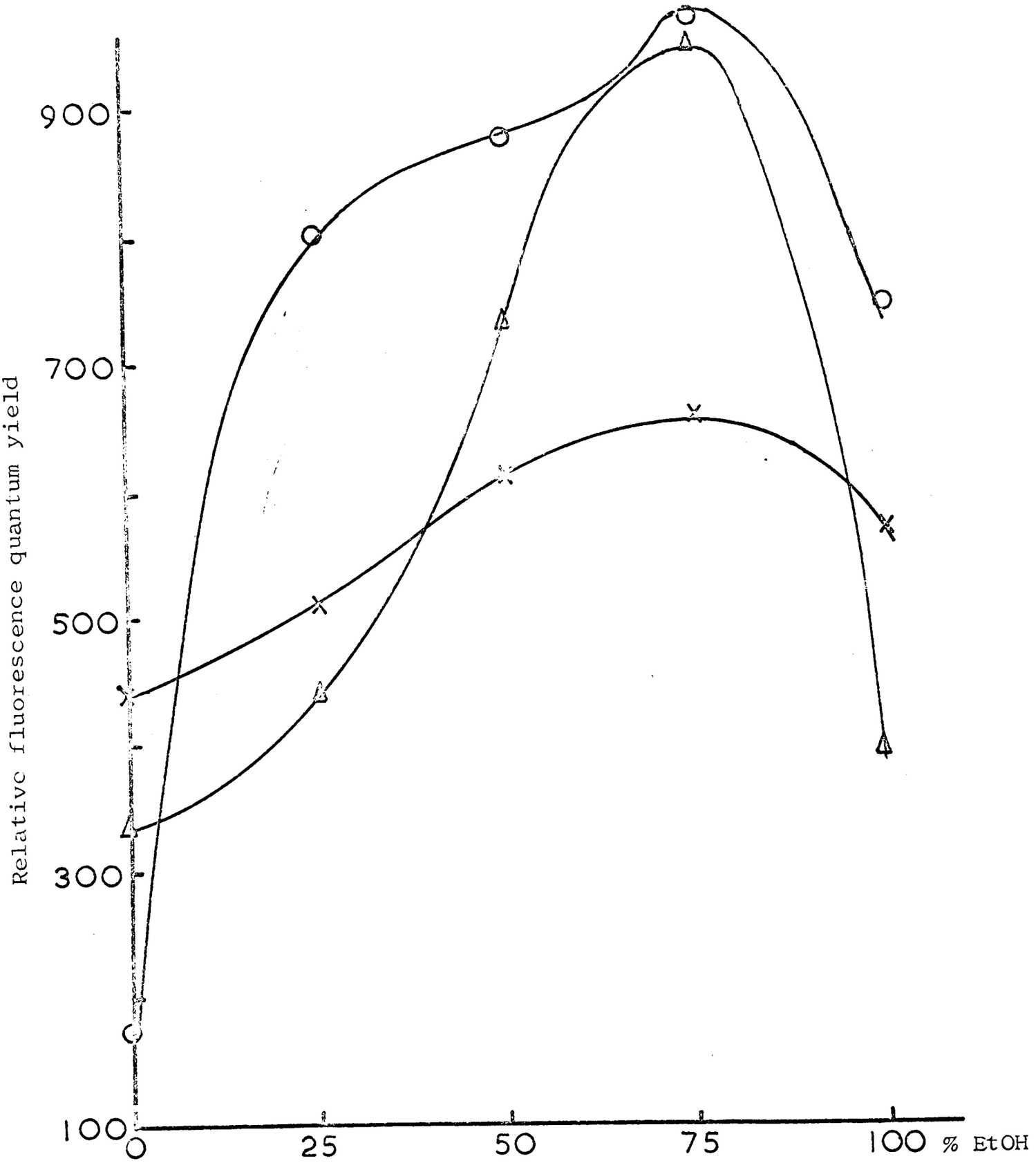

Fig.64. Relative fluorescence quantum yields of ABA (△), ABC (x) and ABS (O) in EtOH/H_2O mixtures.

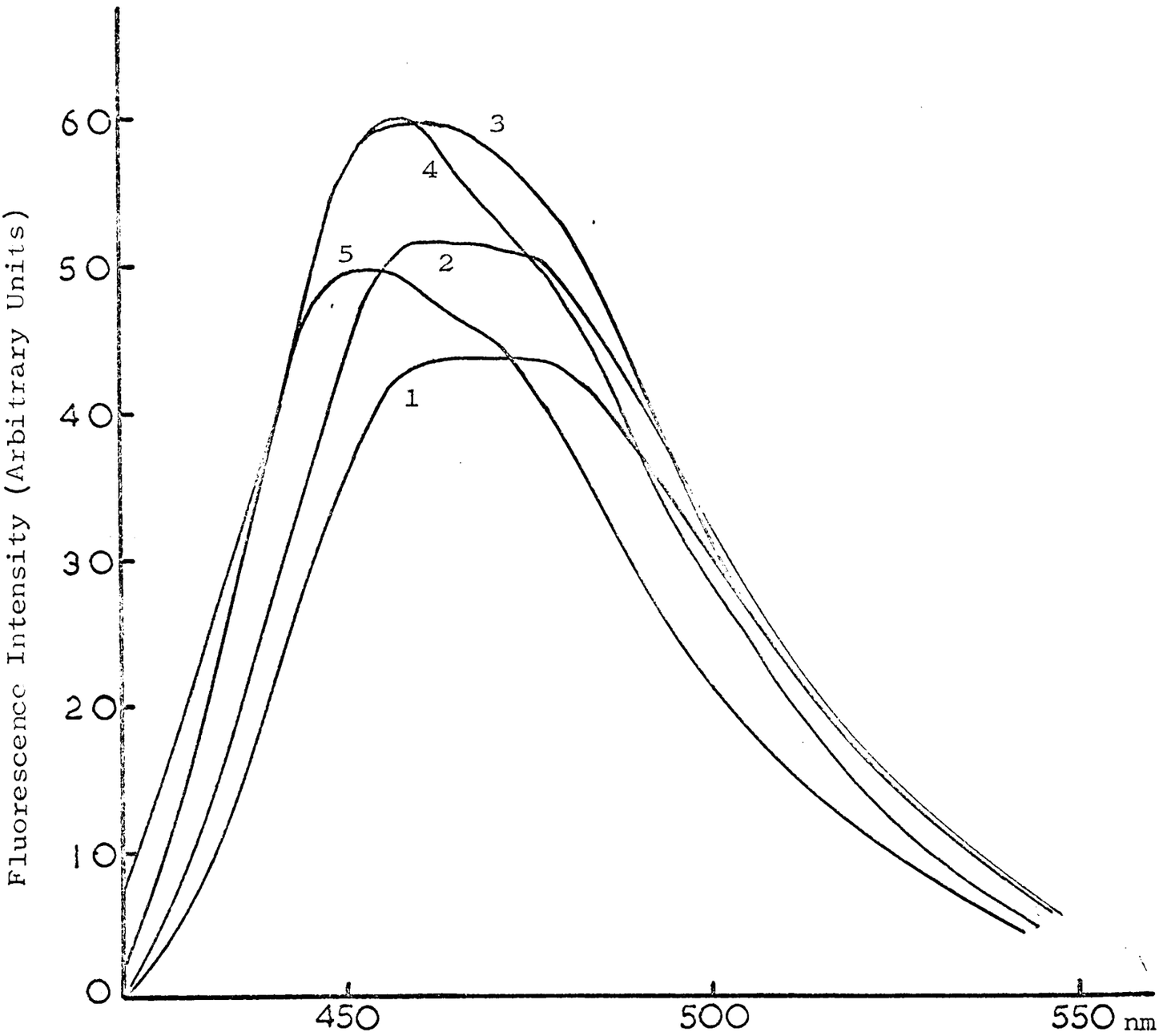

Fig.63. Fluorescence emission spectra of 10μM ABC in ethanol/water mixtures. Excited at 380nm, with bandwidths of 10nm (excitation) and 2nm (emission). 1. H_2O; 2. 25% EtOH; 3. 50% EtOH 4. 75% EtOH; 5. EtOH.

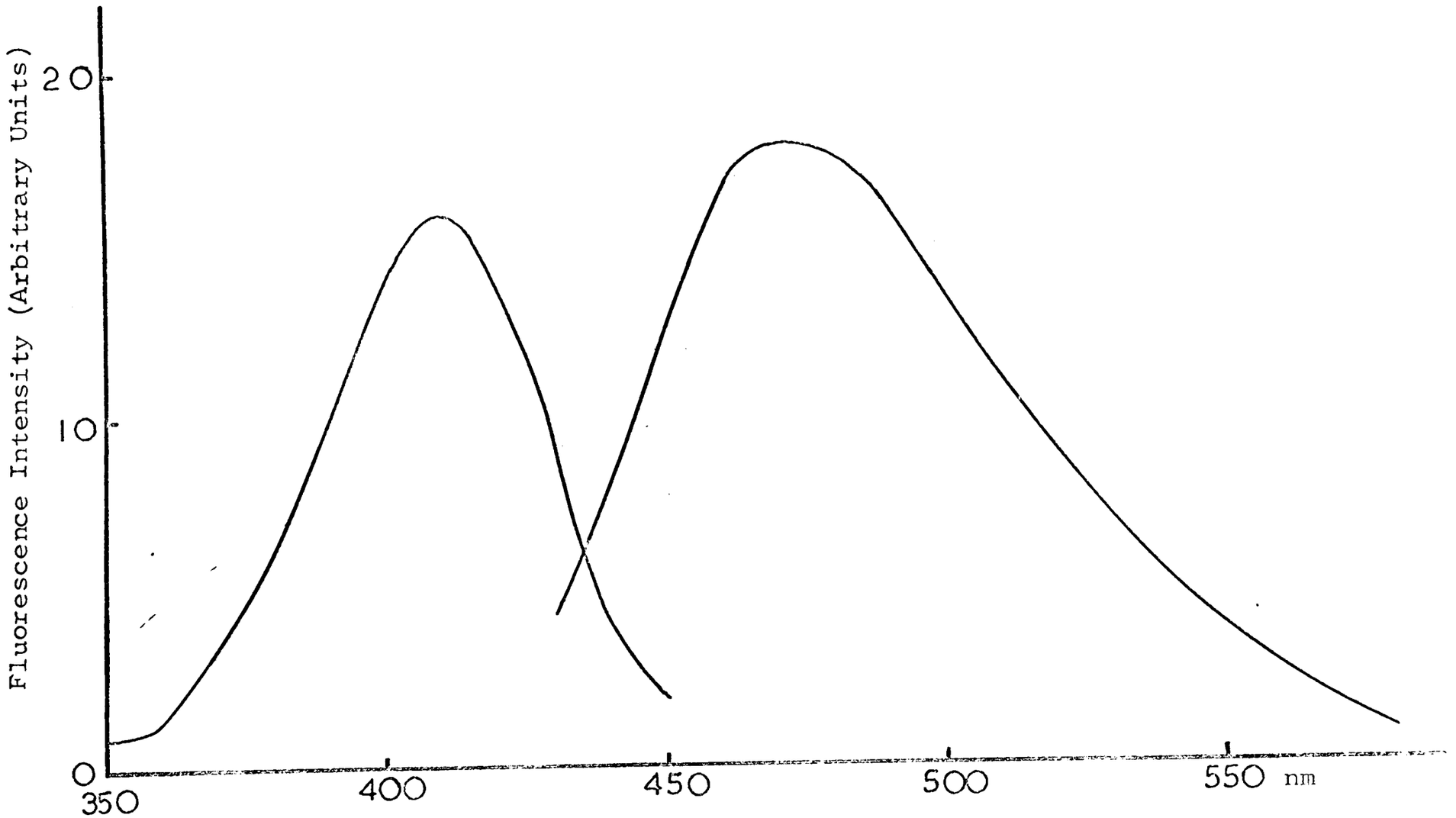

Fig.62 Fluorescence spectra of 5 μM ABA in water. Emission, excited at 400nm, Excitation observed at 500nm.

Table 10

	% composition			
	C	H	N	S
ABA calc	48.5	3.43	5.66	
ABA found	45.2	3.82	6.22	
ABA calc adjusted for assumed water content	45.2	3.95	5.27	
ABC calc	62.9	3.5	7.0	
ABC found	60.65	4.21	6.30	
ABC calc adjusted for water content	56.6	4.25	6.60	
ABS calc	55.0	3.2	6.4	7.3
ABS found	50.6	4.08	6.18	6.96
ABS calc adjusted for water content	49.5	3.91	5.77	6.59

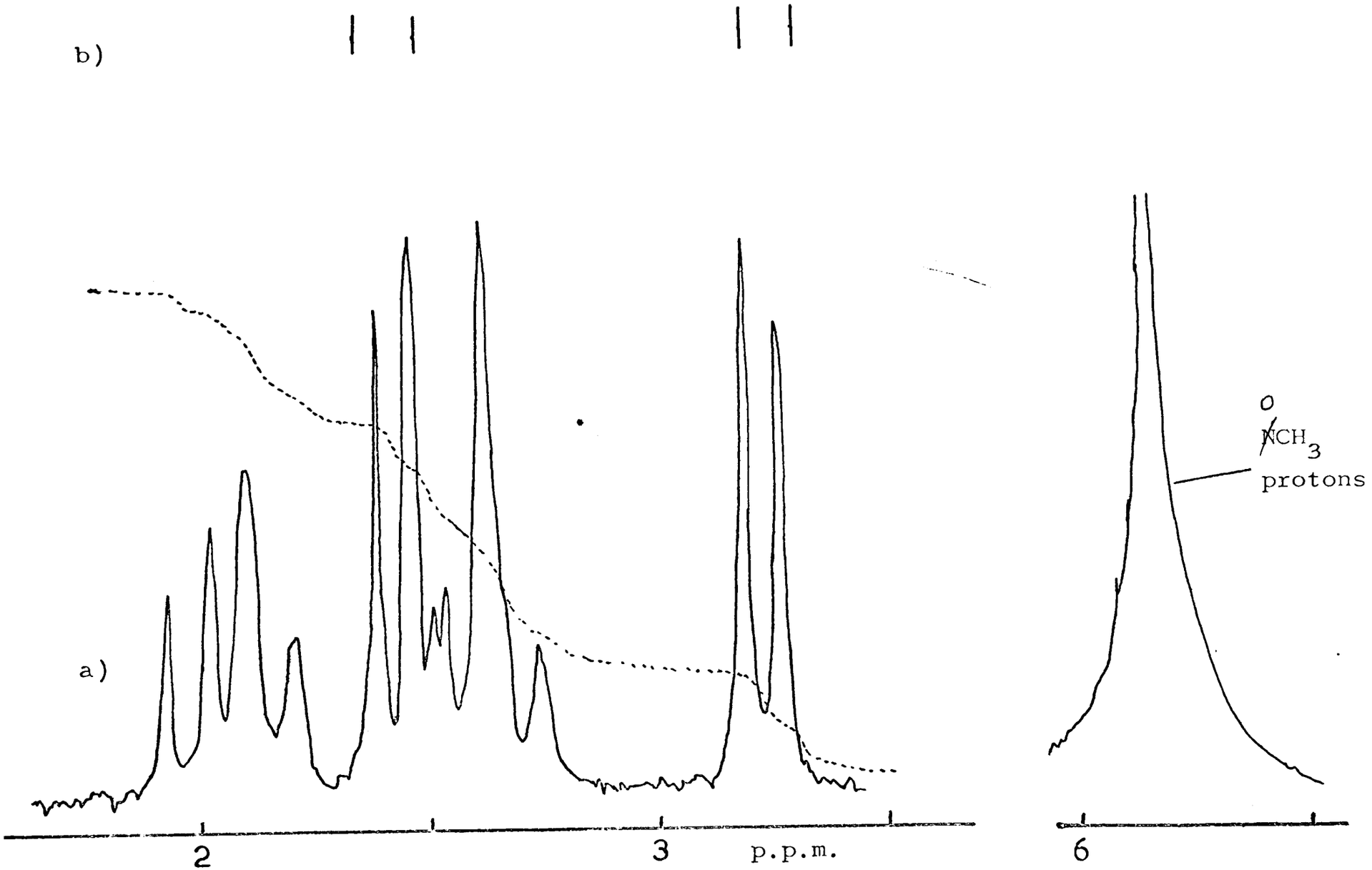

Fig.61. 100 MHz nmr spectra of a) ABS in $DMSOd_6$ b) sulphanilic acid in $DMSO/H_2O$

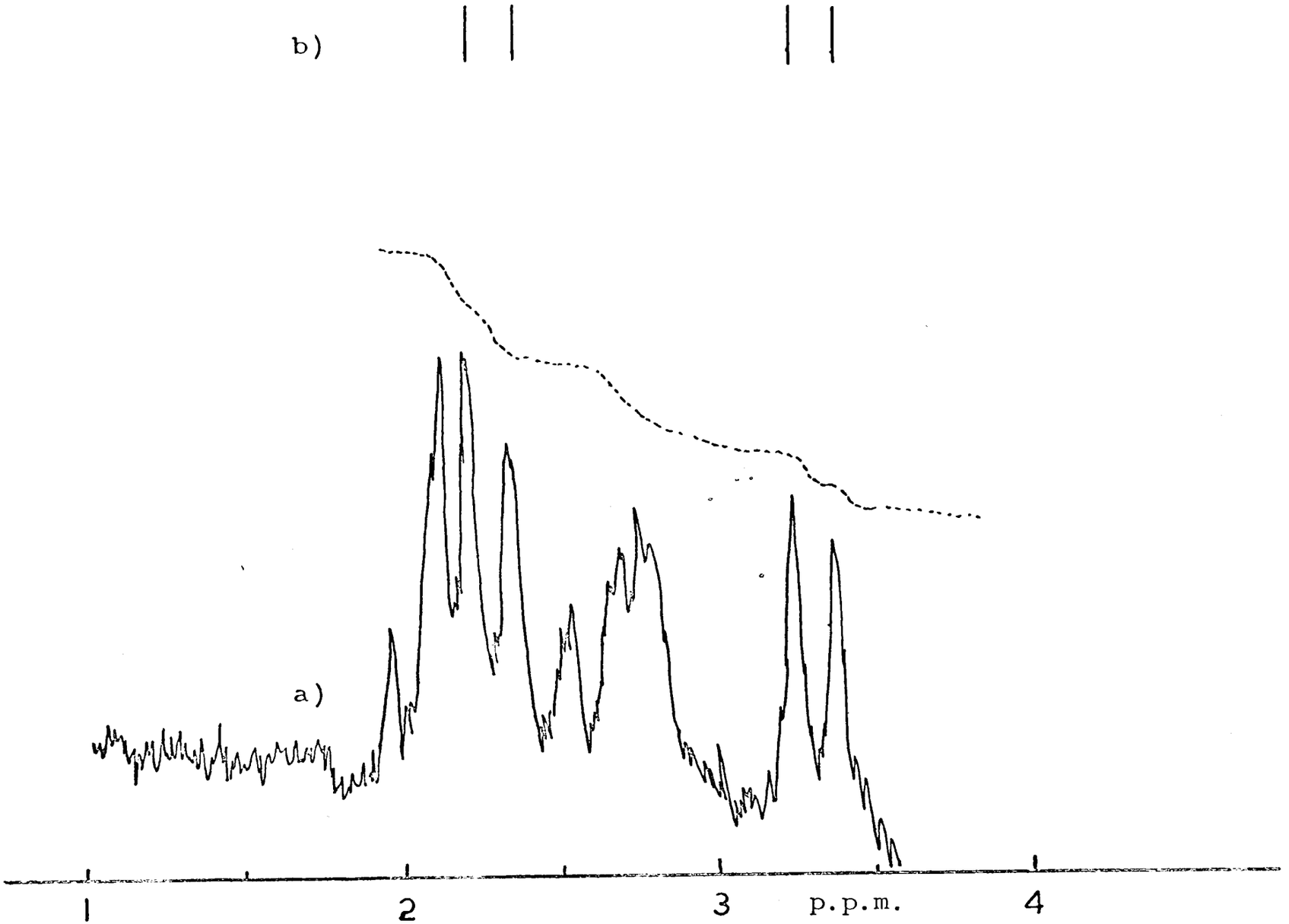

Fig.60. 60 MHz nmr spectra of a) ABC in $DMSOd_6$ b) p amino benzoic acid in $DMSO/H_2O$

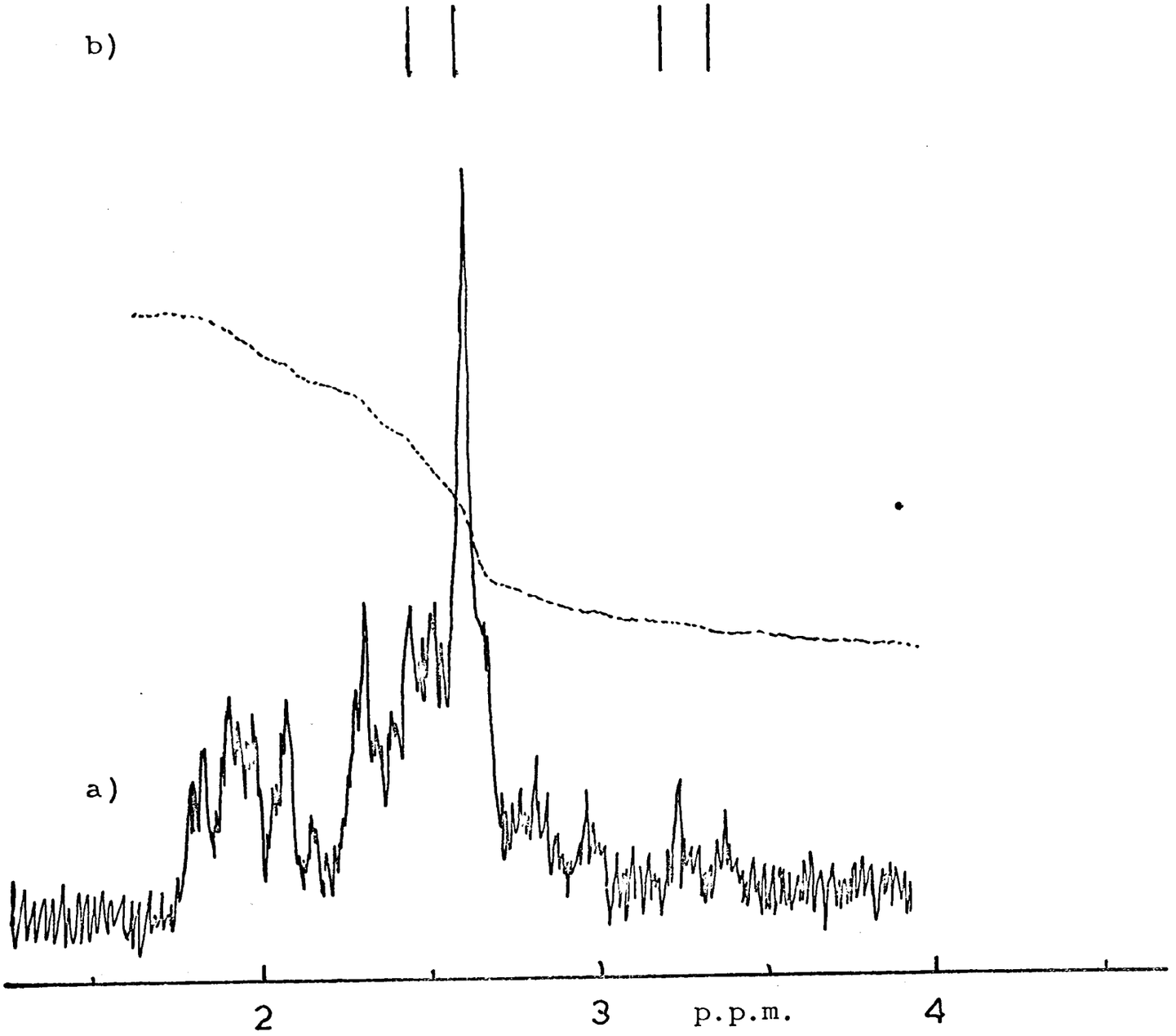

Fig.59. 60 MHz nmr spectra of a) ABA in DMSO b) arsanilic acid in $DMSOd_6$.

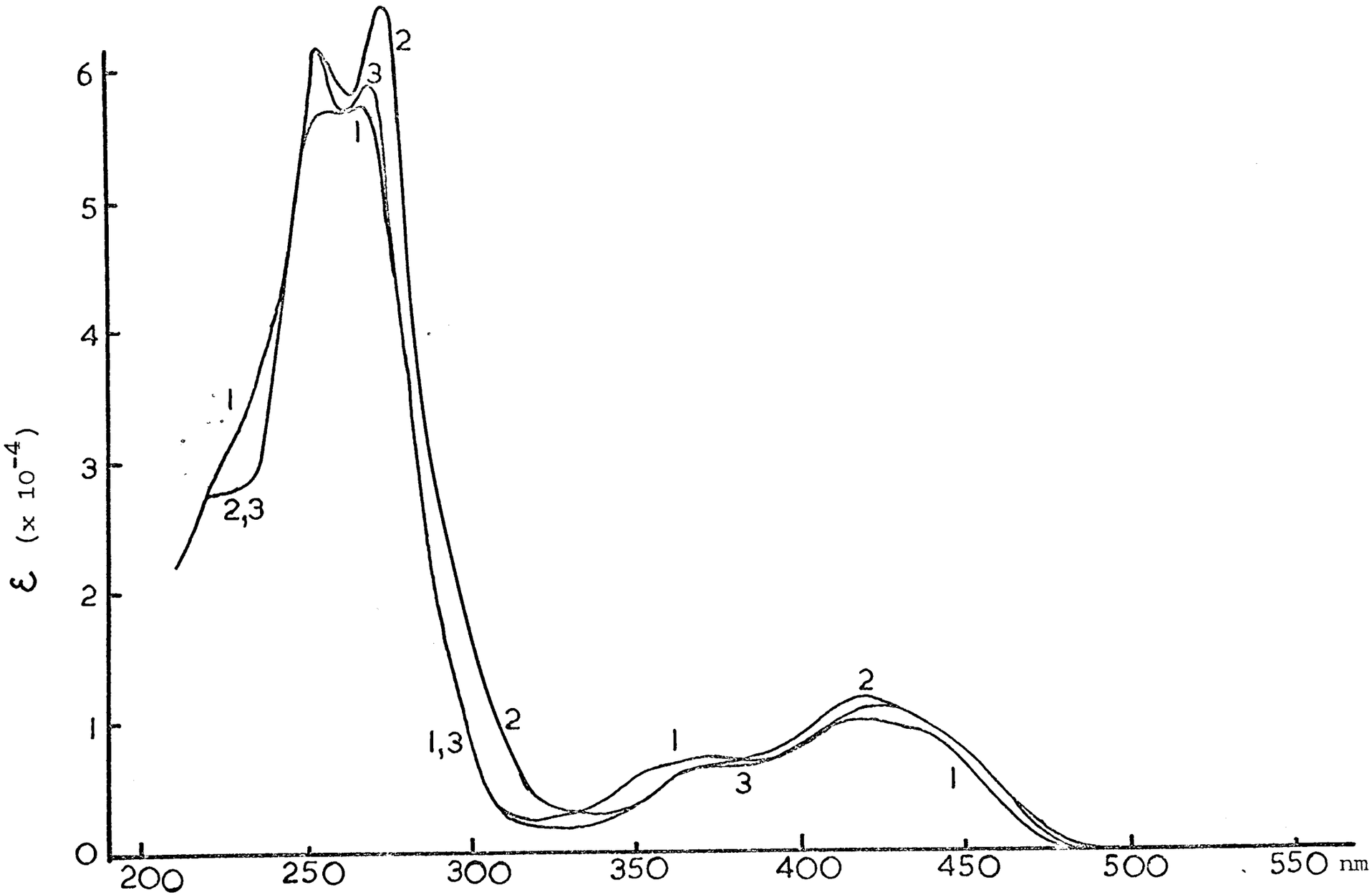

Fig.58. Absorption spectra of ABA, ABC and ABS in Ethanol.

1. ABA; 2. ABC; 3. ABS.

was first mentioned by Weber[234] as being similar to ANS in behaviour. Three derivatives containing $-COO^-$, $-SO_3^-$, $-AsO_3^{2-}$ were prepared and purified as described in the experimental section (p.30). The absorption and nmr spectra are shown in fig.58 and 59-61, with nmr assignments indicated. The poor nmr spectra for ABA and ABC are a result of their low solubility in common nmr solvents. The a_2b_2 pattern of the phenyl protons was assigned by comparison with the original amino benzene acids (fig.59-61). The results of the elemental analyses are shown in Table 10. Carefully run nmr spectra in dry DMSO d_6 enabled the water content of ABC and ABS to be estimated as 2 and $2\frac{1}{2}$ moles per mole respectively. Corrected compositions based on this estimate are also shown in Table 10. The results for ABA are complicated by the fact that it was precipitated from acid and could be a mixture of hydrochlorides.

The fluorescence properties of the three probes were very similar, except that ABS was less fluorescent than the other two. Fig.62 shows a typical fluorescence spectrum. In ethanol/water mixtures intensity and emission peak changed (fig.63) but not in the way expected from ANS. Although the emission maximum varied more or less linearly with ethanol concentration, shifting to the blue as polarity decreased, the relative quantum yield tended to peak at 50-75% ethanol (fig.64 cf PS, p.70).

Addition of ETPH to the three probes caused different effects.

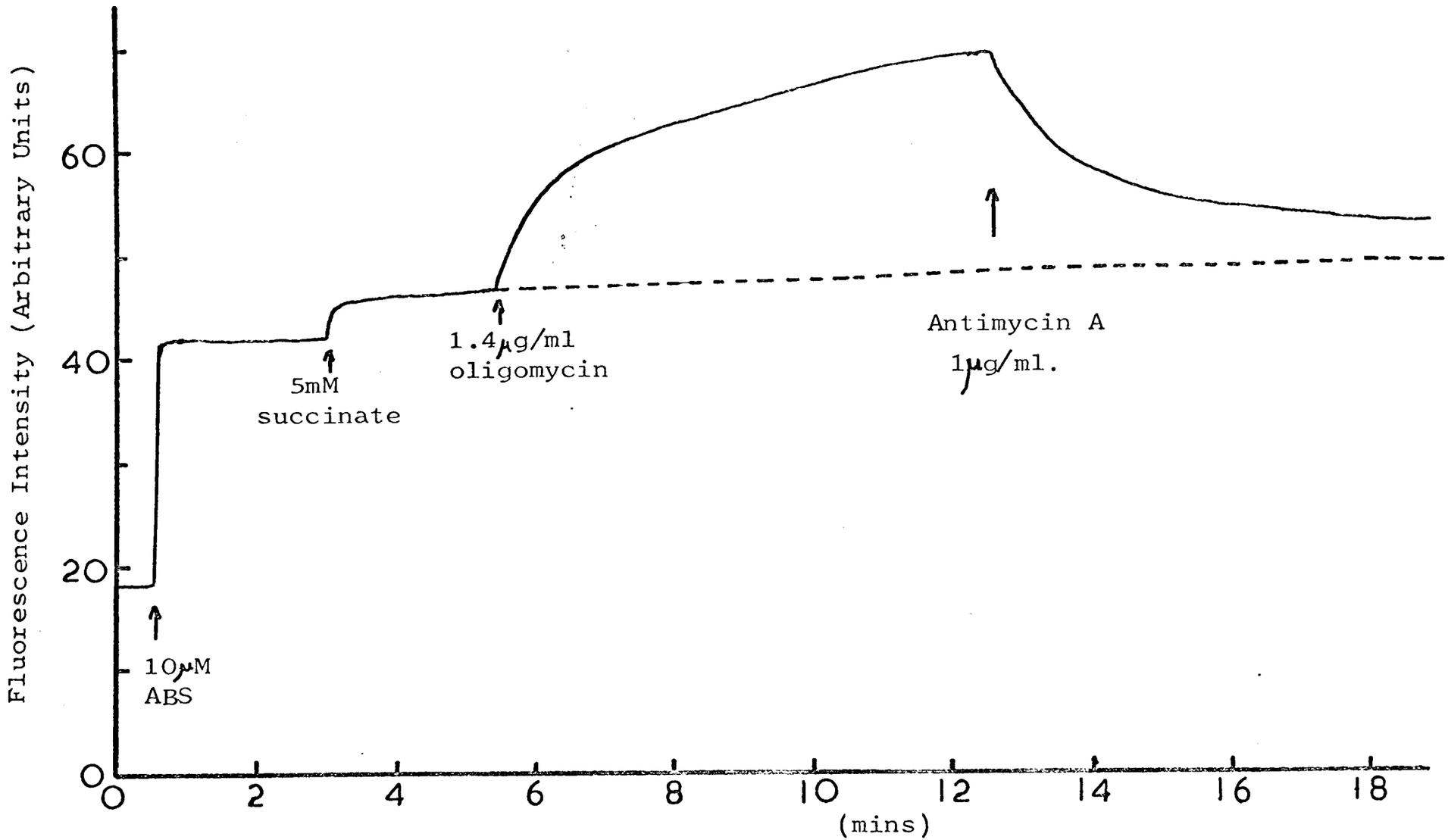

Fig.69. Response of ABS to changes in ESMP (0.3mg/ml) induced by oligomycin and Antimycin A. Excitation 370nm; emission 480nm; 8nm bandwidths. (---) preincubated with antimycin A.

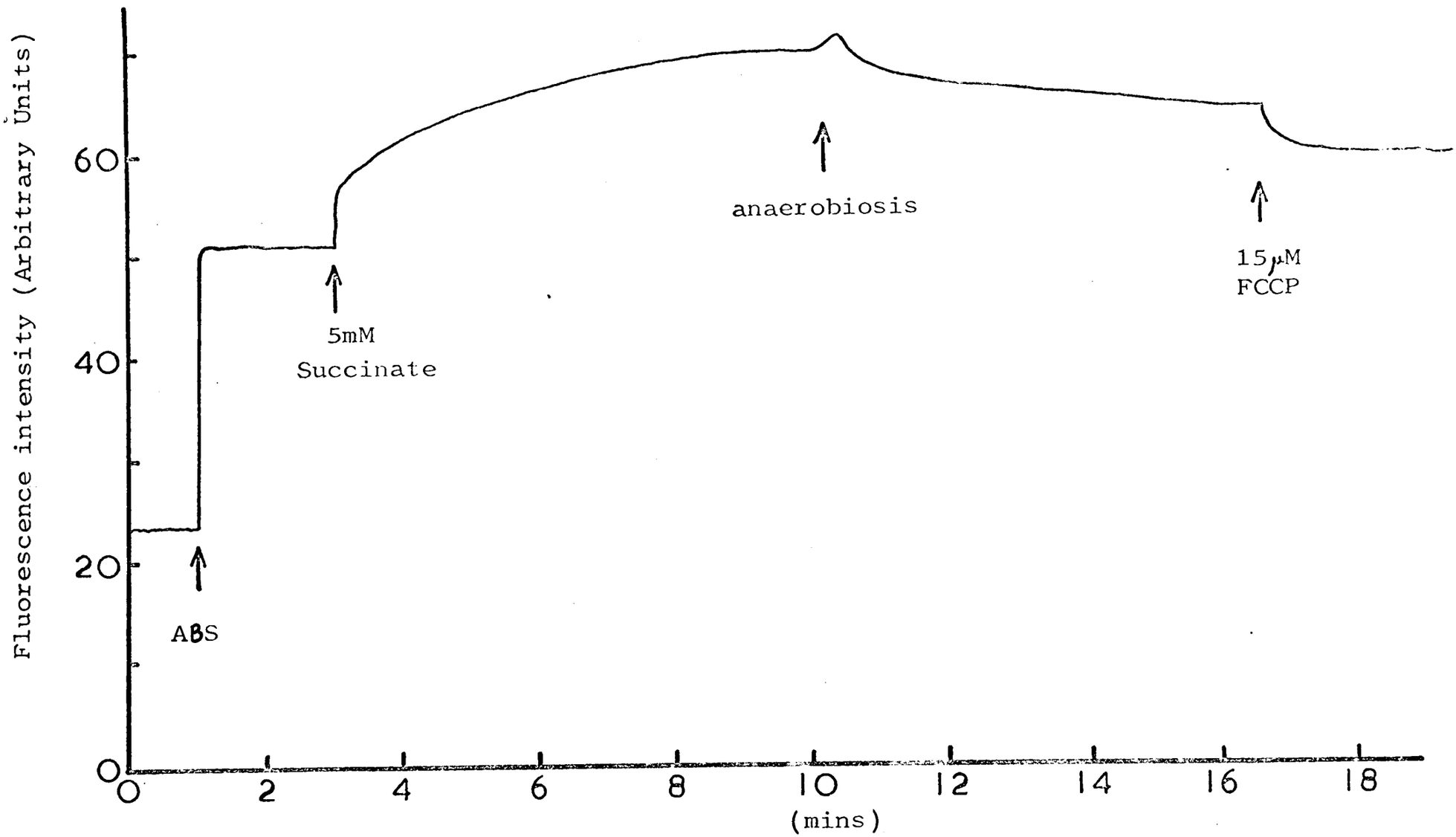

Fig.68. Response to ABS (10μM) to energy dependent changes in OESMP (0.9 mg/ml)

Excitation at 370nm, emission at 480nm, 8nm bandwidths.

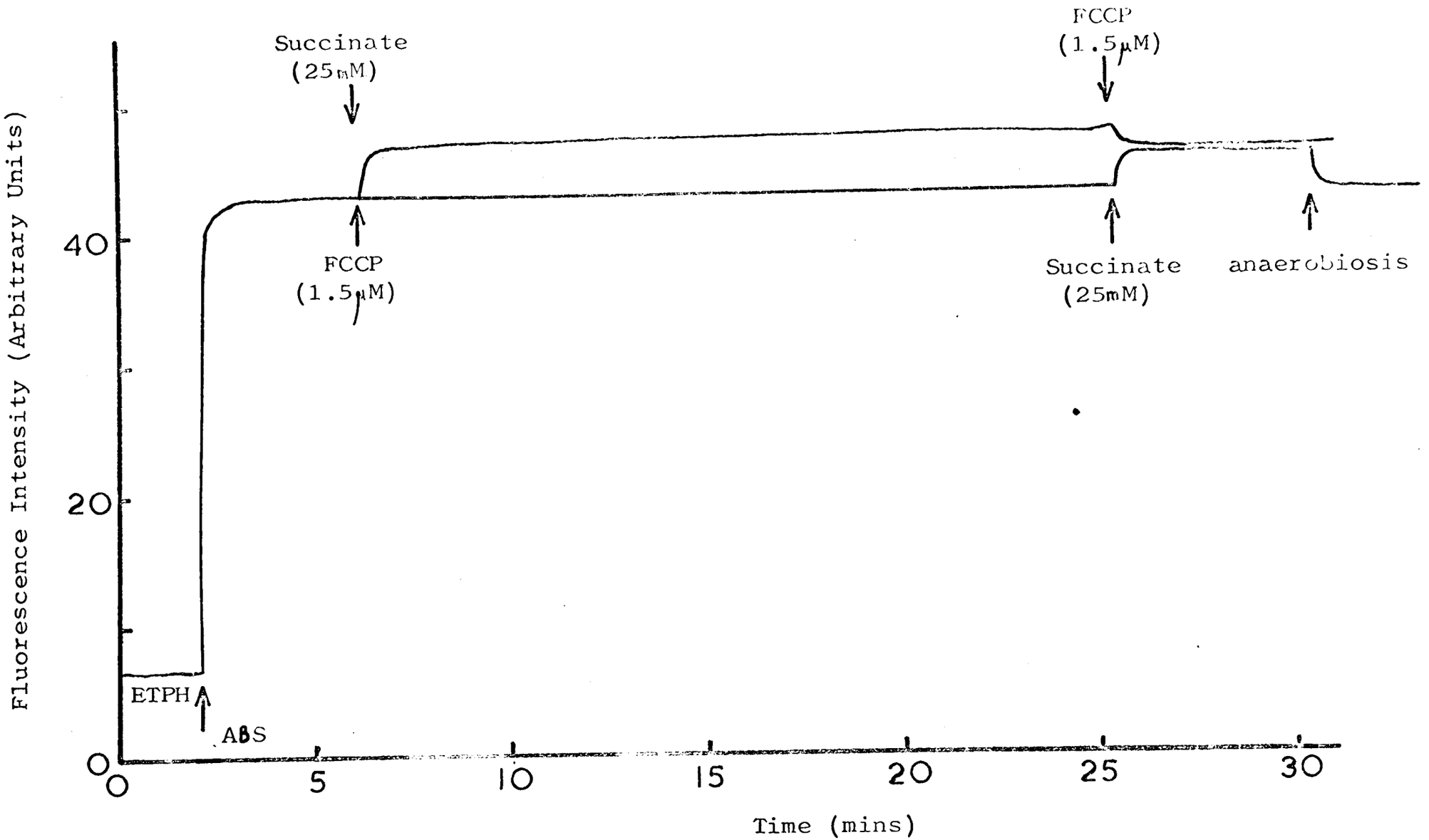

Fig.67. Response of 50μM ABS to energy dependent changes in ETPH.

Fluoresence emission at 500nm excited at 400nm.

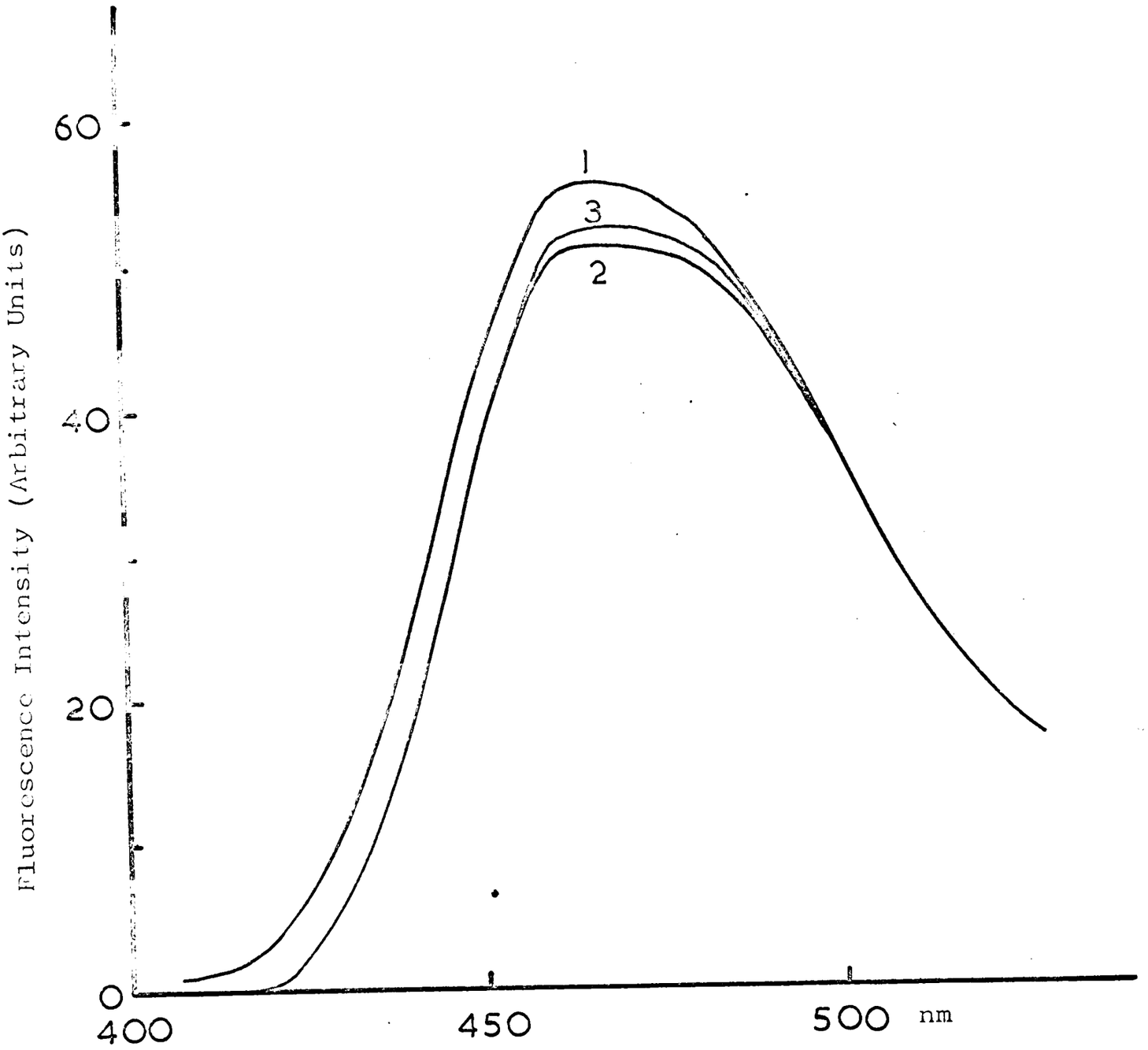

Fig.66. Fluorescence emission spectra of 10μM ABC excited at 380nm. Bandwidths: 10nm for excitation, 2nm for emission.

1. Buffer pH 7.4 2. With resting ETPH (0.33mg/ml)

3. With energised ETPH (0.33mg/ml)

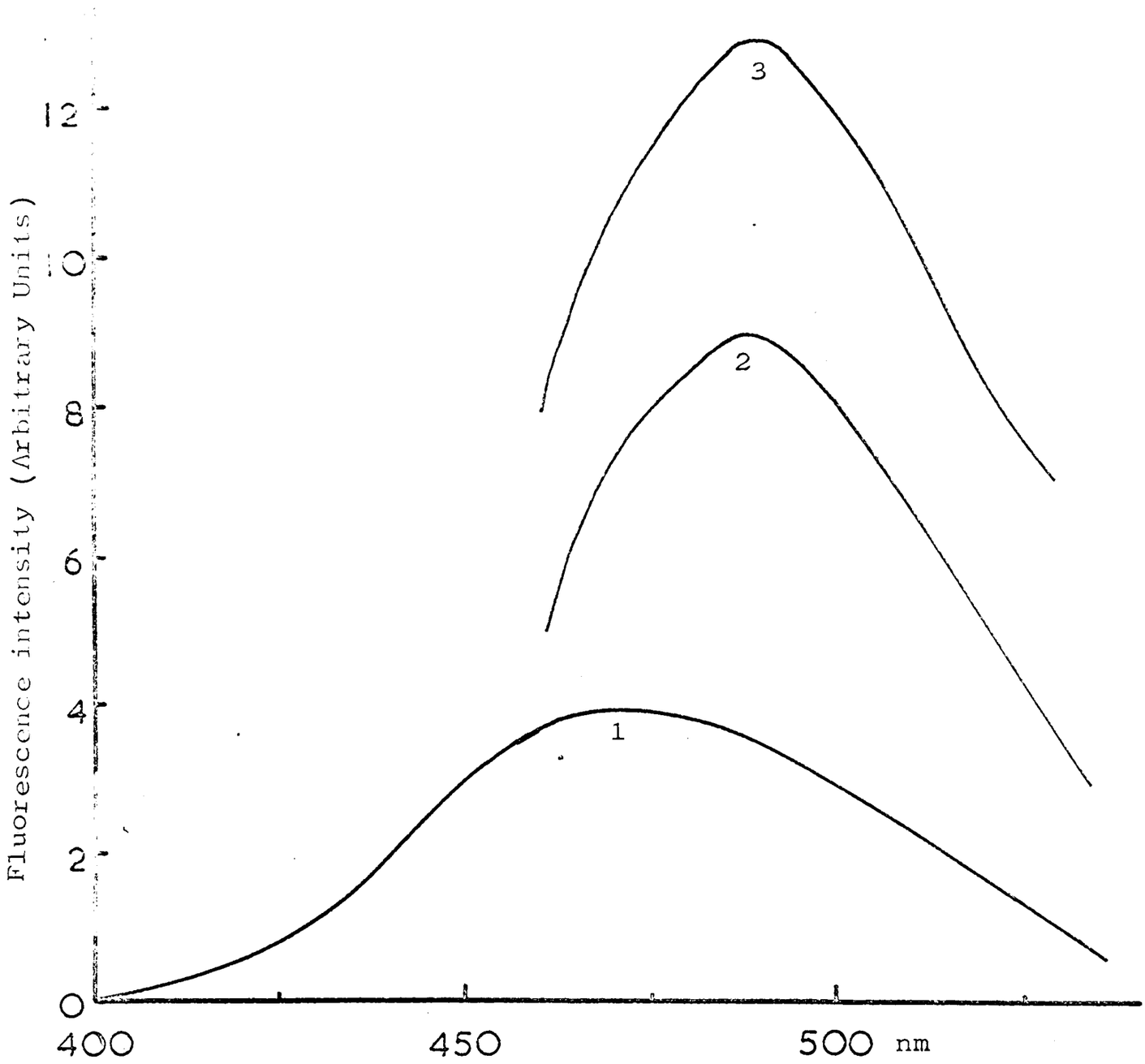

Fig.65 Fluorescence emission spectra of 10μM ABS excited at 380nm. Bandwidths 10nm excitation, 2nm emission.

1. Buffer pH 7.4 2. With ETPH (0.33mg/ml) .

3. With energised ETPH (0.33mg/ml)

ABS fluorescence was enhanced (fig.65) while that of ABC and ABA was very slightly quenched (fig.66). Addition of succinate caused a further enhancement of ABS fluorescence, but had no effect on that of ABC and ABA (figs.65, 66). The apparent shift in ABS fluorescence caused by ETPH is probably distortion due to scattering by ETPH for which correct allowance cannot be made. Further investigation of the energy dependent enhancement of ABS showed that it was biphasic - an almost instantaneous phase followed by a very slow one (fig.67). Anaerobiosis appeared to reverse both these phases but produced only a very slow change, while FCCP reversed only the slow phase. This suggested that the fast phase was related to electron transfer and the slow phase to energy coupling. In order to investigate this further EDTA treated particles were used (ESMP). These will oxidise substrates, but need oligomycin in order to give energy coupling. With OESMP (ESMP incubated with oligomycin) there were the expected fast and slow phases in the enhancement of ABS fluorescence on energisation (fig.68). On anaerobiosis there was a sharp upward kick followed by a slow decline which reversed the slow phase. Again FCCP reversed only the slow phase. On energisation of ESMP there was a rapid jump in the ABS fluorescence followed by a very small slow increase (fig.69). This confirmed that the fast phase was due to a response to electron transfer. On addition of oligomycin there was a large

a)

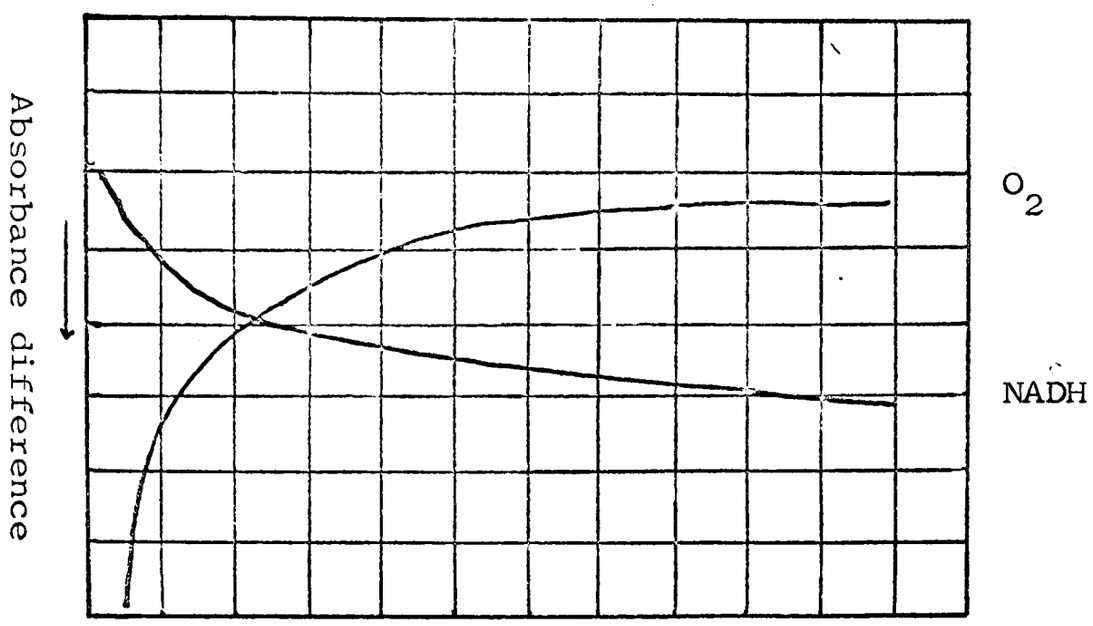

b)

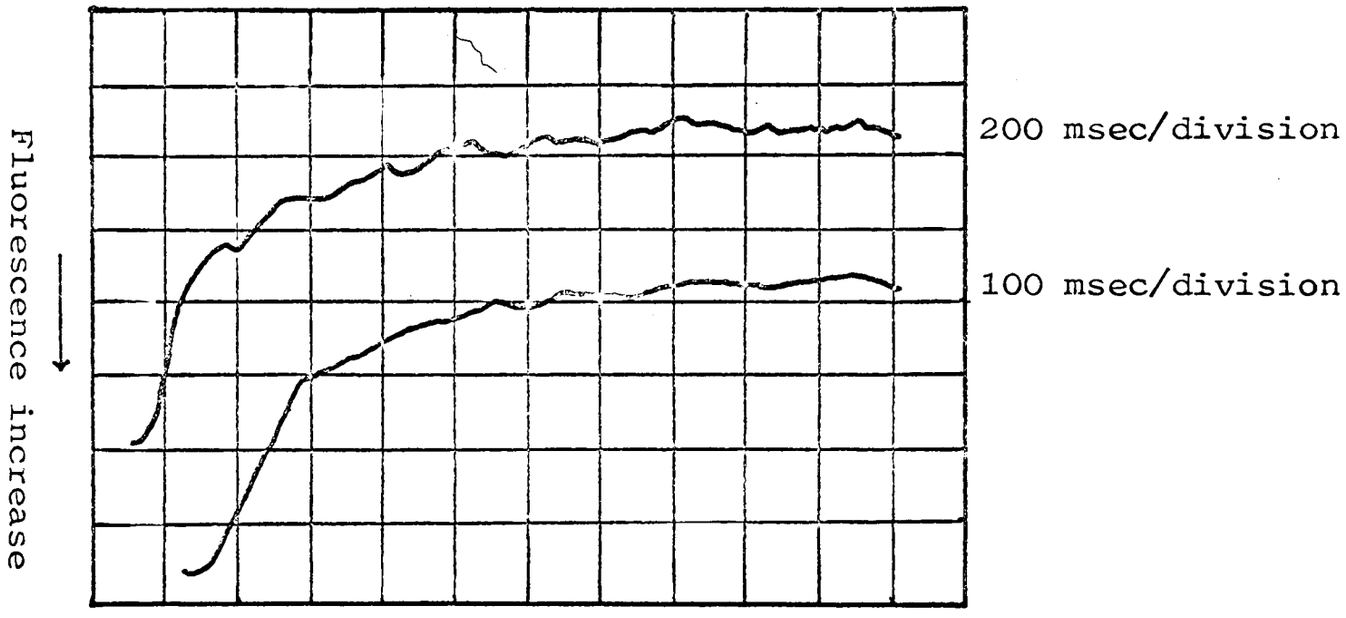

Fig.70. Oscilloscope traces of rapid flow measurements.

a) Cytochrome b reduction by NADH, and oxidation by oxygen pulses.

b) ABS response (excited at 408nm, emission at 510nm) by oxygen pulses.

slow enhancement which was reversed by antimycin A (fig.69). Addition of antimycin A before energisation prevented the oligomycin response, but did not abolish the fast phase of the succinate response (fig.69).

The lack of response for ABA and ABC could be due to their being inhibitors or uncouplers (as might be expected of weak acids). In order to test this, ANS responses and rates of oxygen uptake were measured in the presence of the three probes. At 10 μM all three reduced the ANS response by ca 10% and caused slight increases in the rate of oxygen uptake, i.e. they all appear to cause a small amount of uncoupling. In order to check that all three responded to a biochemical change, BSA was added to the three probes. The following enhancements were observed:-

ABA, 5 fold; ABC, 2 fold; ABS, 50 fold

Thus it seems that this system specifically requires a sulphonate group, rather than any negative charge on the probe.

Rapid reaction measurements

The rapid phase of the ABS response was further investigated by Drs. Chance and Radda at the Johnson Research Foundation, Philadelphia. Using ESMP they compared the rate of cytochrome b oxidation with the fast phase of the ABS response during oxygen pulses (fig.70). The two are comparable ($t_{\frac{1}{2}}$ = 500msec) with ABS slightly slower. However, by studying the electron flow

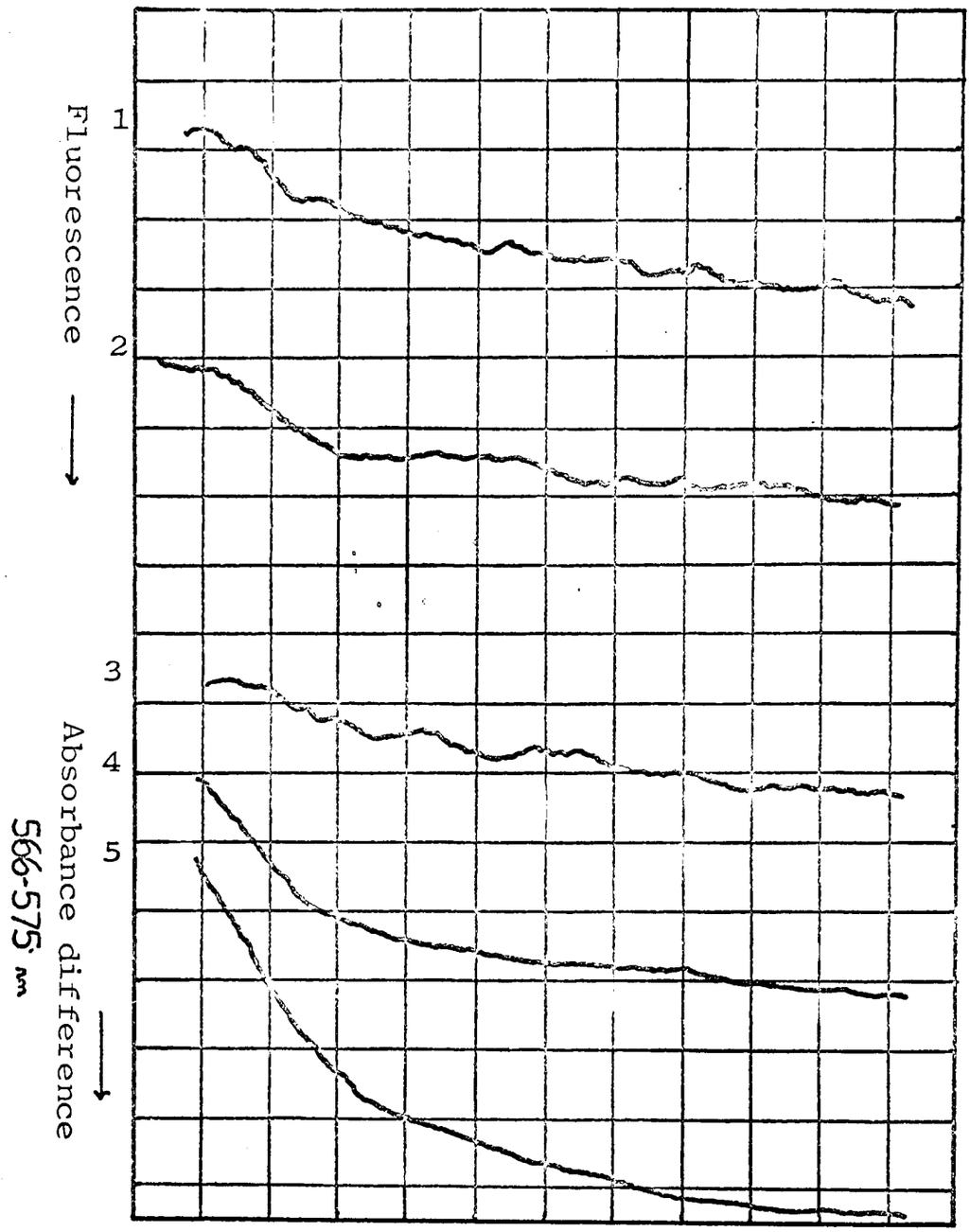

Fig.71. Response of ABS and cyt b to NADH pulses in the presence of Antimycin A.

Upper traces:- ABS fluorescence, excited at 410nm, emission at 510nm.

Lower traces:- Cyt b reduction.

Antimycin concentrations 1. 0; 2. 2μg/ml; 3. 5μg/ml; 4. 2μg/ml; 5. 5μg/ml.

initiated by NADH, it proved possible to separate the ABS and cytochrome b rates. Increasing concentrations of antimycin A changed the rate of Cyt b reduction (increased initial rate and increased extent, but decreased overall rate) but had no effect on the ABS response (fig.71). This again suggests that ABS is responding to a component in the first half of the chain.

This would be compatible with quenching of ABS fluorescence by reduced coenzyme Q. It has since been shown that in ETPH, CoQ quenches ABS fluorescence and that the quenching is partially reversed by energisation (i.e. on oxidation of some of the added CoQ).

Discussion

The aim of this chapter has been two fold:- A. to investigate fully the nature of the energy dependent change in SMP detected by ANS[109] - i.e. the location(s) of the probe binding sites, the nature of the membrane changes which cause the probe responses, and the relation of these changes to oxidative phosphorylation. B. to find out what sort of fluorescent molecule is a good probe of these energy dependent changes.

A. Membrane changes

There are two rates of enhancement for ANS and MNS on binding to ETPH[225]. The fast phases are interpreted as binding on the membrane surface ("fast sites") while the slow phase represents

a subsequent diffusion of the probe into the membrane to "slow" sites. Work in this laboratory has shown that the energy dependent change is in the slow phase only, for ANS, and MNS[223,227]. However, Penefsky et al[236] have reported a rapid response of MNS and TNS (but not of ANS) to energy dependent changes, in addition to the normal slow response. A similar rapid response in ANS fluorescence has been found in this laboratory when damaged ETPH have been used. However, unlike Penefsky's rapid phase, it was not reversible by FCCP.

Having distinguished two types of site, the next problem was to characterise the area of the membrane in which the two types occurred. Energy transfer (Try to ANS and MNS) suggests that the two probes are close to the protein in the membrane, and that on energisation they move slightly closer to the protein[225]. Similar results are obtained with the sarcoplasmic reticulum membrane[103], and erythrocytes[104]. However, polarisation of fluorescence measurements gave a value of p = 0.2 for ANS (p.78) suggesting that ANS is more free to rotate than when bound to a protein (where p = 0.4[44]). The shift and enhancement of ANS fluorescence on binding to ETPH suggest that it is in a hydrophobic environment, and if it were in the lipid phase it would be relatively free to move. An alternative is that ANS binds in an interface region between water and a more hydrophobic area. This would be consistent with the results for

methyl cellulose solutions (p.79) where the ANS polarisation is 0.2. At the concentrations of methyl cellulose used, there are believed to be channels of structured water in a methyl cellulose matrix[237]. The regions of water in ETPH could be structured, and are more likely to be associated with the protein than with the lipid. They will therefore be quite accessible to the solvent outside the membrane.

A further way of examining where ANS binds was to use a probe, similar to ANS, which would bind in the lipid phase, and to compare its behaviour with that of ANS. NPN and retinol both respond to structural changes induced in phospholipid micelles by cholesterol, while ANS does not. This has been explained as ANS binding at the lipid - water interface while NPN and retinol penetrate the lipid phase[229]. This is supported by polarisation measurements which indicate that NPN in micelles is quite free to rotate. Both NPN and retinol bound to ETPH with a rapid enhancement of fluorescence and a small slow phase, but did not respond to energy dependent changes (p.85). This suggests that these molecules are able to enter the lipid phase rapidly, and that the "slow" sites of ANS binding are not due necessarily to difficulty in reaching the more hydrophobic interior of the membrane. Experiments with erythrocyte ghosts showed that denaturation of membrane protein caused a drastic modification

of ANS fluorescence while NPN was unaffected (p.87). Similarly, increasing ionic strength enhanced ANS and not NPN fluorescence (p.87). These observations all point towards ANS (and MNS) binding sites being largely associated with membrane protein, and accessible to the solvent. The work of Ernster has suggested that the slow sites of ANS in ETPH are not accessible to water since only the fast sites are affected by changes in ionic strength[224]. However, Penefsky et al[236] have found a slight dependence of the energy dependent change on ionic strength.

An important question about the location of the ANS binding sites is whether they are associated with a specific part of the oxidative phosphorylation apparatus, or more widely spread, the ANS response being as a result of a more general membrane phenomenon. By energising the membrane with different substrates it was possible to show that the ANS response occurred wherever energy was supplied to the electron transfer chain, though the extent of the response is a measure of the extent of the build up of the energised state (be it chemical, chemiosmotic or conformational) (p.82).

Since the negative charge on ANS was obviously very important in making it bind in a region where it could sense energy dependent changes, it was interesting to see how far the charge could be removed from the fluorophore before response disappeared. In

the GDH system, removal of the charge to a position two carbon atoms further from the aromatic portion of the probe abolished the response (DNS-But vs. DNS-γ-but p.49). With ETPH this sort of increase apparently did not matter since both PB and DNS-γ-but responded to energy dependent changes (p.89). As the charge was moved further away (e.g. ABS p.91) the probe was still energy dependent, and started to sense electron transfer changes. Waggoner and Stryer[238] have investigated the properties of probes based on anthracene, in phosphatidyl choline bilayers. As the distance between the anthracene moiety and the polar group of the side chain is increased, the polarity of the anthracene's environment (as determined by λ_{max} not intensity) decreases, indicating that the anthracenoyl group is buried further and further into the hydrophobic interior of the lipid bilayer. It is tempting to suppose that in ETPH the negative charge on the probe takes it to a region where it can sense energy dependent changes, but as the fluorophore to charge distance increases, the fluorophore moves further into the hydrophobic region, through an area where it can sense electron transfer.

The foregoing discussion has indicated the nature of the region in which ANS and similar probes bind to ETPH. The possible causes of enhancement of probe fluorescence must now be discussed. The increased fluorescence intensity on energis-

ation could be due to an increase in binding, or to an increase in quantum yield (caused by decreased polarity, increased viscosity or decreased quenching). Binding parameters were measured for ANS and MNS by the conventional technique (i.e. extrapolation of a limiting enhancement, followed by Scatchard plots). These measurements indicated both an increase in binding and an increase in quantum yield on energisation[223,225]. Azzi has tried to argue[239] that the enhancement is due solely to an increase in binding, but his results are based on centrifugation procedures which require particles to remain aerobic for long periods (ca 30 mins) in a highly concentrated form. It seems likely that at best, his measurements are of binding to anaerobic particles. The increase in quantum yield is not accompanied by a detectable shift in emission maximum. This suggests that the increase is due not to a change in polarity or viscosity, but to a decrease in some sort of quenching process. The most obvious cause is a decrease in quenching by water (a quencher of ANS[20]) as a result of decreased contact with water within the membrane.

The conventional methods of measuring binding parameters used above involve various extrapolations. The difficulties of the commonly used methods have been critically reviewed by Deranleau[240]. In particular it is important that a large part of the saturation curve is covered (ca 75%) in order to obtain

meaningful secondary plots. In systems where there are multiple equilibria, linear secondary plots will be obtained only if the individual microscopic dissociation constants (and hence the spectroscopic changes caused by binding) are identical or very similar. Neither of these two criteria is normally fulfilled. Most authors assume that if a Scatchard plot gives a straight line with a negative slope, the differences between binding constants are small. The filtration technique developed for measuring PS binding (p.41) was used to measure ANS binding. The results confirmed the data obtained by conventional techniques (p.75).

One way of separating the movement of probe from the quantum yield change would be to use a covalently attached probe. The preliminary results with NBD-Cl indicated that energisation exposes more -SH groups, and that the -SH groups in ESMP are more reactive than those in ETPH.

A second way of separating the two effects was to examine the uncoupling kinetics. A rapid phase common to all the probes was observed, followed by a slow phase (p.77). The latter was characteristic of each probe and could be correlated with the rate at which the probes diffused out of the membrane after uncoupling (p.78). The fast phase appears to be a decrease in quantum yield associated with some rapid membrane change.

A third way of effecting the separation was to use a probe

whose fluorescence was not polarity sensitive, and which would therefore respond to a different parameter of its environment. Such a probe was PS. Its fluorescence proved to be solvent sensitive in water/ethanol mixtures, a fact which could only to some extent be explained by the variation in viscosity. The shape of fig.33 (i.e. variation of monomer fluorescence with ethanol concentration) is very close to being the mirror image of the refractive index curve (fig.34). It seems therefore that the PS monomer fluorescence intensity is inversely related to the solvent polarisability. On binding to ETPH, PS fluorescence was quenched slightly (p.71). This could be due to light scattering by the particles. There are quite marked light scattering changes on energisation, but there is disagreement over whether they are simultaneous with[241], or preceded by[242] the changes detected by ANS.

On energisation PS fluorescence at 400nm (monomer) decreased while that at 500nm (excimer) increased (but with a lag phase) (p.71). The excimer formation on energisation could be due to an increase in concentration (as a result of increased binding or of a decrease in volume of the space in which PS binds) or to a decrease in viscosity, or to a combination of these. Comparison of the PS uncoupling kinetics with those of MNS and ANS showed that it detected the same rapid phase as the other two (p.77). This, together with the similar structures of the three probes,

suggested that they bind in the same area of the membrane. The changes in polarisation of fluorescence and life-times of ANS and MNS on energisation indicated that there was no significant increase in viscosity on energisation (p.78). The small increase was in the wrong direction to cause an increase in PS excimer fluorescence, and so could be dismissed as a cause of the observed changes.

Attempts to obtain binding parameters for PS by the filtration technique failed, producing nonsensical Scatchard plots. However, the data could be used to compare the actual amounts of PS bound to energised and resting particles, (the amount bound doubled on energisation -p.76) and also to estimate how much of the membrane PS occupied:-

From the concentration dependence of PS fluorescence in water (fig.32) it was possible to estimate (by the ratio of 400nm:500nm fluorescence) that the local concentration of PS in the energised membrane must be of the order of 1M. Using the estimated reciprocal density of the membrane (0.84 ml/g[109]) and the amount of PS bound (8.8μM) it was possible to calculate the local concentration of PS in the membrane, assuming uniform distribution throughout the membrane, as 10mM. It seems therefore, that PS occupies about 1% of the energised membrane volume. The data are not accurate enough to detect a change

in occupancy between resting and energised membrane. The increase in excimer fluorescence is much larger than the change in binding which must indicate that only a fraction of the PS molecules bind at sites where they respond. This means that the above calculation overestimates the concentration and that the occupancy is less than 1%.

The uptake of PS on energisation was not large enough to account for the observed excimer fluorescence. The other possible reason for the increase in PS concentration (and hence in excimer fluorescence) was a decrease in volume of the area in which PS binds i.e. the excimer fluorescence could be used as a volume indicator. It was postulated (p.79) that the decrease in volume was due to expulsion of water from the membrane on energisation. This hypothesis was investigated in a number of ways, notably by examining the responses of ANS and MNS in D_2O and H_2O. In buffer the fluorescence of both probes is increased in D_2O since this is a less efficient quencher than H_2O. A smaller, but significant, isotope effect was present when the probes bound to ETPH (both energised and resting - p.82). This indicated that the bound probes are in restricted contact with the solvent in both states of ETPH, i.e. as seen from earlier studies, they are not completely buried in the lipid phase. This is in contrast to several workers who chose to interpret their results

in terms of ANS binding predominantly to the lipid phase[243,108]

The isotope effects on ANS and MNS dropped on binding to ETPH to 57% and 63% respectively of their values in buffer. On energisation these values changed to 55% and 50% respectively (p.81). This indicated that energisation caused a large decrease in the contact which MNS has with the solvent. In view of the fact that only ca 25% of the probe molecules are bound within the membrane, this could mean that water is completely excluded from the 'slow' sites after energisation.

Two further points are worth mentioning:-

a) Energisation causes a smaller increase in ANS quantum yield in D_2O than in H_2O (p.81). Since D_2O quenches ANS fluorescence less than H_2O does, movement of water away from ANS will cause a smaller increase in fluorescence in D_2O than in H_2O. If the enhancement were by any other mechanism, the effect would be the same in D_2O as in H_2O.

b) It is quite likely that the probes bind at an interface between a hydrophobic region and an aqueous region. If this is so, the amino group of MNS will be more deeply buried in the hydrophobic region than is that of ANS. The water quenching of ANS fluorescence is believed to involve the amino group (p.9), and so decreased contact with water would have a larger effect on MNS than on ANS. This was in fact observed, suggesting that energisation causes MNS to become more deeply buried. Rapid

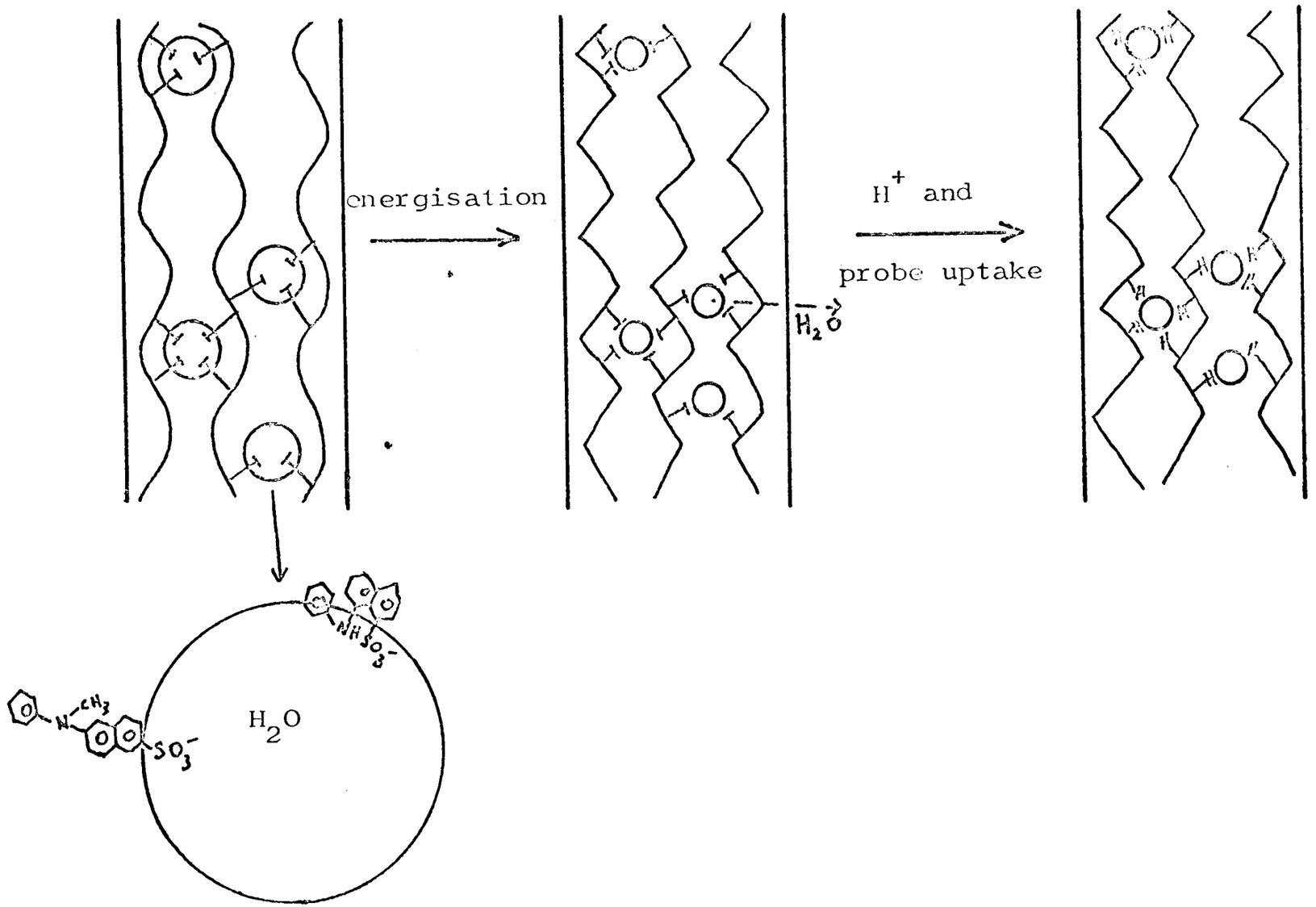

Figs. 72A 72B 72C

D_2O/H_2O exchanges was demonstrated in the energised state (p.81) so the decreased contact must be as a result of removal of water from the environment of the probes.

With all the above observations in mind, it is possible to propose a mechanism of energisation which involves expulsion of water from the membrane (cf Williams[213]). It is envisaged that the three probes (PS, MNS, ANS) bind within the membrane (slow sites) at the surfaces of pockets of water (fig.72A). Energisation causes a rapid structural change which expels water (fig.72B). This is followed by (or more or less simultaneous with) uptake of ANS and protons (fig.72C). The expulsion of water causes the pockets of water to shrink, as detected by the probes, and also forces ionised carboxyl side-chains into the hydrophobic region. These then need to take up protons in order to become stabilised in their new environment. The disappearance of negative charge from the pockets of water also allows more negatively charged probe molecules to bind. This dehydrated membrane can then drive the phosphorylation of ADP (which produces water).

B. Probe structure

Two main questions had to be answered concerning the type of structure needed for a fluorescent molecule to be a good probe:-

(i) what structural characteristics impart environmental

sensitivity?

(ii) what is the importance of the charged group in directing the probe to an area in the membrane where it can sense structural changes?

The environmental factors which affect fluorescence were discussed in the introduction (p.2-9). It appears that the anilino-naphthalene derivatives will be good probes for polarity changes since they have a large dipole-moment change on excitation (giving a large shift in λ_{max}) and restriction of the freedom of rotation about the amino group causes large intensity changes. In aqueous systems they also have the advantage of being quenched by water. However, it is important to realise that the mechanism of fluorescence enhancement of this type of molecule is not well understood, and that, therefore, the shift in λ_{max}, not the change in intensity, should be used as a measure of environmental polarity. Many workers have used intensity changes to measure binding site polarity[11,~~125~~ 236]. For following changes in viscosity and rigidity other probes will be more useful. Pyrene derivatives with their special property of excimer formation are particularly suitable for measuring viscosity changes, while molecules like retinol are able to sense changes in rigidity.

Probably of more importance though in biochemical systems is the problem of directing the probe to a relevant site. A

negative charge was necessary for a probe to sense the structural change in GDH (p.51). As might have been expected, neutralisation of the charge on MNS abolished its response to energy dependent changes in SMP (p.84). However, in this case a marked gradation could be seen with various neutral probes. By making the MNS amides with progressively longer alkyl substituents the rate of interaction with SMP was slowed down (p.84). However, less polar neutral probes like NPN and retinol interacted as rapidly with SMP as did ANS and MNS. Obviously the slowing down of the MNS amides must be some sort of size effect not one of limited access to the lipid phase.

Having established that a negative charge was necessary, it was expected that increasing the distance between the aromatic part of the probe and the negative charge would alter the way in which the probe responded. Thus in SMP it was possible with various probes (e.g. DNS-γ-but, ABS, PB) and in comparison with the work of Stryer, Chance et al[238,244], to draw up a rough scale of distances:-

⊖ responds to energy dependent changes only	also responds to electron transfer	buried
5Å ANS, MNS	10 - 12Å ABS	? 20Å

An outstanding question now was whether or not there was any specificity for the type of charge on the probe. The commonly used probes are all sulphonates (MNS, TNS, ANS) though it has been

shown that the DNS amino acids (p.89) and PB (p.90) can be used as probes. The fact that these probes respond less (i.e. smaller enhancements and shifts) could be due to several things:- the different charge; the increased distance between the charge and the fluorophore; or decreased sensitivity to polarity changes. What was needed was a series of closely related probes in which the only change was in the type of charge. The 9-anilino-acridines fulfilled this requirement, and were shown to have very similar fluorescence properties in water/ethanol mixtures (p.91). They illustrated well the fact that intensity depends on viscosity and quenching as well as polarity (p.91). However, only the sulphonate (ABS) was enhanced by ETPH or responded to energisation (p.92). This seems to indicate that a sulphonate group is preferred, while in certain circumstances a $-COO^-$ will do. The reasons for this are probably similar to the reasons why organic sulphonates are good detergents i.e. the right combination of pK_a, ion complexing ability, and lipid solubility, rather than some more specific requirement of SMP.

The increased distance between charge and fluorophore in ABS resulted in its also responding to electron transfer. This response was a result of some process associated with that part of the electron transfer chain which precedes the antimycin A site (p.93). From preliminary experiments it was suggested that the probe response and coenzyme Q oxidation were related (p.94).

APPENDICES

APPENDIX 1

R_F values for dansyl amino acids in Solvent E on Silica gel G.

	R_F		R_F
DNS-OH	0.98	DNS-isp	0.84
DNS-NH_2	0.95	DNS-Try	0.85
DNS-Ala	0.86	DNS-Cys	0.77
DNS-Asp	0.74	DNS-Glm	0.84
DNS-But	0.94	DNS-Gly	0.86
DNS-Glu	0.70	DNS-His	0.87
DNS-Leu	0.87	DNS-Phe	0.87
DNS-Met	0.91	DNS-Nor	0.94
DNS-Pro	0.83	DNS-γBut	0.75
DNS-Ser	0.83		

9-anilino acridines in pyridine:butanol:water (20:40:40).

ABA	0.60
ABC	0.95
ABS	0.70

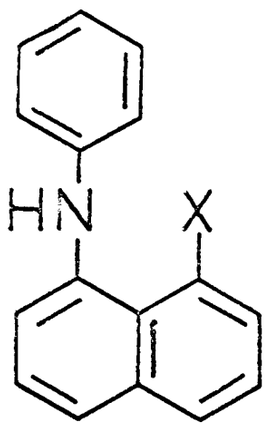

	X =
ANS	SO_3^-
NPN	H

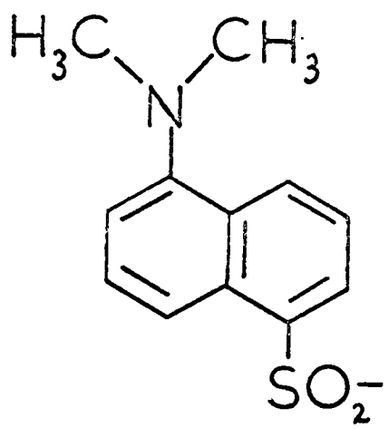

DNS-

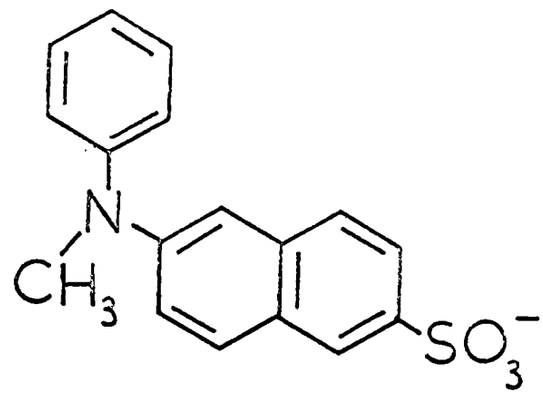

MNS

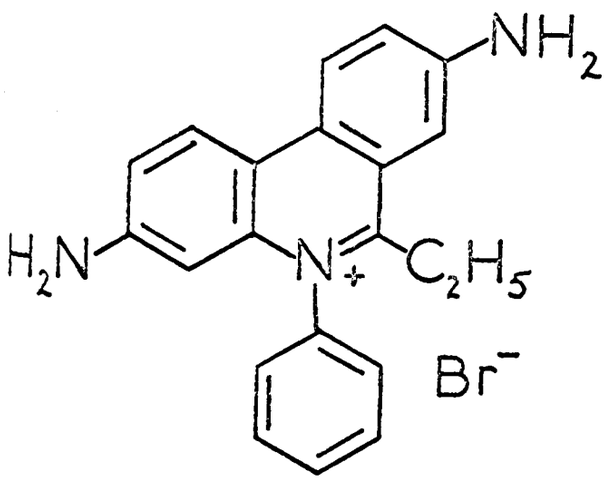

Ethidium bromide

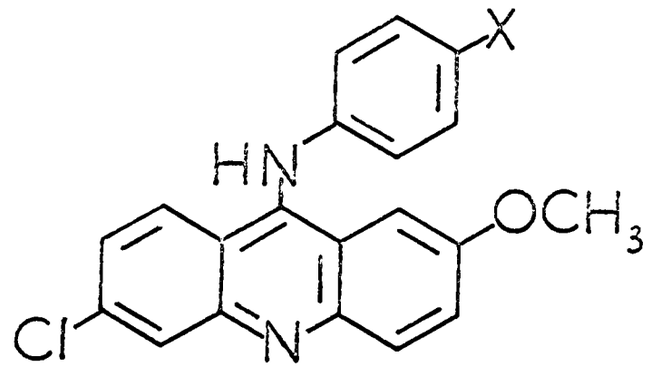

	X =
ABA	$-A_5O_3^{2-}$
ABC	$-COO^-$
ABS	$-SO_3^-$

REFERENCES

References

1. Williams, R.J.P. Quart. Rev. Chem. Soc. 24, 331, (1970). (Tilden Lecture).
2. Cohn, M. Quart. Rev. Biophys. 3, 61, (1970).
3. Birkett, D.J., Dwek, R.A., Radda, G.K., Richards, R.E., & Salmon, A.G., submitted to Eur. J. Biochem. (1970).
4. a) McConnell, H.M., & McFarland B.G. Quart. Rev. Biophys. 3, 91, (1970).
   b) Price, N.C. in "Amino Acids, Peptides and Proteins", Vol.II ed. G.T. Young, Chem. Soc. London, (1970) p.127.
5. Chance, B., & Mela, L. J. Biol. Chem. 241, 4588, (1966).
6. Basu, S. Adv. Quantum Chem. 1, 45, (1964).
7. Wehry, E.L. in "Fluorescence - Theory, instrumentation and practice", ed. G.G. Guilbault, Edward Arnold (1967) p.37.
8. Lippert, E. Z. Electrochem. 61, 962, (1957).
9. Onsager, L. J. Am. Chem. Soc. 58, 1486, (1936).
10. Kosower, E.M. J. Am. Chem. Soc. 80, 3253, (1958).
11. Turner, D.C. & Brand, L. Biochemistry, 7, 3381, (1968).
12. Balasubramaniyan, V. Chem. Rev. 66, 567, (1966).
13. Ainsworth, S. & Flanagan, M.T. Biochim. Biophys. Acta. 194, 213, (1969).
14. Thomson, A.J. J. Chem. Phys. 51, 4106, (1969).
15. Parker, C.A. "Photoluminescence of Solution", Elsevier, Amsterdam (1968).

16. Horrocks, A.R., Medinger, T., & Wilkinson, F. Photochem. Photobiol. 6, 21, (1967).

17. Camerman, A., & Jensen, L.H. Science 165, 493, (1969).

18. Stryer, L. J. Mol. Biol. 13, 482, (1965).

18a. Weber, G. & Shinitzky, M. Proc. Nat. Acad. Sci. 65, 823, (1970).

19. Kasha, M. in "Fluorescence - Theory, instrumentation and practice", ed. G.G. Guilbault, Edward Arnold (1967), p.201.

20. Stryer, L. J. Am. Chem. Soc. 88, 5708, (1966).

21. Eisinger, J. in "Molecular Luminescence", ed. E.C. Lim, Benjamin, (1969), p.185.

22. Döller, E., & Förster, Th. Z. Phys. Chem. 34, 132, (1962).

23. Förster, Th. Disc. Farad. Soc. 27, 1, (1959).

24. Weber, G. Adv. Protein Chem. 8, 415, (1953).

25. Brand, L. & Witholt, B. in "Methods in Enzymology" Vol.XI, ed. C.W. Hirs, Acad. Press (1967), p.776.

26. Edelman, G.M. & McClure, W.O. Acc. Chem. Res. 1, 65, (1968).

27. Stryer, L. Science, 162, 526, (1968).

28. Radda, G.K. in "Current Topics in Bioenergetics" Vol.4. ed. D.R. Sanadi, Acad. Press (1970) in the press.

29. Brocklehurst, J.R. in "Amino Acids, Peptides & Proteins" vol.II, ed. G.T. Young, Chem. Soc., London, (1970) p.123.

30. Chen, R.F. in "Fluorescence - Theory, instrumentation and practice", ed. G.G. Guilbault, Edward Arnold (1967), p.443.

31. Weber, G. & Young, L.B. J. Biol. Chem. 239, 1415, (1964).

32. Daniel, E. & Weber, G. Biochemistry, 5, 1893, (1966).

33. Weber, G. & Daniel, E. Biochemistry, 5, 1900, (1966).

34. Weber, G. & Anderson, S.R. Biochemistry, 4, 1942, (1965).

35. Anderson, S.R. & Weber, G. Biochemistry, 4, 1948, (1965).

36. Laurence, D.J.R. Biochem. J., 51, 168, (1952).

37. Witholt, B. & Brand, L. Biochemistry, 9, 1948, (1970).

38. Anderson, S.R. & Weber, G. Biochemistry, 8, 371, (1969).

39. Anderson, S.R. Biochemistry, 8, 4838, (1969).

40. Pasby, T.L. & Weber, G. Biochemistry, 9, (1970) in the press.

41. Rosen, C-G. & Weber, G. Biochemistry, 8, 3915, (1969).

42. Duke, J.A., McKay, R. & Bolts, J. Biochim. Biophys. Acta. 126, 600, (1966).

43. Cheung, H.C. & Morales, M.F. Biochemistry, 8, 2177, (1969).

44. Dodd, G.H. & Radda, G.K. Biochem. J. 114, 407, (1969).

45. Thompson, W. & Yielding, K.L. Arch. Biochem. Biophys. 126, 399, (1968).

46. Jallon, J.M., Di Franco, A. & Iwatsubo, M. Eur.J.Biochem. 13, 428, (1970).

47. Price, N.C. & Radda, G.K. Biochem. J. 114, 419, (1969).

48. Brand, K. FEBS Lett. 7, 235, (1970).

49. Winkler, M. J. Mol. Biol. 4, 118, (1962).

50. Parker, C.W. & Osterland, C.K. Biochemistry, 9, 1074, (1970).

51. Berns, D.S. & Singer, S.J. Immunochem. 1, 209, (1964).

52. McClure, W.O. & Edelman, G.M. Biochemistry, 6, 559, (1967).

53. McClure, W.O. & Edelman, G.M. Biochemistry, 6, 567, (1967).

54. Wang, J.L. & Edelman, G.M. Fed. Proc. 29, 402, (1970).

55. Lynn, J. & Fasman, G.D. Biochem. Biophys. Res. Comm. 33, 327, (1968).

56. Winkler, M.H. Biochemistry, 8, 2586, (1969).

57. Chen, R.F. Arch. Biochem. Biophys. 120, 609, (1967).

58. Parker, C.W., Yoo, J.J., Johnson, M.C., & Godt, S.M. Biochemistry, 6, 3408, (1967).

59. Cheung, H.C., Smith, L. & Cooke, R. Fed. Proc. 29, 667, (1970).

60. Birkett, D.J., Radda, G.K. & Salmon, A.G. FEBS Lett. (1970) in the press.

61. Winer, G.W. & Schwert, A.D., Biochim. Biophys. Acta, 29, 424, (1958).

62. Churchich, J.E. & Wold, F. Biochemistry, 2, 781, (1963).

63. Bayley, P.M. & Radda, G.K. Biochem. J. 98, 105, (1966).

64. Sund, H. Acta Chem. Scand. 15, 940, (1961).

65. Fisher, H.F. & McGregor, L.L. Biochim. Biophys. Acta, 43, 557, (1960).

66. Sund, H. Acta Chem. Scand. 19, 390, (1965).

67. Tomkins, G.M., Yielding, K.L. & Curran, J.F. J. Biol. Chem. 237, 1704, (1962).

68. Theorell, H. & Winer, A.D. Arch. Biochem. Biophys. 83, 291, (1959).

69. Weiner, H. Arch. Biochem. Biophys. 126, 692, (1968).

70. Kim, S.J. & Anderson, B.M. J. Biol. Chem. 244, 1547, (1969).

71. Hsu, R.Y. & Lardy, H.A. J. Biol. Chem. 242, 527, (1967).

72. Blomquist, C.H. J. Biol. Chem. 244, 1605, (1969).

73. Cortijo, M. & Shaltiel, S. Biochem. Biophys. Res. Comm. 39, 212, (1970).

74. Churchich, J.E. & Farrelly, J.G. J. Biol. Chem. 244, 3685, (1969).

75. Kierzenbaum, F., Dandliker, J. & Dandliker, W.B. Immunochem. 6, 125, (1969).

76. Steiner, R.F. & Edelhoch, H. Chem. Rev. 62, 457, (1962).

77. Horton, H.R. & Koshland, D.E. Jnr. in "Methods in Enzymology", Vol.XI. ed. C.W. Hirs Acad. Press, (1967), p.856.

78. Chen, R.F. Arch. Biochem. Biophys. 133, 263, (1969).

79. Klotz, I. in "Protein Structure and Function", Brookhaven Symp. in Biology, 13, (1960), p.25.

80. Young, M. Biochim. Biophys. Acta, 71, 206, (1963).

81. Gally, J.A. & Edelman, G.M. Biochim. Biophys. Acta., 94, 175, (1965).

82. Massey, V., Harrington, W.F. & Hartley, B.S. Disc. Farad. Soc. 20, 24, (1955).

83. Churchich, J.E. Arch. Biochem. Biophys. 97, 574, (1962).

84. Young, D.M. & Potts, J.T. Jnr. J. Biol. Chem. 238, 1995, (1963).

85. Wahl, P. & Timashef, S.N. Biochemistry, 8, 2945, (1969).

86. Wahl, P. & Weber, G. J. Mol. Biol. 30, 371, (1967).

87. Anderson, S.R. Biochemistry 8, 1394, (1969).

88. Rawitch, A.B., Hudson, E. & Weber, G. J. Biol. Chem. 244, 6543, (1969).

89. Knopp, J.A. & Weber, G. J. Biol. Chem. 244, 6309, (1969).

90. Johnson, P. & Thornton, A.C.R. Biochem. J. 115, 725, (1969).

91. Cowgill, R.W. Biochim. Biophys. Acta. 168, 417, (1968).

92. Bernstein, R.S., Wilchek, M. & Edelhoch, H. J. Biol. Chem. 244, 4398, (1969).

93. Velick, S.F. J. Biol. Chem. 233, 1455, (1958).

94. Price, N.C. & Radda, G.K. submitted to Biochim. Biophys. Acta (1970).

95. Galley, W.C. & Stryer, L. Proc. Nat. Acad. Sci. 60, 108, (1968).

96. Badley, R.A. & Teale, F.W.J. J. Mol. Biol. 44, 71, (1969).

97. Stryer, L. & Haugland, R.P. Proc. Nat. Acad. Sci. 58, 719, (1967).

98. Conrad, R.H. & Brand, L. Biochemistry, 7, 777, (1968).

99. Newton, B.A. J. Gen. Microbiol. 10, 491, (1954).

100. Burns, V.W. Biochem. Biophys. Res. Comm. 37, 1008, (1969).

101. Rubalcava, B., de Muñoz, D.M. & Gitler, C. Biochemistry, 8, 2742, (1969).

102. Freedman, R.B. & Radda, G.K. FEBS Lett. 3, 150, (1969).

103. Gitler, C., Rubalcava, B. & Caswell, A. Biochim. Biophys. Acta. 193, 479, (1969).

104. Tasaki, I., Watanabe, A., Sandlin, R. & Carnay, L. Proc. Nat. Acad. Sci. 61, 883, (1968).

105. Tasaki, I., Carnay, L., Sandlin, R. & Watanabe, A. Science 163, 683, (1969).

106. Kasai, M., Changeux, J-P. & Monnerie, L. Biochem. Biophys. Res. Comm. 36, 420, (1969).

107. Kasai, M., Podleski, T.R. & Changeux, J.P. FEBS Lett. 7, 13, (1970).

108. Vanderkooi, J. & Martonosi, A. Arch. Biochem. Biophys. 133, 153, (1969).

109. Azzi, A., Chance, B., Radda, G.K. & Lee, C.P. Proc. Nat. Acad. Sci. 62, 612, (1969).

110. Chance, B., Radda, G.K. & Lee, C.P. in Round Table Discussion on Electron Transport and Energy Conservation, eds. J.M. Tager, S. Papa, E. Quagliarello, & E.C. Slater, Bari (1969) p.19.

111. a) Smith, A.L. in "Methods in Enzymology", Vol.XI ed. C.W. Hirs, Acad. Press., (1967), p.81.

b) Crane, F.L., Glenn, J.L. & Green, D.E. Biochim. Biophys. Acta, 22, 475, (1956).

112. a) Beyer, R.E. in "Methods in Enzymology", Vol.X, ed. R.W. Estabrook & M.E. Pullman, Acad. Press (1967) p.186.

b) Hansen, M. & Smith, A.L. Biochim. Biophys. Acta, 81, 214, (1964).

113. Linnane, A.W. & Titchener, E.B. Biochim. Biophys. Acta 38, 469, (1960).

114. Dodge, J.T., Mitchell, C. & Hanahan, D.J. Arch. Biochem. Biophys. 100, 119, (1963).

115. Cory, R.P., Becker, R.R., Rosenbluth, R. & Isenburg, I. J. Am. Chem. Soc. 90, 1643, (1968).

116. Rinderknecht, H. a) Experientia 16, 430, (1960), b) Nature 193, 167, (1962).

117. Dupré, D.J. & Robinson, F.A. J. Chem. Soc. (1945), 549.

118. Boulton, A.J., Ghosh, P.B. & Katritzky, A.R. J. Chem. Soc. B, (1966), 1004.

119. Gray, W.R. in "Methods in Enzymology", Vol.XI, ed. C.W. Hirs, Acad. Press, (1967), p.469.

120. Gray, W.R. & Hartley, B.S., unpublished paper. cf. Biochem. J. 89, 59P, (1963).

121. Millar, D., Minzghor, K. & Steiner, R. Biochim. Biophys. Acta, 65, 153, (1962).

122. Morse, D. & Horecker, B.L. Anal. Biochem. 14, 429, (1966).

123. Seiler, N. & Wieckmann, J. Experientia, XX, 559, (1964).

124. Parker, C.A. in "Advances in Photochemistry", Vol.II, eds. W.A. Noyes, G.S. Hammond & J.N. Pitts, Interscience, (1964), p.305.

125. Clark, L.C. Trans. Am. Soc. Art. Sci. Int. Organs, 2, 41, (1956).

126. Olson, J.A. & Anfinson, C.B. J. Biol. Chem. 197, 67, (1952).

127. Lowry, O.H., Rosebrough, N.J., Farr, A.L. & Randall, R.J. J. Biol. Chem. 193, 265, (1951).

128. Marler, E. & Tanford, C. J. Biol. Chem. 239, 4217, (1964).

129. Appella, E. & Tomkins, G.M. J. Mol. Biol. 18, 77, (1966).

130. Sund, H. Acta Chem. Scand. 17, S102, (1963).

131. Frieden, C. J. Biol. Chem. 234, 815, (1959).

132. Fisher, H.F., Cross, D.G. & McGregor, L.L. Nature, 196, 895, (1962).

133. Eisenberg, H. & Tomkins, G.M. J. Mol. Biol. 31, 37, (1968).

134. Sund, H., Pilz, I. & Herbst, M. Eur. J. Biochem. 7, 517, (1969).

135. Reisler, E., Pouyet, J. & Eisenberg, H. Biochemistry, 9, 3095, (1970).

136. Horne, R.W. & Greville, G.D. J. Mol. Biol. 6, 506, (1963).

137. Reisler, E. & Eisenberg, H. Biopolymers, 9, 113, 877, (1970).

138. Engel, P.C. & Dalziel, K. Biochem. J. 115, 621, (1969).

139. Engel, P.C. & Dalziel, K. Biochem. J. 118, 409, (1970).

140. Struck, J. Jnr. & Sizer, I.W. Arch. Biochem. Biophys. 86, 260, (1960).

141. Caughey, W.S., Smiley, J.D. & Hellerman, L. J. Biol. Chem. 224, 591, (1957).

142. Tomkins, G.M. & Yielding, K.L. Cold Spring Harbour Symp. Quant. Biol. 26, 331, (1961).

143. Yielding K.L., Tomkins, G.M., Bitensky, M.W. & Talal, N. Canad, J. Biochem. 42, 727, (1964).

144. Frieden, C. Biochem. Biophys. Res. Comm. 10, 410, (1963).

145. Tomkins, G.M., Yielding K.L., Curran, J.F., Summers, M.R. & Bitensky, M.W. J. Biol. Chem. 240, 3793, (1965).

146. Frieden, C. J. Biol. Chem. 238, 3286, (1963).

147. Colman, R.F. & Frieden, C. Biochem. Biophys. Res. Comm. 22, 100, (1966).

148. Talal, N. & Mushinski, J.F. Fed. Proc. 22, 289, (1963).

149. Dodd, G.H. & Radda, G.K. Biochem. Biophys. Res. Comm. 27, 500, (1967).

150. Brocklehurst, J.R. Part II Thesis, Oxford, (1968).

151. Ballard, S.G. Part II Thesis, Oxford, (1970).

152. Baker, B.R. J. Theoret. Biol. 3, 446, (1962).

153. Churchich, J.E. Biochim. Biophys. Acta 147, 32, (1967).

154. Yielding, K.L. & Holt, B. J. Biol. Chem. 242, 1079, (1967).

155. Malcolm, A.D.B. D.Phil Thesis, Oxford, (1970).

156. Malcolm, A.D.B. Unpublished observations, (1970).

157. Smith, E.L., Landon, M., Piszkiewicz, D., Brattin, W.J., Langley, T.J. & Melamed, M.D. Proc. Nat. Acad. Sci., 67, 724, (1970).

158. Frieden, C. Biochim. Biophys. Acta, 47, 428, (1961).

159. Dickenson, F.M. Private Communication, (1969).

160. Korn, E.D. Ann. Rev. Biochem. 38, 263, (1969).

161. Korn, E.D. Fed. Proc. 28, 6, (1969).

162. Finean, J.B. Quart. Rev. Biophys. 2, 1, (1969).

163. Zahler, P.H. Experientia, 25, 449, (1969).

164. Hall, D.O. & Palmer, J.M. Nature, 221, 717, (1969).

165. Pullman, M.E. & Schatz, G. Ann. Rev. Biochem. 36, 539, (1967).

166. Korn, E.D. Science, 153, 1491, (1966).

167. Fernandez-Moran, H. & Finean, J.B. J. Biophys. Biochem. Cytol. 3, 725, (1957).

168. Sjörstrand, F.S. J. Ultrastruct. Res. 9, 561, (1963).

169. Sjörstrand, F.S. & Barajas, L. J. Ultrastruct.Res. 25, 121,(1968).

170. Fernandez-Moran, H. Science, 140, 381, (1963).

171. Fernandez-Moran, H., Oda, T., Blair, P.V. & Green, D.E. J. Cell Biol. 22, 63, (1964).

172. Parsons, D.F. Science, 140, 985, (1963).

173. Stasny, J.T. & Crane, F.L. J. Cell Biol. 22, 49, (1964).

174. Penniston, J.T., Harris, R.A., Asai, J. & Green, D.E. Proc. Nat. Acad. Sci. 59, 624, (1968).

175. Harris, R.A., Penniston, J.T., Asai, J. & Green, D.E. Proc. Nat. Acad. Sci. 59, 830, (1968).

176. Green, D.E. & Harris, R.A. FEBS Lett. 5, 241, (1969).

177. Kagawa, Y. & Racker, E. J. Biol. Chem. 241, 2475, (1966).

178. Racker, E. & Horstman, L.L. J. Biol. Chem. 242, 2547, (1967).

179. Christiansen, R.O., Loyter, A., Steensland, H., Saltzgaber, J. & Racker, E. J. Biol. Chem. 244, 4428, (1969).

180. Wrigglesworth, J.M., Packer, L. & Branton, D. Biochim. Biophys. Acta, 205, 125, (1970).

181. Brenner, S. & Horne, R.W. Biochim. Biophys. Acta. 34, 103, (1959).

182. Blais, J.J.B.P. & Geil, P.H. Biopol. 8, 275, (1969).

183. Lenard, J. & Singer, S.J. Proc. Nat. Acad. Sci. 56, 1828, (1966).

184. Wrigglesworth, J.M. & Packer, L. Arch. Biochem. Biophys. 133, 194, (1969).

185. Glaser, M., Simpkins, H., Singer, S.J., Sheetz, M. & Chan, S.I. Proc. Nat. Acad. Sci. 65, 721, (1970.)

185a. Lenard, J. & Singer, S.J. Science, 159, 738, (1968).

186. Maddy, A.H. & Malcolm, B.R. Science, 150, 1616, (1965).

187. Graham, J.M. & Wallach, D.F.H. Biochim. Biophys. Acta. 193, 225, (1969).

188. Kamat, V.B. & Chapman, D. Biochim. Biophys. Acta, 163, 411, (1968).

189. Sheetz, M.P. & Chan, S.I. Abstract 7 in "N.m.r. in Biological Systems", Oxford, (1970).

190. a) Metcalfe, J.C., Seeman, P. & Burgen, A.S.V. Mol. Pharmacol. 4, 87, (1968).

b) Metcalfe, J.C. Abstract 3 in "N.m.r. in Biological Systems", Oxford, (1970).

191. Hubbell, W.L. & McConnell, H.J. Proc. Nat. Acad. Sci. 63, 16, (1969).

192. Griffith, O.H. & Waggoner, A.S. Acc. Chem. Res. 2, 17, (1969).

193. McConnell, H.J. in "N.m.r. in Biological Systems", Oxford, (1970).

194. Calvin, M., Wang, H.H., Entine, G., Gill, D., Ferruti, P., Harpold, M.A. & Klein, M.P. Proc. Nat. Acad. Sci. 63, 1, (1969).

195. Gendel, L.Y., Gol'dfel'd, M.G., Kol'tover, V.K. Biofizika, 13, 1114, (1968), (Chem. Abs. 70, 64266u, (1969)).

196. Davson, H. & Danielli, J.F. "The Permeability of Natural Membranes", Cambridge, 1952.

197. Zahler, P.H. & Weibel, E.R. J. Cell Biol. in the press.

198. Lucy, J.A. in "Biological Membranes", ed. D. Chapman, Acad. Press, (1968), p.233.

199. Brierley, G.P. Biochemistry, 9, 697, 708, 714, (1970).

200. Masseri, S. & Azzone, C.F. Eur. J. Biochem. 12, 301, (319,328), (1970).

201. Lehninger, A.L. Biochem. J. 119, 129, (1970).

202. Mandel, L.J. Nature, 225, 450, (1970).

203. Volkenstein, M.V. & Fishman, S.N. Biochim. Biophys. Acta. 203, 1, 10, (1970).

204. Chance, B., Wilson, D.F., Dutton, P.L. & Erecinska, M. Proc. Nat. Acad. Sci. 66, 1175, (1970).

205. Crane, F.L. in "Biological Oxidations" ed. T.P. Singer, Wiley (1968), p.533.

206. Chance, B. & Williams, G.R. Adv. in Enzymology 17, 65, (1956).

207. Gutman, M., Singer, T.P., Beinert, H. & Casida, J.E. Proc. Nat. Acad. Sci. 65, 763, (1970).

208. Gutman, M., Mersmann, H., Luthy, J. & Singer, T.P. Biochemistry, 9, 2678, (1970).

209. Lardy, H.A. & Ferguson, S.M. Ann. Rev. Biochem. 38, 991, (1969).

210. Boyer, P.D. in "Biological Oxidations", ed. T.P. Singer, Interscience, (1968), p.193.

211. Greville, G.D. in "Current Topics in Bioenergetics", Vol.3, ed. D.R. Sanadi, Acad. Press (1969), p.1.

212. Schatz, G. Angew Chem. Int. Ed. 6, 1035, (1967).

213. Williams, R.J.P. in "Current Topics in Bioenergetics", Vol.3, ed. D.R. Sanadi, Acad. Press, (1969), p.80.

214. Slater, E.C. Nature, 172, 875, (1953).

215. Cross, R.L. & Wang, J.H. Biochem. Biophys. Res. Comm. 38, 848, (1970).

216. Wang, J.H. Science, 167, 25, (1970).

217. Mitchell, P. Nature, 191, 144, (1961).

218. Liberman, E.A. & Skulachev, V.P. Biochim. Biophys. Acta, 216, 30, (1970).

219. Slater, E.C. Eur. J. Biochem. 1, 317, (1967).

220. Grinius, L.L., Jasaitis, A.A., Kadziauskas, Y.U.P., Liberman, E.A., Skulachev, V.P., Topali, V.P., Tsofina, L.A. & Vladimirova, M.A. Biochim. Biophys. Acta, 216, 1, (1970).

221. Williams, R.J.P. J. Theoret. Biol. 3, 209, (1962).

222. Jardetsky, O. Nature, 211, 969, (1966).

223. Freedman, R.B. D.Phil. Thesis, Oxford, (1969).

224. Nordenbrand, K. & Ernster, L. Abstracts of 8th Int. Cong. Biochemistry (1970) p.153.

225. Brocklehurst, J.R., Freedman, R.B., Hancock, D.J. & Radda, G.K. Biochem. J. 116, 721, (1970).

226. Hancock, D.J. B.Sc. Thesis, Oxford, (1969).

227. Lee, C.P. & Radda, G.K. Bari Symp. (1970) in the press.

228. Birkett, D.J., Price, N.C., Radda, G.K. & Salmon, A.G. FEBS Lett. 6, 346, (1970).

229. Radda, G.K. & Smith, D.S. FEBS Lett. 9, 287, (1970).

230. Radda, G.K. & Smith, D.S. Unpublished observations, (1970).

231. Lepecq, J-B. & Paoletti, C. J. Mol. Biol. 27, 87, (1967).

232. Caswell, A.H. & Gitler, C. Fed. Proc. 29, 605, (1970).

233. Chance, B. Proc. Nat. Acad. Sci. 67, 560, (1970).

234. Weber, G. & Laurence, D.J.R. Biochem. J. 56, xxxi, (1954).

235. Timmerman's "Physico-chemical constants" Vol.4 Interscience (1960) p.189 - 202.

236. Datta, A. & Penefsky, H.S. J. Biol. Chem. 245, 1537, (1970).

237. Penzer, G.R. Part II Thesis, Oxford, (1966).

238. Waggoner, A.S.& Stryer, L. Proc. Nat. Acad. Sci. 67, 579, (1970).

239. Azzi, A. Biochem. Biophys. Res. Comm. 37, 254, (1969).

240. Deranleau, D. J. Am. Chem. Soc. 91, 4044, 4050, (1969).

241. Chance, B. & Lee, C.P. FEBS Lett. 4, 181, (1969).

242. Packer, L., Donovan, M.P. & Wrigglesworth, J.M. Biochem. Biophys. Res. Comm. 35, 832, (1969).

243. Feinstein, M.B., Spero, L. & Felsenfield, H. FEBS Lett. 6, 245, (1970).

244. Chance, B. unpublished observations